

Robust experimental methods to study in-vivo pre-steady
state kinetics of primary metabolism in *Saccharomyces*
cerevisiae

Mlawule Reginald Mashego

**Robust experimental methods to study in-vivo pre-steady
state kinetics of primary metabolism in *Saccharomyces
cerevisiae***

PROEFSCHRIFT

ter verkrijging van de graad van doctor
aan de Technische Universiteit Delft,
op gezag van de Rector Magnificus prof. dr. ir. J. T. Fokkema,
voorzitter van het College voor Promoties,
in het openbaar te verdedigen op donderdag 3 november 2005 om 13.00 uur
door

Mlawule Reginald MASHEGO

Master of Science in Biotechnology
University of Zimbabwe
geboren te Bushbuckridge, Zuid Afrika

Dit proefschrift is goedgekeurd door de promotor:

Prof. dr. ir. J. J. Heijnen

Samenstelling promotiecommissie:

Rector Magnificus	voorzitter
Prof. dr. ir. J. J. Heijnen	Technische Universiteit Delft, promotor
Prof. dr. J. T. Pronk	Technische Universiteit Delft
Prof. dr. M. Reuss	Universität Stuttgart, Duitsland
Prof. dr. J. C. Portais	Université Paul Sabatier, Toulouse, Frankrijk
Dr. D. Schipper	DSM
Dr B. M. Bakker	Vrije Universiteit Amsterdam
Prof. dr. ir. J. P van Dijken	Technische Universiteit Delft
	Reserveid

The studies presented in this thesis were performed at the Delft University of Technology, Faculty of Applied Sciences, Bioprocess Technology Section. The research was financially supported by the board of the Delft University of Technology (Bonusregeling Excellent Onderzoek), DSM and the Dutch Ministry of Economic Affairs (NWO-CW project 99601). The Bioprocess Technology section is part of the Kluyver Centre for Genomics of Industrial Fermentation, which is supported by the Netherlands Genomics Initiative.

Contents

	Page
Chapter 1	7
General introduction	
Chapter 2	29
Critical evaluation of sampling techniques for residual glucose determination in carbon limited chemostat culture of <i>Saccharomyces cerevisiae</i>	
Chapter 3	39
MIRACLE: Mass Isotopomer Ratio Analysis of U- ¹³ C-Labeled Extracts. A new method for accurate quantification of changes in concentrations of intracellular metabolites	
Chapter 4	55
Changes in the metabolome of <i>Saccharomyces cerevisiae</i> associated with evolution in aerobic glucose-limited chemostats	
Chapter 5	79
In vivo kinetics with rapid perturbation experiments in <i>Saccharomyces cerevisiae</i> using a 2 nd Generation BioScope	
Chapter 6	105
Metabolome dynamic responses of <i>Saccharomyces cerevisiae</i> on simultaneous rapid perturbations in external electron acceptor and electron donor	
Chapter 7	135
Transient response of metabolome/fluxome of aerobic chemostat cultivated <i>S. cerevisiae</i> to increased CO ₂ concentration	
Conclusions and outlook	151
Summary	155
Samenvatting (Summary in Dutch)	157
Acknowledgements	159
Curriculum Vitae	161
List of publications	163

General Introduction

Metabolic Engineering

Improvement of bioprocess performance has traditionally relied on classical random mutagenesis of wild type microbial isolates followed by selection of superior mutants as well as media and fermentation process optimization. This strategy has had outstanding successes as has been demonstrated in the antibiotic (e.g. penicillin) and amino acids (e.g. glutamate and lysine) industries (Aida et al, 1986). Although successful in the past, it has some inherent disadvantages, such as labour and resource intensity, which renders it less attractive due to its trial and error approach. In addition, the mutations leading to the superior qualities of the selected microorganisms are undefined/ unknown. Furthermore, random mutagenesis might lead to the accumulation of undesirable mutations as well. The advent of molecular biology tools (genetic engineering) pioneered with success by Cohen and Boyer in 1973 paved the way for a completely new approach for the introduction of genetic changes in cells thereby manipulating specific cellular metabolic pathways (Table 1). This strategy facilitated optimisation of existing bioprocesses as well as the development of completely new ones. This technology provided the possibility of a more rational approach to microbial strain improvement and led to a new field referred to as metabolic engineering (Bailey, 1991; Stephanopoulos et al, 1998; Nielsen, 2001).

Successful metabolic engineering efforts depend on the quantitative understanding of the in vivo kinetics and regulation of complex metabolic networks. This understanding requires accurate quantitative information on all hierarchical levels of the cell, i.e. genome, transcriptome, proteome, metabolome and fluxome (Figure 1). These hierarchical levels are regulated not simultaneously but rather are regulated at different time's scales as depicted in Figure 2. For the cells, these hierarchical levels ensure robust and well-orchestrated coordination of the in vivo regulation of cellular metabolic response to external stimuli, i.e. by modulating enzyme activity through allosteric regulation via inhibition, activation or covalent modification. This form of metabolic regulation is among the forms of rapid response mechanisms, typically in a time scale of seconds. Alternatively, there is induction/derepression of enzymes that are required but which are not constitutively expressed under certain growth conditions, e.g. diauxic phenomena typical of batch grown *Saccharomyces cerevisiae* culture in a medium containing glucose as a carbon source (Figure 2). During these culture conditions, glucose is used first, partly for ethanol formation as by-product. When glucose is exhausted, the yeast cell turns on the catabolic machinery required for ethanol catabolism as a second carbon source. This level of regulation requires switching of the expression of genes responsible for the enzymes to catabolize ethanol as a carbon source. The process requires typically a minute's to tens of minutes time scale to be activated and functional. The above examples are a small sample of the plentiful possibilities of hierarchical regulatory mechanisms that are at the disposal of biological systems. Successful prediction of the behaviour of this highly integrated and tightly

regulated hierarchical architecture (Figure 1) of biological systems with mathematical models is expected to advance the rapid developing discipline of systems biology. It is realised that successful modelling of complex biological systems needs to be treated holistically and not in individual parts (Kitano, 2002). An analogy to this concept of systems biology is that of a car engine, i.e. understanding how the individual parts of the engine work do not guarantee understanding and hence ability to predict how the engine works as a unit. Systems biology's popularity is fuelled by the rapid increase in analytical power leading to large data sets from all hierarchical levels such as genomics, transcriptomics, proteomics, metabolomics and fluxomics as well as computing power (bioinformatics). We recognize that successful rational engineering of superior cell factories requires understanding of the interaction at all levels of the hierarchical architecture as depicted in figure 1. However, the complexity of the metabolic network demands that choices have to be made. From the point of view of cellular product formation, the kinetics of primary metabolism and connected product pathway(s) are always of interest. Currently, mathematical modelling of primary metabolism focuses mostly on using information on network stoichiometry, metabolic fluxes, metabolite concentrations and enzyme activities.

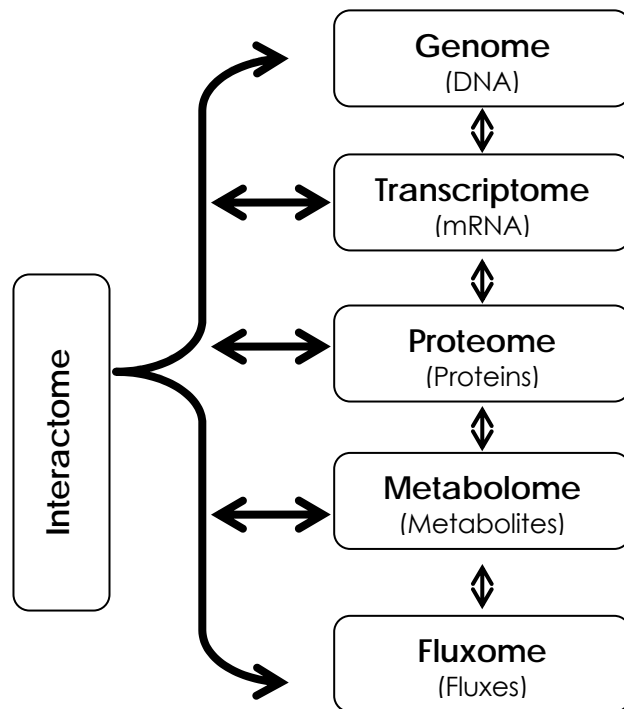


Figure 1 Hierarchical levels of cellular regulation and their interactions

Table	1	Examples	of	metabolic	pathway	engineering	successes
Category		Examples		References			
Heterologous protein production		Hormones; antibiotics; vaccines & novel enzymes					Stephanopoulos et al, 1998
Improvement of yield or productivity		Low value added products (amino acids); ethanol;					Sonderegger et al, 2004; van Maris et al, 2004
		Pyruvate					
Extension of substrate range		Xylose; lactose; starch; xylan; β -glucans,					Kuyper et al, 2004; Burchhardt and Ingram (1992); Brabetz et al, 1999; Penttilä et al, 1987; Domingues et al, 1999a; b; Janse and Pretorius, 1995; Kötter and Ciriacy 1993
Metabolic pathway engineering for new products		Polyketides; novel polyhydroxyalkanoates; antibiotics; indigo; xylitol; 1, 2 and 1,3 propanediol; lactic acid; L-glycerol -3-phosphate					Khosla et al (1999); Murdock et al, (1993); Hallborn et al, (1991); Cameron et al, 1998; Altaras and Cameron, 1999; Lee and Choi (2001); van Maris et al, 2004 ; Nguyen et al, 2004
Pathway for degradation		xenobiotic					Rojo et al, (1987)
Engineering of cellular physiology for process improvement		Glucose repression; pathway					Leloir Klein et al, (1999); Rønnow et al, (1999); Ostergaard et al, (2000)
Elimination of formation		by-products					TAKA amylase production; Oxalic acid production; S. Pedersen et al, (2000); Nissen et al, (2000a; 2000b) cerevisiae anaerobic glycerol formation

Quantitative description of microbial metabolism

Mathematical modelling can be applied in order to describe microbial metabolism in a quantitative way, to predict the behaviour of microorganisms, to obtain a better understanding of their functioning and to guide metabolic redesign. The simplest mathematical model describing a biological system is the so-called black box model. These models treat the cell as a black box in which all intracellular reactions are lumped into one. Only external rates are quantified such as rates of growth and product formation and consumption rates of substrate and oxygen (e.g. μ , q_p , q_s , q_{O_2}). Linear relations can be derived taking for example, the format of the Herbert-Pirt linear equation for substrate consumption (equation 1)

$$q_s = \frac{\mu}{Y_{SX}^{\max}} + \frac{q_p}{Y_{SP}^{\max}} + m_s \quad 1$$

Where,

q_s = specific substrate uptake rate (g substrate/g biomass. h)

Y_{SX}^{\max} = biomass yield parameter (g biomass/g substrate)

μ = specific growth rate (g biomass/g biomass. h)

Y_{SP}^{\max} = product yield parameter (g product/g substrate)

m_s = maintenance parameter (g substrate/g biomass. h)

Such models are effective tools in the optimization of fermentation processes, however, optimisation of the micro-organism itself requires an entirely different approach.

Rational identification of recombinant DNA targets for metabolic engineering of industrial micro-organisms requires detailed mathematical modelling of biological events through construction of *in silico* models of the relevant parts of microbial metabolism. Based on the outcome of the *in silico* model predictions, metabolic redesign can be applied, leading to desired changes in the phenotype of the microorganism. Detailed mathematical modelling of cellular metabolism is widely used in metabolic engineering and can be grouped into two major clusters: i) Stoichiometric modelling and ii) Kinetic modelling.

Stoichiometric modelling

Stoichiometric models of cellular metabolism are based on time invariant characteristics of metabolic networks and essentially describe these metabolic networks as a set of stoichiometric equations representing a system of biochemical reactions e.g. as depicted in figure 3. Major information sources for construction of metabolic network models have been primarily biochemistry textbooks, literature, and, more recently, metabolic pathway databases

e.g. (KEGG; BRENDA) and annotated genomes. An important assumption in stoichiometric models is pseudo steady state conditions. Under these conditions, mass balance constraints on the metabolite pools in the system can be used to determine the intracellular fluxes (Vallino & Stephanopoulos, 1993; van Gulik & Heijnen, 1995; Gombert & Nielsen 2000; Lange, 2002; Förster et al, 2003; Famili et al, 2003; Patil et al, 2004). A set of linear equations is obtained from steady state balancing of the in-put/out-put and intermediate compounds involved. The degree of freedom of the system of linear equations is equal to the total number of reaction rates (unmeasured rates+measured rates) minus the total number of independent linear equations. In order to solve the system mathematically, some rates need to be measured. Depending on the number of measured rates relative to the degrees of freedom, the system can be either determined, over-determined or under-determined (van der Heijden et al, 1994). The system is over determined if the number of measured rates is greater than the degree of freedom or underdetermined if the number of measured rates are lower than the degree of freedom. In case of an under determined system, additional constraints have to be introduced in order to obtain a unique solution. Overdetermined system leads to the redundancy of the data and that allows rigorous statistical data analysis. Such models can be represented by a stoichiometric matrix (S) with the rows representing stoichiometric coefficients of the different metabolites in the metabolic network and the columns representing fluxes through each reaction of the metabolic network. Metabolic flux analysis (MFA) yields the (pseudo) steady state fluxes through the different branches of the network under the investigated conditions. Application of ^{13}C labeled substrates and measurement of isotopomer distributions of metabolites provides extra constraints (the isotope balances) for metabolic flux analysis whereby uncertain cofactor balances can be omitted (Gombert et al, 2001; van Winden, 2002; Christensen et al, 2002).

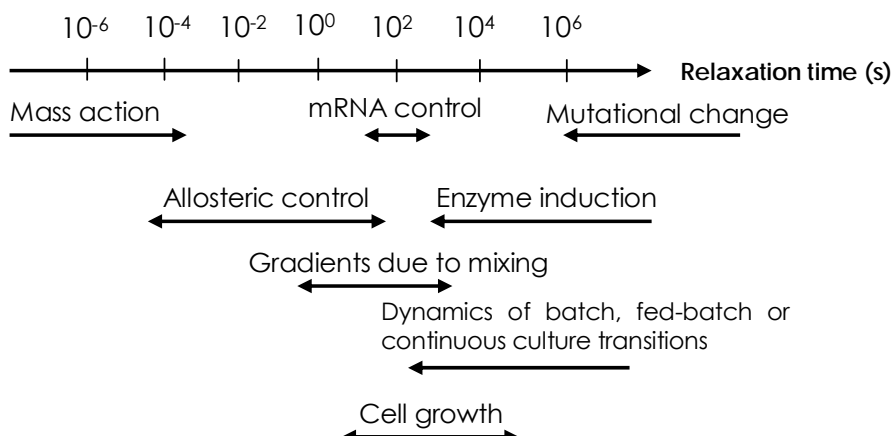


Figure 2 Relaxation times of different cellular processes in comparison with relaxation time of bioreactor operation (Stephanopoulos, et al. 1998)

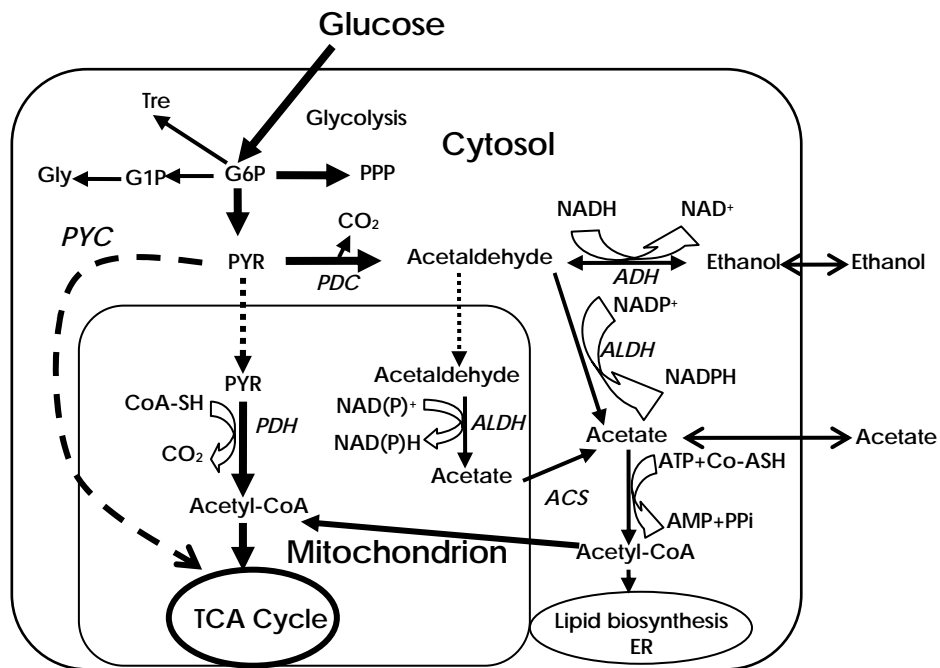


Figure 3 Simplified metabolic network scheme of the primary carbon metabolism in *S. cerevisiae*. Key: *PDH* (Pyruvate dehydrogenase complex); *PYC* (Pyruvate carboxylase); *PYR* (Pyruvate); *PDC* (Pyruvate decarboxylase); *ADH* (Alcohol dehydrogenase); *ALDH* (Acetaldehyde dehydrogenase); *ACS* (Acetyl CoA synthetase); CoA-SH (Coenzyme A); ER (Endoplasmic Reticulum), Tre (Trehalose); G6P (Glucose-6-phosphate); G1P (Glucose-1-phosphate); Gly (Glycogen); PPP (Pentose phosphate pathway).

Kinetic modelling of metabolic reaction networks

A kinetic model defines the metabolic system by combining enzyme rate equations with stoichiometry and mass balances (Rizzi et al, 1997; Vaseghi et al, 1999; Gombert & Nielsen, 2000). The principle of kinetic modelling is illustrated in figure 4 below.

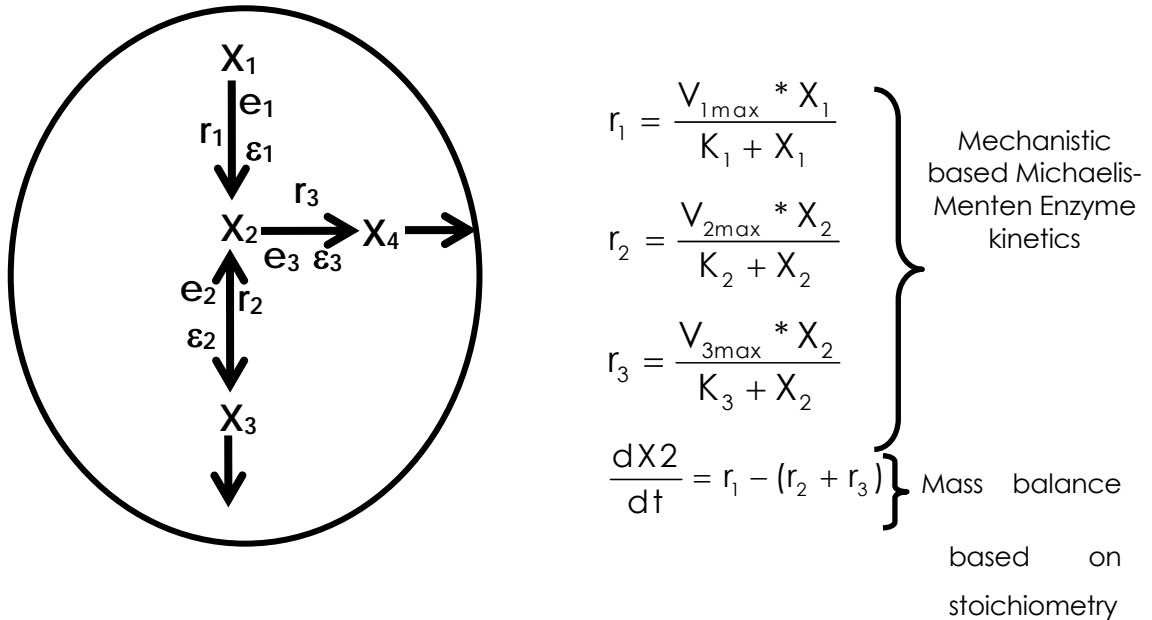


Figure 4 Simplified metabolic network reaction scheme containing four reactants (X_1 ; X_2 ; X_3 and X_4). r_1 ; r_2 and r_3 in kinetic models often mechanistic rate equations for all relevant enzymes are reaction rates catalysed by enzymes e_1 ; e_2 and e_3 with elasticities ε_1 ; ε_2 and ε_3 respectively.

In kinetic models often mechanistic rate equations for the enzymes involved in the metabolic pathway are incorporated, combined with *in vitro* or *in vivo* determined kinetic parameters. It has now been realised that *in vitro* determined kinetic parameters are generally not representative of the *in vivo* kinetic properties due to the entirely different intracellular conditions (pH, osmolarity, crowding) (Schaefer et al, 1999; Vaseghi et al. 1999; Teusink et al, 2000; Wright & Kelly, 1981). Schaefer et al, 1999 concluded from their studies on the conversion of FBP to GAP and DHAP that application of well-known mechanistic models of enzyme reactions studied *in vitro* may not be sufficient to describe the *in vivo* dynamic behavior. Teusink et al, 2000, reported that half of the enzymes matched their predicted flux *in vivo* within a factor 2, whereas for the rest of the enzymes deviations between *in vivo* and *in vitro* kinetics could explain the discrepancies between *in vitro* rate and *in vivo* flux. The parameters of these kinetic functions need therefore to be estimated under *in-vivo* conditions. However, the application of mechanistic rate equations in kinetic models leads to highly complex non-linear systems with a large number of parameters. This greatly hampers the estimation of these parameters from *in-vivo* data including the errors associated with them (Figure 4). A way to

reduce these problems is model simplification. The number of enzyme reaction steps in the models can be drastically reduced by ignoring reactions and pathways that are operating on times scales outside the range of interest (Figure 2) (Stephanopoulos et al. 1998).

Furthermore, enzymatic reaction steps that are catalyzing reversible reactions that are in rapid equilibrium can be lumped, resulting in a significantly reduced model. Further reduction of model complexity can be achieved by using less complicated approximative kinetic formats such as tendency modelling (Visser et al, 2000); lin-log kinetics (Visser & Heijnen, 2003; Visser et al, 2004; Heijnen et al, 2004; Wu et al, 2004; Heijnen 2005); linear (Heinrich et al. 1977; Small and Kacser 1993) and power law kinetics (Savageau, 1976) for dynamic modeling of cellular metabolic reaction networks. The main advantage of these simplified approximate kinetic formats is that they have a reduced number of kinetic parameters while still maintaining a reasonable predictive capability. Recently, an overview was provided of the different approximative kinetic formats and it was concluded that lin-log kinetics (building on the early work by Onsager, 1931; Rottenberg 1973) appears to be the most attractive approximation (Heijnen, 2005).

A general format for lin-log approximative kinetics is given in equation 2 below

$$\frac{v}{J^0} = \frac{e}{e^0} \left(1 + \varepsilon_{x1}^0 \ln \frac{X_1}{X_1^0} + \varepsilon_{x2}^0 \ln \frac{X_2}{X_2^0} + \varepsilon_{x3}^0 \ln \frac{X_3}{X_3^0} \right) \quad 2$$

Where; v = reaction rate; J^0 = reference flux; X_i = intracellular metabolite concentrations and ε_i are the elasticities.

This equation describes the reaction rate as a function of the elasticities (ε_{ij}) and reference state enzyme level, intracellular and extracellular metabolites. The reaction rate is considered proportional to the enzyme level (e) and the influence of the metabolite concentration (X) is taken into account as a linear combination of the logarithmic terms. In metabolic studies, reaction rates are often expressed relative to a well characterised reference steady state, in the equation above such reference state is characterised by the superscript (0) (Visser & Heijnen, 2003; Heijnen et al, 2004). Unlike the other approximative kinetic formats, the lin-log kinetic format provides explicit analytical solutions of steady state fluxes and metabolite concentrations as a function of relatively large changes in enzyme levels.

Metabolic Control Analysis

Metabolic control analysis (MCA) is a mathematical framework that quantitatively relates the changes in system variables (e.g. metabolite concentrations and fluxes) to systems parameters (e.g. enzyme levels) Kacser and Burns 1973; Heinrich et al., 1977; Westerhoff et al, 1991; Fell and Kacser, 1995; Stephanopoulos et al, 1998; Visser & Heijnen 2002). Metabolic control analysis is

concerned with the identification of distribution of control of the flux through an enzyme-catalyzed set of reactions. In a way, MCA attempts to quantitatively describe the behaviour of fluxes and metabolite levels in a metabolic system in response to changes in the independent system variables (enzyme levels) and environmental/external stimuli. Understanding the effect of a change in system parameters on the system independent variables is central to metabolic control analysis. The degree of influence that the variation of a system independent variable has on a system dependant variable determines the level of control of the independent variable (fluxes or metabolite concentrations). Metabolic control analysis (MCA) makes no *a priori* assumptions, such as a first enzyme catalyzed step in a linear pathway is rate limiting or that a first enzyme catalyzed step after a branch point is rate limiting. It defines e.g. a flux control coefficient C^J to express the sensitivity of a flux to an infinitesimal change in enzyme concentration/level (Figure 5).

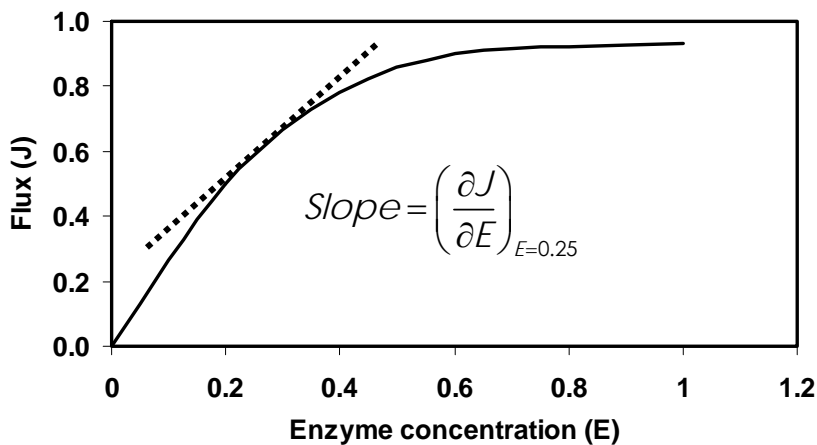


Figure 5 Steady state flux (J) as a function of the activity of an intermediate enzyme (E).

Mathematically, C^J is defined as a fractional change in flux (J) with respect to the fractional change in enzyme level (E) as depicted in equation 3 below (Heinrich et al., 1977; Fell & Kacser, 1995):

$$C^J = \frac{\frac{\partial J/J}{\partial [E]}}{\frac{[E]}{[E]}} = \frac{\partial \ln J}{\partial \ln E} = \frac{\Delta J/J}{\Delta E/E} \quad 3$$

In an enzymatic pathway, the degree of flux control by enzymes constituting the pathway is proposed to be distributed within the individual enzymatic steps of the metabolic network and sum up to unity, i.e. 1, as defined by the summation theorem of the metabolic control framework. Various other control coefficients have been defined such as concentration control coefficients (CCC) as well as response control coefficients (for excellent reviews, see Heinrich et al, 1977; Westerhoff et al, 1991; Fell & Kacser, 1995; Visser & Heijnen, 2002). Central in MCA are

the elasticity parameters ε_{ij} which are the normalized sensitivities of enzyme catalyzed reaction rates to individual metabolite concentrations. Knowledge of the elasticities directly leads to the control parameters. The disadvantage of the traditional MCA framework is that estimation of the elasticity and flux control coefficients requires infinitesimal changes in metabolite and enzyme levels, which is practically difficult to achieve. Furthermore, the main aim of metabolic engineering is to achieve or increase significantly the flux towards a product of choice, hence a larger dynamic range is desirable which the original MCA framework cannot describe. Therefore, variations of the original MCA framework have been proposed taking into account larger non-linear dynamic changes in enzyme and metabolite concentrations (Heinrich et al. 1977; Visser & Heijnen 2003, see an excellent review by Heijnen, 2005).

These developments involve Biochemical Systems Theory (BST), large perturbation MCA; log-linear and lin-log approaches (Heijnen, 2005). Using the lin-log approach it has been shown that elasticities can be obtained from sets of metabolites, fluxes and enzyme activities (Kresnowati et al, 2005). A current bottleneck is to obtain such data sets both from analytical as well as experimental design point of view.

Experimental tools for elucidation of in vivo kinetics in microbial cellular catabolism

Quantitative understanding of complex microbial metabolism and its regulation in-vivo requires accurate information concerning both intracellular and extracellular metabolite pool levels. Such information is commonly obtained under dynamic conditions by carefully designed dynamic perturbation experiments. These dynamic experiments are usually performed in a controlled environment i.e. using chemostat cultivated microorganisms.

Chemostats are continuous cultures of microorganisms in which the required nutrients for growth are all supplied in excess amounts except one, which is in most cases the carbon or nitrogen source (Novick & Szilard, 1950; Tempest and Neijssel, 1981; Theobald et al, 1993; 1997; Visser et al, 2002; 2004; Schmitz et al, 2002; Buchholz et al, 2002; Buziol et al, 2002) (Fig 6).

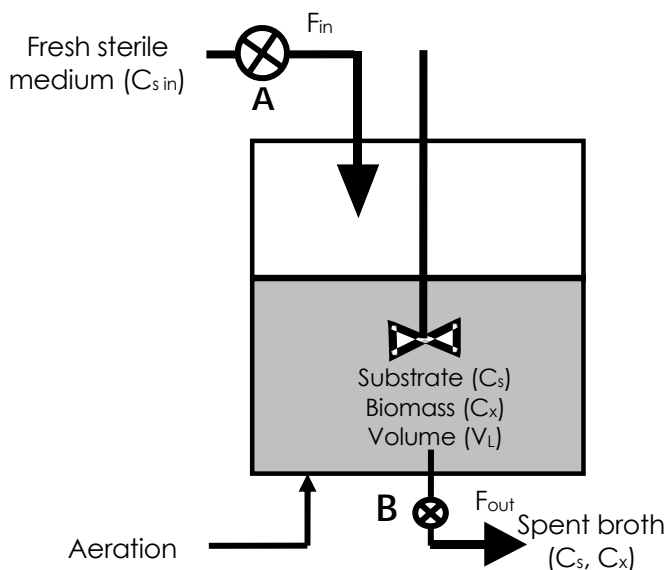


Figure 6 Typical CSTR bioreactor. When valves A and B are closed, the bioreactor is operating in a batch mode. When valve A is open and fresh medium is fed to the bioreactor, the bioreactor is operating in the fed-batch mode, and volume does not remain constant. This mode of bioreactor operation is widely used in industry. When both valve A and B are open and $F_{in} \approx F_{out}$; the bioreactor is operated in continuous mode. The bioreactor volume is constant.

Chemostat cultivation is a preferred mode for cultivating microorganisms, mainly because the specific fluxes can be well controlled and fixed through the dilution rate (D) which under steady state conditions is equal to the specific growth rate (μ). The steady state is defined as a situation in which at least five reactor volume changes have occurred following the end of the batch phase and in which the biomass concentration (C_x), specific oxygen uptake (q_{O_2}) and carbon dioxide production rates (q_{CO_2}) and dissolved oxygen tension remain constant (for detailed review, see, Weusthuis et al, 1994). However, it has been shown that while biomass concentration and biomass specific fluxes are all in steady state, the residual substrate strongly decreases with increased duration time of the chemostat culture (Wick et al, 2001; Weichert et al, 1997; Adams et al, 1985). This indicates that the physiological states of the population might depend on the cultivation time. First indications (Lange, 2002), have been obtained that the intracellular metabolite levels in a chemostat do not reach a steady state level but slowly change as a function of cultivation time. Biomass with a defined steady state therefore might require a fixed time window of biomass age in a chemostat.

Stimulus response experiments with biomass in a defined steady state performed by e.g. an instantaneous increase of the growth limiting substrate of a steady state chemostat culture, has been proposed as a method to elucidate the kinetics of enzymes under in-vivo conditions (Theobald et al, 1993; 1997; Rizzi et al, 1997; Vaseghi et al, 1999). Accurate measurement of metabolite profiles during short term (300 seconds) under highly dynamic conditions requires rapid sampling, instant quenching of cellular metabolism and subsequent measurements of both the intracellular and extracellular metabolite concentrations (Harrison and Maitra 1969; Weibel et al, 1974; De Koning & van Dam 1992; Theobald et al, 1993; 1997, Gonzalez et al, 1997; Schaefer et al, 1999; Visser et al, 2002; Schmitz et al, 2002; Buchholz et al, 2002; Buziol et al, 2002).

These stimulus response experiments have traditionally been performed directly in a chemostat. However, this approach has inherent disadvantages, such as, the loss of the steady state condition, leading to the necessity to start a new chemostat for each perturbation experiment. Also, due to the required short sampling times (<1 second), the sample volume is very limited. This approach is time consuming and relatively expensive. Visser et al, 2002, reported an alternative approach of carrying out perturbation experiments applying a mini plug-flow reactor (BioScope) coupled to a steady state chemostat. The BioScope allows carrying out several perturbation experiments on steady state biomass. The perturbation starts when the flow of steady state broth from the fermentor is mixed with the flow of the perturbing agent in the BioScope. Samples are collected from the flowing broth at different locations along the plug flow reactor. These points of sampling determine the time during which the sampled cells have been exposed to the perturbation and thereby the reaction times.

Metabolite analysis

Quantification of the concentrations of both extracellular, e.g. (glucose, ethanol and acetate) as well as intracellular compounds e.g. (glycolytic and TCA cycle metabolites) is essential for the analysis of the cellular response to externally applied stimuli, e.g. glucose perturbation conditions. Analysis of these metabolites has been traditionally carried out using enzyme-based assays (Bergmeyer et al, 1985). This enzymatic based quantification of extracellular and intracellular metabolites has been in the forefront of the analytical procedures used (Hajjaj et al, 1998; Ruijter & Visser, 1996; Theobald et al, 1993; 1997). However, the available small sample volumes and the large volumes needed in those assays limit the analysis to a few compounds per sample. The reliable quantification of intracellular metabolite concentrations is hindered by the low concentrations of these compounds in cells and is exacerbated by the dilution of the already low metabolite concentrations during the quenching/extraction steps. Furthermore, the complex cellular matrix might interfere with the analysis procedure applied.

The advent of high sensitivity LC-ESI/MS, LC-ESI-MS/MS and GC-MS instruments has broadened the range of techniques available for the quantification of intracellular metabolites as has been reported in *E. coli* and *S. cerevisiae* by Buchholz et al, 2001; 2002; Van Dam et al, 2002; and Castrillo et al, 2003; Farre et al, 2002. The advantage that has led to the increasing use of LC-ESI-MS/MS is its high sensitivity, the simultaneous quantification of many different metabolites and small sample volumes (10 μ L) required for analysis with a detection limit in the sub-pmol range (Van Dam et al, 2002). In addition, the fact that most of the metabolites from central carbon metabolism, i.e. glycolysis, tricarboxylic acid (TCA) cycle and pentose phosphate pathway (PPP), can be analysed in a single injection of 10 μ L sample is fuelling the popularity of these instruments (Van Winden, 2002). A significant disadvantage is the required very laborious procedure of standard additions, calibration, recovery for each metabolite to exclude matrix effects and effects of quenching/extraction.

Outline of the thesis

The aim of the thesis is to develop robust experimental tools for quantification and elucidation of in vivo kinetics of metabolites in primary carbon metabolism in *Saccharomyces cerevisiae*. These tools are vital for successful quantitative analysis of microbial physiology and biochemistry. Such quantitative analysis provides insight into the kinetic and allosteric regulatory mechanisms of metabolic network reactions. These models allow then to calculate the changes in enzyme activities required to achieve a desired objective (e.g. high productivity). It is clear that the implementation of the required changes in enzyme activities requires detailed models of genetic regulation, which is beyond the scope of this thesis.

Chapter 2 is devoted to the development of a rapid sampling and quenching technique for accurate measurement of the concentrations of residual substrate and extracellular metabolites during perturbation experiments. Chapter 3 focuses on the development of a

robust method for quantification of intracellular metabolites of the primary metabolism under steady state as well as dynamic conditions using ^{13}C -labeled intracellular metabolites as internal standards. Chapter 4 addresses in-vivo evolution of *S. cerevisiae* during long-term cultivation in glucose-limited chemostats. Concentrations of intracellular and extracellular metabolites, in vitro specific activities of enzymes involved in the primary metabolism of *S. cerevisiae* as well as cellular shape and size were found to change significantly during a period of 1200 h. As this might indicate a change of enzyme kinetic properties, standardization of cultivation conditions for perturbation response experiments should also include chemostat cultivation time. Chapter 5 focuses on the development of a 2nd generation BioScope design. This design is based on a channel system milled in a Perspex block, for reasons of robustness and reproducibility. To enable manipulation of the gas-phase composition the channel consists of two parts: gas channel and liquid channel, separated by an oxygen (O_2) and carbon dioxide (CO_2) permeable membrane. Chapter 6 explores the use of the 2nd generation BioScope for performing simultaneously dynamic glucose perturbations and perturbation of electron acceptor (using O_2 and acetaldehyde as external acceptor). Manipulation of the specific acetaldehyde and oxygen uptake rates were achieved by manipulating the gas and liquid phase compositions in the BioScope. In chapter 7, the perturbation of a steady state chemostat culture of *S. cerevisiae* by a gaseous compound is investigated. It was found that a step increase of the CO_2 concentration in the aeration gas induced a significant perturbation of primary as well as storage carbohydrate metabolism.

References

- Adams, J. Paquin, C. Oeller, P.W. and Lee L.W., 1985. Physiological characterization of adaptive clones in evolving populations of the yeast *Saccharomyces cerevisiae*. *Genetics*. 110, 173-185.
- Aida K., Chibata I., Nakayama K., Takinami K., Yamada H., 1986. *Biotechnology of amino acid production*. Elsevier. Amsterdam
- Altaras Nedim E. and Cameron Douglas C., 1999. Metabolic Engineering of a 1, 2-Propanediol Pathway in *Escherichia coli*. *Appl Environ Microbiol*. 65, 1180-1185.
- Bailey J.E., 1991. Toward a science of metabolic engineering. *Science*. 252, 1668-1675.
- Bergmeyer H.C., Bergmeyer J., Grass M. (Eds)., 1985. *Methods in enzymatic analysis*. 3rd Edition. Verlag Chemie. Weinheim.

Brabetz W., Liebl W., Schleifer K.H., 1999. Studies on the utilization of lactose by *Corynebacterium glutamicum* bearing the lactose operon of *Escherichia coli*. Arch Microbiol. 155, 607-612.

Buchholz A., Takors R., Wandrey C., 2001. Quantification of intracellular metabolites in *Escherichia coli* K12 using liquid chromatographic-electrospray ionization tandem mass spectrometric techniques. Anal Biochem. 295, 129-137.

Buchholz A., Hurlbaeus J., Wandrey C., Takors R., 2002. Metabolomics: Quantification of intracellular metabolite dynamics. Biomol Eng. 19, 5-15.

Burchhardt G., Ingram L.O., 1992. Conversion of xylan to ethanol by ethanologenic strains of *Escherichia coli* and *Klebsiella oxytoca*. Appl Environ Microbiol. 58, 1128-1133.

Buziol S., Bashir I., Baumeister A., Claassen W., Noisommit-Rizzi N., Mailinger W., Reuss M., 2002. New bioreactor-coupled rapid stopped flow sampling technique for measurements of metabolite dynamics on a sub-second time scale. Biotechnol Bioeng. 80(6), 632-636.

Cameron D.C., Altaras N.E., Hoffman M.L., Shaw A.J., 1998. Metabolic engineering of propanediol pathways. Biotechnol. Prog. 14, 116-125.

Castrillo J.I., Hayes A., Mohammed S., Gaskell S.J. and Oliver S.G., 2003. An optimised protocol for metabolome analysis in yeast using direct infusion electrospray mass spectrometry. Phytochemistry. 62, 929-937.

Christensen B., Gombert A.K., Nielsen J., 2002. Analysis of flux estimates based on ¹³C-labelling experiments. Eur J Biochem. 269(11), 2795-2800.

Cohen S.N., Chang A.C.Y., Boyer H.W., Helling R B., 1973., Construction of biologically functional bacterial plasmids in vitro. Proc Natl Acad Sci U S A. 70(11), 3240-3244.

De Koning W., van Dam K., 1992. A method for the determinations of changes of glycolytic metabolites in yeast on a sub second time scale using extraction at neutral pH. Anal Biochem. 204, 118-123.

Domingues L., Teixeira J.A., Lima N., 1999a. Construction of a flocculent *Saccharomyces cerevisiae* fermenting lactose. Appl Microbiol Biotechnol. 51, 621-626.

Domingues L., Lima N., Teixeira J.A., 1999b. Continuous ethanol fermentation of lactose by a recombinant flocculating *Saccharomyces cerevisiae* strain. *Biotechnol Bioeng.* 64, 692–697.

Famili I., Forster J., Nielsen J., Palsson B.O., 2003. *Saccharomyces cerevisiae* phenotypes can be predicted by using constraint-based analysis of a genome-scale reconstructed metabolic network. *Proc Natl Acad Sci.* 100(23), 13134-13139

Farre E. M., Tiessen A., Roessner U., Geigenberger P., Trethewey R. N., Willmitzer L., 2001. Analysis of the compartmentation of glycolytic intermediates, nucleotides, sugars, organic acids, amino acids, and sugar alcohols in potato tubers using a nonaqueous fractionation method. *Plant Physiol.* 127(2), 685-700.

Fell D., Kacser H. 1995. The control of flux: 21 years on. *Biochem Soc Trans.* 23, 341-366

Förster J., Famili I., Fu P., Palsson B.O., Nielsen J., 2003. Genome-scale reconstruction of the *Saccharomyces cerevisiae* metabolic network. *Genome Res.* 13(2), 244-253.

Gombert A.K., Nielsen J., 2000. Mathematical modelling of metabolism. *Curr Opin Biotechnol.* 11, 180-186.

Gombert A.K., Moreira dos Santos M., Christensen B., Nielsen J., 2001. Network identification and flux quantification in the central metabolism of *Saccharomyces cerevisiae* under different conditions of glucose repression. *J Bacteriol.* 183(4), 1441-51.

Gonzalez, B., Francois, J. and Renaud, M., 1997. A rapid and reliable method for metabolite extraction in yeast using boiling buffered ethanol. *Yeast.* 13, 1347-1356.

Hajjaj H., Blanc P. J., Goma G. and François J., 1998. Sampling techniques and comparative extraction procedures for quantitative determination of intra- and extracellular metabolites in filamentous fungi. *FEMS Microbiol Lett.* 164, 195-200.

Hallborn J., Walfridsson M., Airaksinen U., Ojamo H., Hahn-Hagerdal B., Penttilä M., Kerasnen S., 1991. Xylitol production by recombinant *Saccharomyces cerevisiae*. *Biotechnology.* 9(11), 1090-1095.

Harrison D. E. F., Maitra P. K., 1969. Control of respiration and metabolism in growing *Klebsiella aerogenes*. *Biochem J.* 112, 647-656.

Heijnen J.J., van Gulik W.M., Shimizu H., Stephanopoulos G., 2004. Metabolic flux control analysis of branch points: an improved approach to obtain flux control coefficients from large perturbation data. *Metab Eng.* 6(4), 391-400.

Heijnen J. J., 2005, Approximative kinetic formats used in metabolic network modeling. *Biotechnol Bioeng.* 91, 534-545

Heinrich R., Rapoport S. M., Rapoport T. A., 1977. Metabolic regulation and mathematical models. *Prog. Biophys. Molec. Biol.* 32, 1-82

Janse B.J., Pretorius I.S., 1995. One-step enzymatic hydrolysis of starch using a recombinant strain of *Saccharomyces cerevisiae* producing alpha-amylase, glucoamylase and pullulanase. *Appl Microbiol Biotechnol.* 42(6), 878-883.

Kacser H., Burns J. A., 1973. The control of flux. *Symp. Soc. Exp. Biol.* 27, 65-104

Khosla C., Gokhale R.S., Jacobsen J.R., Cane D.E., 1999. Tolerance and specificity of polyketide synthases. *Annu Rev Biochem.* 68, 219-253.

Kitano H., 2002. System Biology: a Brief overview. *Science.* 295, 1662-1664.

Klein C. J, Rasmussen J. J, Ronnow B, Olsson L, Nielsen J. 1999. Investigation of the impact of MIG1 and MIG2 on the physiology of *Saccharomyces cerevisiae*. *J Biotechnol.* 68(2-3), 197-212.

Kötter P., Ciriacy M., 1993. Xylose fermentation by *Saccharomyces cerevisiae*. *Appl Microbiol Biotechnol.* 38, 776-783.

Kresnowati Penia M.T.A., van Winden Wouter A., Heijnen Joseph. J., 2005. Determination of elasticities, concentration and flux control coefficients from transient metabolite data using linlog kinetics. *Metab Eng.* 7, 142-153

Kuyper M., Winkler A.A., van Dijken J.P., Pronk J.T., 2004. Minimal metabolic engineering of *Saccharomyces cerevisiae* for efficient anaerobic xylose fermentation: a proof of principle. *FEMS Yeast Res.* 4(6), 655-664.

Lange H. C., 2002. Quantitative physiology of *S. cerevisiae* using Metabolic Network Analysis. PhD Thesis. Technical University of Delft.

Lee S.Y., Choi J.I., 2001. Production of microbial polyester by fermentation of recombinant microorganisms. *Adv Biochem Eng Biotechnol.* 71,183-207.

Murdock D., Ensley B.D., Serdar C., Thalen M., 1993. Construction of metabolic operons catalyzing the de novo biosynthesis of indigo in *Escherichia coli*. *Biotechnology.* 11(3), 381-386.

Nguyen H.T.T., Dieterich A., Athenstaedt K., Truong N.H., Stahl U., Nevoigta E., 2004. Engineering of *Saccharomyces cerevisiae* for the production of L-glycerol 3-phosphate, *Metab Eng.* 6, 155-163.

Nielsen J., 2001. Metabolic engineering. *Appl Microbiol Biotechnol.* 55(3), 263-283.

Nissen T.L., Kielland-Brandt M.C., Nielsen J., Villadsen J., 2000a. Optimization of ethanol production in *Saccharomyces cerevisiae* by metabolic engineering of the ammonium assimilation. *Metab Eng.* 2(1), 69-77.

Nissen T.L., Hamann C.W., Kielland-Brandt M.C., Nielsen J., Villadsen J., 2000b. Anaerobic and aerobic batch cultivations of *Saccharomyces cerevisiae* mutants impaired in glycerol synthesis. *Yeast.* 16(5), 463-474.

Novick A., Szilard L., 1950. Description of a chemostat. *Science.* 112, 715-716.

Onsager L., 1931. Reciprocal relations in irreversible processes. *Phys. Rev.* 37, 405-426.

Ostergaard S., Olsson L., Johnston M., Nielsen J., 2000. Increasing galactose consumption by *Saccharomyces cerevisiae* through metabolic engineering of the GAL gene regulatory network. *Nat Biotechnol.* 18(12), 1283-1286.

Patil K.R., Akesson M., Nielsen J., 2004. Use of genome-scale microbial models for metabolic engineering. *Curr Opin Biotechnol.* 15(1), 64-69.

Pedersen H., Christensen B., Hjort C., Nielsen J., 2000. Construction and characterization of an oxalic acid nonproducing Strain of *Aspergillus niger*. *Metab Eng.* 2, 34-41.

Penttila M. E., Andre L., Saloheimo M., Lehtovaara P., Knowles J. K., 1987. Expression of two *Trichoderma reesei* endoglucanases in the yeast *Saccharomyces cerevisiae*. *Yeast.* (3), 175-185.

Rizzi Manfred., Baltés Michael., Theobald Uwe., Reuss Matthias., 1997. In vivo analysis of metabolic dynamics in *Saccharomyces cerevisiae*: II. Mathematical model. Biotechnol Bioeng. 55 (4), 592-608.

Rojo F., Pieper D.H., Engesser K.H., Knackmuss H.J., Timmis K.N., 1987. Assemblage of ortho cleavage route for simultaneous degradation of chloro- and methylaromatics. Science. 238 (4832), 1395-1398.

Rønnow B., Olsson L., Nielsen J., Mikkelsen J.D., 1999. Derepression of galactose metabolism in melibiase producing baker's and distillers' yeast. J Biotechnol. 72, 213-228.

Rottenberg H., 1973. The thermodynamic description of enzyme-catalyzed reactions. The linear relation between the reaction rate and the affinity. Biophys. J. 13, 503-511.

Ruijter G.J.G. and Visser J., 1996. Determination of intermediary metabolites in *Aspergillus niger*. J Microbiol Methods. 25, 295-302.

Savageau M.A., 1976. Biochemical system analysis. Reading (MA): Addison-Wesley Publishing Company.

Schaefer U., Boos W., Takors R., Weuster-Botz D., 1999. Automated sampling device for monitoring intracellular metabolite dynamics. Anal Biochem. 270, 88-96.

Schmitz M., Hirsch E., Bongaerts J., Takors R., 2002. Pulse experiments as a prerequisite for the quantification of in vivo enzyme kinetics in aromatic amino acid pathway of *Escherichia coli*. Biotechnol Progr. 18, 935-941.

Small J.R., Kacser H., 1993. Response of metabolic systems to large changes in enzyme activities and effectors 2. The linear treatment of branched pathway and metabolite concentrations. assessment of the general non-linear case. Eur. J. Biochem. 213, 625-640.

Sonderegger M., Schumperli M., Sauer U., 2004. Metabolic engineering of a phosphoketolase pathway for pentose catabolism in *Saccharomyces cerevisiae*. Appl Environ Microbiol. 70(5), 2892-2897.

Stephanopoulos G.N., Aristidou A. A., Nielsen J., 1998, Metabolic Engineering, Principles and Methodologies, Academic Press, San Diego, USA

Tempest D.W., Neijssel O.M., 1981. Metabolic compromises involved in the growth of microorganisms in nutrient-limited (chemostat) environments. *Basic Life Sci.* 18, 335-356.

Teusink B., Passarge J., Reijenga C.A., Esgalhado E., van der Weijden C. C., Schepper M., Walsh M. C., Bakker B. M., van Dam K., Westerhoff H. V., Snoep J.L., 2000. Can yeast glycolysis be understood in terms of in vitro kinetics of the constituent enzymes? Testing biochemistry. *Eur J Biochem.* 267(17), 5313-5329

Theobald U., Mailinger W., Reuss M. and Rizzi M., 1993. In vivo analysis of glucose-induced fast changes in yeast adenine nucleotide pool applying a rapid sampling technique. *Anal Biochem.* 214, 31-37.

Theobald U., Mailinger W., Baltés M., Reuss M., Rizzi M., 1997. In vivo analysis of metabolic dynamics in *Saccharomyces cerevisiae*: I. Experimental observations. *Biotechnol Bioeng.* 55, 305-316.

Vallino J.J., Stephanopoulos G., 1993. Metabolic flux distributions in *Corynebacterium glutamicum* during growth and lysine overproduction. *Biotechnol. Bioeng.* 41, 633-646.

Van Dam J.C., Eman M.R., Frank J., Lange H.C., van Dedem G.W.K., Heijnen J.J., 2002. Analysis of glycolytic metabolites in *Saccharomyces cerevisiae* using anion exchange chromatography and electrospray ionisation with tandem mass spectrometric detection. *Anal Chim Acta.* 460, 209-218.

Van der Heijden R. T. J. M., Heijnen J. J., Hellinga C., Romein B., Luyben K. C. h. A. M., 1994. Linear constraint relations in biochemical reaction systems: II. Diagnosis and estimation of gross errors. *Biotechnol Bioeng.* 43, 11-20

van Gulik W.M., Heijnen J.J., 1995. A metabolic network stoichiometry analysis of microbial growth and product formation. *Biotechnol Bioeng.* 48, 681-698.

van Maris A.J., Geertman J.M., Vermeulen A., Groothuizen M.K., Winkler A.A., Piper M.D., van Dijken J.P., Pronk J.T., 2004. Directed evolution of pyruvate decarboxylase-negative *Saccharomyces cerevisiae*, yielding a C₂-independent, glucose-tolerant, and pyruvate-hyperproducing yeast. *Appl Environ Microbiol.* 70(1), 159-166.

van Winden W. A., 2002. ¹³C-labeling technique for metabolic network and flux analysis: theory and applications. PhD Thesis. Technische Universiteit Delft.

Vaseghi S., Baumeister A., Rizzi M., Reuss M., 1999. In vivo dynamics of the pentose phosphate pathway in *Saccharomyces cerevisiae*. *Metab Eng.* 1 (2), 128-140.

Visser D., van der Heijden R., Mauch K., Reuss M., Heijnen S., 2000. Tendency modeling: a new approach to obtain simplified kinetic models of metabolism applied to *Saccharomyces cerevisiae*. *Metab Eng.* 2(3), 252-275.

Visser Diana and Heijnen Joseph J. 2002. The Mathematics of Metabolic Control Analysis Revisited. *Metab Eng.* 4, 114-123

Visser D., van Zuylen G.A., van Dam J.C., Oudshoorn A., Eman M.R., Ras C., van Gulik W.M., Frank J., van Dedem G.W., Heijnen J.J., 2002. Rapid sampling for analysis of in vivo kinetics using the BioScope: a system for continuous pulse experiments. *Biotechnol Bioeng.* 79 (6), 674-681.

Visser D., Heijnen J.J., 2003. Dynamic simulation and metabolic re-design of a branched pathway using linlog kinetics. *Metab Eng.* 5(3), 164-176.

Visser Diana., van Zuylen Gertan. A., van Dam Jan C., Eman Michael R., Pröll Angela., Ras Cor., Wu Liang., van Gulik Walter. M., Heijnen Joseph. J., 2004. Analysis of in vivo kinetics of glycolysis in aerobic *Saccharomyces cerevisiae* by application of glucose and ethanol pulses. *Biotechnol Bioeng.* 88 (2), 157-167.

Visser D., Schmid J.W., Mauch K., Reuss M., Heijnen J.J., 2004. Optimal re-design of primary metabolism in *Escherichia coli* using linlog kinetics. *Metab Eng.* 6(4), 378-390.

Weibel K.E., Mor J.R., Fiechter A., 1974. Rapid sampling of yeast cells and automated assays of adenylate, citrate, pyruvate and glucose-6-phosphate pools. *Anal Biochem.* 58, 208-216.

Weichert C. Sauer U. and Bailey J.E., 1997. Use of a glycerol-limited, long-term chemostat for isolation of *Escherichia coli* mutants with improved physiological properties. *Microbiol.* 143, 1567-1574.

Westerhoff H. V., van Heeswijk W., Khahn D., Kell D. B., 1991. Quantitative approaches to the analysis of the control and regulation of microbial metabolism. *Antonie van Leeuwenhoek.* 60, 193-207.

Weusthuis R. A., Pronk J. T., van den Broek P. J. A, van Dijken J. P., 1994. Chemostat cultivation as a tool for studies on sugar transport in yeasts. *Microbiol Rev.* 58 (4), 616-630.

Wick M.L., Quadroni M. and Egli M., 2001. Short- and long-term changes in proteome composition and kinetic properties in a culture of *Escherichia coli* during transition from glucose-excess to glucose-limited growth conditions in continuous culture and vice versa. *Environ Microbiol.* 3(9), 588-599.

Wright B. E., Kelly P. J., 1981. Kinetic models of metabolism in intact cells, tissues, and organisms. *Curr Top Cell Regul.* 19, 103-158.

Wu L., Wang W., van Winden W.A., van Gulik W.M., Heijnen J.J., 2004. A new framework for the estimation of control parameters in metabolic pathways using lin-log kinetics. *Eur J Biochem.* 271(16), 3348-3359.

Critical evaluation of sampling techniques for residual glucose determination in carbon limited chemostat culture of *Saccharomyces cerevisiae*

Abstract

Three sampling techniques for rapid quenching of cellular metabolism and subsequent separation of cells from fermentation broth have been compared. The sampling techniques employed in this study were: (i) Quick freezing of fermentation broth directly in liquid nitrogen. (ii) Quenching metabolism by exposing the fermentation broth to stainless steel beads (4 mm diameter) in a filter syringe pre-cooled to $-18\text{ }^{\circ}\text{C}$. (iii) Withdrawal of the filtrate through a $0.45\text{ }\mu\text{m}$ filter attached to a syringe and a needle inserted directly into the fermentor. It was concluded that use of liquid nitrogen as a quenching method to rapidly arrest cellular metabolism, for quantitative analysis of extracellular glucose is not a very reliable method and that the filter syringe steel beads work very well.

This chapter has been published as: Mashego M. R., van Gulik W. M., Vinke J. L, and Heijnen J. J., 2003. Critical Evaluation of Sampling Techniques for Residual Glucose Determination in Carbon-Limited Chemostat Culture of *Saccharomyces cerevisiae*. *Biotechnol Bioeng.* 83 (4), 395-399.

Introduction

Study of microbial cellular metabolism and its regulation in vivo requires accurate information concerning both intracellular and extracellular metabolite pool levels. Experiments to elucidate the in vivo kinetic properties of metabolic pathways are often performed under highly dynamic conditions. Measurement of the dynamics of intracellular metabolite concentrations during such experiments requires rapid sampling followed by rapid quenching of metabolic activity and subsequent metabolite analysis (Theobald et al, 1997; Lange et al, 2001; Gonzalez et al, 1997; Theobald et al, 1993; Groussac et al, 2000; Hajjaj et al, 1998). Additionally also measurement of the dynamics of extracellular metabolite and/or substrate concentrations is indispensable in these studies on cellular metabolism. However, until now less attention has been paid to the development of reliable methods for rapid arrest of cellular metabolism for extracellular metabolite quantification.-

Usually carbon-limited chemostat cultures are employed in studying the in-vivo kinetic properties of the metabolism of *Saccharomyces cerevisiae*, where a pulse of substrate is added followed by rapid sampling of biomass at 3-5 seconds interval (Theobald et al, 1997). In the literature, several different methods have been described to arrest metabolism for measurement of the residual glucose concentration in glucose limited chemostat cultures of *S. cerevisiae* (Theobald et al 1993; Postma et al, 1989; Van Hoek et al, 1999). Theobald et al, 1993 used pre-cooled tubes containing 10-15 glass beads (diameter 4 mm) at -10°C for rapidly cooling broth and later used pre-cooled tubes filled with 10-15 stainless steel spheres (4mm diameter) -10°C for rapidly cooling the broth for extracellular compounds. The biomass and supernatant are separated by filtration; however, there was no mention of the final broth temperature (Theobald et al, 1997). Postma et al, 1989; Verduyn et al, 1992; Van Hoek et al, 1999 and Diderich et al, 1999 used fast sampling of the broth into liquid nitrogen, followed by thawing in ice with gentle shaking to keep the cell suspension at 0°C . The suspension was later centrifuged to separate biomass from the supernatant.

Until now, no experiments have been published to critically evaluate these different methods. In the present paper, three different methods for rapid arrest of cellular metabolism and/or separation of cells from the extracellular medium are compared:

- 1) Quick-freezing of broth in liquid nitrogen and subsequent thawing and separation of cells from the medium by centrifugation.
- 2) An alternative sampling method for rapid arrest of cellular metabolism employing rapid dropping of fermentation broth into a filter syringe containing pre-cooled stainless steel beads (4 mm diameter), immediately followed by separation of cells and medium by filtration through a $0.45\ \mu\text{m}$ pore size filter. It is a modification of the method reported by Theobald et al, 1997, since in the here presented case defined amount of stainless steel beads are contained in a syringe connected to a $0.45\ \mu\text{m}$ filter allowing immediate filtration of the sample to separate biomass from the filtrate.

3) Direct withdrawal of the extracellular medium from the fermentor via a needle connected to a syringe with 0.45 μm filter. It should be recognised that this method is for reference only, because it cannot be used practically in a pulse experiment where samples are withdrawn at 3-5 seconds interval.

Theory

In order to justify the use of cold stainless steel beads for rapid quenching of cellular metabolism during sampling, we first established the amount and initial temperature of beads required for cooling down a defined amount of broth. Hereby freezing of the yeast cells should be avoided to prevent contamination of the supernatant by the release of intracellular contents. Therefore, the desired final temperature of broth and beads was chosen to be 1°C. From a heat balance equation an expression can be derived for the final temperature, T_{bfinal} , as a function of the amounts and initial temperatures of sample and stainless steel beads (neglecting wall heat effects):

$$T_{\text{bfinal}} = \frac{(VC_p\rho T)^{\text{broth}} + (VC_p\rho T)^{\text{beads}}}{(VC_p\rho)^{\text{broth}} + (VC_p\rho)^{\text{beads}}} \quad (1)$$

where, V = volume; C_P = heat capacity; ρ = density; T = temperature. The amount of stainless steel beads was chosen such that for 5 ml of sample the beads were just covered by the fluid. This amount was found to equal 62 g. In Figure 1, the broth/beads final temperature is plotted as a function of the initial temperature of the beads.

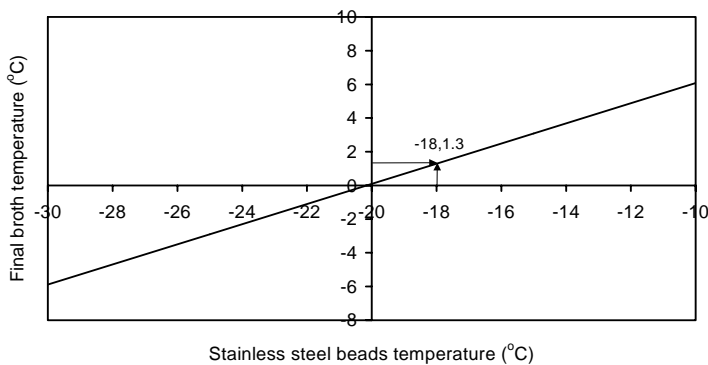


Figure 1 Calculated broth final temperature as a function of stainless steel beads temperature for 62 g stainless steel beads, 5 ml broth volume at 30 °C

Assuming a desired final temperature of 1°C, the initial temperature of the stainless steel beads is calculated to be -18 °C. To prevent clogging, it was chosen to use beads with a diameter of 4 mm. An important point is the time required to cool down the sample. This should be such that in the time between the withdrawal of sample and the separation of cells and extracellular medium no significant uptake of glucose occurs. To obtain an indication of the cooling time,

the time needed to decrease the broth temperature from 30 °C to 5 °C was estimated. The heat transfer from the liquid to the stainless steel beads is determined by the overall heat transfer coefficient (h), for which it holds that:

$$\frac{1}{h} = \frac{1}{h_{sp}} + \frac{1}{h_{liq}} \quad (2)$$

where h_{liq} is the heat transfer coefficient for the liquid phase.

The heat transfer coefficient, h_{sp} , for a sphere can be calculated from:

$$h_{sp} = \frac{k}{R} \quad (3)$$

where k is the thermal conductivity and R is the radius of the sphere. With $k = 0.046$ ($\text{kJ s}^{-1} \text{m}^{-1} \text{K}^{-1}$) for stainless steel it follows that for a stainless steel sphere with a radius of 2 mm the heat transfer coefficient h equals 24 ($\text{kJ s}^{-1} \text{m}^{-2} \text{K}^{-1}$).

The heat transfer coefficient for forced convection around a submerged sphere was calculated according to Bird et al (1960).

For this calculation the Nusselt number (Nu) for turbulent filling of the syringe containing the cold beads was estimated to be equal to 38 (equation 4 below).

$$\text{Nusselt number} = Nu = \frac{h_m D}{k_f} = 2.0 + 0.60 \left(\frac{D v \rho_f}{\mu_f} \right)^{1/2} \left(\frac{C_p \mu}{k} \right)_f^{1/3} \quad (4)$$

The corresponding heat transfer coefficient, h_{liq} , for the liquid phase was calculated to equal 5.7 ($\text{kJ s}^{-1} \text{m}^{-2} \text{K}^{-1}$) indicating that the heat resistance is mainly at the liquid side. Using Eq. (3), the overall heat transfer coefficient was calculated to be 4.6 ($\text{kJ s}^{-1} \text{m}^{-2} \text{K}^{-1}$). Subsequently a numerical simulation of the heat transfer from the 5 ml of broth to 62 g of stainless steel beads was carried out. The result is shown in Figure 2.

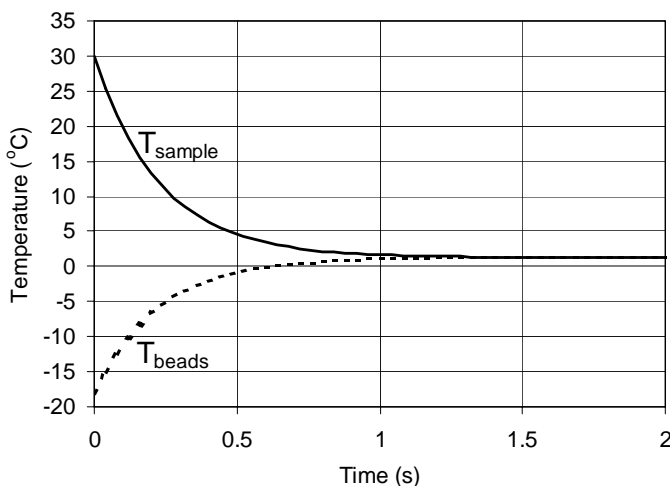


Figure 2 Simulated time profiles of the temperatures of the sample and the beads for 5 ml of sample with an initial temperature of 30 °C and 62 g beads with an initial temperature of -18 °C.

From this figure, it can be inferred that under these conditions cooling of the sample from 30°C to 5°C requires slightly less than 0.5 seconds. In case of a high-density chemostat culture (15 g.l⁻¹ biomass) of *S. cerevisiae*, assuming a Y_{sx} of 0.5 operated at a dilution rate of 0.05 h⁻¹, this would maximally result in the uptake of 0.2 mg of glucose, which is considered acceptable.

Materials and methods

Yeast strain and maintenance

Dr. P. Kötter (Frankfurt, Germany) kindly provided the haploid, prototrophic *Saccharomyces cerevisiae* strain CEN.PK113-7D. Precultures were grown to stationary phase in shake-flasks on mineral medium (Verduyn et al, 1992), adjusted to pH 6.0 and containing 2% (w/v) glucose. After adding glycerol (30%v/v), 2 ml aliquots were stored at -80°C in sterile vials. These frozen stocks were used to inoculate precultures for chemostat cultivation.

Chemostat cultivation

Aerobic glucose-limited chemostat cultures were cultivated at $D=0.05\text{h}^{-1}$ in 7l laboratory fermentors (Applikon, Schiedam, The Netherlands) (Lange et al, 2001). The biomass concentration obtained varied between 3-15 g.l⁻¹ by varying the feed glucose concentration.

Sampling procedure for glucose analysis

Three sampling procedures were investigated in this study: (i) Liquid nitrogen sampling involving direct quick-freezing of the sample in liquid nitrogen. The sample was collected via a side port directly into liquid nitrogen. Fermentor overpressure of 0.3 bars facilitated the broth outflow. Frozen clumps of broth approximately 10 ml were thawed in ice, followed by centrifugation in MSE, Hawk 15/05 bench-top refrigerated micro-centrifuge (Beun. De Ronde, LA, Abcoude, USA) at -6 °C, 11000 rpm for 5 minutes. (ii). Sampling of approximately 5 ml broth directly into a syringe containing stainless steel beads 62 g (4 mm diameter) pre-cooled at -18 °C. The sample did not freeze and was quickly (within seconds) filtered through 0.45 µm pore size filter, (Gelman, Ann Arbor, Michigan). (iii). Direct sampling from the fermentor via a needle (22 cm long, 1.4 mm diameter) and a 0.45 µm pore size filter; (Gelman, Michigan) using a syringe. The supernatant was analysed for residual glucose.

Residual glucose analysis

Glucose analysis was performed spectrophotometrically (Agilent 8453-UV-visible spectroscopy system, Waldbronn, Germany) using Boehringer Mannheim Enzymatic bioanalysis (kit no. 0716251) according to the manufacturer's instructions.

Results and Discussion

Initially, the liquid nitrogen sampling method was applied to arrest cellular metabolism of *S. cerevisiae* CEN.PK 113-7D prior to the determination of the residual glucose concentration in different glucose limited chemostats. The results are shown in Table I.

Table I. Residual glucose concentration obtained when liquid nitrogen was used to arrest cellular metabolism of *S. cerevisiae* CEN.PK 113-7D grown in chemostat under different feed glucose concentration.

Experiment	No of residence times at sample	Dilution rate (h ⁻¹)	Feed glucose (g.l ⁻¹)	Residual glucose (mg.l ⁻¹)	Biomass (g.l ⁻¹)
1	5	0.05	27.1	169±7	15.0±0.05
2A	4	0.05	13.6	115±7	7.5 ±0.05
2B	6	0.05	13.6	105±3	7.5±0.05
3	5	0.10	6.8	47±0.8	3.4±0.05

It can be seen from Table I that at a dilution rate of 0.05h⁻¹ (experiments 1, 2A and 2B) the measured residual glucose concentration ranges from 169 mg.l⁻¹ to 105 mg.l⁻¹ depending on the influent glucose concentration (or biomass concentration). It is expected that in glucose limited chemostat, an increase of the dilution rate should result in an increased residual glucose concentration. However, doubling of the dilution rate resulted in a lower residual glucose concentration (Table I, experiment 3). The only clear relation is an increase in residual glucose with biomass concentration and glucose feed concentration. However, the residual glucose concentration in carbon-limited chemostat cultures operated at the same dilution rate should be independent of the influent glucose concentration, assuming the endogenous metabolism and the death rate of the cells to be negligible. Furthermore, the measured concentrations appear to be significantly higher than the residual glucose concentrations at similar dilution rate reported in literature for *S. cerevisiae*, which are between 13- 30 mg.l⁻¹ (Theobald et al, 1993, Postma et al, 1989, Van Hoek et al, 1999). The above results triggered us to investigate the reliability of the liquid nitrogen sampling method for residual glucose concentration measurements, by comparing it with alternative sampling methods. Samples were taken from a standard low-density chemostat culture of *S. cerevisiae*, (biomass ≈3.4 g.l⁻¹) operated at a dilution rate of 0.1 h⁻¹. The results are shown in Table II. It can be seen from Table II that the measured residual glucose concentration in a steady state chemostat culture of *S. cerevisiae*

CEN.PK113-7D grown at a dilution rate $D = 0.1 \text{ h}^{-1}$ varied depending on the sampling technique employed.

Table II. Comparison of different sampling methods for residual glucose concentration measurements in a steady state chemostat culture of *S. cerevisiae* CEN.PK113-7D grown at specific growth rate $\mu = 0.1 \text{ h}^{-1}$ biomass concentration $\approx 3.4 \text{ g.l}^{-1}$.

No of residence times	Measured residual glucose concentration (mg.l^{-1})			Biomass (g.l^{-1})
	Liquid nitrogen	Direct filtration	Stainless steel beads	
14	31.2	16.5	16.2	3.4
15	32.6	15.4	14.3	3.4
Average	31.9 ± 0.7	16.0 ± 0.6	15.3 ± 0.95	3.4 ± 0.1

When sampling was carried out using liquid nitrogen an average of $31.9 \pm 0.6 \text{ mg.l}^{-1}$ residual glucose concentration was obtained (Table II). This value is lower than 47 mg.l^{-1} reported in Table I (experiment 3) above, under similar growth conditions. This significant drop is due to the phenomenon we have recently observed in our laboratory that residual glucose concentration tends to drop during prolonged chemostat cultivation of *S. cerevisiae* (unpublished data). This residual glucose concentration is in close agreement with that reported by Postma et al, 1989 for *S. cerevisiae* CBS 8066 of 27 mg.l^{-1} at $D = 0.1 \text{ h}^{-1}$ when liquid nitrogen quenching method was used. However, the two other methods resulted in measured residual glucose concentrations of approximately half the value obtained with the liquid nitrogen sampling method (see Table II). These results are an average of two samplings on different dates from the same culture. It should be mentioned here that direct filtration of the broth through a $0.45 \mu\text{m}$ pore size filter was meant as an independent check for the liquid nitrogen sampling method and the cold stainless steel beads method. It can be seen from Table II that the residual glucose concentration obtained with the direct filtration method, which is the best representative of the substrate concentration inside the fermentor because of the instantaneous separation of cells and surrounding medium, agrees well with the value obtained with the cold stainless steel beads method. It is concluded that the liquid nitrogen sampling technique results in residual glucose concentration that is more than double that obtained when using the other sampling techniques. Finally, to investigate the effect of high biomass density, residual glucose concentration measurements were performed in duplicate high-density chemostat cultures operated at a dilution rate of 0.05 h^{-1} . Sampling was performed with both the liquid nitrogen and stainless steel beads method. The results are shown in Table III.

It can be seen from this table, that the residual glucose concentration measured using the liquid nitrogen sampling technique is similar for both chemostat cultures and equals approximately 70 mg.l⁻¹. This value is approximately four times higher than the value measured using the stainless steel beads method. Also in low-density chemostats (Table II) it was observed that the residual glucose concentration measured using liquid nitrogen sampling was significantly higher than the value measured using the stainless steel beads method, although in this case they differ by a factor two. When the residual glucose concentrations measured with both methods are compared it appears that in case of the high-density chemostat (Table III) the difference (average 54 mg.l⁻¹) is approximately three times higher than in case of the low-density chemostat (Table II, average difference 17 mg.l⁻¹). This indicates that the magnitude of the overestimation of the residual glucose concentration with the liquid nitrogen sampling method is a function of the biomass concentration. A possible explanation for this overestimation might be the release of glucose monomers from trehalose, which forms part of the yeast storage carbohydrate pool and part of the cell wall. It has been observed previously (Lange et al, 2001) that when *S. cerevisiae* is grown at low dilution rates, the cells tend to accumulate relatively high amounts of storage carbohydrates in the form of trehalose and glycogen. Since our chemostat cultures were conducted at low dilution rates (0.05 h⁻¹), it is assumed that during sudden change in broth temperature when the cells are exposed to liquid nitrogen for instant freezing, temperature shock leads to cell wall/membrane leakage and yeast stress, hence glucose monomers can leak out, resulting in an increase of the extracellular glucose concentration in the culture supernatant. Therefore, the thus measured residual glucose concentration obtained from such samples is not representative of the steady state extracellular glucose concentration in the fermentor broth. For example, storage carbohydrates can easily be 5-10 % of cell dry weight, amounting to between 750-1500 mg.l⁻¹ carbohydrates in broth at 15 g.l⁻¹ cell dry weight. Hydrolysis of 5% would already lead to 37-75 mg.l⁻¹ of glucose, which seriously compromises the real extracellular glucose concentration of about 20 mg.l⁻¹.

Conclusions

From our observations, it is concluded that rapid quenching of cellular metabolism through quick freezing of fermentation broth in liquid nitrogen followed by thawing on ice and subsequent centrifugation is not a reliable method when applied for *S. cerevisiae* residual glucose measurements. The two other methods tested, i.e. (i) direct filtration and (ii) rapid cooling of broth using cold stainless steel beads followed by filtration appeared both suitable. Residual glucose measurements in samples obtained with these methods showed comparable and reproducible results in both low and high-density chemostat cultures. Stainless steel beads sampling method has also proved indispensable especially when rapid sampling and arrest/separation of cells are required when following the dynamics of substrate uptake rate in

the short sampling time frame of ≈ 200 seconds (Theobald et al, 1997). It can also be extended to follow dynamics of metabolites such as pyruvate and acetate that are excreted to the growth medium and are found intracellularly.

References

Bird R. B., Steward W. E. and Lightfoot E. N., 1960. Transport Phenomena. John Wiley & Sons. Inc.

Diderich J.A., Schepper M., van Hoek P., Luttik M.A.H., van Dijken J.P., Pronk J.T., Klaasen P., Boelens M.J., Teixeira de Mattos M.J., van Dam K. and Kruckeberg A.L., 1999. Glucose uptake kinetics and transcription of *HXT* genes in chemostat cultures of *Saccharomyces cerevisiae*. The Journal of Biological Chemistry. 274, 15350-15359.

Gonzalez B., Francois J., Renaud M., 1997. A Rapid and reliable method for metabolite extraction in yeast using boiling buffered ethanol. Yeast. 13, 1347-1356.

Groussac E., Ortiz M., François J., 2000. Improved protocols for qualitative determination of metabolites from biological samples using high performance ionic chromatography with conductimetric and pulsed amperometric detection. Enzyme Microb Technol. 26, 715-723.

Hajjaj H., Blanc P.J., Goma G., Francois J., 1998. Sampling techniques and comparative extraction procedures for quantitative determination of intra- and extracellular metabolites in filamentous fungi. FEMS Microbiol Lett. 164, 195-200.

Lange H.C., Eman M, van Zuijlen G., Visser D., van Dam J.C. Frank J., Teixeira de Mattos M.J., Heijnen J.J., 2001. Improved rapid sampling for in vivo kinetics of intracellular metabolites in *Saccharomyces cerevisiae*. Biotechnol Bioeng. 75 (4), 406-415.

Lange H. C., Heijnen J. J., 2001. Statistical reconciliation of the elemental and polymeric biomass composition of *Saccharomyces cerevisiae* Biotechnol Bioeng. 75 (3), 334-344.

Postma E., Scheffers W.A., van Dijken J.P., 1989. Kinetics of growth and glucose transport in glucose-limited chemostat cultures of *Saccharomyces cerevisiae* CBS 8066. Yeast. 5, 159-165.

Theobald U., Mailinger W., Reuss M., Rizzi M., 1993. In vivo analysis of glucose-induced fast changes in yeast adenine nucleotide pool applying a rapid sampling technique. Anal Biochem. 214, 31-37.

Theobald U., Mailinger W., Baltés M., Reuss M., Rizzi M. 1997. In vivo analysis of metabolic dynamics in *Saccharomyces cerevisiae*: I. Experimental Observations, *Biotechnol Bioeng.* 55, 305-316.

Van Hoek W.P.M., Diderich J.A., Schepper M., Luttik M.A.H., van Dijken J.P., Pronk J.T., Klaasen P., Boelens M.J., Teixeira de Mattos M.J., van Dam K., Kruckeberg A.L., 1999. Glucose uptake kinetics and transcription of *HXT* Genes in chemostat cultures of *Saccharomyces cerevisiae*. *J Biol Chem.* 64, 4226-4233

MIRACLE: Mass Isotopomer Ratio Analysis of U-¹³C-Labeled Extracts. A New Method for Accurate Quantification of Changes in Concentrations of Intracellular Metabolites

Abstract

The chapter reports the application of stable isotope dilution theory in metabolome characterisation of aerobic glucose limited chemostat culture of *S. cerevisiae* CEN.PK 113-7D using Liquid Chromatography-Electro Spray Ionisation MS/MS (LC-ESI-MS/MS). A glucose limited chemostat culture of *S. cerevisiae* was grown to steady state at a specific growth rate (μ) = 0.05 h⁻¹ in a medium containing only naturally labeled (99% U-¹²C, 1% U-¹³C) carbon source. Upon reaching steady state, defined as 5 volume changes, the culture medium was switched to chemically identical medium except that the carbon source was replaced with 100 % uniformly (U) ¹³C labeled stable carbon isotope, fed for 4h, with sampling every hour. We observed that within a period of 1 hour approximately 80 % of the measured glycolytic metabolites were U-¹³C labeled. Surprisingly, during the next 3 hours no significant increase of the U-¹³C labeled metabolites occurred. Secondly, we demonstrate for the first time the LC-ESI-MS/MS based quantification of intracellular metabolite concentrations using U-¹³C labeled metabolite extracts from chemostat cultivated *S. cerevisiae* cells, harvested after 4 hours of feeding with 100% U-¹³C labeled medium, as internal standard. This method is hereby termed 'Mass Isotopomer Ratio Analysis of U-¹³C Labeled Extracts' (MIRACLE). With this method each metabolite concentration is quantified relative to the concentration of its U-¹³C labeled equivalent, thereby eliminating drawbacks of LC-ESI-MS/MS analysis such as non-linear response and matrix effects and thus leads to a significant reduction of experimental error and work load (i.e. no spiking and standard additions). By co-extracting a known amount of U-¹³C labeled cells with the unlabeled samples, metabolite losses occurring during the sample extraction procedure, are corrected for.

This chapter has been published as: Mashego M. R., Wu L., Van Dam J. C., Ras C., Vinke J. L., Van Winden W. A., Van Gulik W. M., Heijnen J. J., 2004. MIRACLE: mass isotopomer ratio analysis of U-¹³C-labeled extracts. A new method for accurate quantification of changes in concentrations of intracellular metabolites. *Biotechnol Bioeng.* 85, 620-628.

Introduction

Rational metabolic engineering of industrial microorganisms requires knowledge of *in vivo* kinetic properties of the relevant metabolic pathways. This information is normally obtained from carefully designed stimulus response experiments in which the organism is cultured under substrate-limited conditions until a steady state is reached followed by a sudden disturbance, e.g. a sudden increase of the extracellular substrate concentration. Subsequently the fast dynamic changes of the intracellular metabolite concentrations resulting from the introduced perturbation are monitored (Buchholz et al, 2002; Buziol et al, 2002; Schmitz et al, 2002; Theobald et al, 1993; 1996; Visser et al, 2002). This requires fast sampling of cells and rapid inactivation of all metabolic activity. Weibel et al, 1974, reported a sampling technique for yeast cells with a very short time interval between harvesting and inactivation of the cells followed by extraction of intracellular metabolites. This method laid the foundation for quantitative analysis of the microbial metabolome. The method was further refined and automated by De Koning & Van Dam 1992; Gonzalez et al, 1997; Schaefer et al, 1999; Theobald et al, 1993; 1997; Visser et al, 2002.

The reliable quantification of intracellular metabolite concentrations is hindered by the low concentrations of these compounds in cells and is exacerbated by the dilution of the already low metabolite concentrations during the recovery steps. Furthermore, the complex cellular matrix might interfere with the analysis procedure applied. Enzymatic quantification of intracellular metabolites has been in the forefront of the analytical procedures used (Hajjaj et al, 1998; Ruijter & Visser, 1996; Theobald et al, 1993; 1997), however, the available small sample volumes limit the analysis to a few compounds per sample. The advent of high sensitivity LC-ESI/MS and LC-ESI-MS/MS instruments is broadening the range of techniques available for the quantification of intracellular metabolites as recently reported in *E. coli* and *S. cerevisiae* by Buchholz et al, 2001; 2002; Van Dam et al, 2002; and Castrillo et al, 2003 respectively. The advantage that has led to the increasing use of LC-ESI-MS/MS is its high sensitivity and small sample volumes (10 μ L) required for analysis with a detection limit in the 0.4-0.5pmol range (Van Dam et al, 2002). In addition, the fact that most of the metabolites from central carbon metabolism, i.e. glycolysis, tricarboxylic acid (TCA) cycle and pentose phosphate pathway (PPP), can be analysed in a single injection of 10 μ L sample volume is fuelling the popularity of these instruments (Van Winden, 2002).

It should be mentioned that although the LC-ESI-MS/MS analytical technique is powerful, it still has some drawbacks such as a non-linear response due to ion suppression in the electrospray ionisation, originating from high salt/organic compounds concentration in the eluents, leading to non-linear calibration curves (Shi, 2003). Another drawback is the influence of the sample matrix associated with different microbial cultures on the measurements, for which reason an LC-ESI-MS/MS protocol developed for analysing metabolites in samples derived from *Saccharomyces* cultures cannot be used without validation for the analysis of the same

metabolites in samples derived from *Penicillium*, as we have recently noticed in our laboratory. This requires validation through extensive standard addition and calibration procedures. In addition, metabolite recoveries in the extraction procedure require checking via laborious standard addition experiments for each metabolite of interest.

The above-mentioned drawbacks of the LC-ESI-MS/MS analysis technique for intracellular metabolites could be overcome by introduction of an internal standard for each compound of interest. Shi, (2003) recently demonstrated that by using chromatographically co-eluting structural analogues as internal standards the dynamic linear range of the LC-ESI-MS could be expanded. Freisleben et al, 2003 used stable isotope dilution assays for the quantification of the folate vitamers in food samples by using deuterated isotopomers as internal standards in LC-ESI-MS/MS. As they have argued, internal standards should mimic the analysed compounds as much as possible. A U-¹³C labeled isotopomer of a given compound is therefore a very suitable candidate for use as an internal standard in LC-ESI-MS/MS analysis. It should however, be realised that the commercial availability of these U-¹³C labeled equivalents of the metabolites of the central carbon metabolism is very limited. An appropriate way to obtain these U-¹³C labeled equivalents is *in vivo* synthesis using proper (i.e. containing all metabolites of interest) microorganisms cultivated on U-¹³C labeled substrates. By adding known amounts of U-¹³C labeled cells to unlabeled cell samples prior to the extraction procedure, these can serve as a source of U-¹³C labeled internal standards for all intracellular metabolites to be quantified.

In this paper, we report a novel method for *S. cerevisiae* metabolome characterisation based on the stable isotope dilution theory (De Leenheer and Thienpont, 1992; Griffin et al, 2001). This theory states that the relative signal intensity in a mass spectrometer (MS) of two analytes that are chemically identical but of different stable isotope composition, distinguishable in a mass analyser, are a true representation of the relative abundance of the two analytes in a sample (De Leenheer and Thienpont, 1992; Griffin et al, 2001). The theory is routinely applied in isotope-code affinity tag (ICAT) approach for proteomics studies to quantify relative abundance of proteins in biological samples (Govorun and Archakov, 2002; Griffin et al, 2001; Gygi et al, 1999; Ideker et al, 2001; Nyman, 2001).

As a proof of principle, we here present the application of the above method. We exploited the mass to charge (m/z) difference in an Electro Spray Ionisation Tandem Mass Spectrometer (LC-ESI-MS/MS) to determine the ratio of abundance (relative quantities) of unlabeled to uniformly U-¹³C labeled intracellular glycolytic pathway metabolites in steady state chemostat grown *S. cerevisiae* cultures (Van Dam et al, 2002; Van Winden, 2002). Firstly, the replacement of unlabeled metabolites by their U-¹³C labeled equivalents after the switch to medium containing 100% U-¹³C labeled carbon source was followed. Secondly, fixed amounts of U-¹³C labeled cells were added to unlabeled cell samples before metabolite extraction to serve as internal standard. This was done with the purpose to quantify in a more accurate way 1) steady

state metabolite levels and 2) dynamic (0-60 seconds time window) metabolite levels as a response to a glucose perturbation, in an unlabeled chemostat culture of *S. cerevisiae*.

Material and Methods

Yeast strain and maintenance

The haploid, prototrophic *Saccharomyces cerevisiae* strain CEN.PK113-7D was kindly provided by Dr. P. Kötter (Frankfurt, Germany). Precultures were grown to stationary phase in shake-flasks on mineral medium (Verduyn et al, 1992), adjusted to pH 6.0 and containing 2% (w/v) glucose. After adding glycerol (30% v/v), 2 ml aliquots were stored at -80°C in sterile vials. These frozen stocks were used to inoculate precultures for chemostat cultivation.

Chemostat cultivation

Aerobic glucose-limited chemostat cultures were carried out at a dilution rate (D) of 0.05 h^{-1} in 7l laboratory fermentors (Applikon, Schiedam, The Netherlands) with a 4l working volume (Lange et al, 2001). Two chemostats (A and B) were simultaneously inoculated with overnight grown shake flask cultures of *S. cerevisiae* CEN.PK 113-7D. When the cultures of both chemostats reached 22 generations (i.e. approximately 336 h), the medium feed of chemostat B was switched to the $\text{U-}^{13}\text{C}$ labeled medium described below. Chemostat B was fed with this medium for a period of 4 h. During the $\text{U-}^{13}\text{C}$ labeled feeding period the air supply to chemostat B was passed through columns containing silica and NaOH connected in series respectively, to remove the air moisture and all ($\text{U-}^{12}\text{C}$) CO_2 that would introduce $\text{U-}^{12}\text{C}$ carbon in the metabolites due to the carboxylation reactions.

Medium composition

The molar composition of the unlabeled feed medium used for chemostat A and B has been described previously (Lange et al, 2001). This medium contains a mixed carbon source of 150mM glucose and 31mM ethanol. The addition of ethanol successfully prevented the cultures from oscillations. The molar composition of the $\text{U-}^{13}\text{C}$ labeled feed medium for chemostat B was identical to that of chemostat A except that the carbon sources (glucose and ethanol) were replaced by uniformly ^{13}C labeled glucose and uniformly ^{13}C labeled ethanol (CAS 492-62-6, CAS 70753-79-6 Cambridge Isotope Laboratory Inc., Andover, MA). The biomass concentration supported by this medium composition is approximately 14.5gDW.l^{-1} .

Rapid sampling and quenching

Rapid sampling was performed with an automated sampling system with minimal dead volume (Lange et al, 2001). With this system, 1 ml (± 0.05) of broth was withdrawn from the fermentor in approximately 0.7 seconds and injected directly into 5 ml of 60% (v/v) methanol/water at -40

°C for immediate quenching of metabolic activity. The exact amounts of broth withdrawn were quantified by weighing the sample tubes before and after sampling.

Metabolite extraction

The quenched samples were centrifuged for 5 minutes in a cooled (-20 °C) centrifuge (Heraeus Biofuge stratos, Heraeus Instruments, GmbH, Germany) at 2000g. The rotor was pre-cooled at -40 °C to prevent warming-up of the samples to temperatures above -20 °C. After decanting, the cell pellet was resuspended in 5 ml of 60 % (v/v) methanol/water solution (-40 °C) and again centrifuged for 5 minutes. This additional washing step served to effectively remove extracellular components. The supernatant was decanted and the intracellular metabolites were extracted from the remaining pellet using boiling ethanol (based on Gonzales et al, 1997). According to this method, 5 ml of boiling ethanol solution (75 % v/v ethanol/water) was added to the pellet; the tube was vortexed for a few seconds to resuspend the pellet and placed into a hot water bath at 95 °C for a period of 3 minutes. Immediately thereafter, the tubes with the ethanol extracts were cooled down to -40 °C in a cryostat. The ethanol extracts were evaporated to dryness in a Rapid-Vap (Labconco Corporation, Kansas City, MO, USA) for 110 minutes under controlled vacuum and temperature. The dried residue was dissolved in 500 µl Milli-Q water and centrifuged for 5 minutes at 3000 g (Heraeus Biofuge stratos, Heraeus Instruments, GmbH, Germany). The resulting extract was stored at -80 °C until analysis (Fig 1).

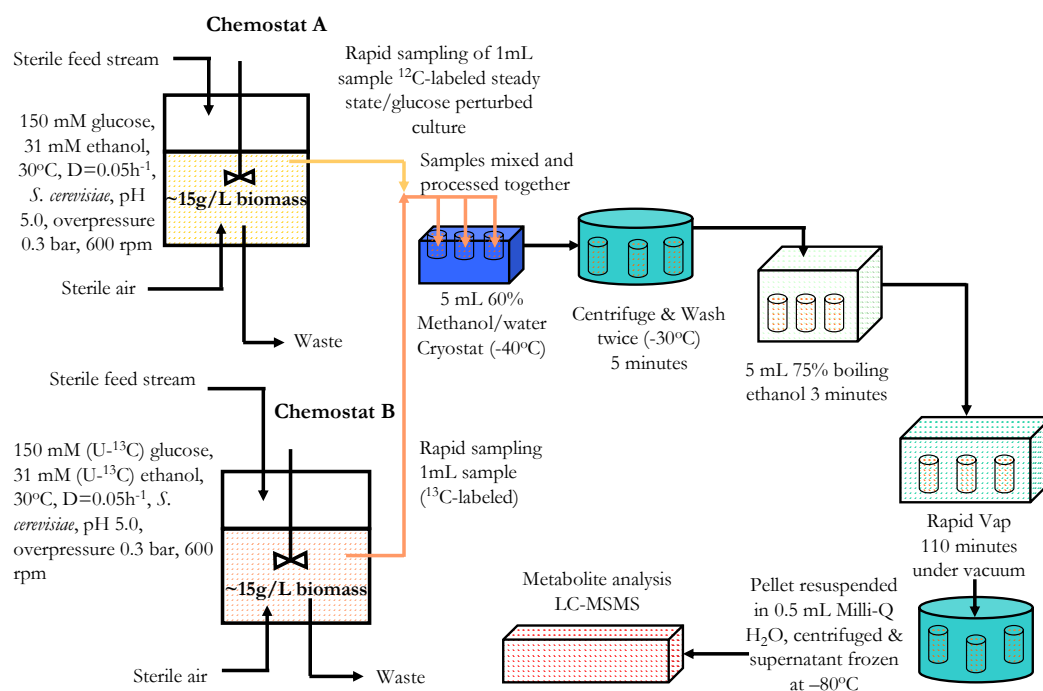


Figure 1 Schematic flow sheet representation of the experimental protocol

U-¹³C Labelling and co-extraction of labeled and non-labeled biomass

During the 4 hours feeding period of chemostat B with U-¹³C labeled medium, rapid sampling was performed at an hourly interval to follow the replacement of the unlabeled intracellular metabolites by their U-¹³C labeled equivalents.

After 4 h of U-¹³C labeled feeding, rapid sampling was performed to withdraw 40 samples of 1 ml each from chemostat B within a period of 10 minutes. Each sample was directly quenched in 5 ml of 60 % (v/v) methanol/water solution at -40 °C. The quenched samples were weighed and thereafter centrifuged for 5 minutes at 2000 g in a cold centrifuge as described above. After resuspension of the pellets in 5ml of 60 % (v/v) methanol/water (-40 °C), they were kept at -40 °C in a cryostat to be used as quenching medium for subsequent sampling from the unlabeled chemostat A. After the second sampling, the tubes were weighed again to determine the exact amounts of sample withdrawn from unlabeled chemostat A. The combined biomass samples were processed according to the procedure described under "metabolite extraction".

Steady state sampling and pulse response experiment

Using the rapid sampling procedure, 8 steady state samples were taken from unlabeled chemostat A and directly quenched in the tubes containing the U-¹³C labeled sample pellets from chemostat B, suspended in 5ml 60 % (v/v) methanol/water solution at -40 °C. Further processing of the samples was performed according to the method described under "metabolite extraction". Subsequently, chemostat A was perturbed by a sudden increase of the extracellular glucose concentration to 0.5 g.l⁻¹. A second series of 16 samples was taken from chemostat A during a period of 60 seconds after the stepwise increase of the extracellular glucose concentration. The sampling and metabolite extraction procedures were the same as for the steady state samples.

LC-ESI-MS/MS analysis of mass isotopomer ratios

The LC-ESI-MS/MS method for quantification of the glycolytic intermediates in *S. cerevisiae* has been described previously (Van Dam et al, 2002). The analysis of mass isotopomer ratios of intracellular metabolites was performed as described in Van Winden (2002).

The replacement of the unlabeled intracellular metabolites by their U-¹³C labeled equivalents was followed by determining the U-¹²C fraction of each metabolite as the ratio between the peak area corresponding with mass M+0 (i.e. U-¹²C) and the sum of the peak areas corresponding with the masses M+0 and M+N (i.e. sum U-¹²C and U-¹³C), where M is the (U-¹²C) molecular mass and N is the number of carbon atoms of the molecule. Each ratio was determined from duplicate samples analysed at least in triplicate. (Note that a fraction of the metabolites may have intermediary masses (M+l, where l<N) during the isotope replacement). However, this occurrence has no effect on the presented results. The peak area ratios (U-¹²C/U-

^{13}C labeled) of glycolytic metabolites in the combined biomass samples are determined as the ratios of peak areas corresponding with masses $M+0$ and $M+N$.

Results and Discussion

Replacement of $\text{U-}^{12}\text{C}$ with $\text{U-}^{13}\text{C}$ labeled glycolytic metabolites

Figure 2 represents the *in vivo* replacement time profile of the unlabeled glycolytic pathway intermediates by their $\text{U-}^{13}\text{C}$ labeled equivalents in *S. cerevisiae* after switching from unlabeled medium feed to a 100% $\text{U-}^{13}\text{C}$ labeled medium feed. Based on the literature data of intracellular metabolite pool sizes and reaction rates it was estimated that more than 97% of the metabolite pools would be replaced with $\text{U-}^{13}\text{C}$ labeled metabolites within 4h following the medium switch to $\text{U-}^{13}\text{C}$ labeled substrate (Theobald et al, 1997; Visser et al, 2002), hence the $\text{U-}^{13}\text{C}$ labeled medium was fed for this duration.

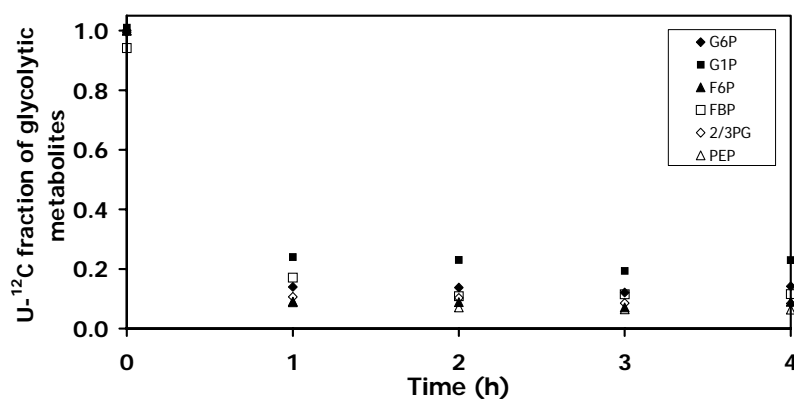


Figure 2 $\text{U-}^{12}\text{C}$ metabolite replacement profiles of glycolytic metabolites after medium switch from unlabeled to uniformly ^{13}C labeled carbon source

As Figure 2 shows, over 80% of the glycolytic metabolites are replaced by $\text{U-}^{13}\text{C}$ labeled equivalents in the first 1h, after which there seems to be an isotopic steady state. It can be inferred from Figure 2 that a much longer feeding time with $\text{U-}^{13}\text{C}$ labeled mixture of glucose and ethanol is required for complete isotopic replacement. The observed incomplete replacement of the unlabeled metabolites in central carbon metabolism was initially not expected. It is speculated that the fractions of unlabeled metabolite that remain do originate from mobilised unlabeled storage sugars such as glycogen and trehalose, which are subjected to continuous turnover (Francois and Parrou, 2001). It is known that *S. cerevisiae* accumulates storage carbohydrates, i.e. glycogen and trehalose under carbon-limited conditions. Moreover, the intracellular concentration of storage carbohydrates has been reported to increase with decreasing growth rates (Paalman et al., 2003, Sillje et al., 1999). Under the cultivation conditions we applied, the amount of storage material is approx. 10% of the biomass dry weight. The $\text{U-}^{13}\text{C}$ labeled glucose taken up by the cells will initially result in a fast replacement of unlabeled glucose-6-P by $\text{U-}^{13}\text{C}$ labeled glucose-6-P. However, a slow turnover

of storage carbohydrates (that are initially still fully unlabeled and of which the time to reach 100% U-¹³C labelling is much longer due to its size) causes the formation of some U-¹²C-labeled G6P (via the G1P intermediate). Therefore, 100% U-¹³C labelling of both the glucose-1-P and glucose 6-phosphate pool may take as much time as complete labelling of the storage carbohydrate pool. If it is assumed that 10 % of the glucose fed passes at least one time through the storage pool it can be calculated that it takes 30 hours to reach 95 % U-¹³C labelling of glucose-6-P. The fact that glucose-1-phosphate (G1P), which forms a connection between the glycolysis and the storage sugar metabolism, shows the slowest isotopic replacement (see Figure 2) supports this hypothesis. It was further observed that the replacement of unlabeled by U-¹³C labeled TCA cycle metabolites took even longer time and after 4 h, a significant fraction of these metabolites was still unlabeled (data not shown). The observed slow replacement profile can be explained partially by the complexity of the lower part of central carbon metabolism in *S. cerevisiae* especially, when considering the exchanges occurring between TCA cycle metabolites such as α -ketoglutarate and large pools of e.g. glutamate. The graphs in Figure 3 show ten measurements of the isotope replacement in the glycolytic intermediates G6P and PEP one hour after switching the unlabeled fermentor to 100 % U-¹³C labeled mixture of ethanol and glucose medium. The graphs show the areas of the M+0 peaks (corresponding to the U-¹²C metabolite) versus the summed areas of the M+0 and M+N peaks (corresponding to the U-¹²C plus U-¹³C metabolite) of the glycolytic intermediates G6P and PEP.

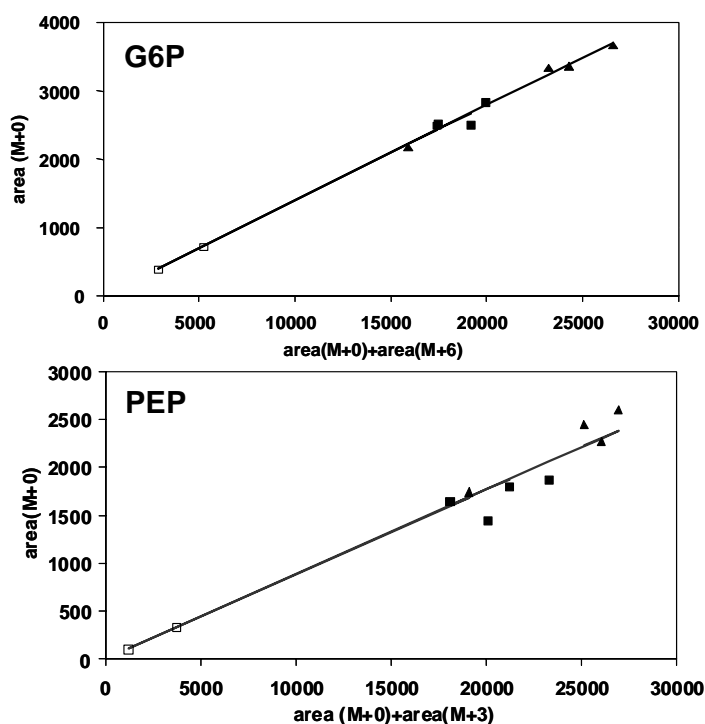


Figure 3 The areas of the M+0 peaks versus the summed areas of the M+0 and M+N peaks (N=6 for G6P; N=3 for PEP) after one hour of U-¹³C labeled medium feeding. ▲: sample 1, ■: sample 2A, □: sample 2B (after failure of ion suppressor). The straight line in the graphs denotes the constant fraction line, having a slope of 0.14 for G6P and 0.09 for PEP.

The presented data are four analyses of sample 1 and six analyses of sample 2 (where the two samples are duplicates). During the analysis, the ion suppressor failed which resulted in an incomplete removal of the sodium ions in the eluate of the LC. This led to an increase of the ion suppression in the LC-MS interface, which gave decreasing peak areas (especially visible for the data of sample 2B in Figure 3). It can be seen that although the absolute areas are strongly varying due to the reasons mentioned above, the ratios are remarkably close to the 'constant fraction' lines in both graphs. This proves the MIRACLE principle: the relative amounts of the unlabeled and fully labeled compounds are much less sensitive to experimental conditions than their absolute amounts.

Comparison of U-¹²C/U-¹³C peak area ratios and absolute concentrations of glycolytic metabolites for the co-extracted samples

Table I presents the average U-¹²C/U-¹³C peak area ratios and absolute concentrations during steady state cultivation of the glycolytic metabolites in the combined and co-extracted samples from chemostat A (unlabeled) and chemostat B (after 4 h of feeding with U-¹³C labeled carbon source).

Table I. Average U-¹²C/U-¹³C peak area ratios and absolute concentrations for all measured glycolytic pathway metabolites in *Saccharomyces cerevisiae* CEN.PK 113-7D

Compound	U- ¹² C/U- ¹³ C- peak area ratio (-)	Relative standard deviation (%)	U- ¹² C metabolite concentration ($\mu\text{mol/gDW}$)	Relative standard deviation (%)
G6P	2.15	6.8	2.81	11.9
F6P	2.23	8.4	0.59	14.5
G1P	2.76	12.0	0.61	13.6
F1, 6BP	1.06	11.4	0.48	12.3
2/3PG	1.73	8.8	1.40	10.7
PEP	1.51	5.7	1.46	10.2

The procedure of using the U-¹²C/U-¹³C peak area ratios is based on the assumption that there are no co-eluting compounds with the same molecular weight (MW), the same fragmentation pattern and the same number of U-¹²C atoms. To verify this, we checked the retention times of all the known isomers and found no co-eluting compounds except for glucose-1-P, which is co-eluting with mannose-1-P. Both compounds have the same fragments, but due to the different intensities of the fragments, it is possible to distinguish between the two (Van Dam et al, 2002).

Absolute concentrations were obtained according to van Dam et al, 2002. Because the intracellular metabolite pools were not completely U-¹³C labeled after 4 hours feeding period with 100% U-¹³C labeled substrate, the peak area ratios presented are corrected for the carry-

over of unlabeled metabolite from the samples of chemostat B. This carry over was determined for each compound as an average from eight separate steady state samples analysed in triplicate. Correction for U-¹²C carry-over was done by subtracting the average peak area corresponding to unlabeled metabolite per millilitre sample of chemostat B, from the total peak area corresponding to unlabeled metabolite measured in the combined samples prior to calculation of the U-¹²C/U-¹³C peak area ratios.

It can be seen from Table I that the standard deviations of the U-¹²C/U-¹³C peak area ratios are below 10 %, except for G1P and F1, 6BP, whereas those of the absolute concentrations are all above 10 %. This demonstrates that the relative quantification of metabolite concentration based on the peak area ratios of U-¹²C/U-¹³C is more accurate when compared to the absolute measured metabolite concentration, which proves that the MIRACLE principle works.

MIRACLE principle applied to a perturbed steady state *S. cerevisiae* culture

We subsequently applied the MIRACLE principle to a glucose perturbed chemostat culture of *S. cerevisiae*, in which we followed the dynamic response of the U-¹²C/U-¹³C peak area ratios of the glycolytic metabolites over a period of 60 seconds. The peak area ratios are measured in samples from the steady state and during the perturbation. The change in the U-¹²C/U-¹³C peak area ratio (perturbation sample relative to steady state sample) corresponds to the change in metabolite concentration (C/C^0), perturbation relative to steady state concentration. The results are depicted in Figures 4 to 6 and show the calculated concentrations of unlabeled glycolytic metabolites relative to their steady state values (C/C^0). It can be seen from these Figures that during the first 60 seconds following the glucose perturbation there is a steady increase in intracellular glucose-6-phosphate (G6P), fructose-6-phosphate (F6P), glucose-1-phosphate (G1P) and fructose-1, 6-bisphosphate (F1, 6BP). On the contrary, the lower glycolytic pathway metabolites, i.e. 2/3-phosphoglycerate (2PG/3PG), phosphoenolpyruvate (PEP) sharply decrease following the glucose pulse. Pyruvate sharply increases in the first 8 seconds after the perturbation, followed by a steady decrease to the initial steady state level after 50 seconds. The dynamic behaviour of these glycolytic metabolites is very well comparable to those observed by other researchers (Buziol et al, 2002; Theobald et al, 1997; and Visser et al, 2002), following a glucose pulse to aerobic carbon limited chemostat cultures of *S. cerevisiae*.

What is of significance in the work presented here is that the uniformly ¹³C labeled steady state samples/metabolites are co-extracted with the samples from the perturbed cultures, providing a U-¹³C labeled internal standard for each metabolite. Quantification of metabolite levels relative to their U-¹³C labeled equivalent, effectively eliminates the non-linear response of the electro spray ionisation (ESI) of the mass spectrometer because the peak area ratio of the U-¹²C labeled compound to its U-¹³C labeled equivalent co-eluting in the LC is not affected by the ion suppression phenomena associated with LC-ESI-MS/MS. A second advantage is that when these known amounts of uniformly ¹³C labeled internal standards are added prior to the

extraction procedure, also partial loss of metabolites during extraction is corrected for. Compared to the traditional approach, which requires spiking and standard addition for each metabolite (Van Dam et al, 2002); this U-¹³C internal standard method (MIRACLE) in principle provides more accurate metabolome data with much less work (no spiking and standard addition, etc.). Table I shows that the standard deviations of the U-¹²C/U-¹³C peak area ratios are clearly better in this experimental set-up. In the work reported here, U-¹³C labeled cells of which the metabolites were not 100 % U-¹³C labeled were used in the co-extraction with unlabeled cells. A further improvement in accuracy is therefore achievable by using 100 % U-¹³C labeled metabolites. These metabolites can be obtained by growing cells on U-¹³C substrates during the entire cultivation period. Currently these aspects are being pursued in our laboratory.

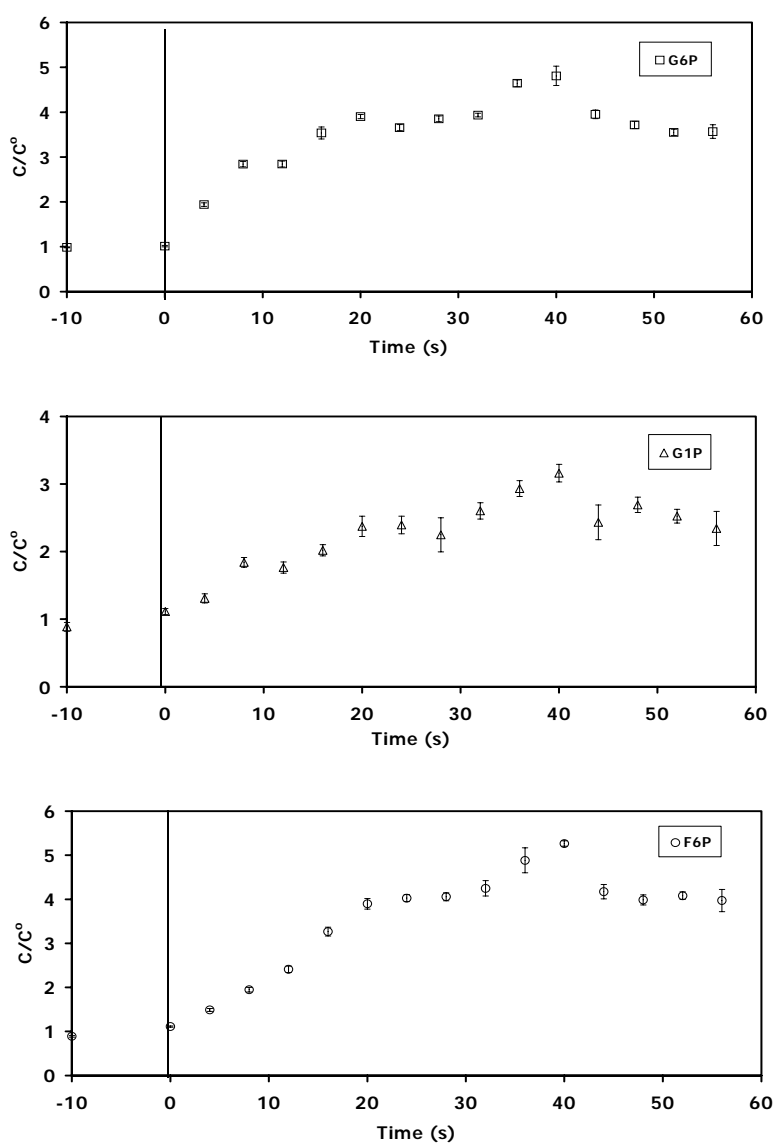


Figure 4 Changes in glucose-6-phosphate, fructose-6-phosphate and glucose-1-phosphate levels relative to the steady state values during a glucose perturbation experiment in an aerobic glucose limited chemostat of *S. cerevisiae* (Co is the average of the two steady state data points: t=0 and t=-10)

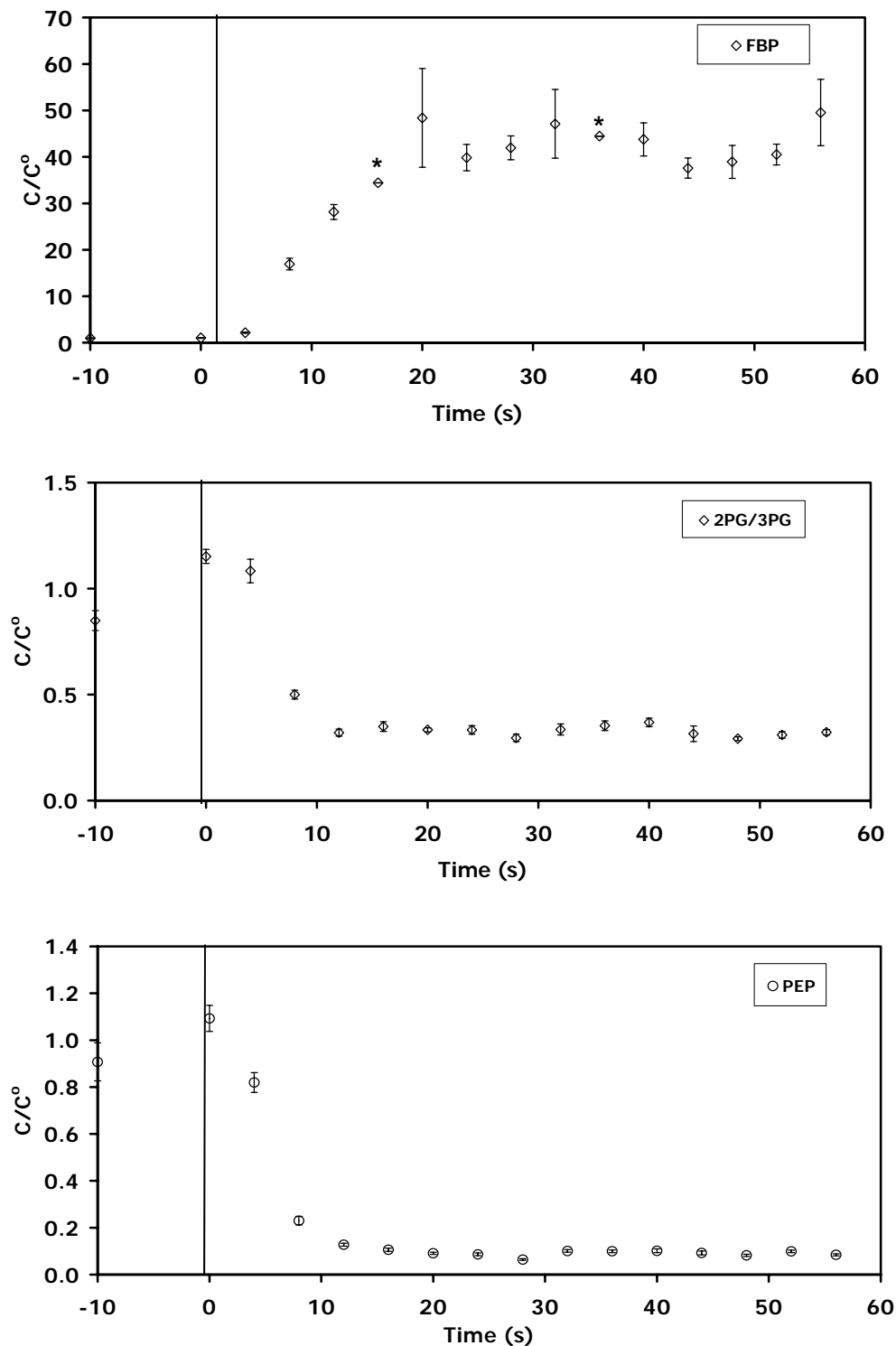


Figure 5 Changes in fructose-1, 6-bisphosphate, 2/3-phosphoglycerate and phosphoenolpyruvate levels relative to the steady state values during a glucose perturbation experiment in an aerobic glucose limited chemostat of *S. cerevisiae* (C_0 is the average of the two steady state data points: $t=0$ and $t=-10$). * On two data points of fructose -1, 6 -bisphosphate graph represents single measurement

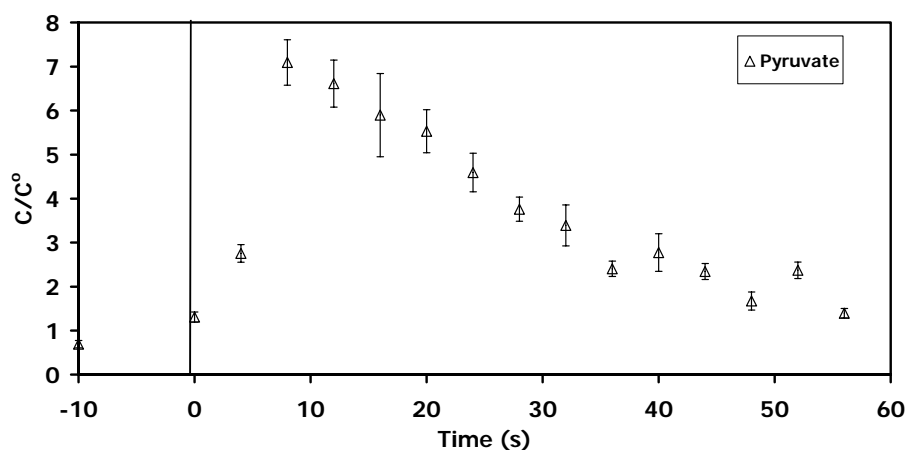


Figure 6 Change in pyruvate level relative to the steady state values during a glucose perturbation experiment in an aerobic glucose limited chemostat of *S. cerevisiae* (C_0 is the average of the two steady state data points: $t=0$ and $t=-10$)

Conclusions

A proof of principle has been presented of the quantification of intracellular metabolites by using $U\text{-}^{13}\text{C}$ labeled equivalents as internal standards (MIRACLE). In the presented results, we had to correct for the observed incomplete isotopic replacement after 4 h of $U\text{-}^{13}\text{C}$ labeled substrate feeding. Ideally, the metabolite extract that is used as an internal standard mixture should be 100 % $U\text{-}^{13}\text{C}$ labeled, which will lead to significant lower standard deviation in measured metabolite changes.

Based on the results (Table I), the MIRACLE principle is shown to be a powerful and robust innovation to date for reliable quantification of concentration changes in intracellular metabolites. Significant advantages of this method are elimination of the non-linear MS response, much less work (no spiking and standard additions needed), small sample volumes of 10 μl , high accuracy of the LC-ESI-MS/MS and much higher accuracy compared to traditional methods. This method has great potential for accurate quantification of changes in intracellular metabolite concentrations.

References

Bailey J.E., 1991. Towards a science of metabolic engineering. *Science*. 252, 1668-1675.

Buchholz A., Takors R., Wandrey C., 2001. Quantification of intracellular metabolites in *Escherichia coli* K12 using liquid chromatographic-electrospray ionization tandem mass spectrometric techniques. *Anal Biochem*. 295, 129-137.

Buchholz A., Hurlebaus J., Wandrey C., Takors R., 2002. Metabolomics: Quantification of intracellular metabolite dynamics. *Biomol Eng.* 19, 5-15.

Buziol S., Bashir I., Baumeister A., Claassen W., Noisommit-Rizzi N., Mailinger W., Reuss M., 2002. New bioreactor-coupled rapid stopped flow sampling technique for measurements of metabolite dynamics on a sub-second time scale. *Biotechnol Bioeng.* 80(6), 632-636.

Castrillo J.I., Hayes A., Mohammed S., Gaskell S.J., Oliver S.G., 2003. An optimised protocol for metabolome analysis in yeast using direct infusion electrospray mass spectrometry. *Phytochemistry.* 62, 929-937.

De Koning W., Van Dam K., 1992. A Method for the determination of changes of glycolytic metabolites in yeast on a sub-second time scale using extraction at neutral pH. *Anal Biochem.* 204, 118-123.

De Leenheer A.P., Thienpont L.M., 1992. Applications of isotope dilution-mass spectrometry in clinical chemistry, pharmacokinetics & toxicology. *Mass Spectrom Rev.* 11, 249-307.

Freisleben A., Schieberle P., Rychlik M., 2003. Specific and sensitive quantification of folate vitamers in foods by stable isotope dilution assays using high-performance liquid chromatography-tandem mass spectrometry. *Anal Bioanal Chem.* 376, 149-156.

Gonzalez B., Francois J., Renaud M., 1997. A rapid and reliable method for metabolite extraction in yeast using boiling buffered ethanol. *Yeast.* 13, 1347-1356.

Govorun V.M., Archakov A.I., 2002. Proteomic technologies in modern biomedical science. *Biochemistry (Mosc).* 67 (10), 1341-1359.

Griffin T.J., Aebersold R., 2001. Advances in proteome analysis by mass spectrometry, *J Biol Chem.* 276 (49), 45497-45500.

Gygi S.P., Rist B., Gerber S.A., Turecek F., Gelb M.H., Aebersold R., 1999. Quantitative analysis of complex protein mixtures using isotope-coded affinity tags. *Nat Biotechnol.* 17, 994-999.

Hajjaj H., Blanc P. J., Goma G., François J., 1998. Sampling techniques and comparative extraction procedures for quantitative determination of intra- and extracellular metabolites in filamentous fungi. *FEMS Microbiol Lett.* 164, 195-200.

Ideker T., Thorsson V., Ranish J.A., Christmas R., Buhler J., Eng J.K., Bumgarner R., Goodlett D.R., Aebersold R., Hood L., 2001. Integrated genomic and proteomic analyses of a systematically perturbed metabolic network. *Science*. 292, 929-934.

Lange H.C., Eman M., van Zuijlen G., Visser D., van Dam J.C. Frank J., Teixeira de Mattos M.J., Heijnen J.J., 2001. Improved rapid sampling for in vivo kinetics of intracellular metabolites in *Saccharomyces cerevisiae*. *Biotechnol Bioeng.*, 75 (4), 406-415.

Nyman T.A., 2001. The role of mass spectrometry in proteome studies. *Biomol Eng.* 18, 221-227.

Paalman J.W.G., Verwaal R., Slofstra S.H., Verkleij A.J., Boonstra J., Verrips C.T., 2003. Trehalose and glycogen accumulation is related to the duration of the G1 phase in *Saccharomyces cerevisiae*. *FEMS Yeast Res.* 3, 261-268.

Ruijter G.J.G., Visser J., 1996. Determination of intermediary metabolites in *Aspergillus niger*. *J Microbiol Methods*. 25, 295-302.

Schaefer U., Boos W., Takors R., Weuster-Botz D., 1999. Automated sampling device for monitoring intracellular metabolite dynamics. *Anal Biochem*. 270, 88-96.

Schmitz M., Hirsch E., Bongaerts J., Takors R., 2002. Pulse experiments as a prerequisites for the quantification of in vivo enzyme kinetics in aromatic amino acid pathway of *Escherichia coli*. *Biotechnol Prog.* 18, 935-941.

Shi G., 2003. Application of co-eluting structural analog internal standards for expanded linear dynamic range in liquid chromatography/electrospray mass spectrometry. *Rapid Commun Mass Spectrom.* 17, 202-206.

Sillje H.H.W., Paalman J.W.G., Ter Schure E.G., Olsthoorn S.Q.B., Verkleij A.J., Boonstra J., Verrips C.T., 1999. Function of trehalose and glycogen in cell cycle progression and cell viability in *Saccharomyces cerevisiae*. *J Bacteriol.* 181, 396-400.

Theobald U., Mailinger W., Reuss M., Rizzi M., 1993. In vivo analysis of glucose-induced fast changes in yeast adenine nucleotide pool applying a rapid sampling technique, *Anal Biochem*. 214, 31-37.

Theobald U., Mailing W., Baltus M., Reuss M., Rizzi M., 1997. In Vivo Analysis of Metabolic Dynamics in *Saccharomyces cerevisiae*: I. Experimental Observations, *Biotechnol Bioeng.* 55, 305-316.

Van Dam J.C., Eman M.R., Frank J., Lange H.C., van Dedem G.W.K., Heijnen J.J., 2002. Analysis of glycolytic metabolites in *Saccharomyces cerevisiae* using anion exchange chromatography and electrospray ionisation with tandem mass spectrometric detection. *Anal Chim Acta.* 460, 209-218.

Van Winden W.A., 2002. ¹³C-Labeling technique for metabolic network and flux analysis, Theory and Application. PhD Thesis. Technical University of Delft.

Verduyn C., Postma E., Scheffers W.A., Van Dijken J.P., 1992. Effect of benzoic acid on metabolic fluxes in yeasts: A continuous culture study on the regulation of respiration and alcoholic fermentation. *Yeast.* 8, 501-517.

Visser D., van Zuylen G.A., van Dam J.C., Oudshoorn A., Eman M.R., Ras C., van Gulik W.M., Frank J., van Dedem G.W., Heijnen J.J., 2002. Rapid sampling for analysis of in vivo kinetics using the BioScope: a system for continuous pulse experiments. *Biotechnol Bioeng.* 79 (6), 674-681.

Weibel K.E., Mor J.R., Fiechter A., 1974. Rapid sampling of yeast cells and automated assays of adenylate, citrate, pyruvate and glucose-6-phosphate pools. *Anal Biochem.* 58, 208-216.

Weuster-Botz D. and de Graaf A.A., 1996. Reaction engineering methods to study intracellular metabolite concentrations. *Adv Biochem Eng Biotechnol.* 54, 75-108.

Changes in the Metabolome of *Saccharomyces cerevisiae* Associated with Evolution in Aerobic Glucose-Limited Chemostats

Abstract

The effect of culture age on intra and extracellular metabolite levels as well as on in-vitro determined specific activities of enzymes of central carbon metabolism has been investigated during evolution for over 90 generations of *S. cerevisiae* CEN.PK 113-7D in an aerobic glucose/ethanol limited chemostat at a specific dilution rate of 0.052 h⁻¹. It was found that the fluxes of consumed (O₂, glucose/ethanol) and secreted compounds (CO₂) did not change significantly during the entire cultivation period. However, morphological changes were observed, leading to an increased cellular surface area. During 90 generations of chemostat growth not only the residual glucose concentration decreased, also the intracellular concentrations of trehalose, glycolytic intermediates, TCA cycle intermediates and amino acids were found to have decreased with a factor 5-10. The only exception was glyoxylate, which showed a 5-fold increase in concentration. In addition to this the specific activities of most glycolytic enzymes decreased by a factor 5-10 as well during long-term cultivation. Exceptions to this were hexokinase, phosphofructokinase, pyruvate kinase and 6-phosphogluconate dehydrogenase of which the activities remained unchanged. Furthermore, it was found that the concentrations of the adenylate nucleotides as well as the energy charge of the cells did not change in a significant manner. Surprisingly the specific activities of glucose-6-phosphate dehydrogenase (G6PDH), malate synthase (MS) and isocitrate lyase (ICL) were observed to have increased significantly during 90 generations of chemostat cultivation. These changes seem to indicate a pattern where metabolic overcapacities (for reversible reactions), and storage pools (trehalose, high levels of amino acids and excess protein in enzymes) are lost during the evolution period. The driving force is proposed to be a growth advantage in the absence of these metabolic overcapacities.

This chapter has been published as: Mlawule R. Mashego, Mickel. L. A.Jansen., Jacobus L. Vinke, Walter M. van Gulik, Joseph J. Heijnen, 2005. Changes in the Metabolome of *Saccharomyces cerevisiae* Associated with Evolution in Aerobic Glucose-Limited Chemostats. FEMS Yeast Research. 5, 419-430.

Introduction

Systems biology aims at understanding the structure, organisation and dynamics of cellular and organismal function at its entirety, rather than from the characterisation of individual parts of a cell or organism (Kitano, 2002). Obtaining this understanding requires functional genomic, proteomic and metabolomic data obtained from well-designed experiments (Aggarwal & Lee, 2003). The obtained knowledge is subsequently incorporated in descriptive and mechanistic models of biological phenomena based on a computational /mathematical framework, with the goal of some predictive ability. Such models facilitate metabolic engineering of cells, dedicated to rational improvement of cellular properties through directed introduction of genetic changes using recombinant DNA technology (Bailey, 1991; Nielsen 2001). Successful application of this model based metabolic engineering approach relies heavily on the understanding of the *in-vivo* kinetics and regulation of complex cellular metabolic networks. This understanding requires accurate information on all hierarchical levels of the cell, i.e. genome, transcriptome, proteome, metabolome and fluxome. Quantitative study of the structure and regulation of these metabolic networks requires cultivation of cells under well-defined conditions, that is, in a chemostat where all required nutrients for growth are in excess except one (Novick & Szilard, 1950). This growth-limiting nutrient is most often the carbon source; however, other limiting nutrients (nitrogen or phosphorus) have been used as well (Novick & Szilard, 1950; Weibel et al, 1974; Tempest & Neijssel, 1981; Theobald et al, 1993; 1997; Buccholz et al, 2002; Schmitz et al, 2002; Visser et al, 2002). It should be realised, however, that continuous substrate limited cultivation puts a specific selective pressure on the population. It has been shown that prolonged chemostat cultivation leads to evolutionary adaptation of the cells to the culture conditions (Novick & Szilard, 1950; Adams et al, 1985; Weichert et al, 1997; Notley-McRobb & Ferenci, 1999; Manche et al, 1999; Wick et al, 2001; Steiner & Sauer, 2003). A general observation has been that the residual substrate concentration decreases and the cellular surface area increases with time due to competition for the growth limiting substrate during such evolution experiments. Recently, transcriptome analysis has been used to study microbial evolution. A culture of baker's yeast that underwent 450 generations of glucose-limited chemostat growth was analysed (Brown et al, 1998; Ferea et al, 1999). When compared to the parental strain, which produced ethanol, resulting in suboptimal biomass yields, it was found that at the end of the experiment the culture sustained steady state growth at significantly lower residual glucose concentrations, increased biomass yield and without ethanol production. The observed decrease of the residual glucose concentration was correlated with increased mRNA levels for high affinity hexose transporters (Brown et al, 1998; Ferea et al, 1999). Furthermore, it was observed that genes with altered expression levels in the three cultures included genes in glycolysis, TCA cycle, oxidative phosphorylation and metabolite transport (Ferea et al, 1999).

More recently, strains of *Saccharomyces cerevisiae* isolated after 100-500 generations of growth in glucose-limited chemostats have been studied at the DNA level by assessing changes in DNA copy number at single-gene resolution (Dunham et al, 2002). Major results were that most of the evolved strains appeared to be aneuploid as the result of gross chromosomal rearrangements due to translocations and amplifications in a region of chromosome IV that includes the high-affinity hexose transporters. Most recently, the combined transcriptome/proteome during evolution of *S. cerevisiae* in aerobic glucose limited chemostat was studied (Jansen M. L. A. personal communication). It was observed that the specific activities of many glycolytic enzymes decreased by a factor 2-8 and that the correlation between transcript levels and glycolytic enzyme activities was weak. In addition, the response of the evolved strain to glucose excess was different leading to a lower μ^{\max} and temporarily absence of ethanol secretion. These findings show that prolonged cultivation of *S. cerevisiae* under glucose-limited conditions does not only lead to a decreased concentration of the growth limiting substrate glucose due to competition but also to significant changes in primary metabolism. The evolutionary driving force for these changes remains to be elucidated.

In the present research this problem is addressed by studying the effect of long-term chemostat cultivation on the combined levels of enzymes and metabolites in the primary metabolism of *S. cerevisiae* i.e. proteome and metabolome.

Materials and Methods

Yeast strain and maintenance

Dr. P. Kötter (Frankfurt, Germany) kindly provided the haploid, prototrophic *Saccharomyces cerevisiae* strain CEN.PK113-7 D. Precultures were grown to stationary phase in shake-flasks on mineral medium adjusted to pH 6.0 (Verduyn et al, 1992) containing 2% (w/v) glucose. After adding glycerol (30%v/v) to the stationary phase culture, 2 ml aliquots were stored at -80°C in sterile vials. These frozen stocks were used to inoculate precultures for chemostat cultivation.

Preculture conditions

Precultures were grown overnight in 100 ml mineral medium (Verduyn et al, 1992) in 500 ml Erlenmeyer flasks at 220 RPM and 30°C on an orbital shaker (New Brunswick, New Jersey, USA).

Chemostat cultivation

Aerobic glucose/ethanol limited chemostat cultures were grown at a dilution rate (D) of 0.052 h^{-1} in 7l laboratory fermentors with a working volume of 4 l (Applikon, Schiedam, The Netherlands) as reported previously (Lange et al, 2001). The feed medium (Lange et al, 2001) contained a mixed carbon source of 150 mM glucose and 31mM ethanol. The addition of a small amount (7% of total carbon) of ethanol successfully prevented the cultures from

metabolic oscillations. The biomass concentration supported by this medium composition is approximately $14.5 \pm 0.3 \text{ g.l}^{-1}$.

Determinations of biomass dry weight concentration

Samples of 5 ml culture broth were filtered through a pre-weighed $0.45 \mu\text{m}$ membrane filter (Supor^R-450, Gelman Sciences, Ann Arbor, Michigan, USA) in triplicate, washed twice with 5 ml de-ionised water and dried for 48 h at $70 \text{ }^\circ\text{C}$ in an oven, followed by weighing.

Determination of residual glucose and ethanol concentrations

Approximately 5 ml of broth was rapidly withdrawn from the fermentor, instantaneously cooled to $1 \text{ }^\circ\text{C}$ followed by immediate filtration as described previously (Mashego et al, 2003). Determination of the residual glucose and ethanol concentrations in the obtained filtrate were performed spectrophotometrically (Agilent 8453-UV-visible spectroscopy system, Waldbronn, Germany) using Enzymatic bio-analysis kits (respectively kit no. 0716251 and 176290 Boehringer Mannheim, Germany) according to the manufacturer's instructions.

Rapid sampling, quenching and metabolite extraction

The applied procedures for fast sampling of broth from the fermentor, quenching of metabolic activity and subsequent extraction of metabolites from the biomass have been described previously (Mashego et al, 2004).

LC-ESI-MS/MS analysis of glycolytic and TCA cycle metabolites

Glycolytic and TCA cycle intermediates were measured in the cell extracts prepared above using LC-ESI-MS/MS (van Dam et al, 2002).

Trehalose analysis

Intracellular trehalose analysis was performed by ion-exchange high-pressure liquid chromatography (HPLC) using an Aminex HPX-87H, 300 mm x 7.8 ion exchange column with a 30 x 4.6 mm guard column (Bio-rad Laboratories, Inc. Hercules, CA, USA). The mobile phase was 1mM phosphoric acid at a flow rate of 0.6 ml. min^{-1} at $60 \text{ }^\circ\text{C}$. The HPLC setup further consisted of a Waters 717 auto sampler connected to a Waters 510 HPLC pump with 410 differential refractometer detector. The trehalose (T-0167) standard was obtained from Sigma-Aldrich (St. Louis, MO, USA).

Measurement of adenine and pyrimidine nucleotides

Intracellular ATP determination was performed using the ATP Bioluminescence Assay Kit CLS II (Cat. no. 1699 695, Roche Diagnostics GmbH, Mannheim, Germany) according to the

manufacturer's instructions in black Costar 96 well micro titre plates. Luminescence was read on Mediators PhL plate reader, (Mediators Diagnostics GmbH, Wien, Austria).

ADP and AMP determination were performed enzymatically based on myokinase (MK), pyruvate kinase (PYK), and lactate dehydrogenase (LDH) (Bergmeyer et al, 1985). The assay was performed in white flat bottom Costar 96 well, ½ area micro titre plates (Corning Inc, USA) by following NADH fluorescence in a Tecan Genios micro titre plate reader, (Tecan, Salzburg, Austria). Excitation wavelength was 340 nm while the emission wavelength was at 465 nm. The NAD assay was based on the enzymatic cycling method reported previously (Visser, 2002) performed in 96 well micro titre plates in a Tecan Genios micro titre plate reader (Tecan, Salzburg Austria).

Cell-free extracts preparation and enzyme assays

Cell free extracts were prepared as described previously (van Hoek et al, 1998). Enzyme assays in cell free extracts were performed as described previously (van Hoek et al, 1998). Specific enzymes activities of the glyoxylate cycle enzymes (malate synthase and isocitrate lyase) were performed as described previously (de Jong-Gubbels et al, 1995).

Image analysis

Microscopic images were taken using an Olympus IMT-2 reverse microscope and analysed using Olympus camera adaptor, a CCD camera, Olympus MTV-3 and image analyser Leica Qwin, version pro 2.2 software.

Results

General observations and culture morphology

Two duplicate chemostats of *S. cerevisiae* were run at a dilution rate of 0.052 h⁻¹, for 80-90 generations. Metabolic oscillations were absent indicating that the use of ethanol as co-substrate was effective in preventing this behaviour. From a macroscopic point of view, both chemostats displayed steady state behaviour during the entire cultivation period. It was observed that the biomass concentration, the specific substrate uptake rate and the specific rates of oxygen consumption and carbon dioxide production did not change significantly during 1200 h of chemostat cultivation (results not shown). Average values are shown in Table 1. The carbon and electron balance, calculated from these rates are close to 100%. The metabolism was fully respiratory, as judged by a respiratory quotient (RQ) of approximately one, (see Table 1) which was expected for the mixed glucose/ethanol substrate used.

With respect to the cell morphology, cell shape changed clearly from oval to more elongate (see Figure 1), resulting in an increased surface area. From electron microscopy carried out at various time points it was observed that the cellular ultra structures (mitochondria, vacuole and

nucleus) did not show notable volume changes during 90 generations of chemostat cultivation (data not shown).

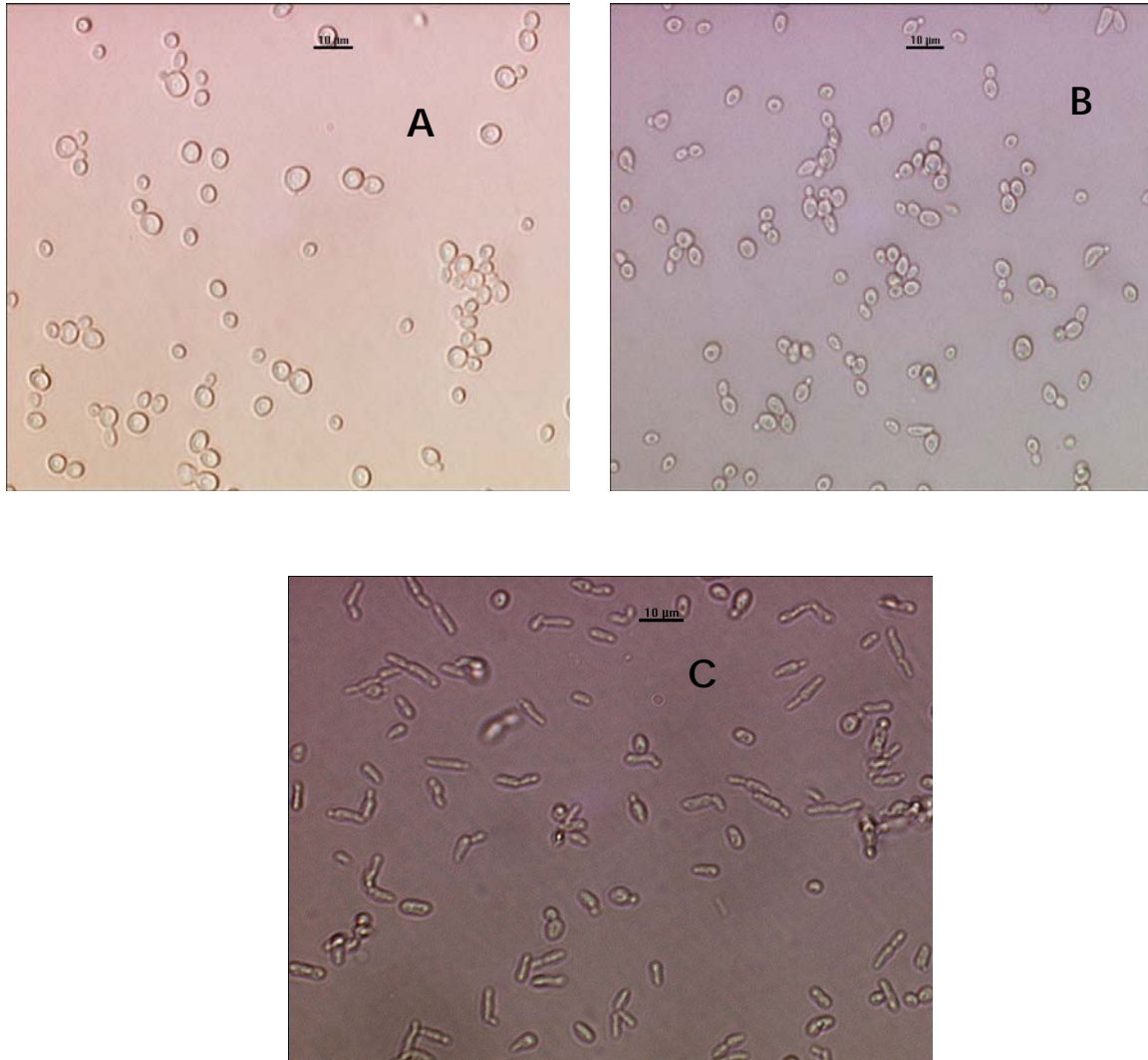


Figure 1 Morphological changes of *S. cerevisiae* during long-term cultivation in aerobic glucose/ethanol limited chemostat culture: 10 (A), 40 (B) and 80 (C) generations: The indicator bar represents 10 µm.

Table 1 Average biomass dry weight concentration, specific ethanol uptake rate (q_{ethanol}); specific glucose uptake rate (q_{glucose}); specific carbon dioxide evolution rate (q_{CO_2}); specific oxygen uptake rate (q_{O_2}) and respiratory quotient (RQ) with their 95% confidence intervals. All values are averages of 15 independent measurements, evenly distributed over the entire cultivation period.

D	Biomass	q_{ethanol}	q_{glucose}	q_{CO_2}	q_{O_2}	RQ	
(h ⁻¹)	(g.l ⁻¹)	(mol ethanol.C- mol biomass ⁻¹ .h ⁻¹)	(mol glucose.C- mol biomass ⁻¹ .h ⁻¹)	(mol CO ₂ .C-mol biomass ⁻¹ .h ⁻¹)	(mol O ₂ .C-mol biomass ⁻¹ .h ⁻¹)	(-)	
Chemostat 1	0.0521 ± 0.0004	14.20 ± 0.30	0.0029±0.0001	0.0141±0.0004	0.043 ± 0.001	0.043 ± 0.001	1.00 ± 0.01
Chemostat 2	0.0522 ± 0.0005	14.53 ± 0.21	0.0029±0.0001	0.0138±0.0003	0.038 ± 0.001	0.039 ± 0.001	0.99 ± 0.01

Residual substrates

During prolonged chemostat cultivation, the residual glucose concentration was found to decrease with more than a factor 2 from 20 mg.l⁻¹ to about 8 mg.l⁻¹ (Figure 2). In contrast, the residual ethanol concentration did not change and remained at values between 2.3 and 2.5 mg.l⁻¹ (data not shown).

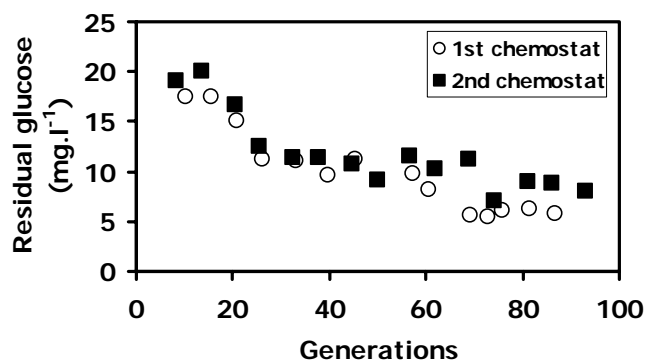


Figure 2 Residual glucose during long-term aerobic glucose/ethanol limited chemostat cultivation of *S. cerevisiae* CEN.PK 113-7D in two duplicate experiments.

In-vitro determined specific enzyme activities

In Tables 2 & 3 the in-vitro, measured specific activities of the enzymes of the upper and lower parts of the glycolytic pathway in *S. cerevisiae*, determined at different time points during long-term chemostat cultivation, are shown. It can be inferred from these tables that most of the measured enzyme activities decrease with a factor 2 to 5 during 90 generations of chemostat cultivation. Notable exceptions are the activities of hexokinase, phosphofructokinase, alcohol dehydrogenase and pyruvate kinase of which the activities remain nearly constant. A remarkable observation was that the measured activities of the two glyoxylate pathway enzymes, isocitrate lyase and malate synthase, as well as the first enzyme of the pentose phosphate pathway, glucose-6-phosphate dehydrogenase increased significantly during long-term chemostat cultivation (Fig 3).

Table 2 Specific activities of enzymes of the upper part of glycolysis (U. mg protein⁻¹) during long term aerobic glucose/ethanol limited chemostat cultivation of *S. cerevisiae* CEN.PK 113-7D at a dilution rate of 0.052 h⁻¹.

Number of generations	Hexokinase		PGI		PFK		FBA		TPI		G3PDH	
	I	II	I	II	I	II	I	II	I	II	I	II
10	2.4	2.8	-	4.6	0.4	0.3	1.6	1.5	111.5	126.0	6.6	6.5
23	-	2.8	4.4	4.7	-	0.3	-	1.7	-	113.3	-	6.3
35	2.4	-	-	-	-	-	1.2	-	102.4	-	4.7	-
47	-	3.2	-	3.8	-	0.4	-	-	-	-	-	-
58	2.5	2.9	3.3	3.8	0.4	-	1.1	-	63.8	66.7	3.2	3.5
74	3.4	2.8	3.2	2.7	0.4	-	0.5	0.6	33.3	28.7	2.1	2.6
94	3.6	3.1	3.0	2.8	0.4	0.3	0.5	0.5	37.1	-	2.0	1.4

Key: Phosphoglucose isomerase (PGI); Fructose-1,6-bisphosphate aldolase (FBA), Triose phosphate isomerase (TPI); Glyceraldehyde-3-phosphate dehydrogenase (G3PDH); I = Chemostat 1; II = Chemostat 2.

Table 3 Specific activities of enzymes of the lower part of glycolysis (U. mg protein⁻¹) during long-term aerobic glucose/ethanol limited chemostat cultivation of *S. cerevisiae* CEN.PK 113-7D at a dilution rate of 0.052 h⁻¹

Number of generations	PGK		ENO		PYK		PDC		ADH	
	I	II	I	II	I	II	I	II	I	II
10	13.4	13.5	1.1	1.0	3.1	3.5	0.6	0.6	13.9	13.1
23	-	12.3	-	0.8	3.1	3.9	0.5	0.6	10.6	10.6
35	8.4	-	0.8	-	3.1	-	0.6	-	11.7	-
47	-	-	-	0.5	-	2.8	-	-	-	11.3
58	5.4	6.6	0.3	0.4	2.5	-	0.4	0.4	11.0	9.6
74	3.9	3.4	0.3	-	2.8	-	0.4	0.4	11.5	13.1
94	3.7	1	-	0.2	2.8	2.8	0.4	-	13.1	-

Key: Phosphoglycerate kinase (PGK); Enolase (ENO); Pyruvate kinase (PYK), Pyruvate decarboxylase (PDC) Alcohol dehydrogenase (ADH). I = Chemostat 1; II = Chemostat 2.

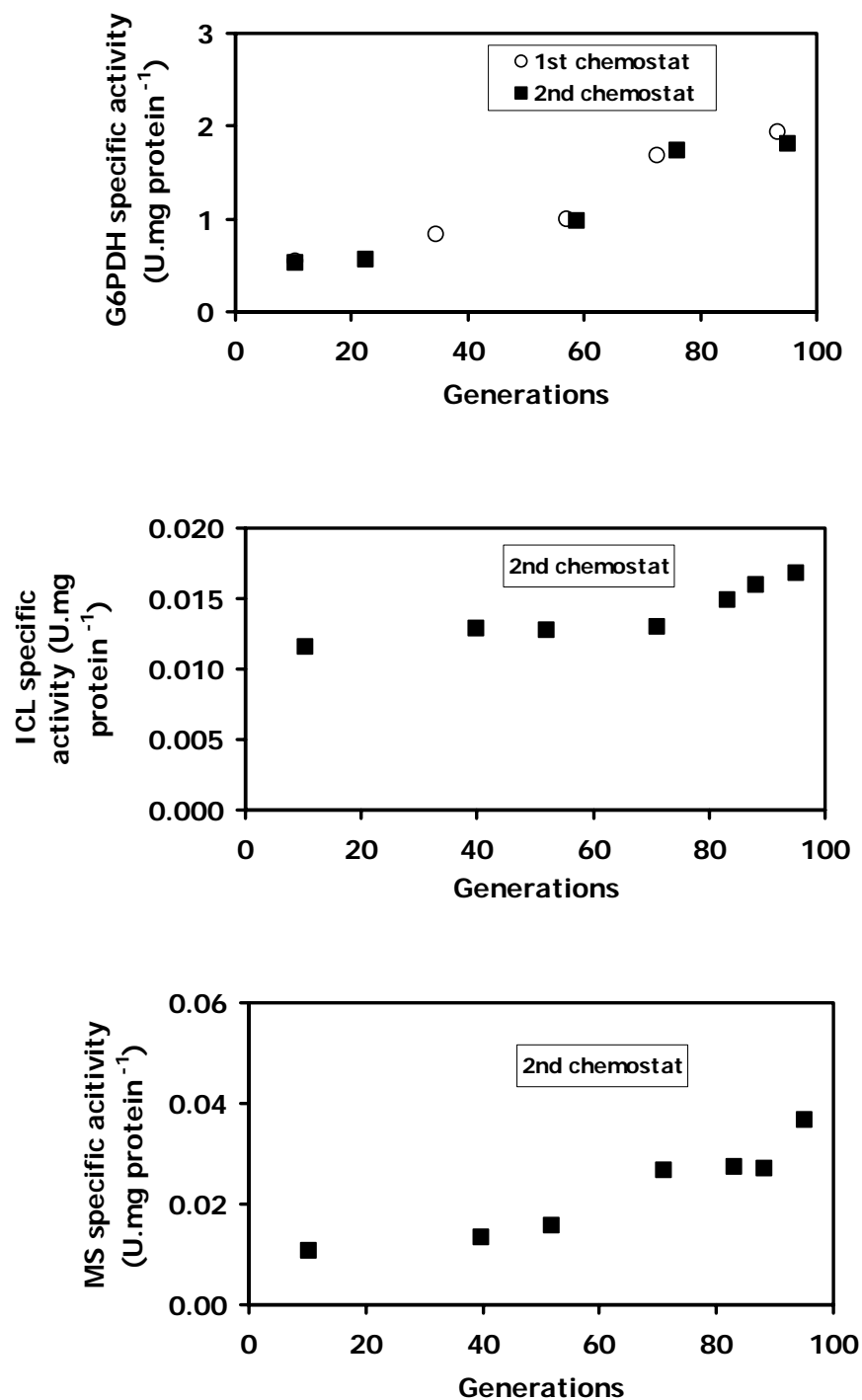


Figure 3 Enzymes with increasing in-vitro specific activities in the pentose phosphate pathway (glucose-6-phosphate dehydrogenase), and the glyoxylate pathway (isocitrate lyase and malate synthase) during long term aerobic glucose/ethanol limited chemostat cultivation of *S. cerevisiae* CEN.PK 113-7D

Intracellular metabolites

In Figure 4A, the results of the measurements of the intracellular adenine and pyridine concentrations are shown. It can be seen from this figure that no significant changes occur in the intracellular concentration of ATP during 90 generations of chemostat cultivation. In addition, the ADP concentration as well as the sum of AMP, ADP and ATP, for which we have only figures for chemostat 2, does not seem to change during the cultivation period. The calculated energy charge (Atkinson, 1968) showed very little change and remained at a value between 0.8 and 0.9. Only the concentration of the pyridine nucleotide NAD was found to decrease slightly during long-term cultivation.

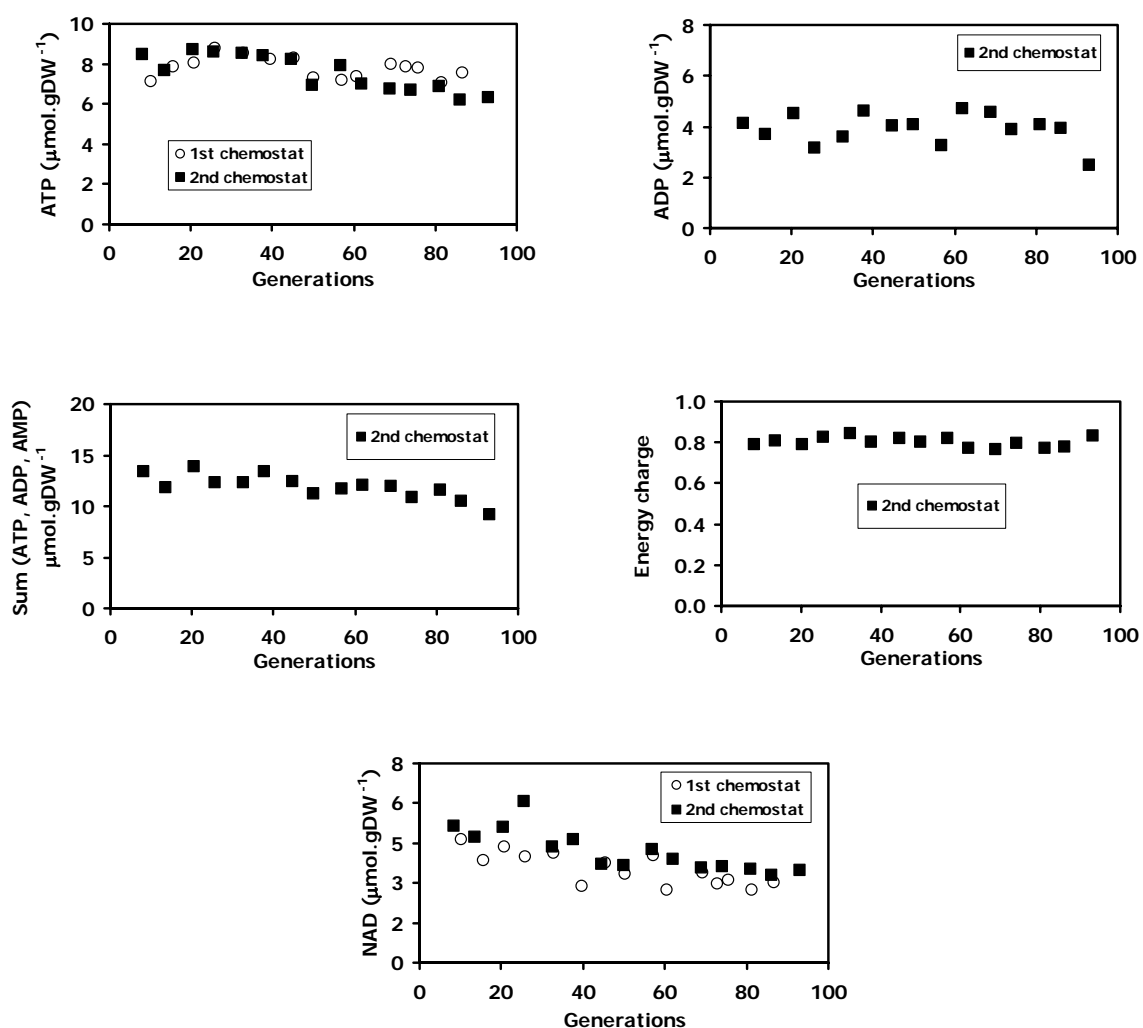


Figure 4A Intracellular concentrations of ATP, ADP, total adenine nucleotides and NAD during long-term aerobic glucose/ethanol limited chemostat cultivation of *S. cerevisiae* CEN.PK 113-7D.

In Figure, 4B-C time patterns are shown of the intracellular concentrations of trehalose, glycolytic intermediates and TCA cycle intermediates. Almost all measured concentrations,

were found to decrease significantly (2-10 fold) within a cultivation period of 80-90 generations. The only two exceptions were succinate, of which the concentration remained constant and glyoxylate of which the concentration strongly increased.

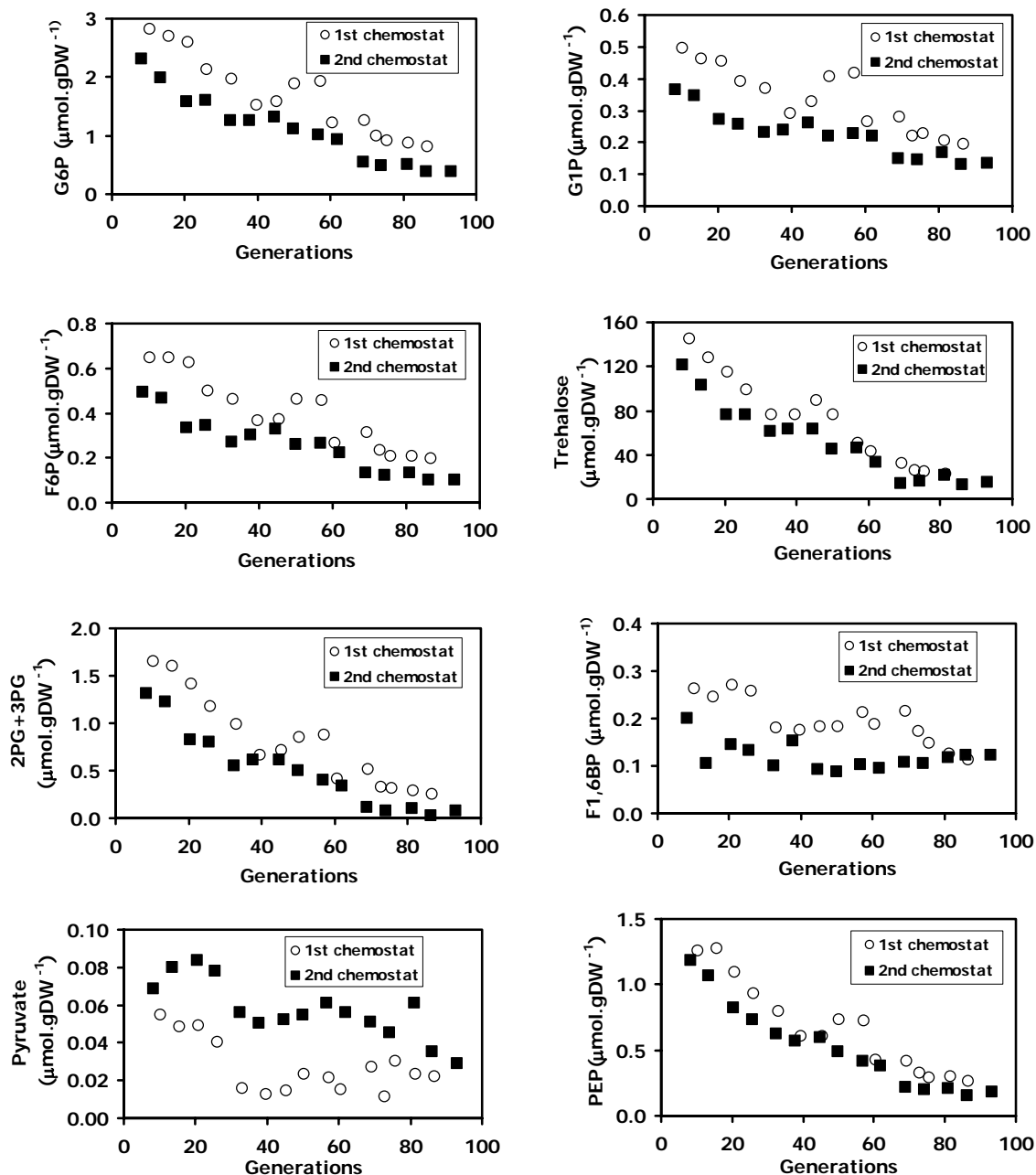


Figure 4B Intracellular concentrations of glycolytic intermediates (G6P, G1P, F6P, 2/3phosphoglycerate, phosphoenolpyruvate, pyruvate) and trehalose during long-term aerobic glucose/ethanol limited chemostat cultivation of *S. cerevisiae* CEN.PK 113-7D.

In Figure 4D time patterns are shown of the intracellular concentrations of the amino acids aspartate, glutamate and alanine which are present in relatively high concentrations (3-25 $\mu\text{mol.gDW}^{-1}$) and are directly derived from primary metabolites (oxaloacetate, α -ketoglutarate

and pyruvate). The concentrations of these amino acids were observed to decrease very significantly (approximately 5 fold). Comparing the changes in the concentrations of the α -keto acids (pyruvate, α -ketoglutarate) and their related amino acids (alanine and glutamate) shows that there is a close correspondence. In addition, the concentrations of the keto acids decreased with a factor of 3. The other amino acids were present at a much lower concentration ($0.2\text{-}1\mu\text{mol.gDW}^{-1}$) and did not show significant changes (data not shown).

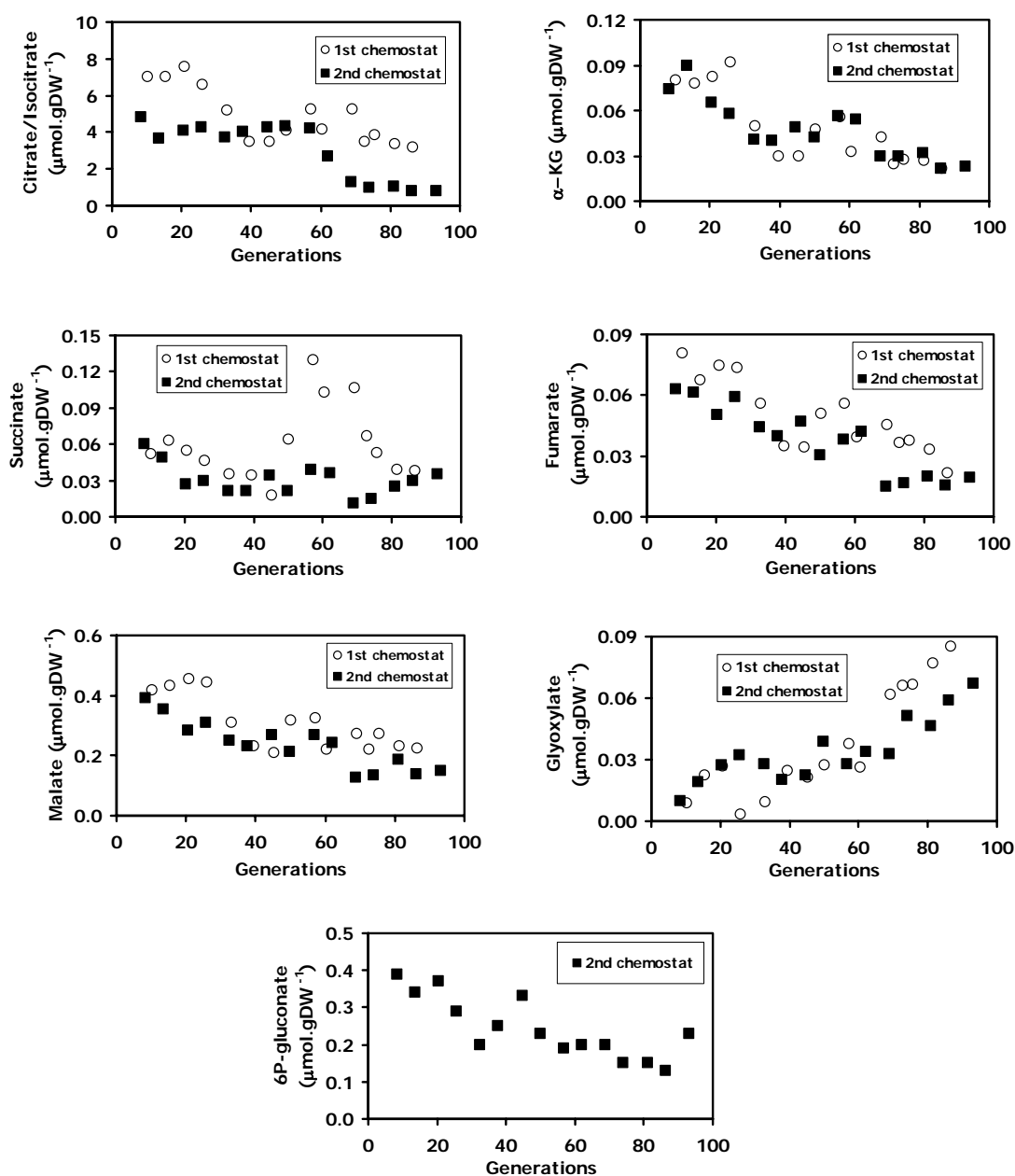


Figure 4C Intracellular concentrations of TCA cycle intermediates (α -ketoglutarate, fumarate, malate, sum of citrate+isocitrate, succinate) and glyoxylate during long-term aerobic glucose/ethanol limited chemostat cultivation of *S. cerevisiae* CEN.PK 113-7D.

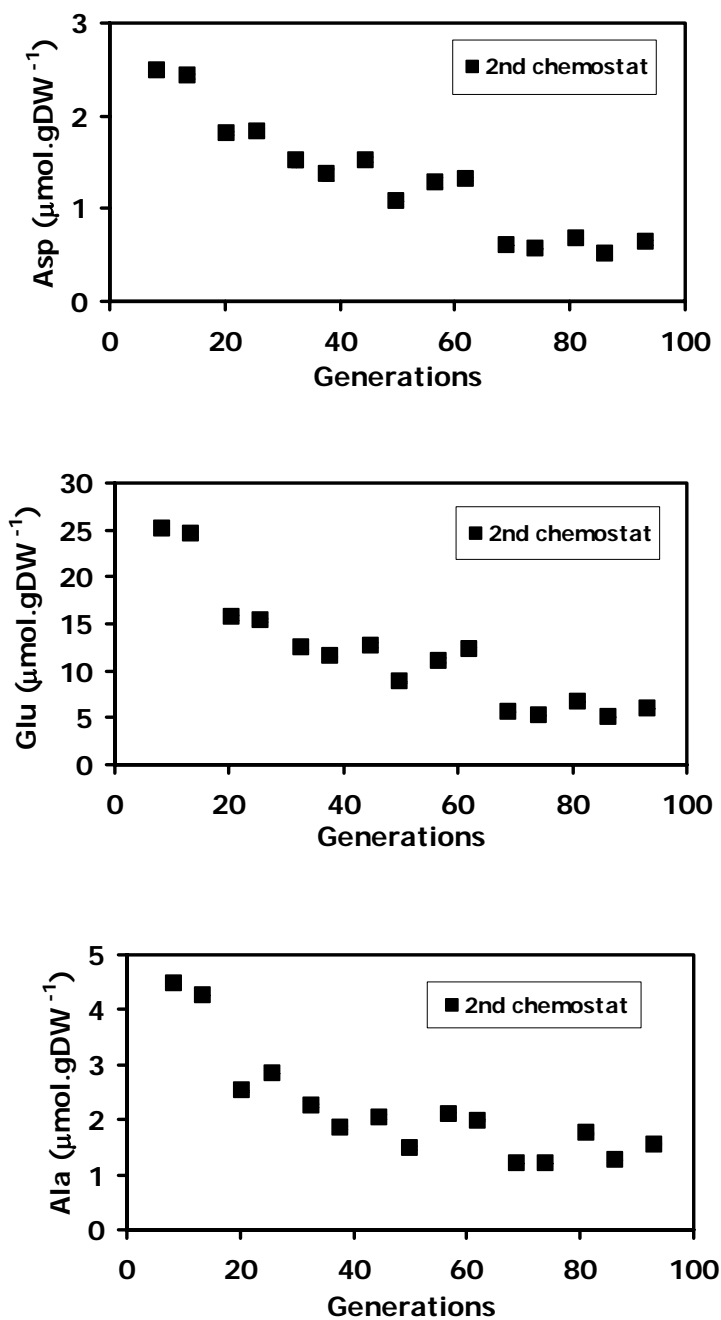


Figure 4D Aspartate, glutamate and alanine concentration, during long-term aerobic glucose/ethanol limited chemostat cultivation of *S. cerevisiae* CEN.PK 113-7D. Error bars representing the standard deviations of duplicate analyses of the same sample were in all cases smaller than the symbol size and are therefore not visible.

Discussion

Long-term cultivation of *Saccharomyces cerevisiae* under carbon limited chemostat conditions did not result in any significant change in biomass concentration, specific consumption rates of substrate, oxygen and specific carbon dioxide production. Therefore, from a macroscopic

point of view, the culture could be considered to be in steady state during the whole cultivation period of 90 generations. However, from measurements of residual substrate level, intracellular metabolite concentrations and specific activities of a large number of enzymes from primary metabolism it was inferred that the cellular properties must have changed tremendously during long term chemostat cultivation. From these observations, the culture could therefore not be considered as steady state within the time frame of observation of 90 generations. The observed decrease of the residual concentration of the growth limiting substrate is probably the result of competition between mutant culture members, where a larger cellular surface area (morphology changing from sphere to elongated) and a more effective substrate transport result in competitive selective advantage. Such changes have been reported before (Adams et al, 1985; Weichert et al, 1997; Notley-McRobb & Ferenci, 1999; Manche et al, 1999; Wick et al, 2001; Steiner & Sauer, 2003; Ferea et al, 1999). These results also agree with the *S. cerevisiae* evolution experiment at dilution rate of 0.1 h^{-1} , (Jansen M. L. A. personal communication).

This is the first time that intracellular concentrations of a large number of primary metabolites have been measured during a chemostat evolution of *S. cerevisiae* and the results reported here provide new and significant information on the possible mechanisms of cellular adaptation. These measurements revealed that the observed decrease of the residual glucose concentration coincided with significant decreases of the concentrations of a large number of primary metabolites. When glucose transport is passive, as is the case for facilitated diffusion in *S. cerevisiae*, and no changes occur in the transport capacity and the glucose consumption rate, a decrease of the extracellular glucose concentration must result in a decrease of the intracellular glucose concentration in order to maintain the driving force for glucose transport over the cell membrane. From our chemostat experiments, it was found that the biomass specific glucose uptake rate (q_s) did not change significantly during long-term cultivation, in spite of the observed decrease of the residual glucose concentration from 0.11 to 0.04 mM (Fig 2). At a constant biomass concentration, this would have resulted in an increase of the specific glucose uptake rate of 0.05%, which is practically unobservable.

Furthermore, it was found that there was only a limited change in the capacity of the passive glucose transporter during long-term glucose limited chemostat cultivation of *S. cerevisiae* (Jansen M. L. A. personal communication). From these findings, it can be concluded that the driving force for glucose diffusion must remain nearly constant, leading to a decreasing intracellular glucose concentration. A decreasing intracellular glucose concentration causes, (through kinetic interactions) that all other glycolytic and TCA cycle intermediates concentration decrease significantly. For example, because the flux through hexokinase is constant (= specific glucose uptake rate), and the hexokinase specific activity hardly changes (Table 1 & 2) the driving force of the rate of reaction must remain similar. This means that a decreasing intracellular substrate concentration must be compensated by a decreasing

concentration of the produced glucose-6-phosphate (G6P), which is clearly observed. Similar arguments can explain the trend observed that nearly all glycolytic and TCA cycle metabolites decrease in concentration.

Parallel to the decreasing metabolite concentrations, it was observed that the specific activities of almost all glycolytic enzymes decreased with a factor 3-5. Similar decreases in enzyme activities as well as unchanging activities of the three enzymes (HK, PFK, PYK) have also been observed for long term chemostats of *S. cerevisiae* grown at a different dilution rate (Jansen M. L. A. personal communication). From the fact that the uptake rate (q_s) of glucose remained the same, it can be inferred that the glycolytic flux also remained constant. A baffling question arises as to how to reconcile the fact that the glycolytic flux remains unchanged while there is a strong decrease in the specific enzyme activities in many reactions of this pathway. A possible explanation is that the reactions of which the enzyme activities have been found to decrease operate close to equilibrium, which means that these enzymes have a very large overcapacity. Therefore, decreasing enzyme activities do not affect significantly the rates of these reactions. An equilibrium situation occurs when the mass action ratio, which is calculated from the measured intracellular metabolite concentration, remains constant and close to the equilibrium constant. The mass action ratio was calculated for reactions catalyzed by PGI, PGK and ENO. They were found to remain constant during long-term chemostat cultivation and close to the reported equilibrium constants of these reactions (data not shown). Hence, it can be concluded that reactions, which are catalyzed by enzymes, which exhibit decreased specific activities during long-term chemostat cultivation, are probably reversible reactions under in-vivo conditions. In agreement with this, it was observed that for the known irreversible steps in glycolysis (hexokinase, phosphofructokinase and pyruvate kinase), (Nelson & Cox, 2000), the enzyme activities did not change. Moreover, the specific activity of glucose-6-phosphate dehydrogenase, the irreversible first step in the pentose phosphate pathway, was observed to increase. The reason for this could be to maintain a constant flux through the pentose phosphate pathway at a decreasing G6P concentration.

The observed changes in enzyme levels and metabolite concentrations are likely to have been caused by metabolic adaptation to a chemostat environment, which does not change and therefore does not require metabolic overcapacities, which can deal with large fluctuations in substrate availability. Usually a temporary excess of substrate requires very large metabolic overcapacities e.g. high enzyme activity in glycolysis. In a chemostat substrate excess does not occur and thus there is no need for enzyme overcapacities. Indeed, the activities of many glycolytic enzymes representing in total about 4% of the dry biomass (van Hoek, 2000), were found to decrease several fold as discussed above. Temporary lack of substrate is usually counteracted by mobilization of storage carbohydrates such as trehalose and glycogen (Schulze et al, 1995; Ribeiro et al, 1999; Argüelles et al, 2000; Francois & Parrou, 2001; Arvindekar & Patil, 2002). For example, trehalose is initially present at a concentration of 150 $\mu\text{mol. gDW}^{-1}$.

However, also the free amino acid pool, which is relatively large (35-50 μ mol.gDW⁻¹) at start of the evolution experiment as well as the excess amounts of glycolytic enzymes, can be considered as sources of stored carbon to be used when external substrate is absent. These available intracellular storage type substrates (trehalose, glycogen, amino acids and proteins) can be estimated at about 50-100 mg. gDW⁻¹ (van Hoek et al, 1998; van Hoek, 2000 and presented amino acid data). During the evolution experiment, for a period of 90 generations under glucose limited conditions the size of these internal pools were observed to decrease with about a factor 5. Clearly, these pools represent a metabolic burden under the conditions of a strictly continuous supply of external substrate as occurs in a chemostat. Cells which convert all consumed substrate directly to productive biomass have apparently in a chemostat, a competitive advantage over the cells which store large amounts of substrate in high levels of trehalose and amino acids or make high levels of glycolytic enzymes. The competitive advantage probably lies in the absence of the energy needed for the operation of e.g. the storage process where direct production of glucose-6-phosphate from glucose using hexokinase costs one ATP per glucose-6-phosphate, whereas when glucose is converted first into trehalose, which is subsequently used to produce glucose-6-phosphate, the energy need is 2.5 mol ATP per mole G6P.

The lower concentrations of intracellular amino acids, aspartate, glutamate and alanine (Fig 4D) directly result in proportionally lower concentration of the α -ketoacids (α -ketoglutarate, oxaloacetate coupled to malate, pyruvate), (Fig 4B), because of the reversible transaminase reactions. This is supported by the observation that the calculated mass action ratio of the transaminase reaction (PYR+GLU \leftrightarrow ALA+ α -KG), does hardly change during the evolution experiment (data not shown). The resulting lower pyruvate concentration possibly limits the normal anaplerotic reaction catalyzed by pyruvate carboxylase and makes the alternative glyoxylate pathway for the production of C4 intermediates more favourable. Indeed, in the later part of the evolution experiment, it was observed that the two glyoxylate pathway enzymes (isocitrate lyase and malate synthase) increased their specific activities and the concentration of the pathway intermediate glyoxylate was observed to increase concomitantly. Also significant is that the concentration of succinate, the product of this pathway, remains almost constant whereas the concentrations of all other TCA cycle intermediates decrease by a factor 2-4. This constancy can be due to extra succinate production/supply from the glyoxylate pathway, which counteracts a decrease in succinate concentration. With all these changes, it is remarkable to see that the concentrations of the energy nucleotides (ATP and NAD), do not change significantly; showing that homeostasis of conserved moieties seems crucial for maintaining a competitive organism. The obtained ATP and ADP levels are very comparable to the values reported elsewhere (Theobald et al, 1993). An energy charge of 0.9 was reported previously for *S. cerevisiae* under similar conditions (Theobald et al, 1993). It appears that the energy charge is independent of the specific growth

rate of *S. cerevisiae* because the specific growth rate applied previously (Theobald et al, 1993) was 0.1 h^{-1} while, in the present case, it was 0.052 h^{-1} . Clearly, this energy related conserved moieties do not change significantly their levels and sums.

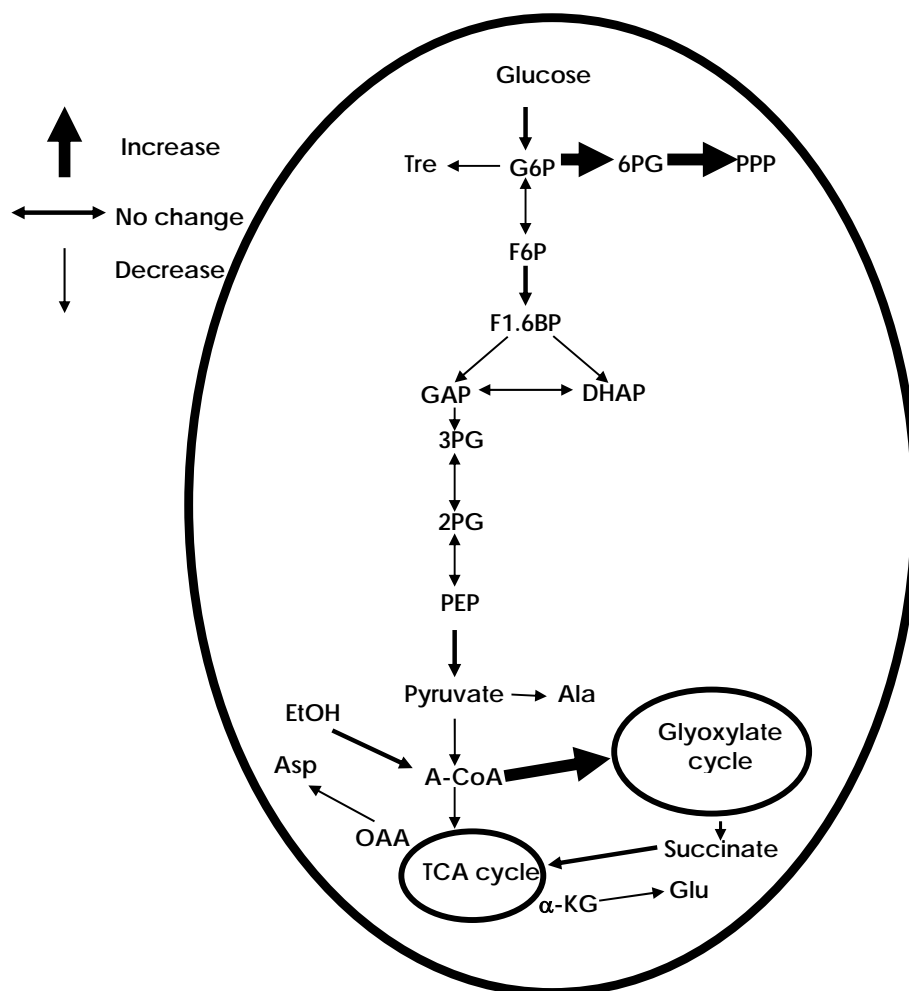


Figure 5 Summary of the physiological changes associated with the adaptation of *S. cerevisiae* during long-term aerobic glucose/ethanol limited chemostat cultivation a dilution rate of 0.052 h^{-1} . Key: G6P (Glucose 6 phosphate); F6P (Fructose 6 phosphate); F1,6BP (Fructose 1,6 bisphosphate); GAP (Glyceraldehyde 3 phosphate); DHAP (Dihydroxyacetone phosphate); 3PG (3 Phosphoglycerate); 2PG (2 Phosphoglycerate); PEP (Phosphoenolpyruvate); A-CoA (Acetyl Coenzyme A); EtOH (Ethanol), 6PG (6-phosphogluconate); PPP (Pentose phosphate pathway); Tre (Trehalose); Ala (Alanine); OAA (Oxaloacetate); Asp (Aspartate); α -KG (α -Ketoglutarate); Glu (Glutamate)

Conclusions

Prolonged cultivation (90 generations) of *S. cerevisiae* under glucose limited chemostat conditions leads to a dramatic metabolic adaptation with strongly reduced levels of enzymes, metabolites and storage material. Figure 5 shows the overall picture of the metabolic

adaptations which were observed. This adaptation involves two phenomena: 1. a lower residual glucose level due to competition for the growth limiting substrate, 2. a metabolic adaptation that gives growth advantage due to a decreased metabolic burden. The former adaptation has been observed before, while the latter is new. The metabolic burden relates to the presence of large pools of intracellular carbon (trehalose, amino acids and excess metabolic capacity in glycolytic enzymes) which is supposed to allow *S. cerevisiae* to survive temporary excess and absence of substrate as usually occurs in nature. In a constant environment of a chemostat, there is no need for such capacities, the maintenance of which costs energy and therefore presents a metabolic burden. Hence, losing these capacities is energetically favourable and therefore a competitive growth advantage is achieved, which explains the adaptation observed. This adaptation is characterized (Figure 5) by: 1. constant fluxes, 2. by a steep decrease in concentrations of glycolytic and TCA cycle intermediates, trehalose, α -keto acids related amino acids and levels of enzymes catalyzing reversible reactions, 3. constant adenine nucleotides and constant or increasing levels of enzymes which catalyze irreversible reactions, 4. induction of the glyoxylate cycle as a possible alternative for the normal anaplerotic reaction (pyruvate carboxylase) in response to the very low intracellular pyruvate level.

Finally, it should be realized that such evolution of microbial populations in a chemostat has some relevant consequences. Studies of in-vivo kinetics of microbial cultures are performed using chemostat grown cultures (Theobald et al, 1993; Visser et al, 2002). The result of such an experiment can therefore be expected to depend on the culture age. This means that for cultivation of biomass for reproducible in vivo kinetic experiments, not only the same conditions should be applied (e.g. temperature, pH, medium composition and dilution rate), but also the same cultivation time. In addition, the chemostat is advocated as an ideal tool to obtain, through evolution, microorganisms with desirable properties (Sauer, 2001). This research shows that these evolved organisms might have the disadvantage of being less capable to handle temporary absence or excess of substrate as might occur in large-scale fermentation equipment due to insufficient mixing.

Acknowledgements

We thank Professor J. T. Pronk for continued interest in the work. Angela ten Pierick, Jan van Dam, Cor Ras and Adam Hassane are acknowledged for analytical work. NWO and DSM are acknowledged for financial support.

References

Adams J. Paquin C. Oeller P.W., Lee L.W., 1985. Physiological characterization of adaptive clones in evolving populations of the yeast *Saccharomyces cerevisiae*. *Genetics*. 110, 173-185.

Aggarwal K., Lee, K.H., 2003. Functional genomics and proteomics as a foundation for systems biology. *Brief Funct Genomic Proteomic*. 2 (3), 175-184.

Atkinson D.E., 1968. The energy charge of the adenylate pool as a regulatory parameter. interaction with feedback modifiers. *Biochem*. 7 (11), 4029-4034.

Argüelles J.C., 2000. Physiological roles of trehalose in bacteria and yeasts: a comparative analysis. *Arch Microbiol*. 174, 217-224.

Arvindekar A.U., Patil N.B., 2002. Glycogen-a covalently linked component of the cell wall in *Saccharomyces cerevisiae*. *Yeast*. 19, 131-139.

Bailey J.E., 1991. Toward a science of metabolic engineering. *Science*. 252, 1668-1675.

Bergmeyer H.C., Bergmeyer J., Grass M. (Eds.), 1985. *Methods in enzymatic analysis*. 3rd Edition. Verlag Chemie. Weinheim.

Brown C.J., Todd K. M., Rosenzweig R.F., 1998. Multiple duplication of yeast hexose transport genes in response to selection in glucose-limited environment. *Mol Biol Evol*. 15 (8), 931-942.

Buchholz A., Hurlbaus J., Wandrey C., Takors R., 2002. Metabolomics: quantification of intracellular metabolite dynamics. *Biomol Eng*. 19, 5-15.

De Jong-Gubbels P., Vanrolleghem P., Heijnen J.J., van Dijken J.P., Pronk J.T., 1995. Regulation of carbon metabolism in chemostat cultures of *Saccharomyces cerevisiae* grown on mixtures of glucose and ethanol. *Yeast*. 11, 407-418.

Dunham M.J., Badrane H., Ferea T., Adams J., Brown P.O., Rosenzweig F., Botstein D., 2002. Characteristic genome rearrangements in experimental evolution of *Saccharomyces cerevisiae*. *Proc Natl Acad Sci USA*. 99 (25), 16144-16149.

Ferea T.L., Botstein D., Brown P.O., Rosenzweig R.F., 1999. Systematic changes in gene expression patterns following adaptive evolution in yeast. *Proc Natl Acad Sci USA*. 96, 9721-9726.

Francois J., Parrou J.L., 2001. Reserve carbohydrates metabolism in the yeast *Saccharomyces cerevisiae*. *FEMS Microbiol Rev*. 25, 125-145.

Kitano H., 2002. System Biology: a Brief overview. *Science*. 295, 1662-1664.

Lange H.C., Eman M., van Zuijlen G., Visser D., van Dam J.C., Frank J., Teixeira de Mattos M.J., Heijnen J.J., 2001. Improved rapid sampling for in vivo kinetics of intracellular metabolites in *Saccharomyces cerevisiae*. *Biotechnol Bioeng*. 75 (4), 406-415.

Manché K., Notley-McRobb L., Ferenci T., 1999. Mutational adaptation of *Escherichia coli* to glucose limitation involves distinct evolutionary pathways in aerobic and oxygen-limited environments. *Genetics*. 153, 5-12.

Mashego M. R., van Gulik W. M., Vinke J. L., Heijnen J. J., 2003. Critical evaluation of sampling techniques for residual glucose determination in carbon-limited chemostat culture of *Saccharomyces cerevisiae*. *Biotechnol Bioeng*. 83 (4), 395-399.

Mashego M. R., Wu L., Van Dam J. C., Ras C. Vinke J. L., Van Winden W. A., Van Gulik W. M., Heijnen J. J., 2004. MIRACLE: mass isotopomer ratio analysis of U-¹³C-labeled extracts. A new method for accurate quantification of changes in concentrations of intracellular metabolites. *Biotechnol Bioeng*. 85(6), 620-628.

Nelson D.L., Cox M. M., 2000. *Lehninger principles of Biochemistry*. 3rd Edition. Worth publishers. USA.

Nielsen J., 2001. Metabolic engineering. *Appl Microbiol Biotechnol*. 55(3), 263-283.

Notley-McRobb L., Ferenci T., 1999. Adaptive *mgI*-regulatory mutations and genetic diversity evolving in glucose-limited *Escherichia coli* populations. *Environ Microbiol*. 1(1), 33-43.

Novick A., Szilard L., 1950. Description of the chemostat. *Science*. 112, 715-716.

Novick A., Szilard L., 1950. Experiments with the chemostat on spontaneous mutations of bacteria. *Proc Natl Acad Sci USA*. 36, 708-719.

Ribeiro M.J., Leao L.S., Morais P.B., Rosa C.A., Panek A.D., 1999. Trehalose accumulation by tropical yeast strains submitted to stress conditions. *Antonie van Leeuwenhoek*. 75(3), 245-2551.

Sauer U., 2001. Evolutionary engineering of industrially important microbial phenotypes. *Adv Biochem Eng Biotechnol*. 73,129-169.

Schmitz M., Hirsch E., Bongaerts J., Takors R., 2002. Pulse experiments as a prerequisites for the quantification of in vivo enzyme kinetics in aromatic amino acid pathway of *Escherichia coli*. *Biotechnol Progr.* 18, 935-941.

Schulze U., Larsen M. E., Villadsen J., 1995. Determination of Intracellular trehalose and glycogen in *Saccharomyces cerevisiae*. *Anal Biochem.* 228, 143-149.

Steiner P., Sauer U., 2003. Long-term continuous evolution of acetate resistant *Acetobacter aceti*. *Biotechnol Bioeng.* 84(1), 40-44.

Tempest D.W., Neijssel O. M., 1981. Metabolic compromises involved in the growth of microorganisms in nutrient-limited (chemostat) environments. *Basic Life Sci.* 18, 335-356.

Theobald U., Mailinger W., Reuss M., Rizzi M., 1993. In vivo analysis of glucose-induced fast changes in yeast adenine nucleotide pool applying a rapid sampling technique. *Anal Biochem.* 214, 31-37.

Theobald U., Mailinger W., Baltés M., Reuss M., Rizzi M., 1997. In vivo analysis of metabolic dynamics in *Saccharomyces cerevisiae*: I. experimental observations. *Biotechnol Bioeng.* 55, 305-316.

Van Dam J. C., Eman M. R., Frank J., Lange H.C., van Dedem G. W. K., Heijnen J. J., 2002. Analysis of glycolytic intermediates in *Saccharomyces cerevisiae* using anion exchange chromatography and electrospray ionisation with tandem mass spectrometric detection. *Anal Chem Acta.* 460, 209-218.

Van Hoek W. P. M., van Dijken J.P., Pronk J. T., 1998. Effect of specific growth rate on fermentative capacity of bakers Yeast. *Appl Environ Microbiol.* 64, 4226-4233.

Van Hoek W. P. M., 2000. Fermentative capacity in aerobic cultures of bakers' yeast. PhD Thesis. Technische Universiteit Delft.

Verduyn C., Postma E., Scheffers W. A., Van Dijken J. P., 1992. Effect of benzoic acid on metabolic fluxes in yeasts: a continuous culture study on the regulation of respiration and alcoholic fermentation. *Yeast.* 8, 501-517.

Visser D., van Zuylen G. A., van Dam J. C., Oudshoorn A., Eman M. R., Ras C., van Gulik W. M., Frank J., van Dedem G. W., Heijnen J. J., 2002. Rapid sampling for analysis of in vivo kinetics using the BioScope: a system for continuous pulse experiments. *Biotechnol Bioeng.* 79 (6), 674-681.

Visser D., 2002. Measuring and modeling in vivo kinetics of primary metabolism. PhD Thesis. Technische Universiteit Delft. 151-173.

Weibel K. E., Mor J. R., Fiechter A., 1974. Rapid sampling of yeast cells and automated assays of adenylate, citrate, pyruvate and glucose-6-phosphate pools. *Anal Biochem.* 58, 208-216.

Weichert C., Sauer U., Bailey J. E., 1997. Use of a glycerol-limited, long-term chemostat for isolation of *Escherichia coli* mutants with improved physiological properties. *Microbiol.* 143, 1567-1574.

Wick M. L., Quadroni M., Egli M., 2001. Short- and long-term changes in proteome composition and kinetic properties in a culture of *Escherichia coli* during transition from glucose-excess to glucose-limited growth conditions in continuous culture and vice versa. *Environ Microbiol.* 3(9), 588-599.

In vivo kinetics with rapid perturbation experiments in *Saccharomyces cerevisiae* using a 2nd Generation BioScope

Abstract

We present a robust 2nd generation BioScope: a system for continuous perturbation experiments. Firstly, the BioScope design parameters, (i.e. pressure drop, overall oxygen (O₂) and carbon dioxide (CO₂) mass transfer, mean residence time distribution and plug flow characteristics) were evaluated. The average overall mass transfer coefficients were estimated to be 1.8E-5 m.s⁻¹ for O₂ and 0.34E-5 m.s⁻¹ for CO₂. It was determined that the O₂/CO₂ permeable membrane accounted for 75% and 95% of the overall resistance for O₂ and CO₂ respectively. The Peclet number (Pe) of the system was found to be >500 for liquid flow rates between 1 and 4 mL.min⁻¹, ensuring plug flow characteristics. Secondly, steady state intracellular metabolite concentrations obtained using direct rapid sampling from the fermentor were compared with those obtained by rapid sampling via the pre-perturbation sample port of the BioScope. With both methods the same metabolite levels were obtained. Thirdly, glucose perturbation experiments were carried out directly in the fermentor as well as in the BioScope, whereby steady state *Saccharomyces cerevisiae* cells from a glucose/ethanol limited chemostat were perturbed by increasing the extracellular glucose concentration from 0.11 to 2.8 mM. Intracellular and extracellular metabolite levels were measured within a time window of 180 seconds. It was observed that the dynamic metabolite concentration profiles obtained from both perturbations were nearly the same, with the exception of the C4 metabolites of the TCA cycle, which might be due to differences in culture age.

To be submitted for publication in metabolic engineering.

Introduction

Recently metabolic engineering has taken centre stage in advancing modern industrial biotechnology progress and will undoubtedly continue to play a key role in its future development. Successful metabolic engineering efforts dedicated to rational improvement of cellular physiology through directed introduction of genetic changes using recombinant DNA technology relies on a thorough understanding of the *in vivo* regulation of complex metabolic networks and fluxes (Bailey, 1991; Nielsen, 2001). Understanding of microbial metabolism and its *in-vivo* kinetics requires accurate information concerning both intracellular and extracellular metabolite pool levels. Elucidation of the *in-vivo* kinetic properties of microbial metabolism can be obtained from short term dynamic experiments. These experiments are usually carried out by perturbing cells grown under well defined, steady state, conditions i.e. cultivated in a chemostat. To obtain accurate snapshots of metabolite concentrations during the highly dynamic conditions initiated by the perturbation, rapid sampling and fast quenching of metabolism is required. Weibel et al, 1974, reported a sampling technique for yeast cells with a very short time interval between harvesting and quenching of metabolism followed by extraction of intracellular metabolites. This method laid the foundation for quantitative analysis of the microbial metabolome. The method was further refined and automated by De Koning & van Dam 1992; Theobald et al, 1993; 1997; Gonzalez et al 1997; Schaefer et al, 1999; Visser et al, 2002; 2004. Measurements of intracellular metabolite concentrations during dynamic glucose perturbation experiments on yeast have successfully been performed (Theobald et al, 1993; 1997; Visser et al, 2002; Schmitz et al, 2002; Buchholz et al, 2002; Buziol et al, 2002).

Instead of perturbing the steady state chemostat culture a small second reactor coupled to a chemostat can be applied to carry out the actual dynamic experiment. Such a device, the BioScope, has been developed previously (Visser et al, 2002) and is based on a mini plug flow reactor equipped with sample ports at different positions. This system greatly facilitates perturbation experiments because the perturbation is applied outside the chemostat and hence the steady state is not disturbed. In the BioScope the perturbation starts when a small constant flow of broth from a chemostat is mixed with a constant flow of a perturbing agent such as, but not limited to glucose. Samples are collected at various locations along the plug flow reactor representing different residence times/reaction times. The 1st generation BioScope yielded satisfactory results but had some drawbacks. Some of the drawbacks were: 1) the design was based on serpentine construction of oxygen permeable silicone tubing (0.8 mm internal diameter). The construction was manual, hence very laborious and time consuming. 2) The serpentes were not identical, necessitating individual characterisation. 3) The serpentes were very sensitive because they were made from flexible silicone tubing therefore handling them would easily influence their characteristics. These drawbacks led to the design of the 2nd generation BioScope.

The presented research consists of three parts: Firstly, the characterisation of the design parameters, i.e. pressure drop, estimation of the overall oxygen and carbon dioxide mass transfer coefficient (K_{ov}), mean residence time distribution and plug flow characteristics. Secondly, steady state metabolite concentration levels obtained using direct rapid sampling from the fermentor were compared with those obtained by rapid sampling via the pre-perturbation sample port of the BioScope. Thirdly, we compared the results of glucose perturbations carried out on a steady state chemostat culture of *S. cerevisiae* and in the BioScope.

Materials and Methods

Yeast strain, maintenance and preculture conditions

The haploid, prototrophic *Saccharomyces cerevisiae* strain CEN.PK113-7D was kindly provided by Dr. P. Kötter (Frankfurt, Germany). Precultures were grown to stationary phase in shake-flasks on mineral medium (Verduyn et al, 1992), adjusted to pH 6.0 and containing 2 % (w/v) glucose. After adding glycerol (30 %v/v), 2 mL aliquots were stored at $-80\text{ }^{\circ}\text{C}$ in sterile vials. These frozen stocks were used to inoculate precultures for chemostat cultivation.

Precultures were grown overnight in 100 mL of mineral medium (Verduyn et al, 1992), contained in 500 mL Erlenmeyer flasks at 30°C with shaking at 220 RPM in an incubator shaker (New Brunswick, New Jersey, USA).

Chemostat cultivation

Aerobic glucose/ethanol limited chemostat cultures were grown at a dilution rate (D) of 0.05 h^{-1} in 7 L laboratory fermentors with a working volume of 4 L (Applikon, Schiedam, The Netherlands) as reported previously (Lange et al, 2001). The synthetic feed medium used was based on the medium described by Verduyn et al, (1992) and contained as carbon source a mixture of 75 mM glucose and 15.5 mM ethanol. The addition of ethanol successfully prevented the culture from metabolic oscillations. The biomass concentration supported by this medium is approximately $7.2\text{ g. L}^{-1} \pm 2\%$. The dissolved oxygen tension (DOT) in the fermentor during steady state condition was measured but not controlled and was always above 80 % saturation. The aeration rate of the reactor was 1.7 L. min^{-1} . The reactor was operated at an over pressure of 0.3 bars. The stirrer speed was 600 RPM, and the temperature was controlled at $30\text{ }^{\circ}\text{C}$. The pH of the culture was controlled at 5.0 by automatic titration with 4 M KOH.

BioScope construction

The 2nd generation BioScope design is based on two hemi spherical channels with a diameter of 1.2 mm milled in a Perspex block, separated by a silicone membrane of 0.6 mm thickness that allows diffusion of O_2 and CO_2 (Fig 1A-B). The channel is configured according to a two

dimensional (2D) serpentine geometry, ensuring plug-flow characteristics. The surface to area ratio is $2122 \text{ m}^2/\text{m}^3$. The total volume is 3.46 mL ; the total channel length is 6.51 m . The BioScope block is placed in a temperature controlled cabinet. The sampling ports are located at the following distances in meters relative to the substrate addition point: -0.09 ; 0.27 ; 0.54 ; 0.8 ; 1.1 ; 1.5 ; 1.9 ; 2.6 ; 3.3 ; 4.9 and 6.5 corresponding to sampling ports 1 to 11 respectively as indicated in figure 1B. Sampling port 1 is the pre-perturbation port and allows sampling of the broth shortly before addition of the perturbing agent. The serpentine channels are connected with each other and with the sampling needles via pieces of flexible silicone tubing with an internal diameter of 0.8 mm . These flexible connecting tubing's were necessary for the two way pinch valves allowing automatic sample collection. This design offers robust and precise channel geometry with the possibility and flexibility of manipulating the gas phase composition in the gas channel, e.g. instantaneous transition from aerobic to anaerobic conditions. This drastically increases the possibility to subject the biomass to different perturbations. Different perturbations lead to much richer data sets, which facilitate the estimation of kinetic parameters.

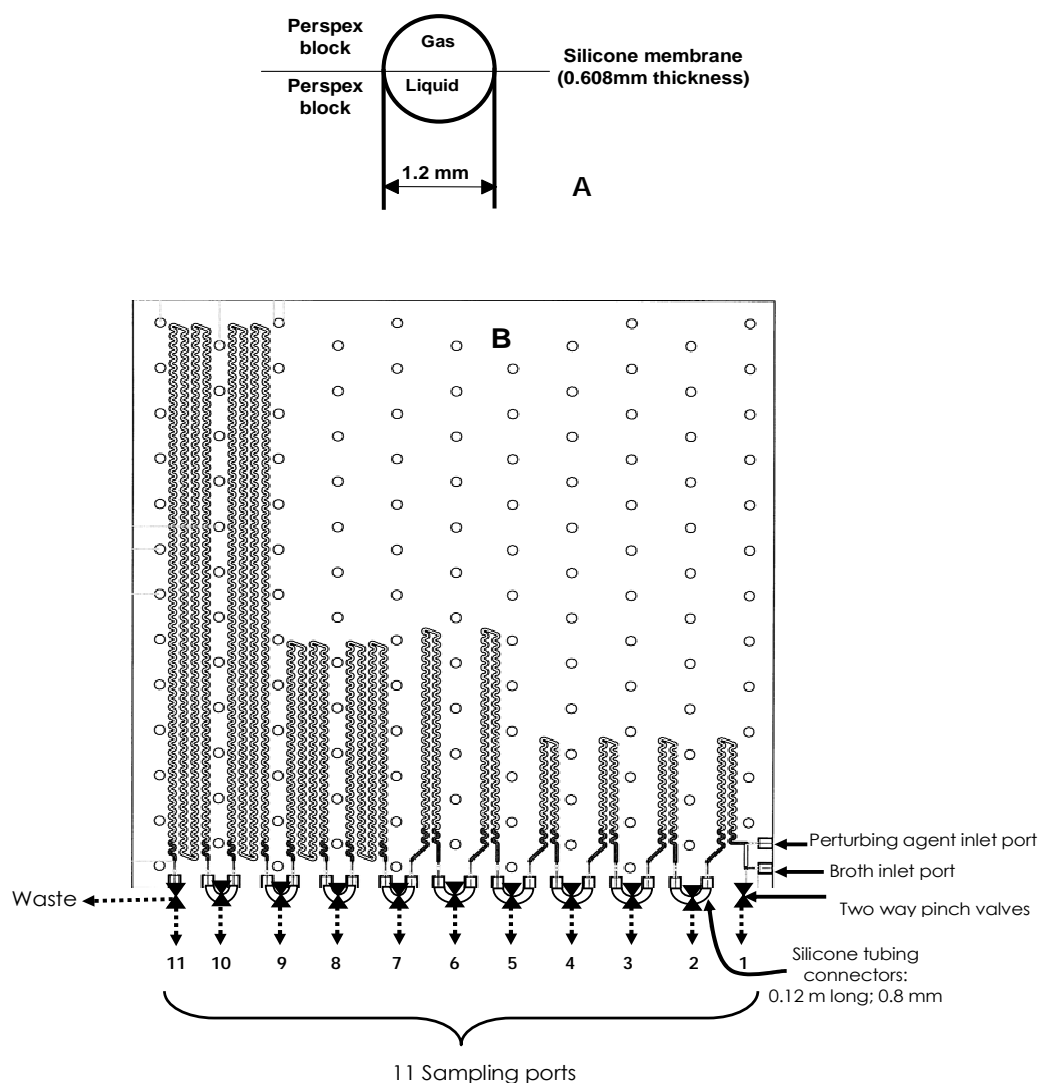


Figure 1 A. Cross section of the BioScope channel; B. 2D serpentine channel geometry of the BioScope.

Measurement of residence time distributions of the BioScope

Residence time distributions were measured at different liquid flow rates by applying a step change in salt concentration at the entrance of the BioScope combined with conductivity measurements at all sample ports according to Visser et al (2002). Two reservoirs, containing water and 0.5 M KCl solution were connected to the BioScope respectively. A peristaltic pump (Ismatec, ISM 930, ISMATEC SA, Labortechnik, CH-8152, Glattenbrugg-Zurich, Switzerland) was used to feed both solutions to the BioScope at constant flow rates. A continuous flow of water was fed to the system via the broth entrance port. An additional flow of water was fed to the system via the entrance port for the perturbation solution at a flow rate which was 10% of the total flow rate. Then at $t=0s$, the additional flow of water was instantaneously changed to a 0.5 M KCl solution, while keeping the flow rate at the same value. This was done by means of a computer controlled two way valve (3/2 solenoid valve S305-05 E63 12 VDC, A&E Engineering). These experiments were carried out for total flow rates of 1, 2, and 4 mL.min⁻¹. A flow through conductivity cell was connected to the outlet of the sampling port of the BioScope to be measured. The conductivity of the liquid stream flowing through this cell was measured using an ED40 Electrochemical detector (Dionex Sunnyvale, CA, USA). The experiment was repeated at least five times per sampling port and was conducted for all eleven sampling ports of the BioScope. The residence time distribution of the conductivity cell itself was measured separately using the same method. This was necessary for the correction of the measured residence time distribution of the different sampling ports for dispersion caused by the conductivity cell. The residence time and the Peclet number were calculated according to Visser et al (2002).

Mass transfer experiments with H₂O and broth

Deoxygenated water (N₂ saturated) in a 2 L stirred vessel maintained at 30 °C was continuously fed to the broth entrance of the BioScope at a flow rate of 2 mL.min⁻¹. Simultaneously the gas channel was continuously flushed with air (20.95 % oxygen) at a constant gas flow rate of 130 mL. min⁻¹. The dissolved oxygen tension (DOT) of the liquid stream was measured in all the sampling ports of the BioScope using a flow through cell in which the dissolved oxygen probe (Mettler Toledo) was mounted. During the experiment, it was ensured that no oxygen transfer occurred via the connecting tube between the deoxygenated stirred vessel and the BioScope by using thick walled (4 mm) marprene oxygen impermeable tubing with an internal diameter of 0.9 mm. The experiment was repeated with fully oxygenated water (air saturated) as described above, while the gas channel part of the BioScope was continuously flushed with N₂ gas at a constant flow rate of 130 mL.min⁻¹. The dissolved oxygen tension (DOT) was measured at every sample port as described above. The overall oxygen mass transfer coefficient (K_{ov}) was estimated from the measured DOT profiles using equation 5 below.

Fermentation broths can show different O₂ transfer properties than water. Therefore, similar experiments as described above were carried out with carbon starved non-respiring *S.*

cerevisiae culture broth. Starved broth was prepared by chemostat cultivation of *S. cerevisiae* to steady state, and subsequently switching off the medium feed pump, followed by a starvation period of minimally three days. Non respiring conditions were satisfied when there was negligible O₂ consumption and CO₂ production. These conditions were confirmed by measurement of the CO₂ and O₂ concentrations in the off gas. Subsequently the fully oxygenated (air saturated) starved broth was continuously fed to the broth entrance of the BioScope at a flow rate of 2 mL.min⁻¹ while the gas channel was continuously flushed with N₂ gas at a constant flow rate of 130 mL.min⁻¹. The dissolved oxygen tension (DOT) of the carbon starved non-respiring yeast culture broth was measured at every sample port as described above. The overall oxygen mass transfer coefficient (K_{ov}) was estimated from the measured DOT profile using equation 5 below.

Estimation of the oxygen (O₂) overall mass transfer coefficient (K_{ov}) of the BioScope

The cross sectional area (A) of the liquid channel of the BioScope which is a semi circle is given by:

$$A = \frac{1}{8} * \pi * D_i^2 \quad (1)$$

Where; D_i= internal diameter of the channel, which is 1.2 E-3 m

The gas exchange area (a) of an infinitesimal element of length (dx) of the BioScope channel is given by:

$$a = D_i * dx \quad (2)$$

The steady state oxygen mass balance for this infinitesimal element is written in the absence of O₂ consumption as:

$$\Phi_v * C_{O_{2,L}} - \Phi_v * (C_{O_{2,L}} + dC_{O_{2,L}}) + k_{ov} * D_i * dx * (C_{O_{2,L}}^* - C_{O_{2,L}}) = 0 \quad (3)$$

This can be rewritten as:

$$-\Phi_v * \frac{dC_{O_{2,L}}}{dx} + k_{ov} * D_i * (C_{O_{2,L}}^* - C_{O_{2,L}}) = 0 \quad (4)$$

From the mass balance for oxygen (equation 4), the relation for the dissolved oxygen concentration as a function of the channel length (x) can be derived with the superficial liquid

velocity $\left(v = \frac{\Phi * 8}{\pi * D_i^2} \right)$:

$$C_{O_{2,L}}(x) = C_{O_{2,L}}^* - \exp\left(\frac{-8 * K_{ov} * X}{v * \pi * D_i}\right) * (C_{O_{2,L}}^* - C_{O_{2,L}}) \quad (5)$$

When the gas phase contains N_2 , $C^*_{O_2,L} = 0$, while for air, $C^*_{O_2,L} = 0.245 \text{ mmol. L}^{-1}$ at 30°C . The parameter k_{O_2} was estimated from the measured DOT profiles by a least squares fit (Matlab, The Mathworks, Inc).

Aerobic glucose perturbation in the BioScope

A continuous flow of culture broth from a chemostat was introduced in the BioScope and mixed at a ratio of 1:9 with a continuous flow of aerated 28 mM glucose solution maintained at 30°C to reach an initial glucose concentration of 2.8 mM. The flow rate of the glucose solution was 0.1 mL. min^{-1} and that of the culture broth was 0.9 mL. min^{-1} giving a total flow rate of 1 mL. min^{-1} . With this flow rate the total residence time in the BioScope was 180 seconds. The broth and the glucose solution were pumped using two independent high precision peristaltic pumps (Ismatec, ISM 930, ISMATEC SA, Labortechnik, CH-8152, Glattenbrugg-Zurich, Switzerland). During the experiment the gas channel of the BioScope was continuously flushed with air (20.95 % O_2) at a constant flow rate of 130 mL. min^{-1} . At this airflow rate the O_2 concentration was close to 21% and the CO_2 concentration was close to 0% allowing maximum O_2 transfer and CO_2 removal. Before samples were collected; the BioScope system was operated for at least five residence times (15 minutes) to allow it to stabilize. Automatic sampling was manually started through computer aided activation of the sequentially positioned, two way magnetic pinch valves (Fig 1B). The sampling and quenching procedure for determination of intracellular metabolites was the same as described previously (Visser et al, 2002).

Aerobic glucose perturbation in the fermentor

The same steady state chemostat culture of *Saccharomyces cerevisiae* which had been used to feed the BioScope for the glucose perturbation experiments was perturbed by injection of 20 mL of a 100 g.L^{-1} glucose solution in less than one second. This resulted in an instantaneous increase of the residual glucose concentration from approximately 0.11 mM to 2.8 mM. Rapid injection of the glucose solution was performed with a custom build pneumatic device. Before injection of the glucose solution, 2 rapid samples were taken to determine the steady state metabolite concentrations. Directly after injection of the glucose solution a series of 12 rapid samples were collected during a period of 180 seconds.

Rapid sampling procedures

The applied procedure for rapid sampling and quenching of broth from the chemostat for determination of intracellular metabolites has been described previously (Wu et al, 2005). Also the applied procedure for rapid sampling and quenching of broth from the chemostat for determination of extracellular metabolites (glucose, ethanol and acetate) has been described previously (Mashego et al, 2003).

The sampling and quenching procedure for determination of extracellular metabolites (glucose, ethanol and acetate) during a glucose perturbation experiment carried out with the BioScope was adapted from Mashego et al, (2003). Approximately 2 mL of broth was collected from each sample port of the BioScope into polystyrene sampling tubes with a diameter of 17 mm containing 31g stainless steel beads (4 mm diameter) kept at a temperature of 0 °C in a cryostat (Lauda RK 20 KS, Lauda-kÖningshofen, Germany). As the total flow rate through the BioScope was 1 mL.min⁻¹ the withdrawal of one sample took 2 minutes. At the end of the sample collection period, the contents of the tubes (quenched sample with beads) were transferred to a precooled (4 °C) syringe (30 mL) connected to a 0.45 µm pore size filter (Gelman, Ann Arbor, Michigan, USA) followed by immediate separation of cells and medium by filtration. Samples were stored at -80 °C until analysis.

Metabolite extraction

Intracellular metabolites were extracted from the biomass using the boiling ethanol method as described previously (Mashego et al, 2004; Wu et al, 2005). Before extraction 100 µL of 100% U-¹³C- labelled cell extract was added as internal standard.

Analytical procedures

Biomass dry weight concentration was determined as described previously (Mashego et al, 2005).

Residual glucose analysis was performed spectrophotometrically (Agilent 8453-UV-visible spectroscopy system, Waldbronn, Germany) using (R-Biopharm AG, D-glucose Kit no E0716251, Darmstadt, Germany) according to the manufacturer's instructions.

Acetate and ethanol were analysed by gas chromatography (GC), (chrompack CP 9001, Hewlett Packard, USA) equipped with a liquid sampler flame ionisation detector (FID) (CP 9010, Hewlett Packard, USA). The GC was equipped with a Hewlett Packard HP column of 15 m in length, 0.53 internal diameter and 1.0 µm film thickness. The carrier gas was Helium and the pressure was 70kPa. The conditions for ethanol analysis were as follows: column temperature: 70 °C, injection temperature of 180 °C, detector temperature of 200 °C. The injected sample volume was 0.5 µL. Acetate analysis conditions were similar to the ethanol analysis conditions mentioned above except that the column temperature was 120 °C.

Glycolytic and TCA-cycle intermediates were measured with isotope dilution LC-ESI-MS/MS (IDMS) according to Wu et al, (2005).

Results and Discussion

Pressure drop, mean residence time distributions and Plug flow characteristics of the BioScope

The pressure drop over the liquid channel of the BioScope was measured at each sample port for different flow rates. The results are shown in figure 2A. It can be seen from this figure that, as

expected, the pressure drop increased with increased liquid flow rate and channel length. At the highest liquid flow rate of 6 mL min⁻¹ the measured pressure drop over the entire liquid channel was 1.5 bar. As this value is significantly lower than the maximum pump pressure of 2 bars a stable flow rate could still be obtained. The mean residence time distribution and the Peclet number (Pe), which is indicative for the plug flow characteristics of the BioScope, were also measured for different liquid flow rates. This was done by applying a step change in the salt concentration at the entrance of the BioScope and subsequently measuring the response at each sample port by means of a conductivity meter.

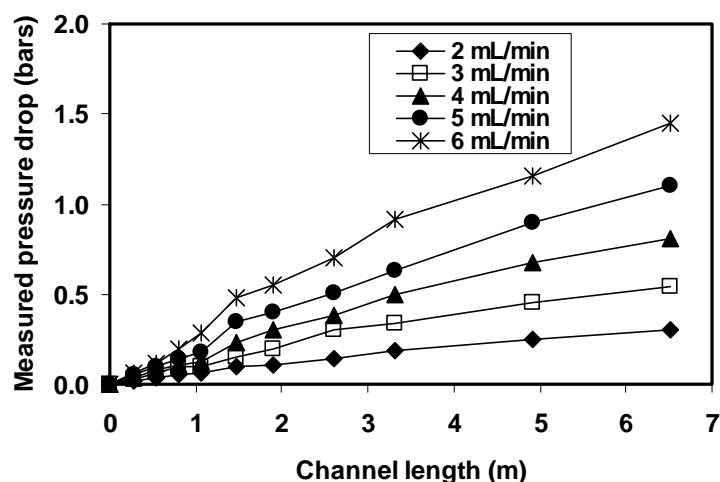


Figure 2A Measured pressure drop as a function of liquid velocity and channel length in the BioScope

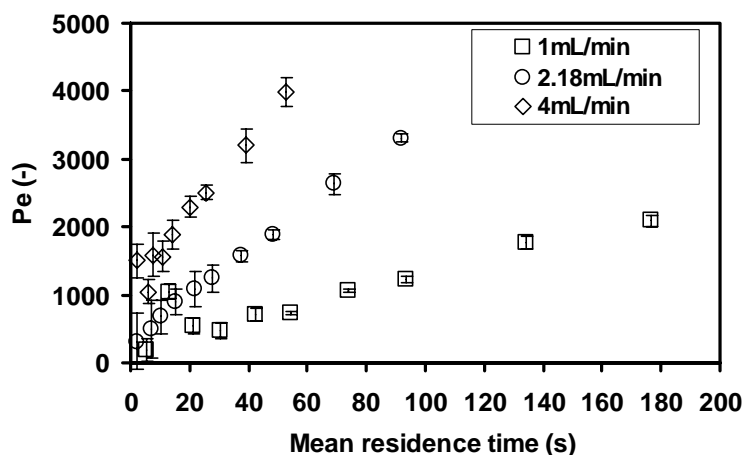


Figure 2B Estimated Peclet number (Pe) as a function of BioScope channel length and liquid velocity. Error bars represents standard deviations between five repeated experiments.

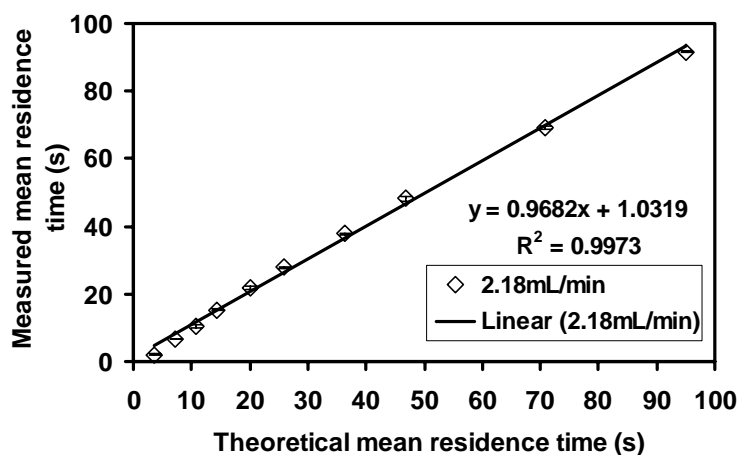


Figure 2C Theoretical mean residence time versus measured mean residence time.

Figure 2B represents Pe as a function of the mean residence time and liquid flow velocity. The value of Pe is a measure for the mixing characteristics of a reactor. It can be calculated that for $Pe > 30$ dispersion effects are negligible and thus plug flow characteristics are satisfied (Visser et al, 2002). The calculated values of Pe for the 2nd generation BioScope were found to be higher than 200 for all mean residence times and different liquid flow velocities (Figure 2B), thus satisfying the plug flow requirement of the new BioScope design. As can be seen from Figure 2B Pe increased with both the increase in liquid flow velocities and mean residence time. This BioScope design also satisfied the estimated theoretical mean residence times (Figure 2C).

Estimation of the overall oxygen mass transfer coefficient

From the measured dissolved oxygen concentration profiles the overall oxygen mass transfer coefficients (K_{ov}) were estimated (Figures 3A-B).

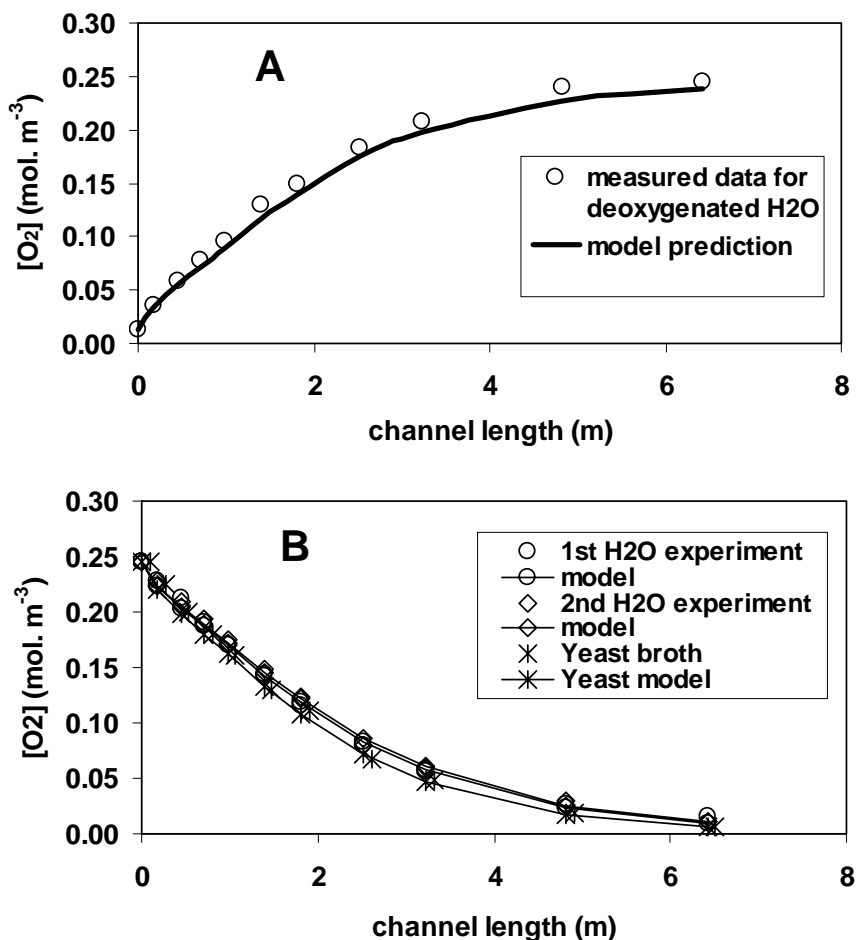


Figure 3 Measured and fitted dissolved oxygen concentration profiles as a function of BioScope channel length.

In addition to H₂O also carbon starved non respiring broth was used in the experimental determination of the overall oxygen mass transfer coefficient (K_{ov}) of the 2nd generation

BioScope. Yeast broth was expected to give the most reliable value for K_{ov} since it represents as close as possible the experimental conditions, with respect to dissolved compounds and rheological characteristics. After the deoxygenated water enters the BioScope, the dissolved oxygen concentration in the deoxygenated water increases, because oxygen is transferred from the gas channel, via the membrane, to the liquid channel. A typical pattern of the measured dissolved oxygen concentrations at the different sample ports when deoxygenated water is fed to the BioScope is shown in Figure 3A. Fig 3B shows the measured concentration profiles when oxygenated water/broth is fed to the BioScope while the gas channel is flushed with N_2 gas, leading to deoxygenation of the liquid. The overall oxygen mass transfer coefficient of this BioScope was estimated to be $1.8E-5 \text{ m}\cdot\text{s}^{-1} \pm 5\%$. Nearly the same values were found for deoxygenated H_2O and starved broth, also when oxygen transfer was in the opposite direction that is when fully air saturated H_2O or starved broth was introduced in the BioScope while passing N_2 gas through the gas channel (Table 1).

Table 1 Comparison of O_2 , CO_2 and overall mass transfer coefficients of the BioScope estimated from H_2O and starved yeast broth DOT measurements. (For the calculations, see Appendix A)

BioScope	H_2O		Yeast broth	
	O_2	CO_2	O_2	CO_2
K_m	2.42E-5	0.36E-5	2.42E-5	0.36E-5
K_L	7.18E-5	6.50E-5	7.18E-5	6.50E-5
K_{ov}	1.81E-5	0.34E-5	1.81E-5	0.34E-5

However, the K_{ov} value obtained for the present BioScope design appears to be lower than that of the 1st generation BioScope for which the overall oxygen transfer coefficient was measured to be $2.99E-5 \text{ m}\cdot\text{s}^{-1}$. This difference is most likely due to the differences in geometry of the two BioScope systems as well as the physical characteristics of the silicone flat membrane used in the 2nd generation BioScope compared to the silicone serpentine of the 1st generation BioScope. The gas transfer area per volume was also very different, i.e. $2122 \text{ m}^2 \cdot \text{m}^{-3}$ for the 2nd generation BioScope vs. $1591 \text{ m}^2 \cdot \text{m}^{-3}$ for 1st generation BioScope respectively. Using the O_2 permeability of the silicone membrane (Visser et al, 2002) it follows that the silicone membrane represents 75 % of the total resistance for O_2 transfer and 95 % of the CO_2 resistance (see Appendix A).

General observations for the chemostat during steady state conditions

Steady state conditions were assumed to be satisfied when there were no observable changes in the off gas carbon dioxide (CO₂) and oxygen (O₂) as well as in the dissolved oxygen concentration. During steady state conditions the measured concentrations of O₂ and CO₂ were 19.90 and 1.06 % respectively. The measured dissolved oxygen concentration was 0.20 mmol. L⁻¹. The dissolved CO₂ concentration was not measured but was calculated, based on the measured concentration in the off gas, to be approximately 0.50 mmol. L⁻¹. The specific carbon dioxide evolution rate (qCO₂) and oxygen uptake rate (qO₂) were calculated to be 0.034±2 % and 0.036±2 % mol. C-mol biomass⁻¹. h⁻¹ respectively and remained constant (data not shown). The carbon metabolism was fully respiratory as judged by the respiratory quotient (RQ) of 0.95±1%, which is expected for the mixed glucose/ethanol substrate used (data not shown). The value for q_{glucose} and q_{ethanol} were 0.013 mol. C-mol biomass⁻¹. h⁻¹ and 0.0028 mol. C-mol biomass⁻¹. h⁻¹ respectively. The redox and carbon balance closed at 100% and 101% respectively.

Comparison of the steady state metabolite levels of the cells harvested using two different sampling procedures

Stimulus response experiments require prior and precise definition of the reference physiological state of the cells, commonly referred to as steady state (Theobald et al, 1993; 1997; Visser et al, 2002). It is also of paramount importance that the physiological steady state of the culture is maintained upon transition from the chemostat to the BioScope. To verify this, intracellular metabolite levels in cells collected directly from the steady state chemostat by means of the rapid sampling technique (Lange et al, 2001) were compared with metabolite levels in cells collected via the pre-perturbation sample port of the BioScope. Samples were taken directly from the fermentor and via the BioScope within a time interval of approximately one hour. It should be noted that the main difference between direct sampling from the fermentor and via the BioScope system is that in case of direct rapid sampling the sample is withdrawn from the reactor in less than 0.7 second, whereas sample withdrawal via the BioScope requires 4 seconds which is the residence time of the broth in the channel between the chemostat and the pre-perturbation sample port of the BioScope. In Table 2 the results of the intracellular metabolite measurements are shown. The presented data are average values for 9 samples analysed in duplicate and are displayed with their 95% confidence intervals. It can be seen from Table 2 that the intracellular concentrations of almost all metabolites are slightly, but not significantly as judged by the overlap in their 95 % confidence intervals, higher in the cells sampled via the BioScope than in cells directly sampled from the chemostat. Malate is the only metabolite whose confidence interval did not overlap and the concentration in the steady state samples taken via the pre-perturbation sample port of the BioScope was significantly

higher. The reason for this is not clear yet. Overall it appears that the physiological state of the cells has not significantly changed upon transfer from the chemostat to the BioScope.

Table 2 Comparison of the intracellular metabolite concentration in samples collected directly from a steady state chemostat fermentor and using BioScope pre-perturbation sample port connected directly to the same chemostat. Data are averages of 9 samples analyzed in duplicate

Metabolite	Fermentor		BioScope	
	Average ($\mu\text{mol.gDW}^{-1}$)	95% confidence interval	Average ($\mu\text{mol.gDW}^{-1}$)	95% confidence interval
G6P	2.23	2.08-2.37	2.53	2.35-2.72
G1P	0.36	0.34-0.39	0.41	0.38-0.43
F6P	0.42	0.39-0.44	0.40	0.37-0.42
FBP	0.39	0.36-0.43	0.42	0.38-0.47
G3P	0.07	0.06-0.08	0.08	0.07-0.09
2/3PG	1.80	1.67-1.92	2.05	1.87-2.23
PEP	1.69	1.56-1.81	1.81	1.67-1.94
Pyruvate	0.12	0.10-0.13	0.16	0.13-0.19
Citrate	4.66	4.41-4.92	4.84	4.55-5.13
α -KG	0.23	0.21-0.25	0.31	0.28-0.34
Succinate	0.11	0.10-0.13	0.17	0.14-0.20
Fumarate	0.12	0.10-0.12	0.19	0.16-0.21
Malate	0.67	0.62-0.72	1.09	0.97-1.20
M6P	1.02	0.96-1.09	1.12	1.04-1.20
T6P	0.43	0.40-0.46	0.43	0.40-0.45
6PG	0.40	0.37-0.43	0.41	0.38-0.44

Glucose consumption during a glucose perturbation

During the glucose perturbations carried out in the fermentor as well as in the BioScope, the extracellular concentrations of glucose, ethanol and acetate were measured as a function of time. In both perturbation experiments the residual glucose concentration was increased instantaneously from a steady state value of 0.11 mM to 2.8 mM followed by a gradual decrease (Fig 4A). It can be seen from this figure that the measured concentration profiles for the BioScope and the fermentor are very similar. Furthermore, it can be inferred from these

patterns that the glucose uptake rate is not constant in time but that different phases can be distinguished. Directly after the addition of the glucose pulse a period of rapid glucose uptake can be observed (phase I), followed by a period of slower uptake (phase II) and again a period of fast uptake (phase III). From the measured concentration profiles, it can be calculated that the hexokinase flux increases 7 fold in phase I and III when compared to the steady state (Fig 4). In phase II, the hexokinase flux is only 4 fold higher compared to the steady state.

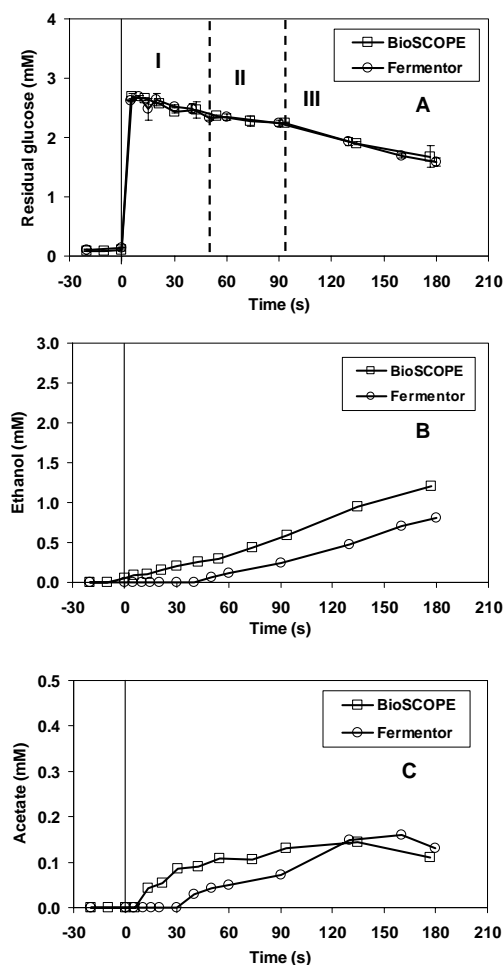


Figure 4 Residual glucose (A), ethanol (B) and acetate (C) concentration profiles during glucose perturbation to steady state culture of *S. cerevisiae* CEN.PK 113-7D in the BioSCOPE and the fermentor respectively. Error bars represents standard deviations between duplicate analyses of the same sample.

Excreted ethanol and acetate

The ethanol concentration profiles during the applied perturbations are also depicted in Fig 4B. A clear difference was observed between ethanol production in the BioSCOPE and the fermentor. In the BioSCOPE, ethanol accumulation was observed to start instantly after the start of the perturbation, whereas when the perturbation was carried out directly in the chemostat a

delay period of approximately 40 seconds was observed. A similar delay was also observed for acetate production (Fig 4C).

Intracellular metabolite dynamic responses during a glucose perturbation

Intracellular metabolite concentration profiles for both the BioSCOPE and the fermentor glucose perturbations are depicted in Figures 5-7.

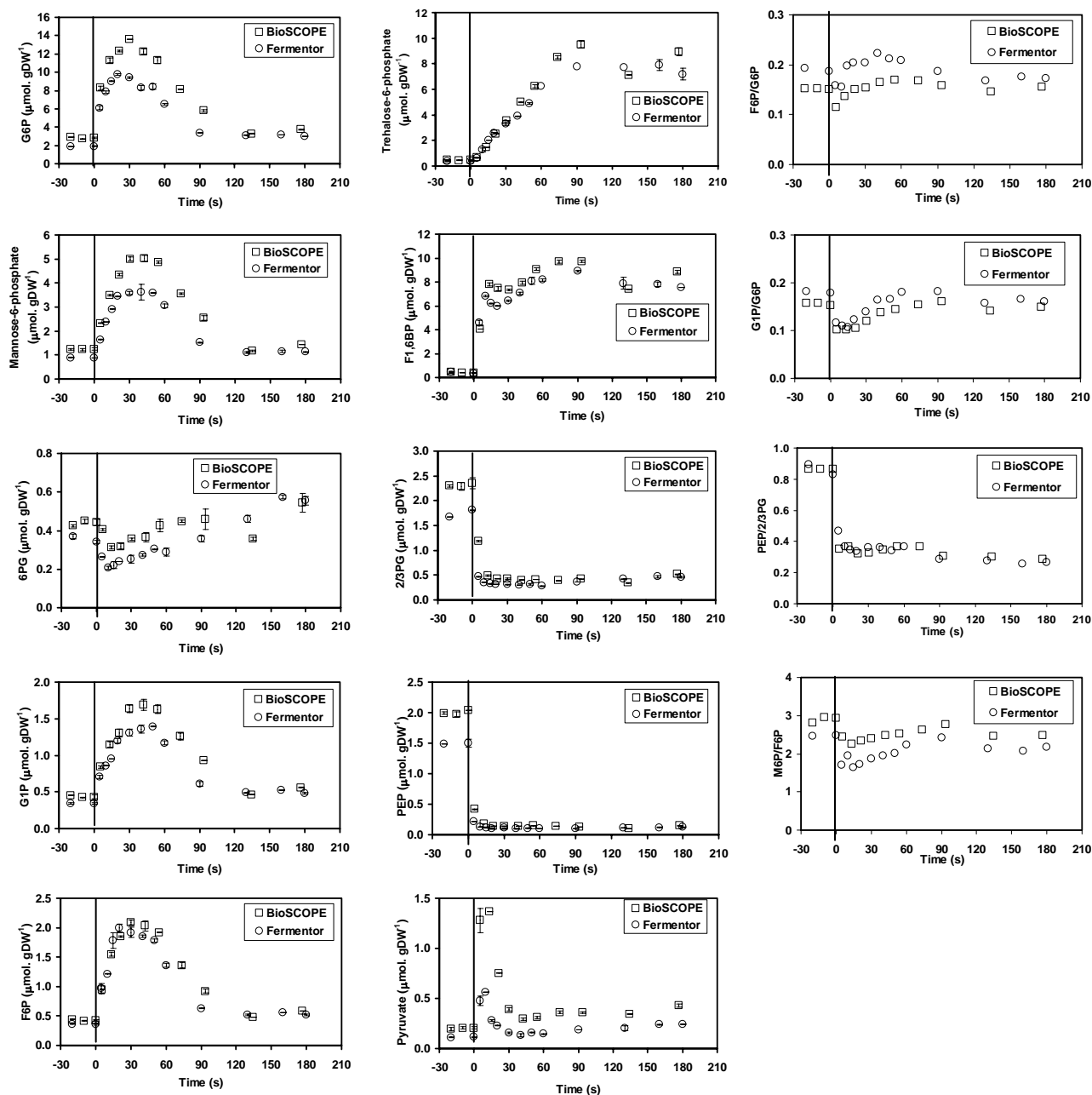


Figure 5 Intracellular glycolytic metabolites, mannose-6-phosphate (M6P), trehalose-6-phosphate (T6P) and 6-phosphogluconate (6PG) concentration profiles, mass action ratios of phosphoglucose isomerase (PGI), phosphoglucose mutase (PGM), enolase and phosphomannose isomerase (PMI) during a glucose perturbation to steady state chemostat culture of *S. cerevisiae* CEN.PK 113-7D in the BioSCOPE and fermentor respectively. Error bars represent standard deviations between duplicate analyses of the same sample.

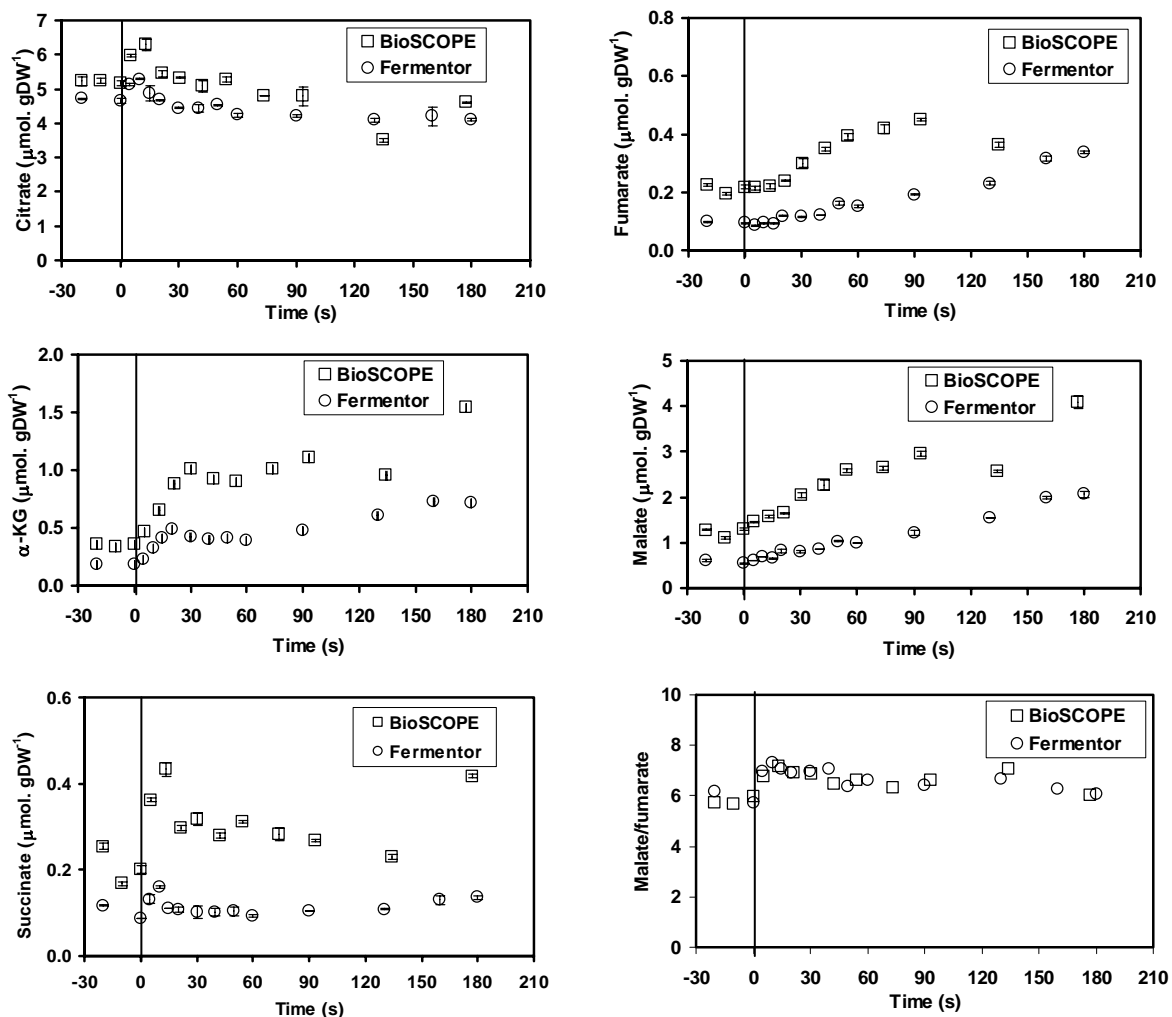


Figure 6 Intracellular TCA cycle metabolites concentration profiles and the mass action ratio of fumarase during a glucose perturbation to steady state chemostat culture of *S. cerevisiae* CEN.PK 113-7D in the BioSCOPE and fermentor respectively. Error bars represents standard deviations between duplicate analyses of the same sample.

It can be seen from these figures that there is a very close correspondence between the perturbation experiments in the BioSCOPE and the fermentor with respect to the glycolytic metabolite levels. However, the measured concentrations of the C4 intermediates of the TCA cycle during the perturbation experiment in the BioSCOPE are significantly higher than when the experiment is carried out in the fermentor. The origin of these differences (which include the above observed differences in the ethanol and acetate profiles) can be several. One hypothesis is that increased CO_2 levels lead to an increased flux through pyruvate carboxylase resulting in increased pools of the C4-metabolites of the TCA cycle. However, it was calculated that the dissolved CO_2 concentration (Appendix B) during the glucose perturbation experiment in the fermentor was 1.48 mM but in BioSCOPE only 1.04 mM. Therefore this explanation is very unlikely.

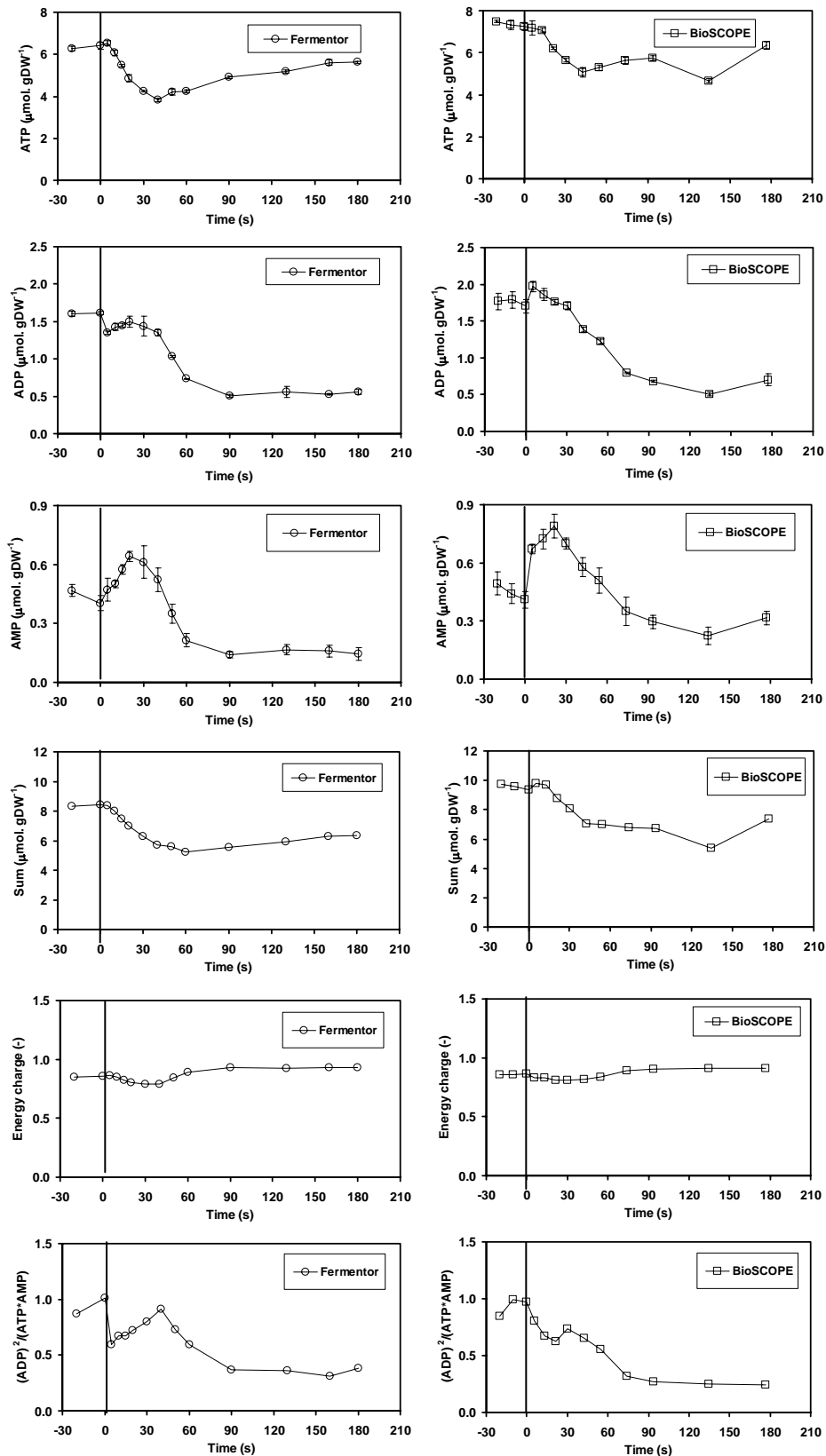


Figure 7 Intracellular adenine nucleotides (ATP, ADP, and AMP) concentration profiles, total sum (ATP+ADP+AMP), cellular energy charge and adenylate kinase mass action ratio during a glucose perturbation to steady state chemostat culture of *S. cerevisiae* CEN.PK 113-7D in the fermentor and in the BioSCOPE. Error bars represents standard deviations between duplicate analyses of the same sample.

Recently it has been observed (Mashego et al, 2005) that in prolonged glucose limited chemostat cultures, the concentrations of many primary metabolites decrease significantly with increasing culture age. In these experiments the fermentor perturbation has been performed 72 h after the BioScope perturbation, which represents 5 generations of growth. When considering that the steady state levels of these metabolites are already lower in the fermentor when compared to the BioScope, this generation difference is more likely to be responsible for the differences observed. This suggest that the observed differences can be attributed to the differences in biomass age, i.e. 8 generations in case of the BioScope perturbation experiment and 13 generations in the fermentor perturbation experiment.

During the first 30 seconds following the glucose perturbation there is a steady increase in intracellular glucose-6-phosphate (G6P), glucose-1-phosphate (G1P), fructose-6-phosphate (F6P), mannose-6-phosphate (M6P) and fructose-1, 6-bisphosphate (F1, 6BP). However, the concentration of G6P, G1P, F6P and M6P decreased after 30 seconds following the glucose perturbation and stabilizes at a new steady state concentration, which is slightly higher than during glucose/ethanol limited culture conditions (Fig 5). F-1, 6-BP concentration do not decrease but rather remains constant at a much higher level compared to the steady state concentration before the perturbation (Fig 5). To the contrary, the lower glycolytic pathway metabolites, i.e. 2/3-phosphoglycerate (2PG/3PG) and phosphoenolpyruvate (PEP) sharply decrease following the glucose perturbation. Pyruvate sharply increases in the first 5 seconds after the perturbation, followed by a steady decrease to slightly higher metabolite concentration level compared to the initial carbon limited steady state culture conditions (Fig 5). The dynamic behaviour of these glycolytic metabolites is very well comparable to those observed by other researchers (Buziol et al, 2002; Theobald et al, 1997; and Visser et al, 2002; Visser 2004), following a glucose perturbation to an aerobic carbon limited chemostat cultures of *S. cerevisiae*.

The concentration of trehalose-6-phosphate (T6P) increased linearly from 0.4 to 10 $\mu\text{mol.gDW}^{-1}$ (Fig 5). The concentration of 6-phosphogluconate (6-PG) dropped from the steady state value of 0.4 $\mu\text{mol.gDW}^{-1}$ to 0.2 $\mu\text{mol.gDW}^{-1}$, 5 seconds following the glucose perturbation (Fig 5). However, it started to increase and stabilised at 0.6 $\mu\text{mol.gDW}^{-1}$ after 150 seconds in both the BioScope and the fermentor. The decrease in 6-PG contradicts with the increase in its primary precursor G6P, suggesting that the in vivo activity of glucose-6-phosphate dehydrogenase (G6PDH) or the rate of this key irreversible pentose phosphate pathway enzyme is not affected by the increase in its substrate, while the in vivo activity of 6-phosphogluconate dehydrogenase (6PGDH) or the enzymes downstream of 6PG increased leading to the pulling or drainage of 6PG. These results contradict an earlier observation that 6PG concentration increases following the increase in G6P, when *S. cerevisiae* is exposed to a glucose perturbation (Vaseghi et al, 1998). The physiological relevance of this behaviour remains to be elucidated.

Mass action ratios of phosphoglucose isomerase (PGI); phosphoglucomutase (PGM); enolase and phosphomannose isomerase (PMI) were calculated as ratios of product to reactants/substrates from the measurements of the intracellular metabolites concentrations and are depicted in figure 5. Steady state mass action ratios of PGI and PGM were found to be between 0.2 and 0.18 respectively. These ratios were perturbed during glucose perturbations and dropped to as low as 0.1 but were quickly restored to the steady state level in less than 40 seconds following a perturbation (Fig 5). PGI mass action ratio is in good agreement with that of 0.2 and 0.29 reported previously (Tewari et al, 1988; Visser et al, 2004.) The rapid restoration of the steady state mass action ratios supports the notion that (PGI) and PGM functions near equilibrium and therefore is not an attractive target for metabolic engineering efforts aiming to increase the flux through this enzymes. Steady state mass action ratios of enolase and PMI were 0.9 and 2.8 respectively and were also perturbed by glucose perturbation (Fig 5). However, the mass action ratios of enolase did not return to the steady state values rather permanently decreased to 0.4 whereas that of PMI appeared to return to the steady state value (Fig 5).

Dynamic responses of the intracellular TCA cycle metabolites (citrate, α -ketoglutarate, succinate, fumarate and malate) and mass action ratio of fumarase are depicted in Fig 6. The concentration of citrate remains constant at 5 $\mu\text{mol.gDW}^{-1}$, whereas that of fumarate and malate increases significantly during a glucose perturbation in both the BioScope and the fermentor. Succinate increases and drops whereas α -KG increases. Mass action ratio of fumarase was perturbed by the glucose perturbation in both systems to the same extent but quickly restored its steady state value (Fig 6). Interestingly, the fumarase mass action ratio is perturbed (>1), which indicates a reversal of reaction from malate to fumarate. These points to a temporary functioning of the reductive branch of the TCA cycle.

Figure 7 represents intracellular adenine nucleotides (ATP, ADP and AMP) dynamic concentration profiles, total sum (ATP+ADP+AMP), the cellular energy charge and the adenylate kinase mass action ratio during a glucose perturbation carried out directly in the fermentor and in the BioScope. ATP concentration decreased instantly from steady state level of 6.5 to 3.8 $\mu\text{mol.gDW}^{-1}$ during the first 40 seconds following the glucose perturbation. The instant drop in ATP concentration is generally considered to be due to the high hexokinase/high upper glycolytic flux requiring ATP for the phosphorylation of glucose and F6P. After 40 seconds ATP increases steadily and reaches a steady state value 180 seconds after the glucose perturbation. ADP concentration also decreases in a similar way as that of the ATP from 1.7 to 0.5 $\mu\text{mol.gDW}^{-1}$ and remains constant at this low value. In contrast, AMP concentration increases instantly in the first 20 seconds of the perturbation from 0.5 to 0.7 $\mu\text{mol.gDW}^{-1}$, followed by a rather sharp decrease to the value of 0.2 $\mu\text{mol.gDW}^{-1}$, which is even lower than the steady state value before the perturbation (Fig 7). Total sum of ATP+AMP+ADP decreased from 9 to about 6 $\mu\text{mol.gDW}^{-1}$ and appeared to return towards the steady state levels at the end. The cellular energy charge (Atkinson 1968) during steady state was calculated to be 0.85 (Fig 7).

Also the cellular energy charge was slightly perturbed by the glucose perturbation during the period of 30 seconds. However, the energy charge is quickly restored to even a higher value of 0.93. This energy charge value has been reported previously for *S. cerevisiae* (Theobald et al, 1993, Mashego et al, 2005). Mass action ratio of adenylate kinase catalyzing the formation of ATP+AMP from 2ADP, was perturbed and dropped by 50% from 0.9 to 0.4 and remained low.

The physiological response and regulation of *S. cerevisiae* central carbon metabolism to glucose perturbation is summarized by a simplified scheme depicted in fig 8. The explanation to this dynamic metabolite response lies in the allosteric regulation of the three key glycolytic enzymes believed to catalyze irreversible reactions, i.e. hexokinase, phosphofructokinase and pyruvate kinase. Increasing hexokinase flux leads to simultaneous increase in the levels of G6P, F6P and F1, 6 BP while at the same time draining the level of ATP. High F1, 6BP and low ATP/AMP ratio stimulates pyruvate kinase activity leading to the instant drop in the pool of 2/3PG and PEP causing an instantaneous increase in pyruvate (Figs 5, 7). Increased F6P activate trehalose- 6-phosphate synthase leading to an increasing trehalose- 6-phosphate which in turn allosterically inhibit hexokinase activity (q_{glucose}) (Gancedo & Flores, 2004; Guillou et al, 2004; Bell et al, 1998; Hohmann et al, 1996; Blazquez et al, 1993). The inhibitory effect of T6P to hexokinase fit very well with the three apparent specific glucose uptake rates/phases as shown in Figure 4A (I; II and III).

Conclusions

The 2nd generation BioScope is a powerful and robust tool that widens the scope for elucidation of in-vivo kinetics through various perturbation experiments. The performance of the 2nd generation BioScope is found to be satisfactory. The main message presented in this paper is that we have designed a 2nd generation BioScope, which is more versatile and flexible e.g. it offers the possibility of manipulating the gas composition in the gas channel, leading to instantaneous switch from aerobic to anaerobic conditions. Furthermore, the maintenance of this 2nd generation BioScope is minimal. Also important design parameters of the 2nd generation BioScope such as plug flow characteristics and oxygen transfer were satisfied. Most importantly, the glycolytic metabolite responses of aerobic glucose/ethanol limited chemostat culture of *S. cerevisiae* to glucose perturbation carried out in the BioScope do show nearly the same concentrations to that when performed directly in the fermentor itself. This holds also for the pentose phosphate pathway (6PG). This shows that the BioScope and the fermentor are identical. The only differences are in the excreted ethanol, acetate and the concentration of C4 TCA cycle intermediates. A possible explanation is that the biomass used in the fermentor perturbation was 5 generations older than the biomass used in the BioScope (8 generations).

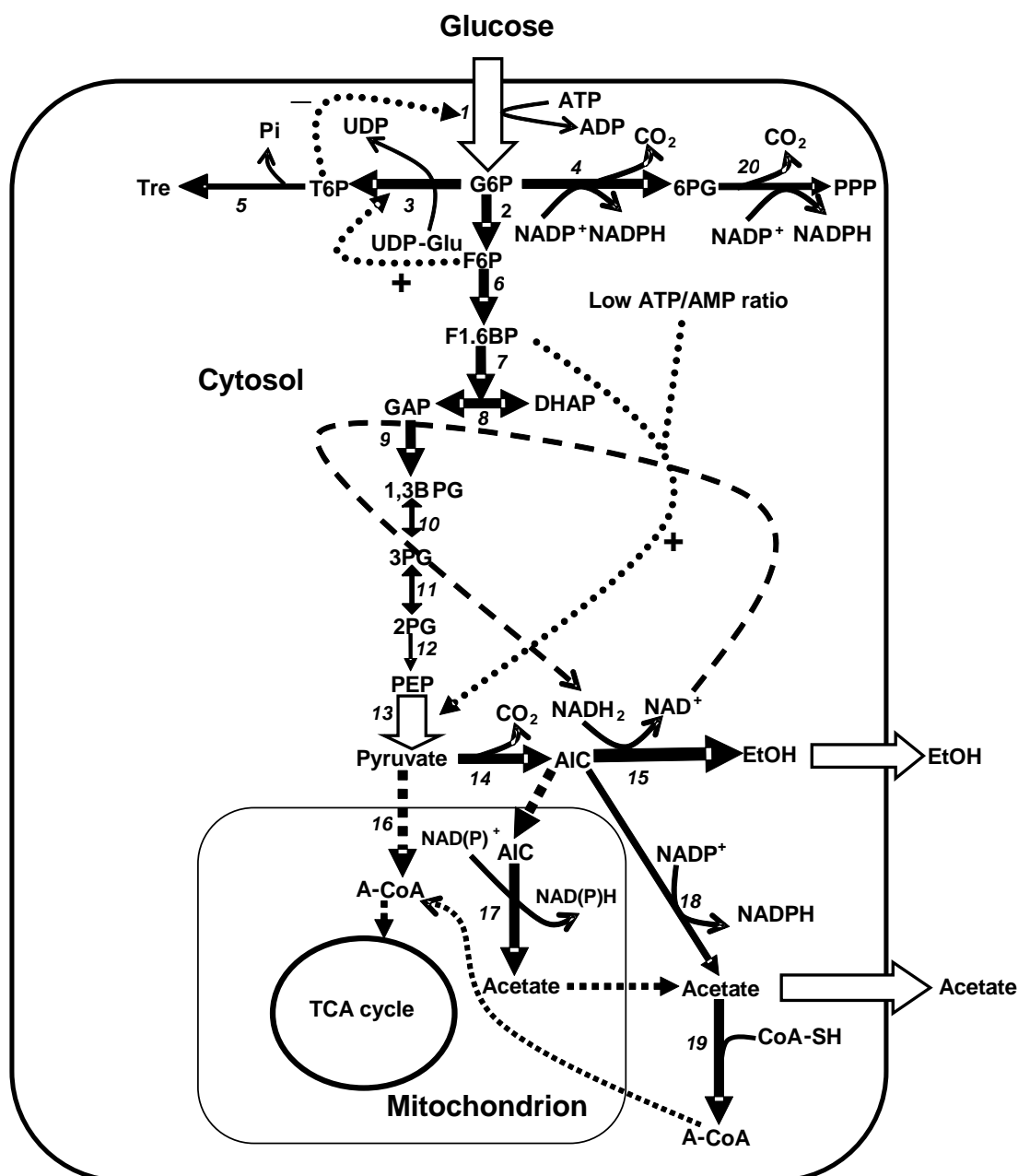


Figure 8 Simplified metabolic network scheme of the primary carbon metabolism in *S. cerevisiae*. Key: (1), Hexokinase); (2) Phosphoglucose isomerase; (3) Trehalose-6-phosphate synthase; (4) Glucose-6-phosphate dehydrogenase; (5) Trehalose- 6-phosphate phosphatase; (6) Phosphofruktokinase; (7) Aldolase; (8) Triosephosphate isomerase (9) Glyceraldehyde-3-phosphate dehydrogenase; (10) Phosphoglycerate kinase; (11) Phosphoglycerate mutase; (12) Enolase; (13) Pyruvate kinase; (14) Pyruvate decarboxylase; (15) NADH dependent alcohol dehydrogenase; (16) Pyruvate dehydrogenase complex; (17) Mitochondrial NAD(P)⁺ dependent acetaldehyde dehydrogenase; (18) Cytosolic NADP⁺ dependent acetaldehyde dehydrogenase (19) (Acetyl CoA synthetase); (20) 6-phosphogluconate dehydrogenase; CoA-SH (Coenzyme A); AIC (Acetaldehyde)

Acknowledgements

We would like to acknowledge Rob Kerste, Geerts Dirk and Tom for technical assistance. Angie ten Pierick; Cor Ras; Jan van Dam; Max Zomerdijk and Johan Knoll for analytical work. Applikon BV (The Netherlands) and DSM Limited (The Netherlands) and NWO for financing the Project

References

Atkinson D.E. 1968. The energy charge of the adenylate pool as a regulatory parameter. Interaction with feedback modifiers. *Biochem. J.* 7 (11), 4029-4034.

Bailey J.E., 1991. Toward a science of metabolic engineering. *Science.* 252, 1668-1675.

Bell W., Sun W., Hohmann S., Wera S., Reinders A., De Virgilio C., Wiemken A., Thevelein J.M., 1998. Composition and functional analysis of the *Saccharomyces cerevisiae* trehalose synthase complex. *J. Biol. Chem.* 273(50), 33311-33319.

Blazquez M.A., Lagunas R., Gancedo C., Gancedo J.M., 1993. Trehalose-6-phosphate, a new regulator of yeast glycolysis that inhibits hexokinases. *FEBS Lett.* 329(1-2), 51-4.

Buchholz A., Hurlbaus J., Wandrey C., Takors R., 2002. Metabolomics: Quantification of intracellular metabolite dynamics. *Biomol Eng.* 19, 5-15.

Buziol S., Bashir I., Baumeister A., Claassen W., Noisommit-Rizzi N., Maillinger W., Reuss, M., 2002. New bioreactor-coupled rapid stopped flow sampling technique for measurements of metabolite dynamics on a sub-second time scale. *Biotechnol Bioeng.* 80(6), 632-636.

Côté P., Bersillon J.L., Huyard A., 1989. Bubble-free aeration using membranes: mass transfer analysis. *J Memb Sci.* 47, 91-106

De Koning W. van Dam K., 1992. A method for the determinations of changes of glycolytic metabolites in yeast on a subsecond time scale using extraction at neutral pH. *Anal Biochem.* 204, 118-123.

Gancedo C., Flores C. L., 2004. The importance of a functional trehalose biosynthetic pathway for the life of yeasts and fungi. *FEMS Yeast Res.* (4-5), 351-359.

Gonzalez B., Francois J., Renaud M., 1997. A rapid and reliable method for metabolite extraction in yeast using boiling buffered ethanol. *Yeast.* 13, 1347-1356.

Guillou V, Plourde-Owobi L., Parrou J. L., Goma G. François J. 2004. Role of reserve carbohydrates in the growth dynamics of *Saccharomyces cerevisiae*. FEMS Yeast Res. 4(8), 773-787.

Hohmann S., Bell, W., Neves M.J., Valckx D., Thevelein J.M., 1996. Evidence for trehalose-6-phosphate-dependent and -independent mechanisms in the control of sugar influx into yeast glycolysis. Mol Microbiol. 20(5), 981-91.

Lange H.C., Eman M., van Zuijlen G., Visser D., van Dam J.C., Frank J., Teixeira de Mattos M.J., Heijnen J.J., 2001. Improved rapid sampling for in vivo kinetics of intracellular metabolites in *Saccharomyces cerevisiae*. Biotechnol Bioeng. 75 (4), 406-415.

Mashego M.R., van Gulik W.M., Vinke J.L., Heijnen J.J., 2003. Critical evaluation of sampling techniques for residual glucose determination in carbon-limited chemostat culture of *Saccharomyces cerevisiae*. Biotechnol Bioeng. 83 (4), 395-399.

Mashego M.R., Wu L., Van Dam J.C., Ras C., Vinke J.L., Van Winden W.A., Van Gulik W.M., Heijnen J.J., 2004. MIRACLE: mass isotopomer ratio analysis of U-¹³C-labeled extracts. A new method for accurate quantification of changes in concentrations of intracellular metabolites. Biotechnol Bioeng. 85, 620-628.

Mashego M. R., Jansen M. L.A., Vinke J. L., van Gulik W.M., Heijnen J.J., 2005. Changes in the metabolome of *Saccharomyces cerevisiae* associated with evolution in aerobic glucose-limited chemostats. FEMS Yeast Res. 5, 419-430.

Nielsen J., 2001. Metabolic engineering. Appl Microbial Biotechnol. 55, 263-283.

Schaefer U., Boos W., Takors R., Weuster-Botz D., 1999. Automated sampling device for monitoring intracellular metabolite dynamics. Anal Biochem. 270, 88-96.

Schmitz M., Hirsch E., Bongaerts J., Takors R., 2002. Perturbation experiments as a prerequisite for the quantification of in vivo enzyme kinetics in aromatic amino acid pathway of *Escherichia coli*. Biotechnol Progr. 18, 935-941.

Tewari YB., Steckler DK., Goldberg RN., 1988. Thermodynamics of isomerization reactions involving sugar phosphates. J Biol Chem. 263(8), 3664-3669.

Theobald U., Mailinger W., Reuss M., Rizzi M., 1993. In vivo analysis of glucose-induced fast changes in yeast adenine nucleotide pool applying a rapid sampling technique. *Anal Biochem.* 214, 31-37.

Theobald U., Mailinger W., Baltés M., Reuss M., Rizzi M., 1997. In vivo analysis of metabolic dynamics in *Saccharomyces cerevisiae*: I. Experimental observations. *Biotechnol Bioeng.* 55, 305-316.

Vaseghi S., Baumeister A., Rizzi M., Reuss M., 1999. In vivo dynamics of the pentose phosphate pathway in *Saccharomyces cerevisiae*. *Metab Eng.* 1 (2), 128-140.

Van Dam J.C., Eman M.R., Frank J., Lange H.C., van Dedem G.W.K., Heijnen J.J., 2002. Analysis of glycolytic intermediates in *Saccharomyces cerevisiae* using anion exchange chromatography and electrospray ionisation with tandem mass spectrometric detection, *Anal Chem Acta.* 460, 209-218.

Verduyn C., Postma E., Scheffers W.A., van Dijken J.P. (1992) Effect of benzoic acid on metabolic fluxes in yeasts: a continuous-culture study on the regulation of respiration and alcoholic fermentation. *Yeast* 8, 501–517.

Visser D., van Zuylen G. A., van Dam J.C, Eman M.R., Pröll A., Ras C., Wu L., van Gulik W.M., Heijnen J.J., 2004. Analysis of in vivo kinetics of glycolysis in aerobic *Saccharomyces cerevisiae* by application of glucose and ethanol perturbations, *Biotechnol Bioeng.* 88 (2), 157-167.

Visser D., van Zuylen G.A., van Dam J.C., Oudshoorn A., Eman M.R., Ras C., van Gulik W.M., Frank J., van Dedem G.W., Heijnen J.J., 2002. Rapid sampling for analysis of in vivo kinetics using the BioScope: a system for continuous perturbation experiments. *Biotechnol Bioeng.* 79 (6), 674-681.

Verduyn C., Postma E., Scheffers W.A., Van Dijken J.P., 1992. Effect of benzoic acid on metabolic fluxes in yeasts: A continuous culture study on the regulation of respiration and alcoholic fermentation. *Yeast.* 8, 501-517.

Weibel K.E., Mor J.R., Fiechter A., 1974. Rapid sampling of yeast cells and automated assays of adenylate, citrate, pyruvate and glucose-6-phosphate pools. *Anal. Biochem.* 58, 208-216.

Wu L., Lange H. C., van Gulik W. M., Heijnen J. J., 2003. Determination of in Vivo oxygen uptake and carbon dioxide evolution rates from off-gas measurements under highly dynamic conditions. *Biotechnol Bioeng.* 81 (4), 448-458

Wu L., Mashego M. R., van Dam J. C., Proell A. M., Vinke J.L., Ras C., van Winden W. A., van Gulik W.M., Heijnen J. J., 2005. Quantitative analysis of the microbial metabolome by isotope dilution mass spectrometry using uniformly ^{13}C -labeled cell extracts as internal standards. *Anal. Biochem.* 336, 164-171.

Appendix A. Mass transfer properties of the BioScope

The overall mass transfer coefficient (K_{overall}) resistance in the BioScope based on the resistance in series model is given by equation (A1) (Côté et al, 1989)

$$\frac{1}{K_{\text{ov}}} = \frac{1}{K_{\text{m}}} + \frac{1}{K_{\text{L}}} + \frac{1}{K_{\text{g}}} \quad (\text{A1})$$

Where,

K_{ov} = overall mass transfer coefficient

K_{m} = membrane transfer coefficient

K_{L} = liquid transfer coefficient

K_{g} = gas transfer coefficient,

K_{ov} is defined here with respect to a driving force in the liquid phase.

Gas transfer resistance ($\frac{1}{K_{\text{g}}}$) is assumed to be negligible due to the high diffusion coefficient;

hence equation (A1) reduces to

$$\frac{1}{K_{\text{ov}}} = \frac{1}{K_{\text{m}}} + \frac{1}{K_{\text{L}}} \quad (\text{A2})$$

The overall oxygen mass transfer coefficient $K_{\text{ov}}(\text{O}_2)$ for H_2O and broth was estimated from the dissolved oxygen tension (DOT) measurements profile data to be $1.81\text{E-}5$ m/s.

Silicone membrane (0.608 mm thickness) transfer coefficient (K_{m}) for (O_2) and CO_2) used in this study was measured using a conventional gas permeation experiment to be $2.42\text{E-}5$ and $0.36\text{E-}5$ m/s respectively.

From equation (A2) using $K_{\text{m}}=2.42\text{E-}5$ and $K_{\text{ov}}=1.8\text{E-}5\text{m/s}$, it can be calculated that the liquid transfer resistance $K_{\text{L}}=7.18\text{E-}5$ m/s, indicating that 75% of the O_2 transfer resistance lies in the silicone membrane used.

K_{LCO_2} can be calculated from the relation

$$\frac{K_{LO_2}}{K_{LCO_2}} = \left(\frac{D_{O_2}}{D_{CO_2}} \right)^{0.5} = 1.1 \quad (A3)$$

It follows that $K_{LCO_2} = 6.52E-5 \text{ m/s}$

It can also be calculated from equation (A2) for CO_2 that $K_{ov}(CO_2)$ is $0.341E-5 \text{ m/s}$ (Table 1), indicating that 95 % of the CO_2 transfer resistance lies in the membrane used.

Appendix B. Calculation of CO_2 accumulation in the BioScope

From the CO_2 mass balance in the BioScope, a relation similar to that in equation 4 can be derived, including the CO_2 production term as

$$-\Phi_V * \frac{dC_{CO_2,L}}{dx} - k_{overall} * Di * (C_{CO_2,L} - C_{CO_2,L}^*) + r_{CO_2} * \frac{\pi}{8} (Di)^2 = 0 \quad B1$$

Integration with the boundary conditions; BioScope channel length (X) = 0 and $CO_{2L} = CO_{2(ferm)}(X)$, gives

$$C_{CO_2,L(X)} = C_{CO_2,L}^* + r_{CO_2} \frac{\pi * Di}{8 * K_{overall}} + \left[CO_{2(ferm)} - \left(C_{CO_2,L}^* + r_{CO_2} \frac{\pi * Di}{8 * K_{overall}} \right) \right] \exp\left(-\frac{\pi * K_{overall} * Di}{\Phi} X \right) \quad B2$$

This equation shows that for large BioScope channel length (X), i.e. exponent goes to zero, the concentration of CO_2 becomes constant and independent of BioScope channel length (X). This concentration is called C^∞

$$C_{CO_2,L}^\infty = C_{CO_2,L}^* + r_{CO_2} * \frac{\pi * Di}{8 * K_{overall}} \quad B3$$

The relation for $CO_{2(X)}$ becomes

$$C_{O_2,L(X)} = C_{CO_2,L}^\infty + (C_{CO_2(ferm)} - C_{CO_2,L}^\infty) \exp\left(-\frac{K_{overall} Di}{\Phi} X \right) \quad B4$$

This equation was used to calculate the dissolved CO_2 in the BioScope.

Metabolome dynamic responses of *Saccharomyces cerevisiae* on simultaneous rapid perturbations in external electron acceptor and electron donor

Abstract

In vivo dynamics of metabolome responses of primary metabolism in *Saccharomyces cerevisiae* CEN.PK 113-7D have been studied using rapid perturbation experiments. Such experiments were highly relevant to elaborate the in vivo kinetics for mathematical models of metabolism, which are needed for selecting gene targets for metabolic engineering. Perturbations were applied to the chemostat cultivated biomass ($D=0.05\text{ h}^{-1}$, aerobic glucose/ethanol-limited) using the BioScope, (which is a mini plug-flow reactor, $V=3.46\text{ mL}$) over a time span of 90 and 180 seconds. In addition to the more conventional glucose perturbations, novel perturbation principles were elaborated to obtain sets of highly different dynamic metabolites responses. The availability of external electron acceptor was decreased from fully aerobic to anaerobic conditions. The changes in metabolome response were limited to the pyruvate node. Acetaldehyde supply was used as an extra external electron acceptor under glucose perturbation condition, which had a strong effect on the metabolome dynamics and nearly gave a higher glycolytic flux. The response of the adenine nucleotides was very remarkable and indicated that its behavior is not dictated by the glycolytic flux but is much more coupled to the cytosolic NADH/NAD⁺ ratio through the equilibrium pool from F-1,6-BP to 2/3PG. Also the electron donor availability was decreased by application of very low glucose concentration. The metabolome response was as expected, opposite to the response to high glucose concentration. Surprisingly, the trehalose storage was not mobilized in the time frame of 180 seconds.

To be submitted for publication in FEMS Yeast Research.

Introduction

A rational approach towards the identification of gene targets for metabolic engineering of (micro) organisms requires quantitative information on in-vivo kinetics of metabolism (Bailey, 1991; Stephanopoulos et al, 1998; Nielsen, 2001).

Stimulus response experiments pioneered by Theobald et al, 1993; performed to *Saccharomyces cerevisiae* grown under carbon limited chemostat conditions has provided a platform for studying in vivo kinetics and regulation of primary central carbon metabolism. Such stimulus response experiments (reviewed by Oldiges & Takors, 2005) are traditionally performed by instantaneous step increase in residual glucose concentration followed by rapid sampling; instant quenching; intracellular metabolite extraction and measurements of the intracellular metabolite concentrations during a short time. The short time scale is important for the assumption of constant enzyme levels, since these experiments are designed to study in vivo kinetics of key regulatory enzymes, whose response to the increased metabolite levels should be dissected from the increase or decrease in enzyme levels. Increase or decrease in enzyme levels as a regulatory mechanism in cells is believed to occur at a longer time frame of several minutes (Stephanopoulos et al, 1998). These techniques are important for success in quantitative analysis and modelling of the in vivo kinetics of metabolism (Harrison & Maitra, 1969; De Koning & van Dam 1992; Theobald et al, 1993; 1997; Gonzalez et al, 1997; Schaefer et al, 1999; Visser et al, 2002; Schmitz et al, 2002; Buchholz et al, 2002; Buziol et al, 2002; Mashego et al, 2004). However, it should be recognized that although glucose perturbation experiments have paved the way and provided valuable information towards understanding the kinetics of primary carbon metabolism (especially glycolysis), other stimulus response experiments using other perturbing agents or a combination thereof are of major interest for increasing our current understanding of in vivo kinetics of the primary cellular metabolism as has recently been demonstrated (Buchholz et al, 2002; Visser et al, 2004). Standard glucose perturbations (Theobald et al, 1993; 1997; Visser et al, 2002; Mashego et al, 2004; Mashego et al, 2005, submitted) perturb primary metabolism from the top, i.e. glucose entrance. This traditional approach leads to quite strong kinetic response of glycolysis, whereas the TCA cycle response is only moderate. Furthermore, the important anaplerotic reactions are less addressed in a glucose perturbation. Hence, other points of perturbations are of general interest as has been most recently attempted in the perturbation of the aromatic amino acid pathway in *Escherichia coli* (Oldiges et al, 2004). For example, perturbation of O₂ uptake can be expected to directly interfere with the redox metabolism and the TCA cycle. Another possibility for perturbing the redox metabolism is to offer an additional external electron acceptor. In yeast, acetaldehyde can be reduced to ethanol, thus draining the NADH produced from glycolysis. Acetaldehyde and glucose perturbation to oscillating yeast culture under fermentation conditions has been performed before (Richter et al, 1975). It was found that NADH level dropped rapidly, ATP piled up leading to less activity of phosphofructokinase. In turn (G6P) and

(F6P) piled up whereas F1, 6BP, GAP and DAP concentrations dropped and remained low (Richter et al, 1975). Furthermore, the anaplerotic route can be expected to be sensitive to CO₂ levels; therefore, the response to different CO₂ levels is of interest too. In the standard glucose perturbation, the glucose concentration is significantly increased leading to strong flux increase. From a kinetic point of view, a lower glycolytic flux is also of major interest. This can be achieved by lowering the glucose concentration.

The recently developed modified BioScope (Mashego et al, 2005, submitted) allows performing different perturbations on the steady state biomass from the same chemostat.

In the present work, perturbations were performed on both electron acceptor and donor in the modified BioScope aiming to elucidate the kinetics of central carbon metabolism in *S. cerevisiae*. Metabolism responds sensitively to changes in both electron donor and electron acceptor. Traditionally perturbations are performed by increasing the availability of electron donor. In this research, electron acceptor availability (lower and higher) as well as electron donor availability (lower) will be studied. Firstly, perturbation experiments have been carried out with glucose perturbation under different conditions of external electron acceptor, where both less acceptor (O₂-limited and anaerobic) and more acceptor (using acetaldehyde) has been applied.

Secondly, a perturbation experiment has been performed with much less electron donor (decreasing glucose flux).

Materials and Methods

Yeast strain and maintenance

The haploid, prototrophic *Saccharomyces cerevisiae* strain CEN.PK113-7D was kindly provided by Dr. P. Kötter (Frankfurt, Germany). Precultures were grown to stationary phase in shake-flasks on mineral medium (Verduyn et al, 1992), adjusted to pH 6.0 and containing 2 % (w/v) glucose. After adding glycerol (30 %v/v), 2 mL aliquots were stored at -80 °C in sterile vials. These frozen stocks were used to inoculate precultures for chemostat cultivation.

Preculture conditions

Precultures were grown in 100 mL mineral medium (Verduyn et al, 1992), contained in 500 mL Erlenmeyer flasks at 30 °C overnight with shaking at 220 RPM in an incubator shaker (New Brunswick, New Jersey, USA).

High and low-density chemostat cultivation

Aerobic glucose/ethanol limited chemostat cultures of *S. cerevisiae* were cultivated at a dilution rate (D) of 0.05h⁻¹ in 7 L laboratory fermentor with a working volume of 4 L at 30°C and pH, 5.0 (Applikon, Schiedam, The Netherlands) as reported previously (Lange et al, 2001; Mashego et al, 2005). The molar composition of the feed medium used has been described

previously (Lange et al, 2001). This medium contains a mixed carbon source of 150 mM glucose and 31 mM ethanol. The addition of ethanol successfully prevented the cultures from oscillations. The biomass concentration (high cell density) supported by this medium composition is approximately 14.5 g/L \pm 2%. The medium composition for low density chemostat culture was as described above except that all medium components were halved, e.g. 75 mM glucose and 15.5 mM ethanol were used instead. The biomass concentration supported by this medium composition is approximately 7.22 g/L \pm 2%. Dissolved O₂ and CO₂ were 0.196 mmol/L and 0.52 mmol/L for both cultures respectively. Specific fluxes, carbon dioxide evolution rate (q_{CO_2}); oxygen uptake (q_{O_2}); $q_{glucose}$ and $q_{ethanol}$ were identical in both chemostats and were 0.039 \pm 2%, 0.042 \pm 2% mol/ C-mol biomass. h, 0.013 mol/C-mol biomass. h and 0.0028 mol/ C-mol biomass. h respectively. The carbon and redox balance closed at 100 and 101%. Perturbations were executed in the modified BioScope as described before.

Experimental design

BioScope glucose perturbations with reduced external electron acceptor (O₂) availability were performed using chemostat cultured biomass at high cell density (14.5 g/L). In such experiments it is necessary to design ways of establishing an instantaneous switch from chemostat aerobic to BioScope anaerobic conditions as the yeast broth leaves the fermentor to enter the BioScope. One attractive and modest way is to reduce the dissolved oxygen tension (DOT) in the chemostat from the normal steady state value of 80% to 27%. This was achieved by blending the aeration gas into the chemostat with 50 % nitrogen gas while maintaining the gas inflow rate of 3.33 L/min. Because the gas flow is not changed, it is expected that the CO₂ concentration in the fermentor remains the same. The oxygen concentration of this gas mixture was confirmed by passing it through a Rosemount NGA 2000 off gas analyser (Fisher-Rosemount, Germany) and it contained indeed 10.47 % oxygen. Secondly, it was also necessary to check the physiological steady state of the culture when the DOT was 27% since, it is necessary to minimize physiological/metabolic changes which may result due to the differences in DOT in the chemostat experienced by the culture. To this end intracellular metabolite concentration levels of the steady state culture growing at a reduced dissolved oxygen tension (DOT) of 27 % were compared with metabolite concentration levels of the same steady state culture growing at 80 % DOT.

The first set of three experiments (Table I on perturbation in O₂ availability) was performed using the high cell density chemostat. The first experiment concerned a glucose perturbation under fully aerobic conditions with continuous flow of a glucose perturbing agent (56 mM glucose solution) to a final concentration of 5.6 mM at the entrance of the of the BioScope. The flow rate of the perturbing agent was 0.2 mL/min whereas that of the culture broth was 1.8 mL/min, leading to a final total constant flow rate of 2 mL/min. The total residence time in the BioScope is then 90 seconds. The gas channel part of the BioScope was continuously flushed with air

(20.95 % O₂) at constant flow rate of 130 mL/min. The depletion of O₂ and enrichment of CO₂ in the gas channel is negligible at this high gas flow rate. The dissolved oxygen tension (DOT) in the fermentor during steady state was constant at 80 % saturation by continuous aeration with air at a constant flow rate of 3.33 L/min and a reactor overpressure of 0.3 bars. DOT in the BioScope was monitored at various sample ports using a dissolved oxygen probe mounted onto a flow cell with a volume of 200 µL. This flow cell was also used for measurements of dissolved CO₂ except that a dissolved CO₂ probe was used (Mettler Toledo CO₂ measuring system, In Pro 5100e, Mettler-Toledo GmbH, Switzerland).

The second experiment involved a glucose perturbation under O₂-limited conditions. The experimental conditions were as described above except that the gas composition in the gas channel of the BioScope was a mixture of 25 % air and 75 % nitrogen gas (N₂). This gas mixture resulted in 5.25 % oxygen concentration in the gas mixture fed to the BioScope at a constant gas flow rate of 130 mL/min. The solubility of O₂ at this gas composition $C^*_{O_2}=0.061$ mmol/L. The oxygen concentration of this gas mixture was confirmed by passing it through Rosemount NGA 2000 off gas analyser (Fisher-Rosemount, Germany). The dissolved oxygen tension of the chemostat was instantaneously reduced from 80% to 27 % DOT as described before so as to minimize excessive oxygen carry over from the chemostat broth into the BioScope. The dissolved oxygen tension of the last sample port of the BioScope was measured with the dissolved oxygen probe as described above and found to be zero. Using the O₂ transfer characteristics of the BioScope (Mashego et al, 2005, submitted), the maximum O₂ transfer rate follows as 9.25 mmol/L. h ($K_{La}= 148/h$, $C^*_{O_2}=0.066$ mmol/L) or $q_{O_2} = 0.69$ mmol/gDW. h (or 0.192 µmol/gDW.s; Table 1). This is about 45 % of the q_{O_2} in the steady state chemostat.

The third experiment concerned a glucose perturbation under anaerobic conditions. The experimental conditions were as described for the oxygen limited (fixed q_{O_2}) glucose perturbation conditions above, except that the gas channel of the BioScope was continuously flushed with nitrogen gas (N₂) at a constant gas flow rate of 130 mL/min. The dissolved oxygen tension of the sample ports of the BioScope was measured as described above in order to ensure that anaerobic conditions are satisfied.

In the previous experiments, reduced availability of the electron acceptor (O₂) during glucose perturbation was performed. However, increased electron acceptor availability during a glucose perturbation is also of interest because of the known redox stress originating from high flux of glyceraldehyde-3-phosphate dehydrogenase (GAPDH). Therefore, a second set of two experiments were performed in the BioScope using biomass from the low cell density (7.22 g/L) chemostat.

The first experiment used a glucose perturbation (2.8 mM glucose) under fully aerobic conditions. The flow rate of the perturbing agent was 0.1 mL/min whereas that of the culture broth was 0.9 mL/min leading to a final total flow rate of 1 mL/min. The residence time in the BioScope is then 180 seconds. The gas channel part of the BioScope was continuously flushed

with air (20.95 % O₂) at 130 mL/min. The dissolved oxygen tension (DOT) in the fermentor during steady state was maintained constant above 80 % saturation (0.196 mM) by continuous aeration with air at a flow rate of 1.67 L/min with a reactor overpressure of 0.3 bars. The carbon dioxide level in the chemostat (0.52 mM) was identical to the high cell density culture because the airflow was halved.

In a second experiment, the availability of the external acceptor was increased by supplying acetaldehyde, which becomes reduced to ethanol and then consumes 1 NADH. Glucose (55.5 mM) and acetaldehyde (32 mM) perturbing agents were pre-mixed via a high precision multichannel peristaltic pump (Ismatec, ISM 930, ISMATEC SA, Labortechnik, CH-8152, Glattenbrugg-Zurich, Switzerland) using two independent tubing's (0.64 mm internal diameter) connected via a Y-piece connector prior to the BioScope entry port. The two perturbation agents flow rates were independently measured to be 0.05 mL/min for glucose solution and 0.05 mL/min for the acetaldehyde solution. Furthermore, the perturbation agents total flow rate of 0.1 mL/min was also verified prior to the commencement of the experiment. The final glucose concentration in the BioScope was similar to that in the glucose only perturbation experiment, i.e. 2.8 mM. The calculated acetaldehyde final concentration at the entrance of the BioScope was 1.5 mM. The experiment was fully aerobic by supplying air (130 mL/min) through the gas channel of the BioScope.

A third set of experiment concerned a decrease of the electron donor under fully aerobic condition, using biomass from the low cell density chemostat. This was achieved by taking biomass from the chemostat into the BioScope without supplying any glucose. The biomass only has the residual glucose present in the supernatant (0.11mM). It can be expected that the dissolved CO₂ concentration in the BioScope drops due to the strongly decreased CO₂ production and the CO₂ stripping over the silicone membrane. In order to maintain a constant CO₂ concentration in the BioScope, dissolved CO₂ was added to the broth taken from the low cell density chemostat such that dissolved CO₂ concentration was tripled instantaneously in the BioScope, i.e. instant increase from 0.52 mM to 1.7 mM. This was achieved by continuously mixing 40% CO₂ saturated H₂O solution at 0.1 mL/min liquid flow rate with 0.9 mL/min broth in the BioScope. The gas channel part of the BioScope was continuously flushed with CO₂ enriched gas mixture containing 5 % CO₂, 20.95% O₂ and the rest was N₂. 5 % CO₂ corresponds to a solubility of 1.45 mM CO₂ in the liquid phase. Therefore, flushing the gas channel of the BioScope with enriched (5 % CO₂) gas mixture ensured near zero CO₂ transfer or limit CO₂ escape from the liquid phase to the gas channel of the BioScope. The dissolved CO₂ in the liquid stream was measured for all the sampling ports of the BioScope using a flow cell in which the dissolved CO₂ probe (In Pro 5100e; Mettler-Toledo GmbH; Switzerland) was mounted. The perturbation experiments using either the high or low cell density chemostat were performed approximately 24h after each other over a total period of three days in the sequence in which they are presented above.

Culture dry weight determinations

Biomass dry weight concentration was determined as described previously (Mashego et al, 2005).

Sampling procedure and analysis for extracellular metabolites (glucose, acetaldehyde, ethanol and acetate)

Rapid sampling, quenching procedure and analysis for extracellular metabolites (glucose, ethanol and acetate) from the BioScope samples were as described previously (Mashego et al, 2003; Mashego et al, 2005, submitted). For validation of the procedure for the determination of the residual acetaldehyde in the glucose+acetaldehyde perturbation, acetaldehyde stock solution (32 mM) kept at 30 °C in the temperature controlled BioScope cabinet was fed through the BioScope and samples collected with simultaneous quenching as described previously for extracellular metabolites (Mashego et al, 2005, submitted). The acetaldehyde concentration was found as expected to be 32mM, pointing to no loss of acetaldehyde during sampling/quenching. At the end of the experiment, (approximately 6 hrs) a sample from acetaldehyde stock solution bottle was also collected in order to check the stability and the concentration of the acetaldehyde at the end of the experimental period. This was necessary because acetaldehyde is known to be very unstable at room temperature and tends to trimerize/evaporate. The concentration of the acetaldehyde stock was found to be 25 mM, leading to a loss of about 20 % in 6 hrs at 30 °C.

Sampling procedure for intracellular metabolites

The BioScope system was flushed with broth and the perturbing agent at least five residence times (7.5-15 minutes) before sampling was started through computer aided automatic activation of the sequentially positioned, two ways pinch valves (Visser et al, 2002). The sampling and quenching procedure for determination of intracellular metabolites was the same as described previously (Visser et al, 2002).

Trehalose extraction, enzymatic hydrolysis and analysis

Samples for intracellular trehalose were extracted using the ethanol boiling method (Mashego et al, 2005). To 100 µL sample from the trehalose extraction procedure, 50 µL trehalase (Sigma-Aldrich, Steinheim, Germany) 0.1 units/mL and 850 µL, 80 mM sodium acetate buffer (pH 5.2) were added. The mixture was incubated at 37°C for 6.5 hours with shaking at 220 RPM in 1.5 mL eppendorf tubes. Glucose concentration in the trehalase hydrolyzed samples was measured enzymatically as described previously (Mashego et al, 2005).

Intracellular metabolite analysis procedure

Intracellular metabolite concentrations were measured in the cell extracts prepared as described previously using LC-ESI-MS/MS (MIRACLE) principle (van Dam et al, 2002; Mashego et al, 2004; Wu et al, 2005).

Results and Discussion

I. Comparison of the physiological steady state of aerobic glucose/ethanol limited chemostat culture of *S. cerevisiae* at 27% and 80% DOT

It is necessary to decrease the dissolved O_2 concentration in the BioScope to very low levels as soon as possible for the perturbation experiments involving different O_2 supply. To achieve this, the chemostat (14.5 g/L biomass) dissolved O_2 was reduced from 0.184 mol/m³ corresponding to 80 % DOT to 0.061 mol/m³ corresponding to 27 % DOT. From the off-gas analysis in the chemostat, it followed that this does not cause any change in q_{CO_2} and q_{O_2} . Furthermore, intracellular metabolite concentration levels representing the physiological steady state of the culture were also compared under both 27 and 80% DOT conditions. Figure 1 shows that the intracellular metabolites do not change and are identical. The values of the metabolite levels are averages of 4 samples analysed in duplicate and the error bars indicate variations between duplicate analyses of the same samples. It is clear that the dissolved O_2 level change from 0.196 to 0.066 mol/m³ has no effect on the physiological state of *S. cerevisiae*. Using the mass transfer characteristics of the BioScope (Mashego et al, 2005, submitted), it could be calculated that the dissolved O_2 in the BioScope drops to near zero level at 0.4 m length of the BioScope channel, corresponding to 6 seconds (See appendix 1). This is true provided that the broth from the chemostat contains 0.066 mol/m³ (27% DOT). For DOT of 80 %, it takes about three times longer to achieve DOT of zero in the BioScope (see Appendix 1). O_2 -limitation in the BioScope can therefore be assumed after a few seconds.

II. Perturbation of external electron acceptor during a glucose pulse

The first set of experiments concerned the lower availability of electron acceptor O_2 . A glucose perturbation was applied under fully aerobic, O_2 -limited and anaerobic conditions (Table 1). The response will be discussed with respect to the effect on uptake and secreted fluxes. Under standard glucose perturbation conditions in the BioScope, there is sufficient dissolved oxygen (>0.05 mmol/L) as depicted in Figure 2A. Also the CO_2 concentration increases from 0.50 to 1 mM. Using the measured dissolved O_2 concentration of 0.05 mmol/L and the O_2 transfer characteristics of the BioScope (K_{La} =148/h; $C^*_{O_2}$ = 0.245 mmol/L and C_x =13.05 g/L allows to calculate that q_{O_2} equals 0.57 μ mol/gDW.s (Table 1).

This is about 20-30% higher than the steady state chemostat value of 0.41 μ mol/ gDW.s (Table 1). A similar increase in q_{O_2} has been found before in a glucose perturbation in the fermentor (Bloemen et al, 2003).

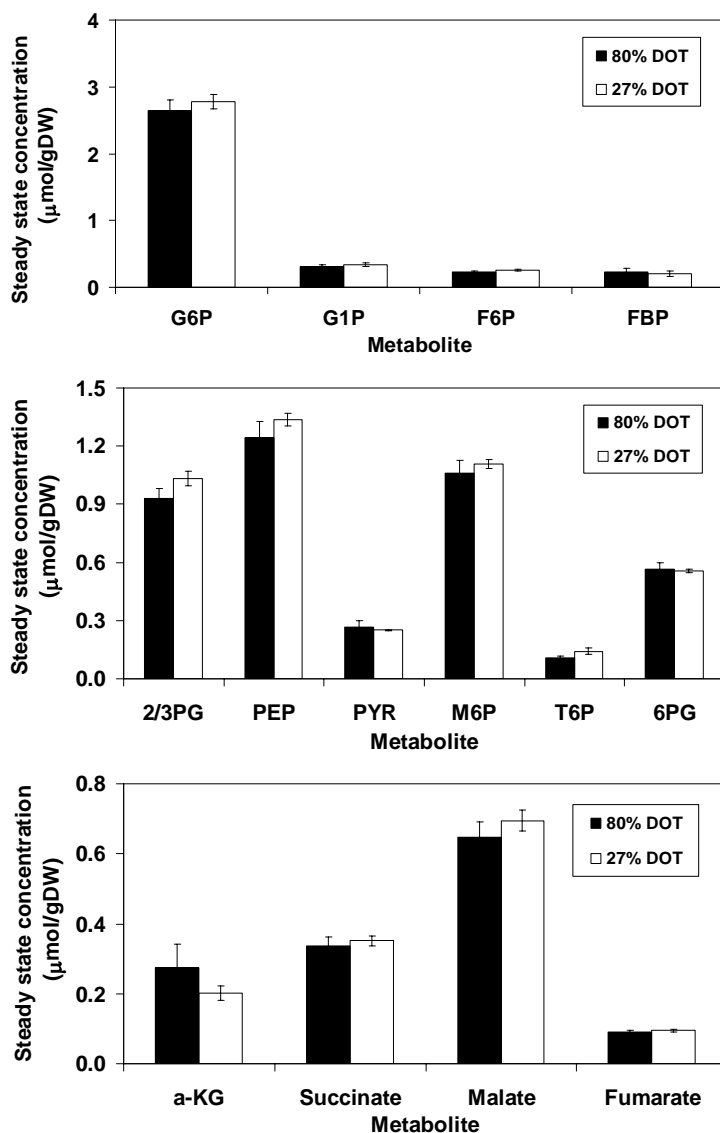


Figure 1 Comparison of intracellular glycolytic, TCA cycle metabolites, 6-phosphogluconate, mannose-6-phosphate and trehalose-6-phosphate concentration of aerobic glucose/ethanol limited steady state chemostat culture of *S. cerevisiae* CEN.PK 113-7D grown at a dilution rate of 0.05 h^{-1} at 27 % and 80 % dissolved oxygen tensions (DOT). Error bars represent standard deviations between analyses of four samples.

Table 1 Comparison of specific uptake rates of glucose (q_{glucose}) and specific oxygen uptake rate (q_{O_2}), with a glucose perturbation (5.8 mM) under fully aerobic, O_2 limited and anaerobic conditions in the BioScope fed with broth from high cell density chemostat.

BioScope perturbation experiments	q_{glucose} $\mu\text{mol (gDW s)}^{-1}$		q_{O_2} $\mu\text{mol (gDW s)}^{-1}$
	Phase I (0 -30 s)	Phase II (30-90 s)	
Glucose/fully aerobic	1.99	1.03	0.57
Glucose O_2 -limited (fixed q_{O_2})	1.93	1.26	0.19
Glucose Anaerobic (Steady state)	1.79 (0.14)	1.19 0.14	0.00 (0.41)

Figure 2B depicts the glucose uptake under fully aerobic; O_2 -limited and anaerobic conditions in the BioScope. In Table 1, q_{glucose} is divided into two distinct phases I and II. Initial flux in phase I (0-30 seconds) during fully aerobic standard glucose perturbations is 3-10 % higher than O_2 -limited and anaerobic glucose perturbations. However, in phase II (30-90 seconds), the situation is reversed, i.e. O_2 -limited and anaerobic perturbation conditions are 15% higher than the q_{glucose} under fully aerobic conditions (Table 1). It appears that the effect of lower O_2 availability on the glucose uptake rate, and hence the rate of glycolysis is limited. With respect to secreted ethanol and acetate, figures 2C-D shows that the O_2 perturbed experiments (O_2 -limited and anaerobic) are quite similar and when compared to the standard fully aerobic perturbation, the ethanol production is much higher and acetate production is much lower.

The effect of the O_2 -supply perturbation on intracellular metabolites is shown in figure 3 which represents the well known intracellular glycolytic intermediates, 6-phosphogluconate (6-PG), mannose-6-phosphate (M6P) and trehalose 6 phosphate (T6P) concentration profiles. There was no significant difference for most metabolite concentration response profiles under the different specific oxygen uptake rates imposed. Only pyruvate seems to be higher for O_2 -limited condition which points to less pyruvate flux into the TCA cycle. The above observed higher ethanol and lower acetate agrees with this higher pyruvate level and that the flux is redirected from respiration (TCA cycle) to fermentation. Figure 3 shows that the dynamic metabolite concentration responses resembles very well known dynamic patterns of glucose perturbations (Theobald et al, 1997; Buziol et al, 2002; Visser et al, 2002; Mashego et al, 2004; Mashego et al, 2005, submitted). Because the glycolytic flux is hardly different, there is no difference in glycolytic intermediates to be expected as well.

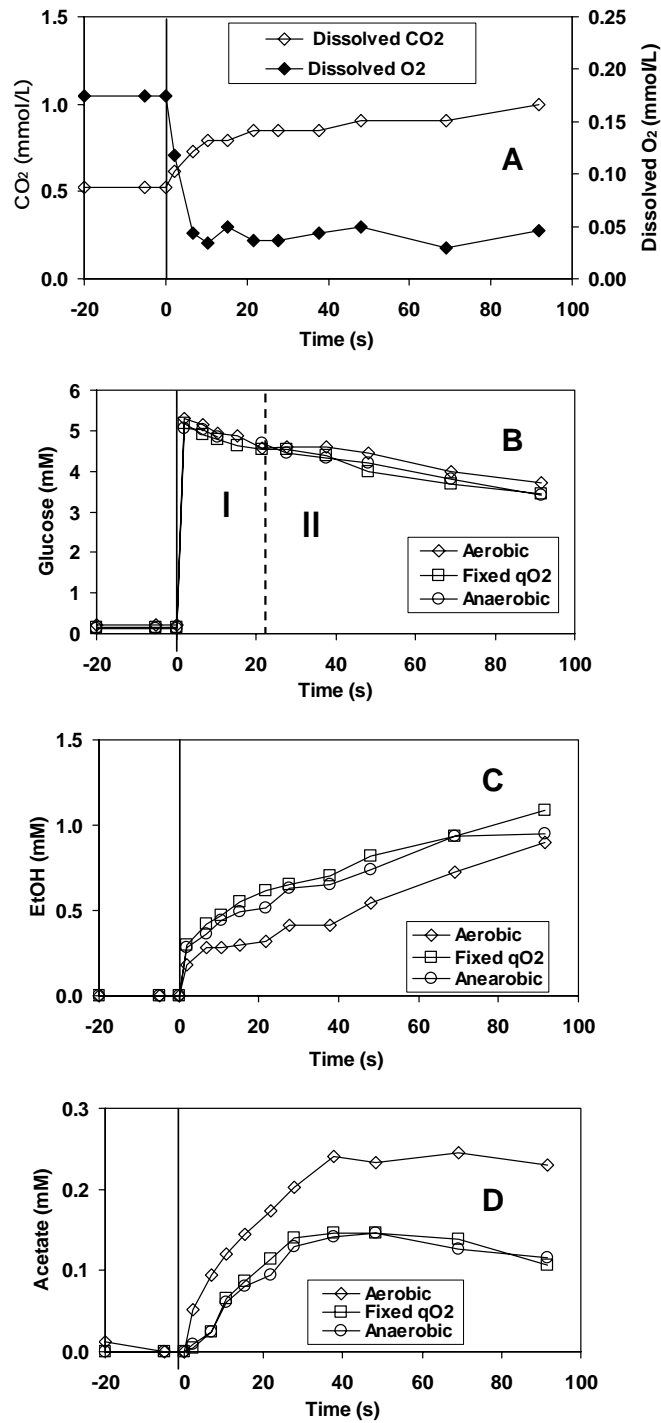


Figure 2 Dissolved carbon dioxide (DCO_2), dissolved oxygen concentration, residual glucose, excreted ethanol and acetate concentration profiles before and during a glucose perturbation to high cell density fully aerobic glucose/ethanol limited chemostat culture of *S. cerevisiae* CEN.PK 113-7D under fully aerobic, O₂-limited and anaerobic conditions in the BioScope. Error bars represent standard deviations between duplicate analyses of the same sample.

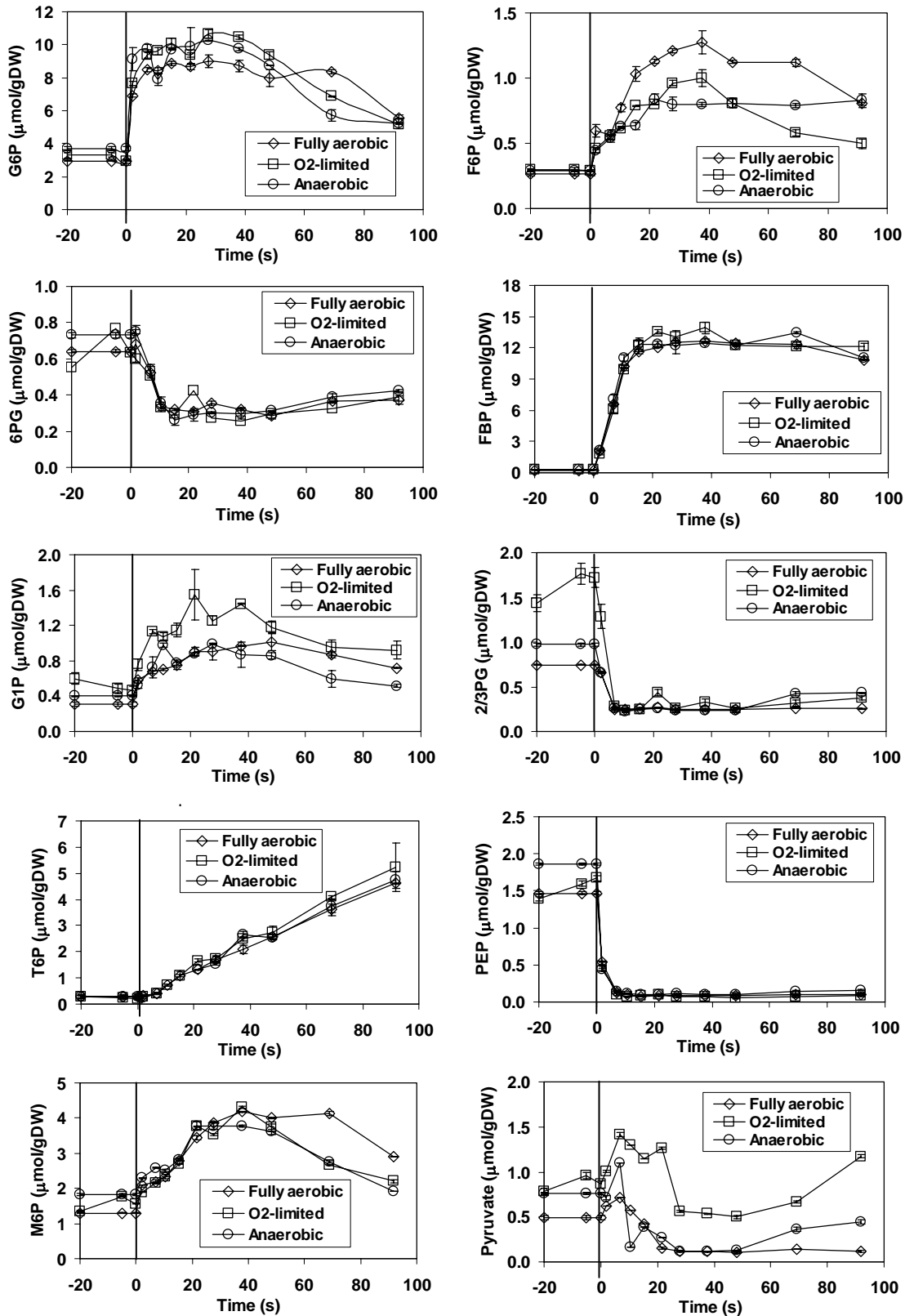


Figure 3 Intracellular glycolytic metabolites, 6-phosphogluconate, trehalose-6-phosphate concentration profiles before and during a glucose perturbation to high cell density fully aerobic glucose/ethanol limited chemostat culture of *S. cerevisiae* CEN.PK 113-7D under fully aerobic, O₂-limited and anaerobic conditions in the BioScope. Error bars represent standard deviations between duplicate analyses of the same sample.

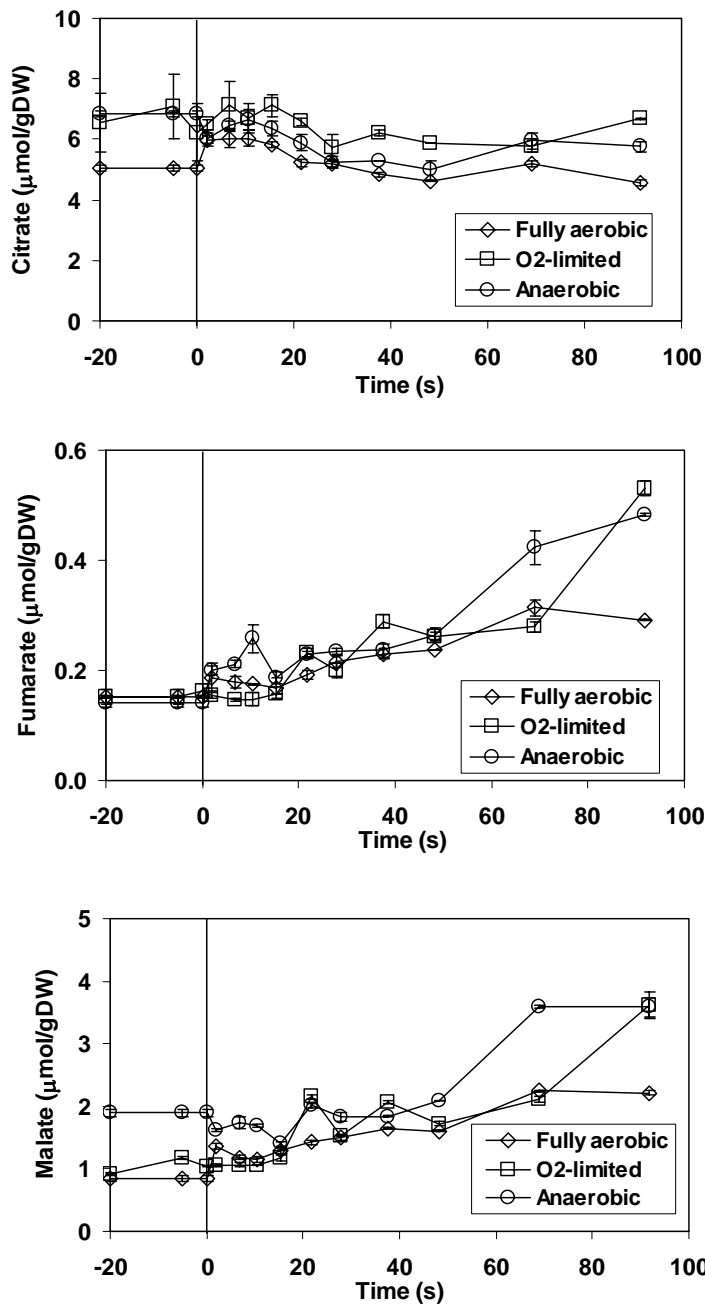


Figure 4 Intracellular TCA cycle metabolites (citrate, fumarate and malate) concentration profiles before and during a glucose perturbation to high cell density aerobic glucose/ethanol limited chemostat culture of *S. cerevisiae* CEN.PK 113-7D under fully aerobic, O_2 -limited and anaerobic conditions in the BioScope. Error bars represent standard deviations between duplicate analyses of the same sample.

The dynamic responses of the TCA cycle intracellular metabolites (citrate, fumarate and malate) are depicted in figure 4. Fumarate seems to be higher in anaerobic glucose perturbation which points to a more reduced state of the cytosol. This further suggests the hypothesis of slightly higher cytosolic NADH/NAD^+ ratio under O_2 -limited perturbation

conditions. This higher redox level with the higher pyruvate level can further explain the observed higher ethanol and lower acetate secretion. In conclusion, O₂ perturbation mainly seems to affect the pyruvate node fluxes due to pyruvate level and the redox level effects and much less the glycolytic metabolites and fluxes.

In the second set of experiments under conditions of a glucose perturbation, the availability of external electron acceptor was increased by supplying acetaldehyde under fully aerobic conditions. Acetaldehyde readily permeates the cell membrane and is easily reduced to ethanol consuming 1 NADH per mol acetaldehyde.

Residual glucose increases instantaneously from steady state value of 0.11 mM to 2.8 mM followed by the gradual decrease in three phases designated I (0-30 s); II (30-94 s); and III (94-177 s) (Fig 5A and Table 2).

Table 2 Comparison of specific uptake rates of glucose (q_{glucose}) and acetaldehyde $q_{\text{acetaldehyde}}$ under steady state culture conditions as well as during fully aerobic glucose only and glucose+acetaldehyde perturbations with a glucose perturbation (2.8 mM) under fully aerobic conditions fed with broth from the low cell density chemostat.

BioScope perturbation experiments	Glucose			Acetaldehyde $q_{\text{acetaldehyde}}$ ($\mu\text{mol/gDW.s}$)
	q_{glucose} ($\mu\text{mol/gDW.s}$) Phase I 5-30 s	Phase II 30-94 s	Phase III 94-177 s	
Glucose/fully aerobic	1.60	0.46	1.06	0.00
Glucose+acetaldehyde/fully aerobic (Steady state)	2.46	0.45	1.09	1.38
	(0.14)	(0.14)	(0.14)	0.00

The initial high glucose flux phase I (0-30 s) was followed by a low flux phase II (30-94 s) and high flux phase III (94-180 s) which fits very well with the apparent inhibition model of hexokinase by an increase of T-6-P, (Fig 6) thus controlling the glycolytic flux (Blazquez et al, 1993; Hohmann et al, 1996; Francois and Parrou, 2001; Gancedo and Flores, 2004; Guillou et al, 2004). The specific glucose uptake rates in phase I for glucose only and glucose+acetaldehyde perturbation experiments were 1.60 and 2.46 $\mu\text{mol/gDW.s}$ respectively leading to a 10 and 18 fold increase for glucose only and glucose+acetaldehyde mixture respectively relative to the steady state q_{glucose} flux (Table 2). The higher glycolytic flux in phase I under glucose+acetaldehyde

perturbation conditions is apparently due to the electron removal by acetaldehyde that freely diffused from the medium into the cell as an external electron acceptor.

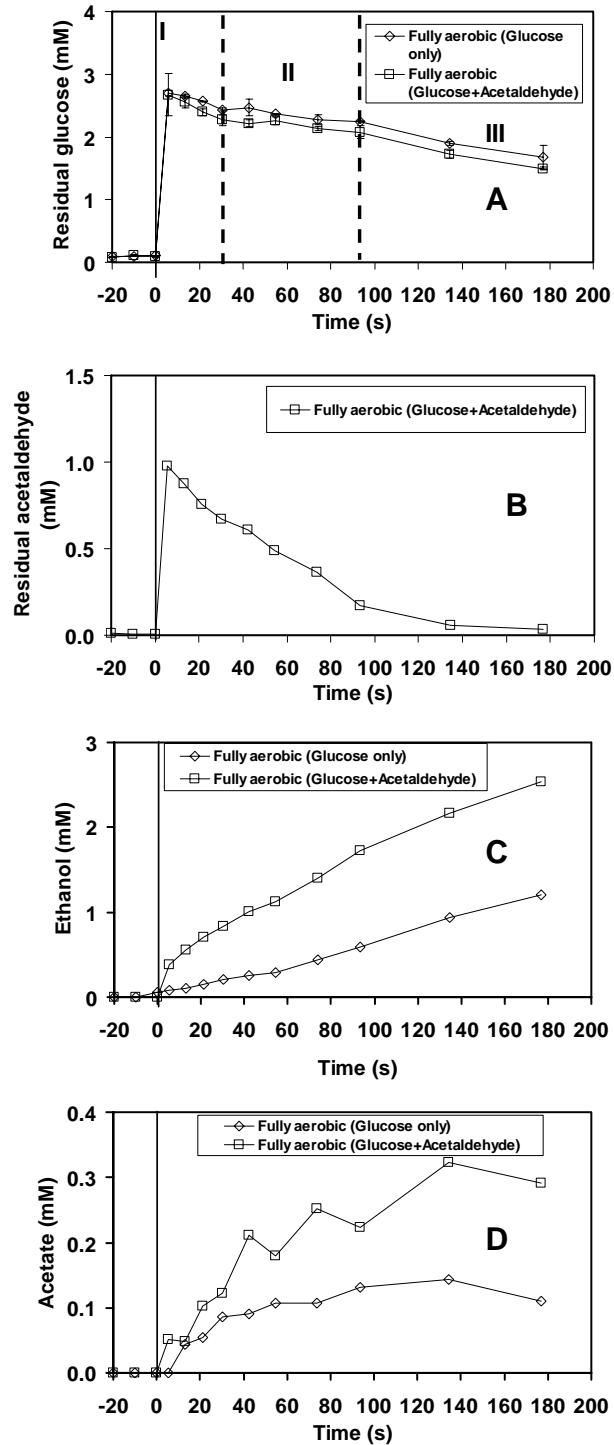


Figure 5 Residual glucose, acetaldehyde, ethanol and acetate concentration profiles before and during fully aerobic glucose only and glucose+acetaldehyde mixture perturbation to low cell density aerobic glucose/ethanol limited chemostat culture of *S. cerevisiae* CEN.PK 113-7D in the BioScope. Error bars represent standard deviations between duplicate analyses of the same sample.

Figure 5B shows that acetaldehyde level in the BioScope increased instantaneously from 0 to 1 mM, 5 seconds after the perturbation and sharply decreased linearly in the first 100 seconds. There is a rapid consumption of acetaldehyde. Figure 5A shows that the presence of acetaldehyde also increases the glucose uptake rate leading to much higher ethanol levels (Fig 5C) and also slightly higher acetate levels (Fig 5D). The specific acetaldehyde uptake rate is calculated to be $1.38 \mu\text{mol/gDW.s}$, which is equivalent to $0.69 \mu\text{mol O}_2/\text{gDW.s}$. Since the $q\text{O}_2$ under standard fully aerobic glucose perturbation conditions is $0.57 \mu\text{mol O}_2/\text{gDW.s}$ (Table 1), it can be calculated that the electron sink is increased from 0.57 to $1.26 \mu\text{mol O}_2$ equivalent/gDW.s, due to acetaldehyde consumption. Both glucose and acetaldehyde were taken up simultaneously by the cells, leading to almost twice as high ethanol and acetate accumulation as was found in glucose only perturbation (Figs 5C-D).

Ethanol production in both cases start after 5 seconds in the BioScope. Figure 5C shows that final ethanol concentration in glucose+acetaldehyde perturbation is 2.5 mM, 1.3 mM more than obtained in glucose only perturbation which is 1.2 mM. The consumption of the added 1 mM acetaldehyde explains an increase of ethanol with maximally 1mM. The remaining increase is due to the increased fermentation of glucose. Fig 5D shows that acetate production is increased from about 0.1mM to 0.25 mM in the presence of acetaldehyde which indicates that a small part of the added acetaldehyde is oxidised into acetate. This increase is probably not due to the increased acetaldehyde concentration because the K_m of acetaldehyde dehydrogenase is known to be very low (Wang et al, 1998). A likely explanation is that the cytosolic NADH/NAD⁺ ratio is lower due to the acetaldehyde/ alcohol conversion as explained below. In summary it appears that the presence of an extra cytosolic electron drain strongly (50%) stimulates the initial glycolytic flux (first 30 seconds) and leads to increased ethanol excretion rates.

The effect of the presence of the additional external electron acceptor acetaldehyde on the intracellular glycolytic and TCA cycle metabolites is shown in figures 6 and 7 respectively. Adenine nucleotides are depicted in figure 8. First, it was observed that the mass action ratios of PGI, PGM were perturbed but quickly returned to steady state values whereas those of enolase and fumarase were also perturbed but remained at lower levels (data not shown). Comparing the effect of a presence of the additional external electron acceptor acetaldehyde it follows that hexose-phosphate pools are lower, F-1, 6-BP is dramatically lower, the C3 pool (2/3PG and PEP) drop less fast and pyruvate increases less fast. These differences are even more remarkable in view of the increased glycolytic flux, which normally causes higher levels of hexose phosphate F-1, 6-BP and a faster drop in the C3-pool. The behaviour of the adenine nucleotides (Fig 8) is even more remarkable. A glucose perturbation normally leads to strong decrease in ATP and increases in ADP and AMP as shown in figure 8. This is usually explained by the increased glycolytic flux, which consumes large amounts of ATP to achieve the hexose phosphorylation. In the presence of the extra external electron acceptor

acetaldehyde, it can be seen that despite the strongly increased glycolytic flux, the nucleotides behave completely opposite. Initially, ATP increases whereas ADP and AMP decrease.

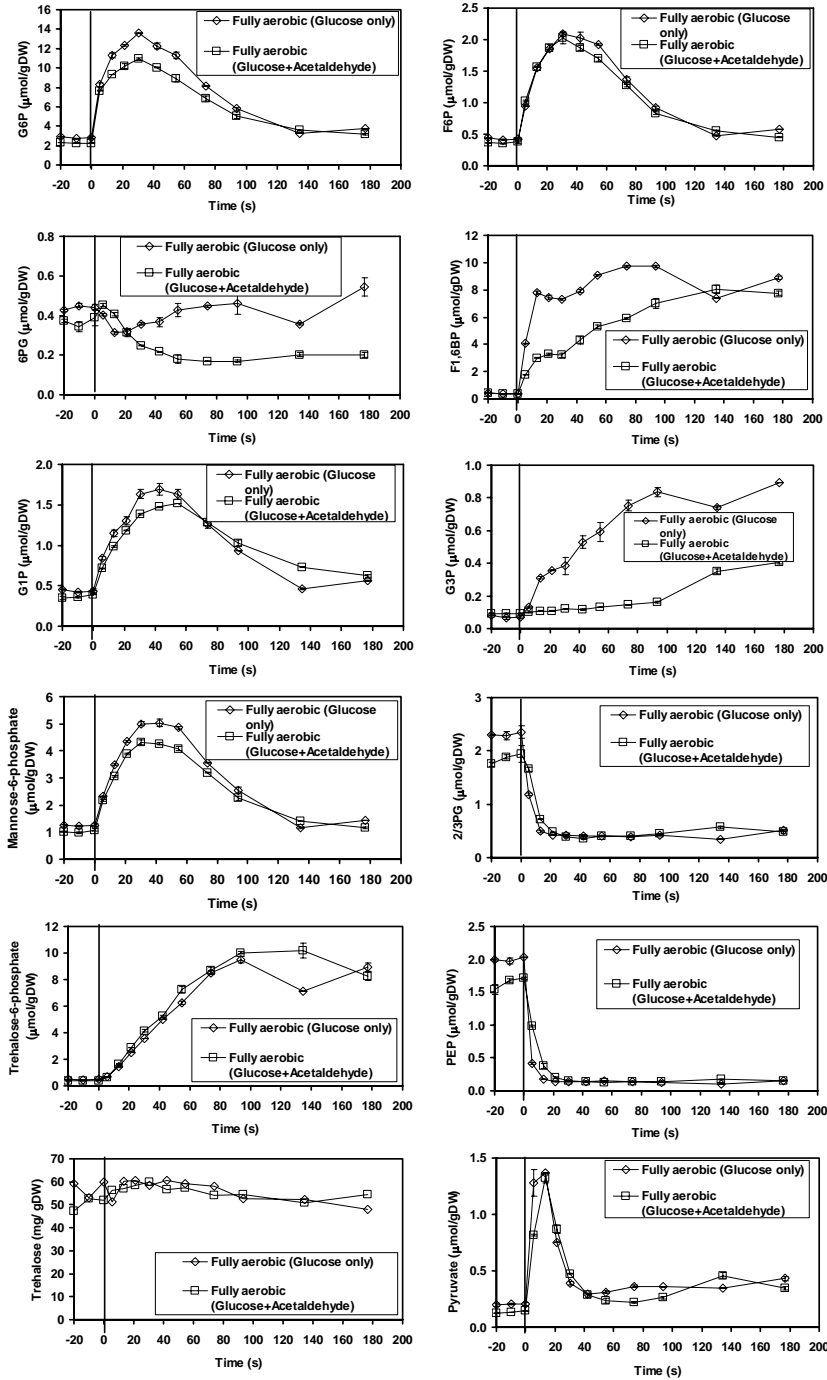


Figure 6 Comparison of intracellular glycolytic metabolites, mannose-6-phosphate, 6-phosphogluconate, trehalose-6-phosphate and trehalose concentration profiles before and during fully aerobic glucose only and glucose+acetaldehyde mixture perturbation to low cell density aerobic glucose/ethanol limited chemostat culture of *S. cerevisiae* CEN.PK 113-7D in the BioScope. Error bars represent standard deviations between duplicate analyses of the same sample.

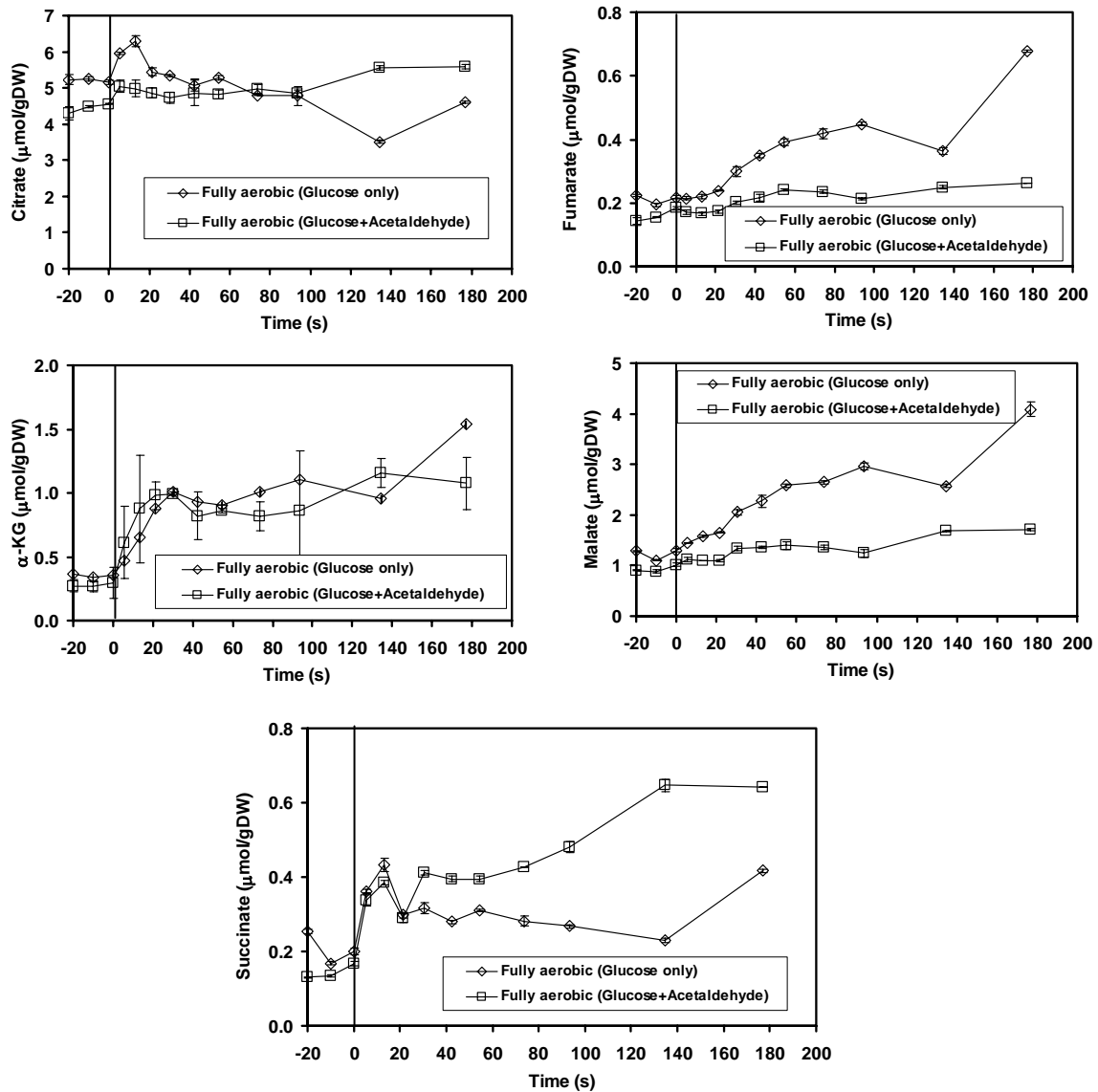


Figure 7 Comparison of intracellular TCA cycle metabolites concentration profiles before and during fully aerobic glucose only and glucose+acetaldehyde mixture perturbation to low cell density aerobic glucose/ethanol limited chemostat culture of *S. cerevisiae* CEN.PK 113-7D in the BioScope. Error bars represent standard deviations between duplicate analyses of the same sample.

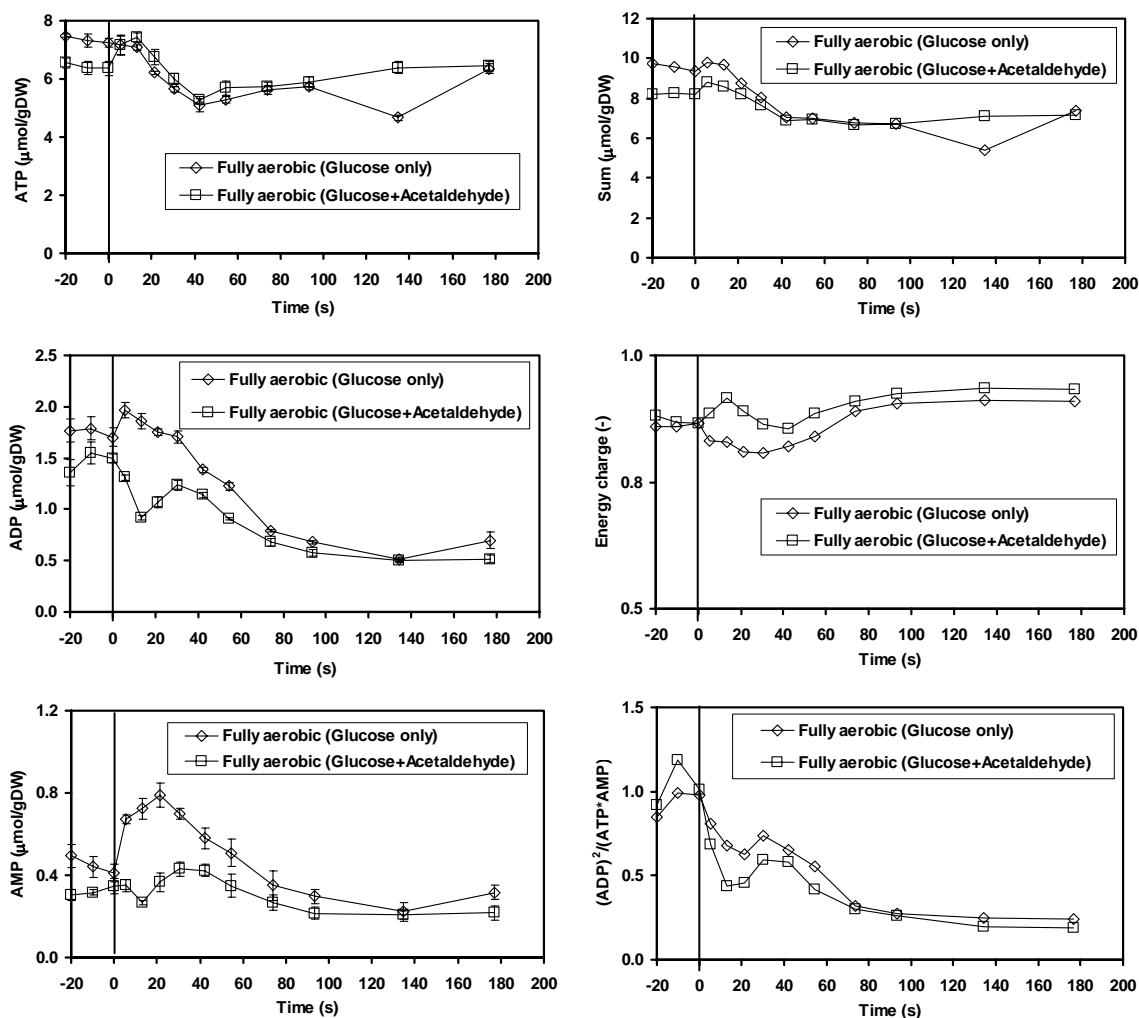


Figure 8 Intracellular adenine nucleotides (ATP, ADP, and AMP) concentration profiles; sum of nucleotides, cellular energy charge and adenylate kinase mass action ratio during fully aerobic glucose only and glucose+acetaldehyde perturbation to low cell density aerobic glucose/ethanol limited chemostat culture of *S. cerevisiae* CEN.PK 113-7D in the BioScope. Error bars represents standard deviations between duplicate analyses of the same sample.

This is even more surprising because ATP production is less because glycolytically produced NADH is diverted through acetaldehyde reduction to ethanol formation thereby not entering the electron transport phosphorylation. This ATP increase phenomenon is in agreement with the observations by Richter et al, (1975). These observations make it unlikely that the usually observed ATP drop is caused by the high glycolytic flux. An alternative explanation is that the behaviour of ATP and ADP is controlled by the set of equilibrium reaction between F-1, 6-BP and 2/3PG, (see equation 1).



The whole set of these reactions is known to be close to equilibrium (Visser et al, 2004) even during a perturbation with increased fluxes. It can be expected that in the presence of acetaldehyde, the cytosolic NADH/NAD⁺ ratio does not increase that high. Indeed, the formation of glycerol-3-phosphate, which usually strongly responds to cytosolic redox stress, increases much slower in the presence of acetaldehyde (Fig 6). Moreover, despite the higher glycolytic flux the level of F-1, 6-BP is much lower (Fig 6) in the presence of acetaldehyde. This is also in agreement with the above equilibrium and the expected much lower cytosolic NADH/NAD⁺ ratio. The fold change in the NADH/NAD⁺ ratio compared to the steady state is easily calculated from the fold change of the intracellular metabolites (assuming a constant pH and concentration of Pi). Figure 9 shows that the presence of acetaldehyde leads to much lower fold change in NADH/NAD⁺ ratio. This shows that acetaldehyde effectively balances the rapid production of glycolytic NADH. It is concluded that because of the equilibrium pool of F-1, 6-BP to 2/3PG, the fold change in redox (NADH/NAD⁺) are coupled to the fold change in ATP/ADP ratio. Redox stress (high fold increase of NADH/NAD⁺) leads to high fold decrease in the ATP/ADP ratio. Acetaldehyde also appears to have a strong effect on 6-PG, leading to its concentration drop. There is much more 6-PG increase in glucose only perturbation, in contrast to the decrease in glucose+acetaldehyde perturbation. This indicates that less NADPH is required from the pentose phosphate pathway, which can be due to the acetaldehyde oxidation to acetate as a source for NADPH, replacing the PPP in the glucose+acetaldehyde. The TCA cycle intermediates (Fig 7) show that fumarate and malate are much less increased due to the action of acetaldehyde. Their increase in a standard glucose perturbation is considered to be due to increased NADH/NAD⁺ ratios leading to a more reduced C4 pool (aspartate, oxaloacetate, malate and fumarate) which agrees with their much less increase in the acetaldehyde experiment where the change in NADH/NAD⁺ is much less. Succinate is much more increased, which can be due to an increased TCA cycle rate, which might be less inhibited due to the lower redox ratio (NADH/NAD⁺). In conclusion, the use of acetaldehyde seems an excellent method to create highly informative perturbations in redox, energy and carbon of all major primary pathways.

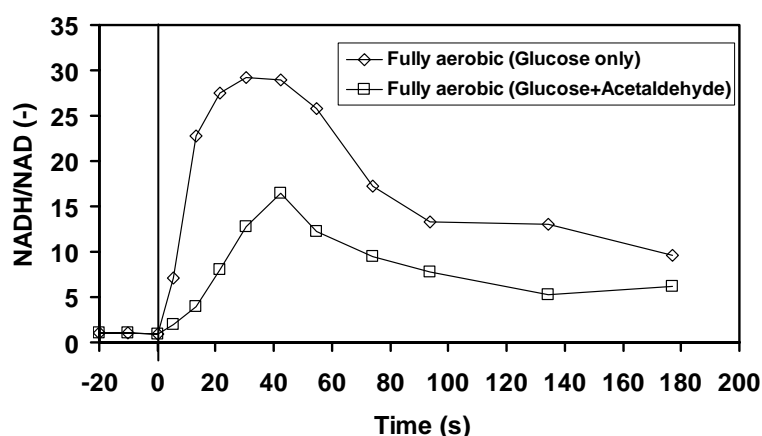


Figure 9 Comparison of NADH/NAD⁺ ratio before and during fully aerobic glucose only and glucose+acetaldehyde perturbation to low cell density aerobic glucose/ethanol limited chemostat culture of *S. cerevisiae* CEN.PK 113-7D in the BioScope.

III. Perturbation by less electron donor supply (no glucose addition)

Figure 10 compares the fully aerobic standard glucose perturbation (2.8 mM) with no glucose addition. The glucose and CO₂ concentration in the BioScope are shown in figure 10A. It can be seen that the glucose concentration slowly drops from 0.11 to 0.03 mM. The dissolved CO₂ concentration is between 1.5 to 2mM, which is comparable to the CO₂ concentration which occurs in a fully aerobic glucose perturbation (1 to 1.5 mM). The glucose uptake flux is obtained from the glucose consumption and is found to drop sharply (Fig 10B).

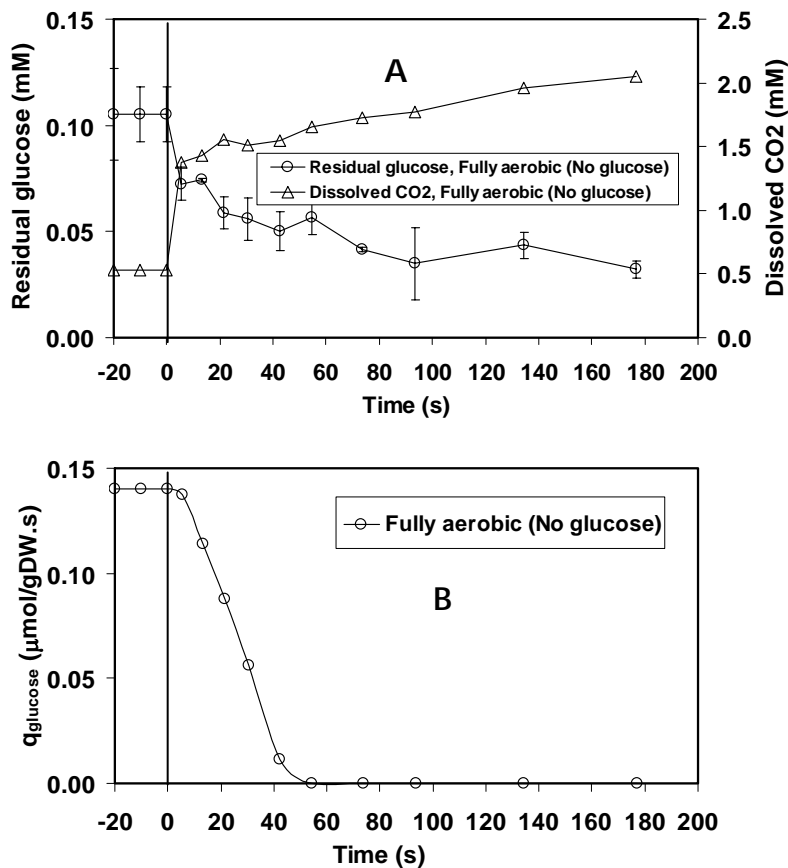


Figure 10 Residual glucose concentration, dissolved CO₂ and specific glucose uptake rate, before and during fully aerobic, no glucose perturbation to low cell density aerobic glucose/ethanol limited chemostat culture of *S. cerevisiae* CEN.PK 113-7D in the BioScope. Error bars represent standard deviations between duplicate analyses of the same sample.

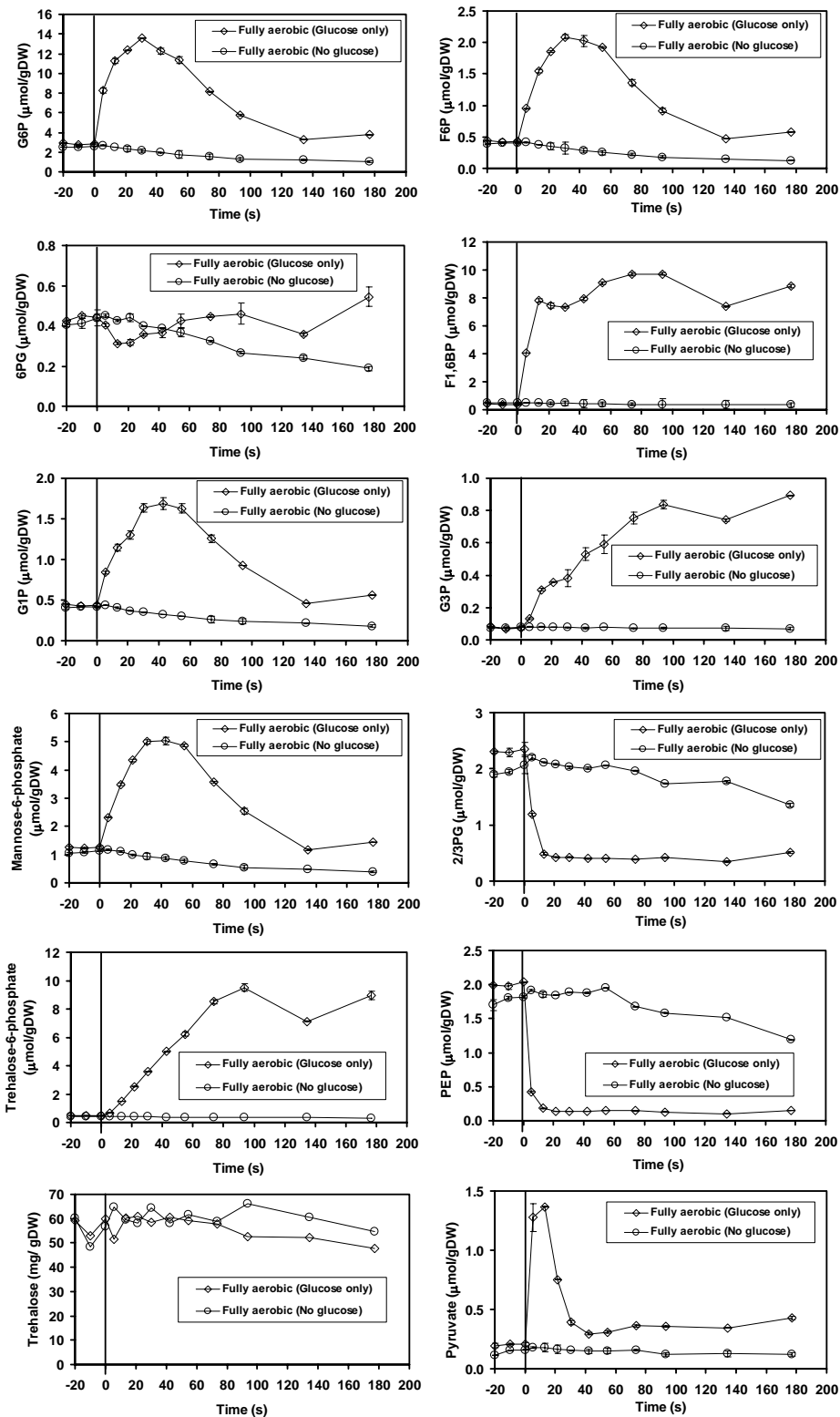


Figure 11 Comparison of intracellular glycolytic metabolites, mannose-6-phosphate, 6-phosphogluconate, trehalose-6-phosphate and trehalose concentration profiles before and during fully aerobic glucose only and no glucose perturbation to low cell density aerobic glucose/ethanol limited chemostat culture of *S. cerevisiae* CEN.PK 113-7D in the BioScope. Error bars represent standard deviations between duplicate analyses of the same sample.

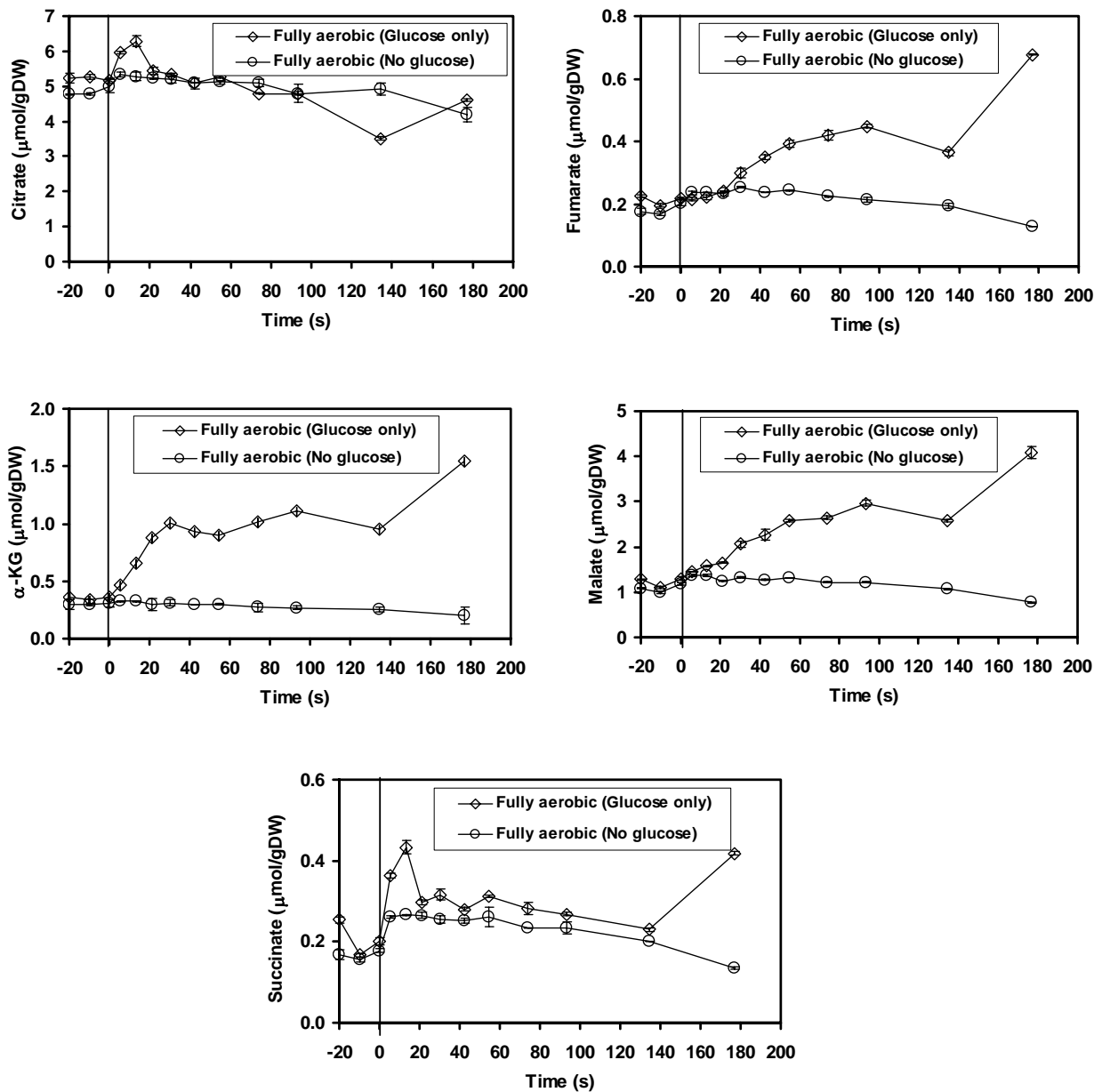


Figure 12 Intracellular TCA cycle metabolites concentration profiles before and during fully aerobic glucose only and no glucose perturbation to low cell density aerobic glucose/ethanol limited chemostat culture of *S. cerevisiae* CEN.PK 113-7D in the BioScope. Error bars represent standard deviations between duplicate analyses of the same sample.

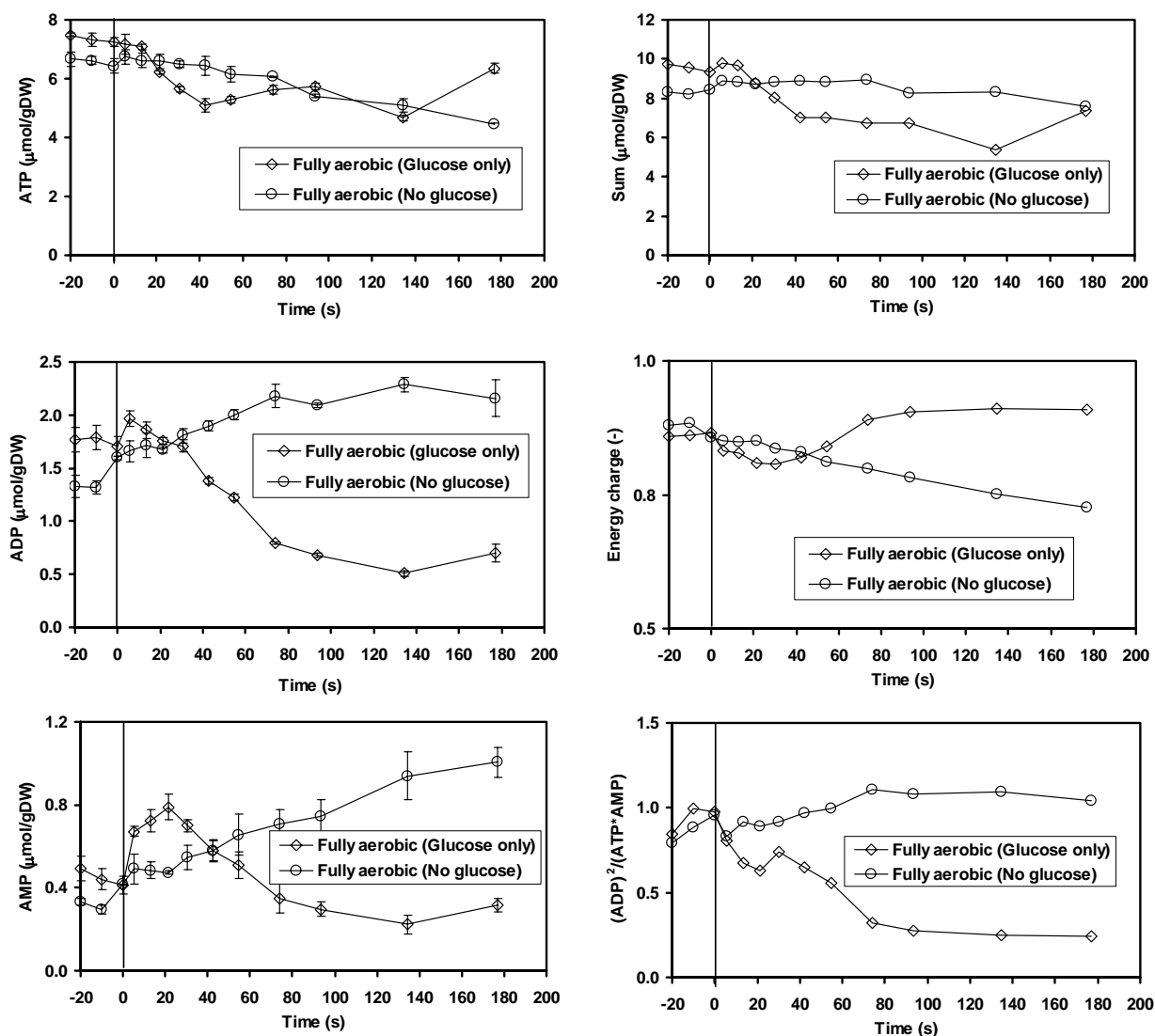


Figure 13 Intracellular adenine nucleotides (ATP, ADP, and AMP) concentration profiles; sum of nucleotides; cellular energy charge and adenylate mass action ratio during fully aerobic glucose only and no glucose perturbation to low cell density aerobic glucose/ethanol limited chemostat culture of *S. cerevisiae* CEN.PK 113-7D in the BioScope. Error bars represents standard deviations between duplicate analyses of the same sample.

The intracellular glycolytic and TCA cycle intermediates and adenylate nucleotides are shown in figs 11, 12 and 13, where the fully aerobic standard glucose only perturbation of (2.8 mM) is compared to the fully aerobic without glucose addition. All known mass action ratios (PGI, PGM, PMI, Enolase, and fumarase) are maintained close to equilibrium (data not shown).

A typical pattern is observed which is opposite to the results for the increased glycolytic flux occurring for an added glucose perturbation. Most notably one observes initially a slight

increase in 2/3PG and PEP, which could be caused by the lower ATP levels in the equilibrium between F1, 6 BP and 2/3PG. Also the lower F-1, 6-BP levels lead to less stimulation of pyruvate kinase.

Glycerol-3-phosphate hardly changes, showing the absence of redox stress. In the TCA cycle, one observes increased initial levels of the C4 pool metabolites, (malate, fumarate and succinate), which might be related to the higher CO₂ level in the experiment and the near equilibrium reaction of pyruvate carboxylase which converts pyruvate, CO₂ and ATP to the C4 pool via oxaloacetate.

The adenine nucleotides show a drastically different pattern with a slow drop in ATP and increases in ADP and AMP. Furthermore, a slow drop in cellular charge is observed. Most notably, there is hardly any change in the nucleotides sum. The adenylate kinase equilibrium is maintained (Fig 13). Intracellular trehalose was also quantified during both perturbations (Fig 11). It was found that there was no significant difference in steady state as well as during a perturbation in both cases. It is remarkable that also in glucose limited (no glucose addition) perturbation, no drop in the trehalose concentration was observed. This is surprising since it is expected that *S. cerevisiae* mobilizes storage carbohydrates (trehalose and glycogen) under starvation conditions (Francois and Parrou, 2001; Gancedo and Flores, 2004; Guillou et al, 2004). It is concluded that the glucose starvation period of 180 seconds is not long enough to trigger mobilization of storage compounds e.g. trehalose. Furthermore, there was still some glucose uptake during the 180 seconds in the BioScope (Figure 10A). This could further explain why trehalose was not mobilized as expected.

Conclusions

A perturbation towards lower O₂ availability (fully aerobic to anaerobic) in the presence of a glucose perturbation shows hardly any effect on glycolysis rate and its metabolites. Only pyruvate concentration is increased and the pyruvate flux is redirected from TCA cycle to ethanol and acetate. The use of acetaldehyde as an additional external electron acceptor under fully aerobic conditions and a glucose perturbation shows a highly significant impact on fluxes and metabolite levels of glycolysis and TCA cycle and especially the adenine nucleotides. The results strongly indicate that the dynamic response of adenine nucleotides is determined by the equilibrium coupling between the redox ratio NADH/NAD⁺ and the nucleotide ratio ATP/ADP caused by the equilibrium pool between F-1, 6-BP and 2/3PG. The perturbation of lower electron donor (glucose) supply shows a dynamic metabolite pattern which is opposite to the known pattern of increased glucose supply. Remarkable is that there is no indication of mobilization of trehalose storage under this conditions.

Acknowledgements

We would like to acknowledge Rob Kerste and Geerts Dirk for technical assistance. Johan Knoll; Cor Ras; Jan van Dam and Max Zomerdijk for analytical work. Applikon BV, Schiedam, The Netherlands; DSM Limited, Delft, The Netherlands and NWO are acknowledged for financing the Project.

References

- Bailey J.E., 1991. Toward a science of metabolic engineering. *Science*. 252, 1668-1675.
- Blazquez M.A., Lagunas R., Gancedo C., Gancedo J.M., 1993. Trehalose-6-phosphate, a new regulator of yeast glycolysis that inhibits hexokinases. *FEBS Lett* 329(1-2), 51-54.
- Bloemen H. H. J., Wu L., van Gulik W. M., Heijnen J. J., 2003. Reconstruction of the O₂ uptake rate and CO₂ evolution rate on a time scale of seconds. *AIChE Journal*. 49 (7), 1895-1908
- Buchholz A., Hurlbaus J., Wandrey C., Takors R., 2002. Metabolomics: Quantification of intracellular metabolite dynamics. *Biomol Eng*. 19, 5-15.
- Buziol S., Bashir I., Baumeister A., Claassen W., Noisommit-Rizzi N., Mailinger W., Reuss M., 2002. New bioreactor-coupled rapid stopped flow sampling technique for measurements of metabolite dynamics on a sub-second time scale. *Biotechnol Bioeng*. 80(6), 632-636.
- De Koning W., van Dam K., 1992. A method for the determinations of changes of glycolytic metabolites in yeast on a subsecond time scale using extraction at neutral pH. *Anal Biochem*. 204, 118-123.
- Francois J., Parrou J.L., 2001. Reserve carbohydrates metabolism in the yeast *Saccharomyces cerevisiae*. *FEMS Microbiol Rev*. 25, 125-145.
- Gancedo C., Flores C., 2004. The importance of a functional trehalose biosynthetic pathway for the life of yeasts and fungi. *FEMS Yeast Res*. 4 (4-5), 351-359.
- Gonzalez B., Francois J., Renaud M., 1997. A rapid and reliable method for metabolite extraction in yeast using boiling buffered ethanol. *Yeast*. 13, 1347-1356.

Guillou V., Plourde-Owobi L., Parrou J. L., Goma G., François J., 2004. Role of reserve carbohydrates in the growth dynamics of *Saccharomyces cerevisiae*. FEMS Yeast Res 4(8), 773-787.

Harrison D. E. F., Maitra P. K., 1969. Control of respiration and metabolism in growing *Klebsiella aerogenes*. Biochem J. 112, 647-656.

Hohmann S., Bell W., Neves M.J., Valckx D., Thevelein J.M., 1996. Evidence for trehalose-6-phosphate-dependent and -independent mechanisms in the control of sugar influx into yeast glycolysis. Mol Microbiol. 20(5), 981-991.

Lange H.C., Eman M., van Zuijlen G., Visser D., van Dam J.C. Frank J., Teixeira de Mattos M.J. and Heijnen J.J., 2001. Improved rapid sampling for in vivo kinetics of intracellular metabolites in *Saccharomyces cerevisiae*. Biotechnol Bioeng. 75 (4), 406-415.

Mashego M.R., van Gulik W.M., Vinke J.L., and Heijnen J.J., 2003. Critical evaluation of sampling techniques for residual glucose determination in carbon-limited chemostat culture of *Saccharomyces cerevisiae*. Biotechnol Bioeng. 83 (4), 395-399.

Mashego M.R., Wu L., Van Dam J.C., Ras C., Vinke J.L., Van Winden W.A., Van Gulik W.M., Heijnen J.J., 2004. MIRACLE: mass isotopomer ratio analysis of U-¹³C-labeled extracts. A new method for accurate quantification of changes in concentrations of intracellular metabolites. Biotechnol Bioeng. 85, 620-628.

Mashego, M. R., Jansen, M. L.A., Vinke, J. L., van Gulik, W.M., Heijnen, J.J., 2005. Changes in the metabolome of *Saccharomyces cerevisiae* associated with evolution in aerobic glucose-limited chemostats. FEMS Yeast Res. 5, 419-430.

Mashego M. R., van Gulik W. M., Vinke J. L., Visser D., Heijnen J. J., In vivo kinetics study with rapid perturbation experiments in *Saccharomyces cerevisiae* using a 2nd generation BioScope. Submitted.

Nielsen J., 2001. Metabolic engineering. Appl Microbial Biotechnol. 55, 263-283.

Oldiges M., Kunze M., Degenring D., Sprenger G. A., Takors R., 2004. Stimulation, monitoring, and analysis of pathway dynamics by metabolic profiling in the aromatic amino acid pathway, Biotechnol progr. 20(6), 1623-1633.

Oldiges M., Takors R., 2005. Applying metabolic profiling techniques for stimulus-response experiments: chances and pitfalls. *Adv Biochem Eng Biotechnol.* 92, 173-196.

Richter O., Betz A., Giersch C., 1975. The response of oscillating glycolysis to perturbations in the NADH/NAD system: A comparison between experiments and a computer model. *Biosystems.* 7(1), 137-146

Schaefer U., Boos W., Takors R., Weuster-Botz D., 1999. Automated sampling device for monitoring intracellular metabolite dynamics. *Anal Biochem.* 270, 88-96.

Schmitz M., Hirsch E., Bongaerts J., Takors R., 2002. Perturbation experiments as a prerequisite for the quantification of in vivo enzyme kinetics in aromatic amino acid pathway of *Escherichia coli*. *Biotechnol Progr.* 18, 935-941.

Stephanopoulos G.N., Aristidou A. A., Nielsen J., 1998. *Metabolic Engineering. Principles and Methodologies.* Academic Press, San Diego.

Theobald U., Mailinger W., Reuss M., Rizzi M., 1993. In vivo analysis of glucose-induced fast changes in yeast adenine nucleotide pool applying a rapid sampling technique. *Anal Biochem.* 214, 31-37.

Theobald U., Mailinger W., Baltés M., Reuss M., Rizzi M., 1997. In vivo analysis of metabolic dynamics in *Saccharomyces cerevisiae*: I. Experimental observations. *Biotechnol Bioeng.* 55, 305-316.

Van Dam J.C., Eman M.R., Frank J., Lange H.C., van Dedem G.W.K. Heijnen J.J., 2002. Analysis of glycolytic intermediates in *Saccharomyces cerevisiae* using anion exchange chromatography and electrospray ionisation with tandem mass spectrometric detection. *Anal Chem Acta.* 460, 209-218.

Verduyn C., Postma E., Scheffers W.A., Van Dijken J.P., 1992. Effect of benzoic acid on metabolic fluxes in yeasts: A continuous culture study on the regulation of respiration and alcoholic fermentation. *Yeast.* 8, 501-517.

Visser D., van Zuylen G.A., van Dam J.C., Oudshoorn A., Eman M.R., Ras C., van Gulik W.M., Frank J., van Dedem G.W., Heijnen J.J., 2002. Rapid sampling for analysis of in vivo kinetics using the BioScope: a system for continuous perturbation experiments. *Biotechnol Bioeng.* 79 (6), 674-681.

Visser D., van Zuylen G. A., van Dam J. C., Eman M. R., Pröll A., Ras Cor., Wu L., van Gulik W. M., Heijnen J. J., 2004. Analysis of in vivo kinetics of glycolysis in aerobic *Saccharomyces cerevisiae* by application of glucose and ethanol perturbations, *Biotechnol Bioeng.* 88 (2), 157-167.

Wang X., Mann C. J., Bai Y., Ni L., Weiner H., 1998. Molecular cloning, characterization, and potential roles of cytosolic and mitochondrial aldehyde dehydrogenases in ethanol metabolism in *Saccharomyces cerevisiae*. *J Bacteriol*, 180 (4), 822-830

Wu L., Mashego M. R., van Dam J. C., Proell A. M., Vinke J.L., Ras C., van Winden W. A., van Gulik W.M., Heijnen J. J., 2005. Quantitative analysis of the microbial metabolome by isotope dilution mass spectrometry using uniformly ¹³C-labeled cell extracts as internal standards. *Anal. Biochem.* 336, 164-171.

Appendix 1

In case of a constant O₂ consumption rate, rO₂ (mol/m³. s) in the BioScope, the O₂ balance can be written as follows

$$-\Phi_v \times \frac{dC_{O_2,L}}{dx} + k_{overall} * Di * (C_{O_2}^* - C_{O_2,L}) - rO_2 * \frac{\pi}{8} * Di^2 = 0 \quad 1$$

Integration of equation 1, using at x=0, C_{O₂}=C_{O₂}(0), leads to the expression

$$\frac{C_{O_2,L} - C_{O_2}^* + rO_2 * \frac{\pi}{8} * \frac{Di}{k_{overall}}}{C_{O_2,L(0)} - C_{O_2}^* + rO_2 * \frac{\pi}{8} * \frac{Di}{k_{overall}}} = e^{\left[\frac{-x}{\frac{\Phi}{k_{overall} * Di}} \right]} \quad 2$$

Using C_{O₂}(0) = 0.066 mol/m³ (DOT=27 %);

C_{O₂}^{*} = 0 (N₂ gas in the gas channel of the BioScope);

rO₂ = 0.007 mol/m³.s;

Di = 1.2 E-3 m;

K_{overall} = 1.9E-5 m/s

ø_v = 2 ml/min = 3.33E-8 m³/s;

leads to

$$\frac{C_{O_2,L} + 0.173}{0.061 + 0.173} = e^{\left[\frac{-x}{1.54} \right]} \quad 3$$

Here, x is the BioScope channel length (m);

C_{O₂} is mol O₂/m³

This equation shows that C_{O₂} = 0 at x = 0.45 m, corresponding to 6 seconds

Transient response of metabolome/fluxome of aerobic chemostat cultivated *S. cerevisiae* to increased CO₂ concentration

Abstract

A steady state aerobic glucose/ethanol limited chemostat ($D=0.05\text{ h}^{-1}$) culture of *Saccharomyces cerevisiae* CEN.PK 113-7D was perturbed by an instantaneous step increase of carbon dioxide (CO₂) concentration in the aeration gas from 0.04% to 1 %, while maintaining the oxygen concentration (O₂) at 20.95% during a period of 120 minutes. This changed the dissolved CO₂ level from 0.5 to 1.5 mM. It was found that this increased CO₂ concentration led after about 3-10 minutes to a strong transient increase in the external fluxes, i.e. (q_{O_2} and q_{CO_2}) as judged by the concentration of the off-gas CO₂ and O₂ as well as dissolved oxygen tension (DOT). This transient occurred at a glucose uptake which does not change, pointing to mobilization of storage carbon as a source of increased metabolism. Glycolytic flux was calculated to be transiently increased with up to a factor 2 during the perturbation. This increased flux reflected itself in an expected response of the concentration of glycolytic intermediates. TCA cycle metabolites also increased most probably due to the stimulatory effect of CO₂ to pyruvate carboxylase (anaplerotic route). Intracellular storage carbohydrates (trehalose and glycogen) decreased sequentially. Also, ATP concentration dropped in two distinct phases similar to that of trehalose and glycogen. Mass action ratios of phosphoglucose isomerase (PGI), phosphoglucomutase (PGM), Enolase, phosphomannose isomerase (PMI) and fumarase were also slightly perturbed but quickly returned to the pre-perturbation steady state levels.

To be submitted for publication in FEMS Yeast Letters.

Introduction

Bakers/brewers yeast (*Saccharomyces cerevisiae*) is a suitable eukaryotic cell model organism for studying in vivo regulation of carbon metabolism. Its popularity among the eukaryotic microbial physiologists has been enhanced by its whole genome sequence published in 1996 (Mewes et al, 1997). Since then, *S. cerevisiae* has been adopted as one of the eukaryotic platforms for metabolic engineering projects designed to study the primary and secondary cellular metabolism. It is envisaged that upon the understanding of the in-vivo kinetics and regulation of primary and secondary metabolism in this organism, this knowledge will be easily translated to the design of superior eukaryotic-based strains (cell factories) for production of high value added fine chemicals or products of pharmaceutical importance.

Quantitative study of the structure and regulation of metabolic reaction networks requires accurate information concerning both intracellular and extracellular metabolite pool levels which is required for the estimation of in vivo kinetic parameters. This information is commonly obtained under dynamic conditions via stimulus response experiments (Theobald et al, 1993). Stimulus response experiments under dynamic conditions (recently reviewed by Oldiges & Takors, 2005) are usually carried out in controlled environment using chemostat cultivation to obtain microorganisms under quantitatively defined steady states which are then perturbed using mainly glucose perturbation (Novick & Szilard, 1950; Tempest and Neijssel, 1981; Theobald et al, 1993; 1997; Visser et al, 2002; 2004; Schmitz et al, 2002; Buchholz et al, 2002; Buziol et al, 2002; Mashego et al, 2004). Traditionally, these experiments are performed via instantaneous step increase in residual growth limiting substrate concentration, rapid sampling, instant quenching and measurements of the intracellular metabolite concentrations during short time experiments, typically 300 seconds (Theobald et al, 1993; 1997; Schaefer et al, 1999; Visser et al, 2002; Schmitz et al, 2002; Buchholz et al, 2002; Buziol et al, 2002; Mashego et al, 2004; Oldiges et al, 2004).

Perturbations at a time scale of several hours are also frequently performed to characterize the response of enzyme degradation/induction.

During such dynamic glucose perturbation experiments, carbon dioxide is among the major primary end products of yeast glucose catabolism under both aerobic and anaerobic conditions and its concentrations easily increases several folds (Wu et al, 2003). Furthermore, in industrial fed-batch bakers yeast production process leads to very high CO₂ levels and the yeast experiences continuously changing CO₂ levels, the effect of which on metabolism is hardly known. This high CO₂ levels invariably will affect the quality, physiology and performance of the final yeast product, e.g. fermentative capacity (van Hoek, 2000). It can therefore be expected that the increased CO₂ will have secondary influence on the dynamic response of *S. cerevisiae* under glucose perturbation conditions. Also, CO₂ is an important component in the metabolism of microorganisms not only as a product but also as a substrate for carboxylation reactions e.g. anaplerotic route catalyzed by pyruvate carboxylase for the production of

oxaloacetate, thus refueling the TCA cycle. There are several other carboxylation reactions present in *S. cerevisiae* such as those catalyzed by phosphoenolpyruvate (PEP) carboxykinase and acetyl-CoA carboxylase (ACC).

The effect of dissolved CO₂ on yeast growth and metabolism has been studied from various aspects (for review, see Jones & Greenfield, 1982). CO₂ partial pressure (pCO₂) increase on aerobic substrate limited fed-batch grown *S. cerevisiae* has been reported to result in a decrease in cell yield and growth rate of *Saccharomyces* in baker's yeast production (Chen & Gutmanis, 1976). Furthermore, inhibition of yeast growth was found to be negligible below 20 % CO₂ concentration in the aeration gas mixture and increased with increase in CO₂ level above 50 % in the gas phase. Higher CO₂ content in the gas phase is reported to inhibit the fermentative activity of baker's yeast (Chen & Gutmanis, 1976). Recently, physiological and genome-wide transcriptional responses of carbon limited aerobic/anaerobic *Saccharomyces cerevisiae* to high carbon dioxide concentrations have been investigated (Aguilera et al, 2005). It was concluded in this study that aerobic metabolism was more sensitive to high CO₂ levels than anaerobic metabolism. Furthermore, the exposure to pCO₂ = 0.75 bar (22.51 mM) dissolved CO₂ under aerobic glucose limited condition led to only 104 changed genes, many of these encoded mitochondrial genes. Interestingly, PEPCCK (a gluconeogenic enzyme) was highly up regulated and the enzyme level was strongly increased. Also pyruvate carboxylase (PYC) was up regulated. Some decarboxylation genes were down regulated (Aguilera et al, 2005). However, in contrast to Chen & Gutmanis, 1976, no reduction in cell yield and growth was observed when *S. cerevisiae* was exposed to high CO₂ levels (Aguilera et al, 2005).

These studies show that *S. cerevisiae*, when exposed for long time (>10 hours) to high CO₂ levels, shows a clear response. Here we present results on the effect at a much shorter time scale (2 hours) of exposure to CO₂ on the metabolite levels as well as metabolic fluxes in a chemostat culture of *S. cerevisiae*.

Materials and Methods

Yeast strain and maintenance

The haploid, prototrophic *Saccharomyces cerevisiae* strain CEN.PK113-7D was kindly provided by Dr. P. Kötter (Frankfurt, Germany). Precultures were grown to stationary phase in shake-flasks on mineral medium adjusted to pH 6.0 (Verduyn et al, 1992) containing 2 % (w/v) glucose. After adding glycerol (30 %v/v) to the stationary phase culture, 2 ml aliquots were stored at -80 °C in sterile vials. These frozen stocks were used to inoculate precultures for chemostat cultivation.

Preculture conditions

Precultures were grown overnight in 100 ml mineral medium (Verduyn et al, 1992) contained in 500 ml Erlenmeyer flasks at 30 °C with shaking at 220 RPM on an orbital shaker (New Brunswick, New Jersey, USA).

Chemostat cultivation

Aerobic glucose/ethanol limited chemostat cultures were grown at 30°C, pH= 5.0, reactor overpressure of 0.3 bars to steady state at a dilution rate (D) of 0.05 h⁻¹ in 7l laboratory fermentor with a working volume of 4 l (Applikon, Schiedam, The Netherlands) as reported previously (Lange et al, 2001; Mashego et al, 2005). The feed medium contained a mixed carbon source of 150 mM glucose and 31mM ethanol. The addition of a small amount (7% of total carbon) of ethanol successfully prevented the cultures from metabolic oscillations. The biomass concentration supported by this medium composition is approximately 14.5±0.3 g.l⁻¹.

CO₂ perturbation in the chemostat

Steady state aerobic glucose/ethanol limited chemostat culture (14.8 g. l⁻¹) biomass of *S. cerevisiae* CENPK113-7D was perturbed by an instantaneous step increase of the dissolved CO₂ concentration via an increase of the CO₂ concentration in the aeration gas to the fermentor from 0.04 % to 1.0 % while maintaining the concentration of O₂ at 20.95 % for a period of 120 minutes. The volumetric gas flow rate before and during the CO₂ step change was kept constant at 3.3 l. min⁻¹. There was no change in medium feed rate. Rapid samples for intracellular and extracellular metabolites were collected at regular time intervals over the period of 120 minutes as described previously (Lange et al, 2001; Mashego et al, 2003). Online off-gas CO₂ and O₂ as well as dissolved oxygen tension (DOT) were also followed during the entire duration of the experiment.

Determinations of biomass dry weight concentration

Biomass dry weight concentration was determined as described previously (Mashego et al, 2005).

Determination of residual glucose concentration

Rapid sampling and instant quenching as well as the determination of residual glucose concentrations was as described previously (Mashego et al, 2003).

Rapid sampling, quenching and intracellular metabolite extraction

The applied procedures for fast sampling of broth from the fermentor, quenching of metabolic activity and subsequent extraction of metabolites from the biomass have been described previously (Mashego et al, 2004; Wu et al, 2005).

Trehalose extraction, enzymatic hydrolysis and analysis

Biomass samples for intracellular trehalose were extracted using the boiling ethanol method as described previously (Mashego et al, 2005). Two hundred micro liters sample from the trehalose extraction procedure, 50 µl trehalase (Sigma-Aldrich, Steinheim, Germany) 0.1 units. ml⁻¹ and

750 µl 80 mM sodium acetate buffer (pH 5.2) were added. The mixture was incubated at 37°C for 6.5 hours with shaking at 200 RPM in 1.5 ml Eppendorf tubes (Parrou et al, 1997). Glucose concentration in the trehalase hydrolyzed samples was measured spectrophotometrically (Agilent 8453-UV-visible spectroscopy system, Waldbronn, Germany) using a commercial glucose enzymatic kit no E0716251 (R-Biopharm AG, Darmstadt, Germany) as described previously (Mashego et al, 2005)

Glycogen extraction, enzymatic hydrolysis and analysis

A variation of the glycogen extraction methods described by Becker et al (1978); Quain et al, (1981) and Parrou et al, (1997) was employed for glycogen extraction from the yeast biomass. Five hundred micro liters of 0.25 M Na₂CO₃ solution were added to 500 µl biomass sample to a final biomass concentration of 14.8 g. l⁻¹. This alkali extraction mixture was immediately placed in boiling water bath in screw capped Eppendorf tubes, and incubated for 10 minutes to stop any metabolic activity. The resulting suspension was sonicated for 10 minutes followed by boiling in a water bath for 110 minutes. The samples were then centrifuged and the supernatant collected. The resulting alkali insoluble fraction was acid extracted with 500 µl 0.5 M perchloric acid (PCA) by boiling in a water bath for 20 minutes to extract the acid soluble glycogen fraction. The samples were centrifuged and the supernatant collected. The resulting acid extracted pellet residue was further acid extracted with 250 µl 0.5 M PCA as described above. The extract was centrifuged once more and both the alkaline and the two acidic fractions were pooled. The pH of the pooled fractions was adjusted to 5.2 by addition of 100 µl of 0.4 M sodium acetate buffer (pH 5.2) and 400 µl of water.

Samples, 250 µl from the pooled fractions and 70 µl amyloglucosidase (Sigma-Aldrich, Steinheim, Germany), 5 units. ml⁻¹ were added to 680 µl 0.4 M sodium acetate buffer (pH 5.2). The solution was incubated overnight at a temperature of 57°C with shaking at 200 RPM in screw capped Eppendorf tubes. At 57°C the co-hydrolysis of trehalose by trehalase is completely inhibited (Parrou et al, 1997), thereby stopping the cross contamination of the glucose resulting from the action of glycogen hydrolysis by amyloglucosidase. Glucose concentration in the samples was measured enzymatically as described previously (Mashego et al, 2005).

Analysis of intracellular glycolytic and TCA cycle metabolites

Intracellular glycolytic, TCA cycle metabolites, 6-PG, M-6-P and T-6-P were measured in the cell extracts using LC-ESI-MS/MS as described previously (van Dam et al, 2002; Mashego et al, 2004; Wu et al, 2005).

ATP analysis

ATP concentration in the samples from the trehalose extraction procedure was measured enzymatically using ATP Bioluminescence Assay Kit CLS II (Roche, Germany) as described previously (Mashego et al, 2005).

Results and Discussion

General steady state observations

The steady state of the chemostat is provided in Table 1. This steady state is characterized by constant biomass concentration and constant concentrations of O₂ and CO₂ in the off gas. Steady state condition is assumed to be satisfied when there were no observable changes in the off gas carbon dioxide (CO₂) and oxygen (O₂) as well as in the dissolved oxygen tension (DOT). The off gas O₂ and CO₂ were 19.72 and 1.15 % respectively. Dissolved O₂ remained constant at 0.196 mmol. l⁻¹ and the dissolved CO₂ was 0.52 mmol. l⁻¹ and remained constant as well. Specific fluxes, carbon dioxide evolution rate (qCO₂) and oxygen uptake (qO₂) were calculated to be 0.039 ± 2% and 0.042 ± 2% mol. C-mol biomass⁻¹. h⁻¹ respectively and remained constant (Table 1). The carbon metabolism was fully respiratory as judged by the respiratory quotient (RQ) of 0.95 ± 1%, which is expected for the mixed glucose/ethanol substrate used (Fig 1C). The carbon and redox balances are satisfied to 98 %.

Within several minutes upon introduction of 1 % CO₂ in the chemostat inflow gas, the dissolved CO₂ concentration tripled very rapidly from steady state value of 0.52 to a value of 1.5 mmol. l⁻¹. The dissolved O₂ level did hardly change in the first 5 minutes (Fig 1A, B). However, after about 5 minutes, there was a surprising transient increase in O₂ consumption and CO₂ production as observed from the depicted O₂ and CO₂ in the off gas. The increase peaked at about 50 minutes and after 80 minutes the O₂ and CO₂ fluxes returned to nearly the pre-perturbation values. The increase in O₂ consumption rate was mirrored in a transient decrease/increase in dissolved O₂ (Fig 1B).

During the transient, the respiratory quotient (RQ) ≈ 1, showing aerobic metabolism and the total amount of extra combusted carbon amounts to 0.04 C-mol for the whole culture (Fig 1D). Because the feed rate was not changed, the extra catabolized carbon must be obtained either from the residual glucose or from storage carbon. The residual glucose slightly decreased with an amount of 7 mg. l⁻¹ (Fig 2A) representing 0.001 mol C and can clearly not account for the observed extra catabolism.

Table 1 Average biomass dry weight concentration, specific ethanol uptake rate (q_{ethanol}); specific glucose uptake rate (q_{glucose}); specific carbon dioxide evolution rate (q_{CO_2}); specific oxygen uptake rate (q_{O_2}) and respiratory quotient (RQ) with their standard deviation. Dissolved O_2 and CO_2 in the chemostat were 0.196 and 0.52 mM respectively.

D	Biomass	q_{ethanol}	q_{glucose}	q_{CO_2}	q_{O_2}	RQ	
(h ⁻¹)	(g.l ⁻¹)	(mol ethanol.C- mol biomass ⁻¹ .h ⁻¹)	(mol glucose.C- mol biomass ⁻¹ .h ⁻¹)	(mol CO ₂ .C-mol biomass ⁻¹ .h ⁻¹)	(mol O ₂ .C-mol biomass ⁻¹ .h ⁻¹)	(-)	
Chemostat	0.05 ± 0.001	14.80 ± 0.30	0.0029±0.0001	0.0141±0.0004	0.039 ± 0.001	0.042 ± 0.001	0.94 ± 0.01

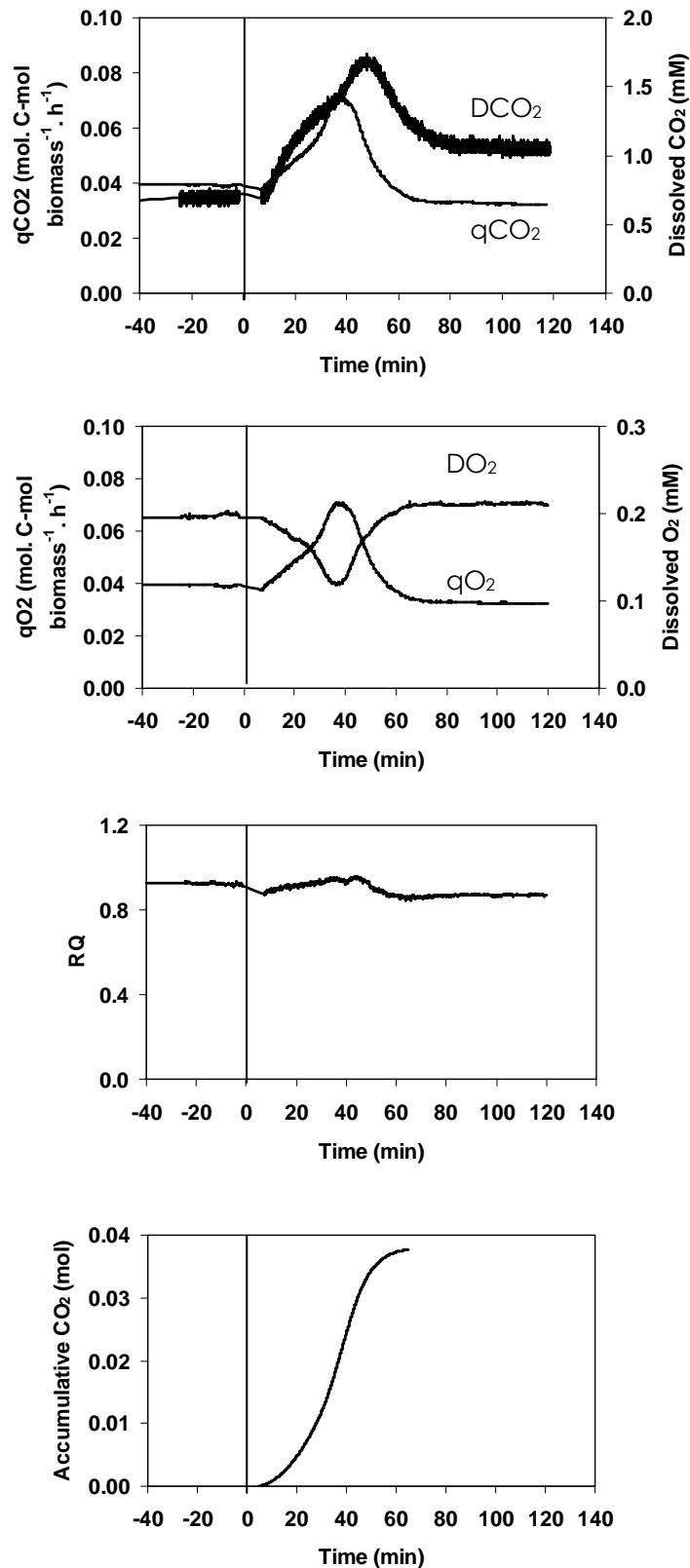


Figure 1 Specific carbon dioxide production rate (q_{CO_2}), dissolved CO_2 concentration, specific oxygen uptake rate (q_{O_2}), dissolved oxygen concentration, respiratory quotient (RQ), and accumulative CO_2 before and during CO_2 perturbation performed to aerobic glucose/ ethanol limited chemostat cultures of *S. cerevisiae* during a period of 120 minutes.

The biomass storage carbon analysis showed that both trehalose and glycogen were rapidly undergoing complicated transients, but after 80 minutes when the O₂ and CO₂ transient was over it appeared that a total amount of (15+15) mg of trehalose and glycogen per gram biomass had disappeared (Figs 2B, C). This represents a total of (60 grams dry biomass present in the fermentor) 1800 mg carbohydrate. Upon normal metabolism, this would lead to an extra CO₂ production of about 0.03 mol CO₂, which is very close to the observed amount of extra CO₂ (Fig 1D). This strongly indicates that mobilization of storage material causes the increased O₂ and CO₂ response. The transient shows an increase in qO₂ and qCO₂ of nearly a factor 2 (Fig 1A, B). Assuming a constant stoichiometry, this leads to a glycolytic flux which nearly doubles during the transient. This extra glycolytic flux seems to be created by a fast mobilization of the storage metabolism.

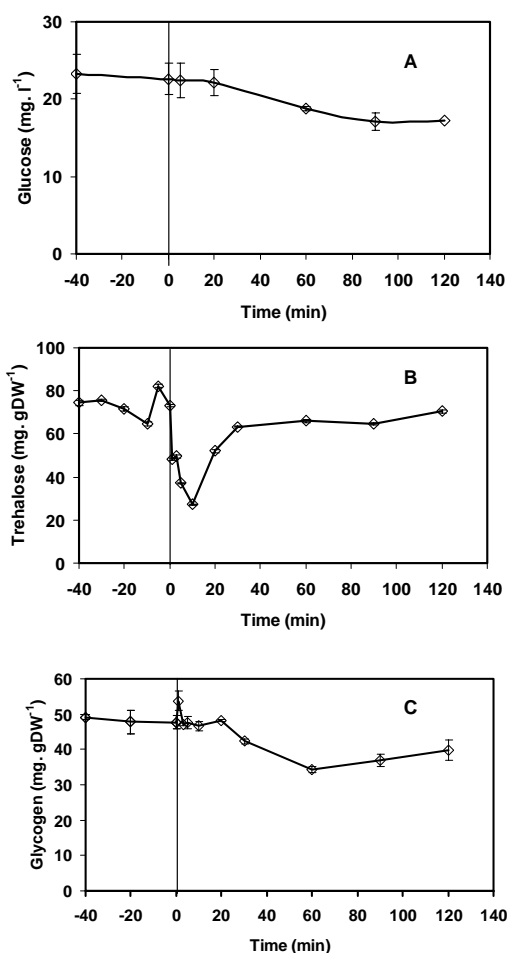


Figure 2 Residual glucose, trehalose and glycogen concentration profiles before and during CO₂ perturbation performed to aerobic glucose/ ethanol limited chemostat cultures of *S. cerevisiae* during a period of 120 minutes.

The response of the intracellular metabolites on this increased flux is shown in Figs 3-4. Carboxylation reactions are probably the most responsive to an increased CO₂ level, the most important reaction is pyruvate carboxylase which converts pyruvate to oxaloacetate (OAA), which is in equilibrium with C4 pool (malate, fumarate and succinate). Fig 3 shows that these metabolites significantly increase in the CO₂ caused transient. This suggests that the anaplerotic

route is stimulated significantly due to the higher CO₂ level. The glycolytic/storage metabolic intermediates are shown in Fig 4 and allow the following observations. Trehalose-6-phosphate (T6P) decreases strongly, suggesting a rapid mobilization of the storage carbon trehalose.

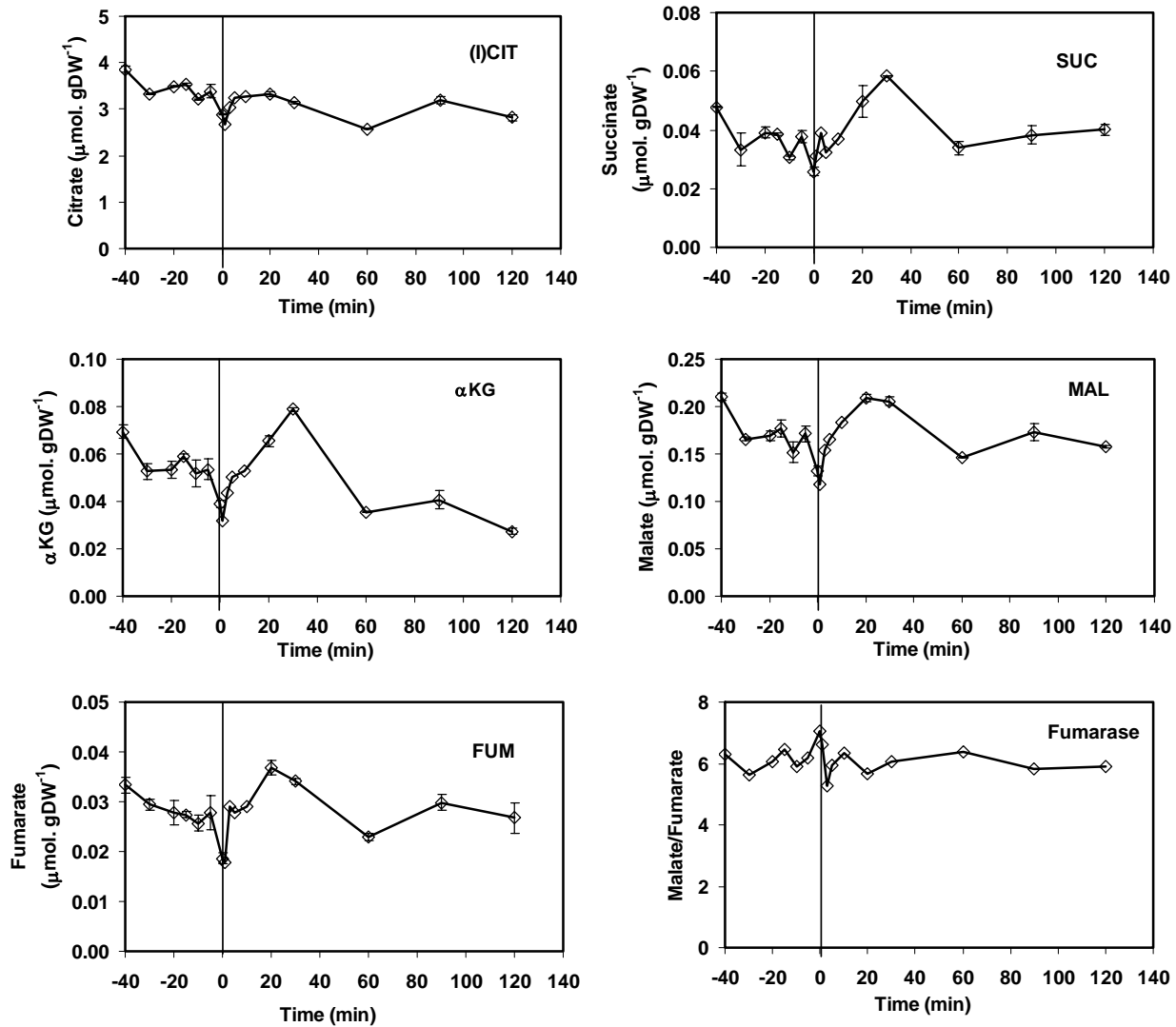


Figure 3 TCA cycle metabolites concentration profiles and fumarase mass action ratio before and during the CO₂ perturbing experiment to aerobic glucose/ethanol limited chemostat culture of *S. cerevisiae* CEN.PK 113-7D for a period of 120 minutes. Error bars represent absolute error between duplicate analyses of the same sample

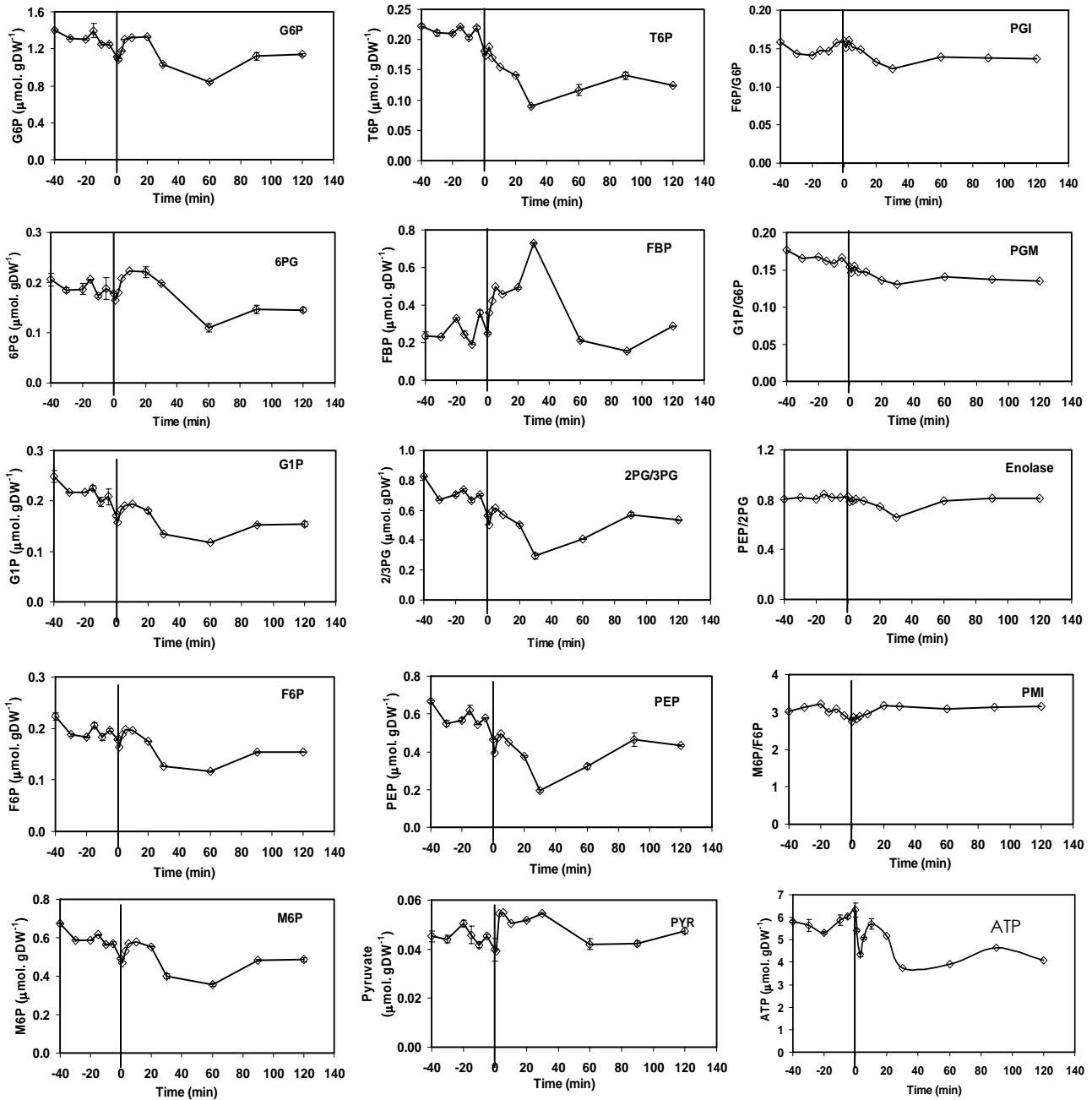


Figure 4 Intracellular glycolytic metabolites, 6-phosphogluconate, mannose-6-phosphate, trehalose-6-phosphate, and the mass action ratios of PGI, PGM, Enolase, PMI and ATP response profiles before and during CO_2 perturbation performed to aerobic glucose/ ethanol limited chemostat cultures of *S. cerevisiae* during a period of 120 minutes. Error bars represent absolute error between duplicate analyses of the same sample.

A higher glycolytic flux can indeed also be recognized from the response of intracellular levels of F1, 6BP; 2/3PG; PEP and pyruvate. It is known from glucose response experiments that a higher glycolytic flux leads to a much higher F1, 6BP and lower levels of PEP and 2/3PG (Theobald et al, 1993; 1997; Visser et al, 2002; Mashego et al, 2004). Also in such perturbation

experiments, the pyruvate level is usually increased due to the pyruvate carboxylase (PYC) activation by the higher F1, 6 BP levels. In this experiment, there is a clear 4-fold increase and decrease of F1, 6 BP, a 2-fold decrease/increase of 2/3PG and PEP and lastly, a slight increase in pyruvate. This strongly suggests a higher glycolytic flux in the transient. Interestingly, this higher flux is accompanied by lower levels of the complete hexose-phosphate pool (G6P, M6P, G1P, and F6P) all of which remain close to equilibrium as judged from the mass action ratio for phosphoglucose isomerase (PGI), phosphoglucomutase (PGM) and phosphomannose isomerase (PMI). Apparently, phosphofructokinase (PFK) can have a higher flux at a lower F6P level. The cause of all this might be the lower ATP level appearing after the CO₂ up-shift (Fig 4), because ATP is known to inhibit PFK. Although the above shows that the metabolite response is in good agreement with the nearly doubled glycolytic flux, it remains to be explained why the ATP concentration drops. Partly this could be due to the extra ATP consumed in the pyruvate carboxylase reaction. In addition, CO₂ after transport over the cell membrane dissociates intracellularly into H⁺ and HCO₃⁻. To maintain the intracellular pH, protons must be extruded and a cation imported (for the charge balance) at the cost of ATP (Shen et al, 2004). Furthermore, since the first and second phases of ATP concentration decrease coincided with trehalose and glycogen concentration drops respectively, it is expected that the released glucose units from the mobilization of this storage compounds especially trehalose hydrolysis by the enzyme trehalase have to be phosphorylated in glycolysis by the action of hexokinase (Francois & Parrou, 2001), which requires ATP.

These results do show that changing CO₂ level creates a drastic dynamic response of metabolism at time scales of ten's of minutes. For in vivo kinetic experiments at time scales of less than 5 minutes as performed in the BioScope (Visser et al, 2002), it would appear that the effect of CO₂ on the metabolic response can be expected to be minor. However, for industrial fermentation processes e.g. fed-batch, where CO₂ concentration can change quickly (minutes) due to the mixing and on hour scale due to increased feeding, these results show that the physiological states of *S. cerevisiae* can be affected profoundly by CO₂.

Conclusions

Increasing CO₂ concentration from 0.5 to 1.5 mM during a short time scale of tens of minutes has severe effects on central carbon metabolism in chemostat cultured aerobic *S. cerevisiae*. Higher CO₂ levels do lead to a transient mobilization of storage carbon (trehalose and glycogen) which in turn leads to nearly doubled glycolytic fluxes and a corresponding dynamic pattern of changes in the concentration of glycolytic intermediates. The trigger for these dynamic events might be the lower ATP level which can be caused by increased energy consumption for carboxylation reactions coupled to phosphorylation of the released glucose units from the storage pool as they enter glycolysis.

Finally, increased CO₂ concentration during the study of in vivo kinetics as performed in the time frame of 3 minutes could be expected to have negligible secondary effect to that of the glucose perturbation itself.

Acknowledgements

We would like to acknowledge Rob Kerste and Dirk Geerts for technical assistance. Cor Ras; Jan van Dam and Johan Knoll for analytical work. Applikon BV (The Netherlands) and DSM Limited (The Netherlands) and NWO for financing the Project

References

Aguilera J., Petit T., de Winde J.H., Pronk J.T., 2005. Physiological and genome-wide transcriptional responses of *Saccharomyces cerevisiae* to high carbon dioxide concentrations. FEMS Yeast Res. 5(6-7), 579-593.

Becker J.U., 1978. A method for glycogen determination in whole yeast cells. Anal Biochem. 86(1), 56-64.

Buchholz A., Hurlbaeus J., Wandrey C., Takors R., 2002. Metabolomics: Quantification of intracellular metabolite dynamics. Biomol Eng. 19, 5-15.

Buziol S., Bashir I., Baumeister A., Claassen W., Noisommit-Rizzi N., Mailinger W., Reuss M., 2002. New bioreactor-coupled rapid stopped flow sampling technique for measurements of metabolite dynamics on a sub-second time scale. Biotechnol Bioeng. 80(6), 632-636.

Chen S.L., Gutmain F., 1976. Carbon dioxide inhibition of yeast growth in biomass production. Biotechnol Bioeng. 18(10), 1455-1462.

Jones R. P., Greenfield P. F., 1982. Effect of carbon dioxide on yeast growth and fermentation. Enzyme Microb. Technol. 4, 210-223.

Lange H. C., Eman M., van Zuijlen G., Visser D., van Dam J. C., Frank J., de Mattos M. J., Heijnen J. J., 2001. Improved rapid sampling for in vivo kinetics of intracellular metabolites in *Saccharomyces cerevisiae*. Biotechnol Bioeng. 75(4), 406-415.

Mashego M. R., van Gulik W. M., Vinke J. L., Heijnen J. J., 2003. Critical evaluation of sampling techniques for residual glucose determination in carbon-limited chemostat culture of *Saccharomyces cerevisiae*. Biotechnol Bioeng. 83(4), 395-399.

Mashego M. R., Wu L., Van Dam J. C., Ras C., Vinke J. L., Van Winden W. A., Van Gulik W. M., Heijnen J. J., 2004. MIRACLE: mass isotopomer ratio analysis of U-¹³C-labeled extracts. A new method for accurate quantification of changes in concentrations of intracellular metabolites. *Biotechnol Bioeng.* 85(6), 620-628.

Mashego M. R., Jansen M. L.A., Vinke J. L., van Gulik W.M., Heijnen J.J., 2005. Changes in the metabolome of *Saccharomyces cerevisiae* associated with evolution in aerobic glucose-limited chemostats. *FEMS Yeast Res.* 5, 419-430.

Mewes H. W., Albermann K., Bähr M., Frishman D., Gleissner A., Hani J., Heumann K., Kleine K. Maierl A., Oliver S. G., Pfeiffer F., Zollner A., 1997. Overview of the yeast genome. *Nature.* 387, 7-8.

Novick A., Szilard L., 1950. Description of the chemostat. *Science.* 112, 715-716.

Oldiges M., Kunze M., Degenring D., Sprenger G. A., and Takors R., 2004. Stimulation, monitoring, and analysis of pathway dynamics by metabolic profiling in the aromatic amino acid pathway, *Biotechnol progr.* 20(6), 1623-1633.

Oldiges M., Takors R., 2005. Applying metabolic profiling techniques for stimulus-response experiments: chances and pitfalls. *Adv Biochem Eng Biotechnol.* 92:173-196.

Parrou J. L., Francois J., 1997. A simplified procedure for a rapid and reliable assay of both glycogen and trehalose in whole yeast cells. *Anal Biochem.* 248(1), 186-188.

Quain D. E., 1981. The determination of glycogen in yeasts. *J Inst Brew.* 87, 289-291.

Schaefer U., Boos W., Takors R., Weuster-Botz D., 1999. Automated sampling device for monitoring intracellular metabolite dynamics. *Anal Biochem.* 270, 88-96.

Shen H. Y., De Schrijver S., Moonjai N., Verstrepen K. J., Delvaux F., Delvaux F.R., 2004. Effects of CO₂ on the formation of flavour volatiles during fermentation with immobilised brewer's yeast. *Appl Microbiol Biotechnol.* 64(5), 636-643.

Schmitz M., Hirsch E., Bongaerts J., Takors R., 2002. Perturbation experiments as a prerequisite for the quantification of in vivo enzyme kinetics in aromatic amino acid pathway of *Escherichia coli*. *Biotechnol Progr.* 18, 935-941.

Tempest D.W., Neijssel O.M., 1981. Metabolic compromises involved in the growth of microorganisms in nutrient-limited (chemostat) environments. *Basic Life Sci.* 18, 335-356.

Theobald U., Mailinger W., Reuss M., Rizzi M., 1993. In vivo analysis of glucose-induced fast changes in yeast adenine nucleotide pool applying a rapid sampling technique. *Anal Biochem.* 214, 31-37.

Theobald U., Mailinger W., Baltés M., Reuss M., Rizzi M., 1997. In vivo analysis of metabolic dynamics in *Saccharomyces cerevisiae*: I. Experimental observations. *Biotechnol Bioeng.* 55, 305-316.

Van Dam J. C., Eman M. R., Frank J., Lange H. C., van Dedem G. W. K., Heijnen J.J., 2002. Analysis of metabolic dynamics in *Saccharomyces cerevisiae* using anion exchange chromatography and electrospray ionization with tandem mass spectrometric detection. *Anal Chem Acta.* 460, 209-218.

Van Hoek W.P.M., 2000. Fermentative capacity in aerobic cultures of bakers' yeast. PhD Thesis. Technische Universiteit Delft.

Verduyn C., Postma E., Scheffers W. A., Van Dijken J. P., 1992. Effect of benzoic acid on metabolic fluxes in yeasts: a continuous-culture study on the regulation of respiration and alcoholic fermentation. *Yeast.* 8(7), 501-517.

Visser D., van Zuylen G. A., van Dam J. C., Oudshoorn A., Eman M. R., Ras C., van Gulik W. M., Frank J., van Dedem G. W., Heijnen J. J., 2002. Rapid sampling for analysis of in vivo kinetics using the BioScope: a system for continuous-pulse experiments. *Biotechnol Bioeng.* 79(6), 674-681.

Visser Diana., van Zuylen Gertan. A., van Dam Jan C., Eman Michael R., Pröll Angela., Ras Cor., Wu Liang., van Gulik Walter. M., Heijnen Joseph. J., 2004. Analysis of in vivo kinetics of glycolysis in aerobic *Saccharomyces cerevisiae* by application of glucose and ethanol perturbations, *Biotechnol Bioeng.* 88 (2), 157-167.

Wu L., Lange H. C., van Gulik W. M., Heijnen J. J., 2003. Determination of in vivo oxygen uptake and carbon dioxide evolution rates from off-gas measurements under highly dynamic conditions. *Biotechnol Bioeng.* 81 (4), 448-458

Wu L., Mashego M. R., Van Dam J. C., Proell A. M., Vinke J. L., Ras C., Winden W. A., Gulik W. M., Heijnen J. J., 2005. Quantitative analysis of the microbial metabolome by isotope dilution mass spectrometry using U-¹³C-labeled cell extracts as internal standards. *Anal. Biochem.* 336, 164-171.

Conclusions and outlook

The purpose of the research presented in the thesis was to develop robust methods and experimental designs for quantitative analysis of primary metabolism in *S. cerevisiae*. To this end, chemostats were used mainly for obtaining reproducible steady state biomass under well-defined conditions. However, it was observed that the residual substrate (glucose) under glucose limited conditions of the chemostats were higher than expected for carbon limited conditions. This observation led to the systematic evaluation of the methods in literature used for determination of residual substrate in carbon-limited chemostats. The importance of the accurate determination of residual substrate concentration is that it allows accurate calculation of specific substrate uptake rate, which is in turn a valuable input variable, especially under dynamic conditions. Rigorous evaluation of the sampling techniques has resulted in the recommendation and subsequent adoption of the cold (-18°C) stainless steel beads quenching method mainly due to its reproducibility and simplicity. Furthermore, accurate measurements of excreted metabolites such as ethanol and acetate produced predominantly during dynamic glucose perturbation experiments to carbon-limited chemostats of *S. cerevisiae* were achieved. This method is easily adapted to other microbial systems as well. Intracellular metabolite measurements are central in the elucidation of microbial metabolic networks and their regulation in vivo. Reliable isotope dilution mass spectrometry (IDMS) methods for reproducibly quantifying a wide number of low molecular weight metabolites from the glycolysis, TCA-cycle and pentose phosphate pathway have been developed. These methods are based on the use of ^{13}C labeled metabolites as internal standards, which are added prior to the extraction step following rapid quenching of cells in cold methanol. This method is termed MIRACLE: Mass Isotopomer Ratio Analysis of ^{13}C -labeled Extracts. The method is superior to the LC-MS/MS method reported by van Dam et al, 2001, since the accuracy is significantly increased. In addition, more metabolites can be quantified in a single run of 10 μl sample injection volume, rendering it very suitable for high throughput screening projects. Furthermore, when compared to the enzymatic based analytical methods (Buchholz et al, 2002; Hajjaj et al, 1998; Ruijter & Visser, 1996; Theobald et al, 1993; 1997; which requires very large sample volumes for quantifying limited number of metabolites, the IDMS method is superior.

A highly important observation was that intracellular primary metabolites of prolonged carbon limited chemostat cultures of *S. cerevisiae* tend to decrease significantly (factor 2-5) during a cultivation period of 90 generations. In depth investigation clearly revealed that these cultures tends to shed the overcapacities in the form of high intracellular metabolite levels and glycolytic enzymes when grown for a prolonged period (> 20 generations) at a constant growth rate under carbon limited conditions. This phenomenon has been observed before in *E. coli* (Adams et al, 1985; Weichert et al, 1997; Notley-McRobb & Ferenci, 1999; Manche et al,

1999; Wick et al, 2001; Steiner & Sauer, 2003) and in *S. cerevisiae* (Brown et al, 1998; Ferea et al, 1999). This observation has led to the conclusion that the notion that chemostats provide consistent “the same” biomass when the same medium and dilution rate are applied needs some revision. It is recommended that chemostat cultivated biomass destined for reproducible in vivo perturbation studies should not only be cultured on the same medium and at the same dilution rate but should also not be cultivated longer than 20 generation as revealed by our results. This ensures steady state grown cells that have always the same intra and extracellular metabolite levels.

Another remarkable finding was that steady state yeast metabolism responds very fiercely to a small change in the dissolved CO₂ concentration. The observed transient response clearly involves storage metabolism, but the trigger is unknown. Finally, the BioScope, an improved version of the system developed by Visser et al, (2002), which is a mini-plug flow reactor for high throughput dynamic experimentation, has been designed and used successfully. The system avoids the direct perturbation of the chemostat since perturbation experiments are performed outside the reactor. Improvements of the new system presented here, includes the possibility of an instantaneous switch from aerobic to anaerobic conditions by supplying N₂ in the gas channel of the BioScope. Furthermore, various perturbation agents other than glucose (e.g. acetaldehyde) can be used on biomass from the same chemostat since the perturbations are performed outside the bioreactor. In addition, it was demonstrated that various experimental designs such as the simultaneous manipulation of both the glucose concentration in the BioScope together with the gas composition fed to the gas channel of the BioScope could be performed leading to enriched data sets. The dynamic concentration profiles of the obtained metabolites are very comparable to those obtained previously (Visser et al., 2002; Theobald et al, 1993; 1997) but also when compared to perturbations performed directly in the fermentor. This research has provided sound analytical and experimental platforms to generate experimental data for the development of in vivo kinetic models of primary metabolism.

It is envisaged that having developed these robust analytical methods and tools for quantification of the primary carbon metabolism, the next step would be to use these tools for perturbing the secondary/ product pathway. This could be achieved by introducing various perturbation agents other than glucose such as those arising from the primary carbon metabolism, e.g. pyruvate, succinate, etc. In addition, inhibitors of certain known enzymatic reaction steps in a metabolic pathway could be used as perturbation agents, to change the reaction rate/ flux through those enzymes. Subsequently, in vivo kinetic parameters should be estimated from the resulting wealth of short term dynamic data. An important issue is now the development of reliable and fast methods to estimate the parameters from the obtained experimental data. Application of approximative kinetic formats, e.g. lin-log kinetics, to avoid the models becoming highly non-linear seems to offer promising prospects. . The remaining challenge is to quantitatively integrate the large quantity of data from all hierarchical levels

(genomics, transcriptomics, proteomics, metabolomics as well as fluxomics together with the inherent regulatory networks associated with biological systems into functional entities, predictable by the mathematical models resulting in *in silico* kinetic models for cellular metabolism and its regulation, incorporating all the levels of control of the biological system.

Summary

In this thesis, robust experimental methods and experimental designs for quantitative analysis of the metabolome (concentrations of relevant metabolites in the cell) of *Saccharomyces cerevisiae* (Bakers yeast) have been presented. In this research, it is essential to obtain a snapshot of intracellular as well as extracellular metabolite concentrations under defined conditions and as a function of time. Therefore, it is necessary to obtain within a fraction of a second, a representative sample from the population of cells and instantly arrest cellular metabolism. Chapter 2, presented a method for the rapid sampling and quenching of cellular metabolism based on cold stainless steel beads dedicated to reliable quantification of excreted metabolites as well as substrates, e.g. ethanol, acetate and glucose. In chapter 3, a new method addressing the shortcomings e.g. non-linearity of the liquid chromatography electro spray ionization mass spectrometry (LC-ESI-MS/MS) due to the saturation of electrospray ionisation as well as loss of metabolites during the boiling ethanol extraction procedure encountered during quenching/extraction and analysis of intracellular metabolites with liquid chromatography mass spectrometry is presented. The problems are overcome by adding for each compound to be analyzed a chemically identical stable isotope (^{13}C -fully labeled) internal standard. For each compound, the ^{12}C peak area relative to the ^{13}C peak area of the corresponding ^{13}C internal standard is measured. The ^{13}C -fully labeled metabolites were obtained by cultivating *S. cerevisiae* on fully labeled glucose and harvesting the biomass followed by extraction. This allows the calculation of the concentration of the ^{12}C compound relative to the known concentration of the ^{13}C labeled compound since the ESI saturation is the same for both ^{12}C and ^{13}C and therefore the ratio is not affected by saturation phenomena. Furthermore, since the ^{13}C labeled internal standard is added prior to the sample extraction in boiling ethanol, partial degradation and recovery problems during the extraction procedure are corrected. Chapter 4 probed the validity of the steady state assumption commonly assumed for substrate-limited chemostat grown cultures used as standard physiological reference for perturbation experiments. It was found for aerobic carbon limited chemostat culture of *S. cerevisiae* that the culture evolved due to substrate competition (in vivo evolution). The residual glucose concentration, intracellular glycolytic and TCA cycle metabolites as well as in vitro determined enzyme activities dropped over an extended cultivation period of more than 90 generations. Surprisingly the specific external fluxes (q_{O_2} , q_{CO_2} , q_{glucose}) as well as biomass yield remained unchanged. Therefore, it is suggested that steady state assumption holds true only for chemostat cultures of less than 20 generations old. Furthermore, the results of perturbation experiments can be expected to depend not only on the applied external stimuli, but also on the culture age as well. This suggests that for cultivation of biomass for reproducible in vivo kinetic experiments, not only the same growth conditions should be applied (e.g. temperature, pH, medium composition and dilution rate), but also the same cultivation time.

In chapter 5 the 2nd generation BioScope design, a mini plug-flow reactor for performing perturbation experiments with the possibility to alter the gas phase composition is presented. It is shown for both extracellular (glucose, ethanol and acetate) as well as intracellular (glycolytic, TCA cycle and adenine nucleotides) that the dynamic metabolite concentration patterns measured during a glucose perturbation experiment carried out in the BioScope were very similar to the results of a similar glucose perturbation carried out directly in the chemostat itself. Chapter 6 shows the successful use of the 2nd generation BioScope as a tool to carry out perturbation experiments. In addition to the more conventional glucose perturbations, novel perturbation principles were elaborated to obtain sets of highly different dynamic metabolite responses. The availability of external electron acceptor (O₂) was decreased from fully aerobic to anaerobic conditions. Furthermore, acetaldehyde was supplied during fully aerobic glucose perturbation experiment as an extra external electron acceptor, thereby increasing both the electron acceptor and donor simultaneously. It was found that changes in metabolome response were limited to the pyruvate node, when external electron acceptor was decreased from aerobic to anaerobic conditions. Acetaldehyde was found to have a strong effect on the metabolome dynamics and also gave a higher glycolytic flux. The response of the adenine nucleotides was very remarkable. During a glucose perturbation in the presence of acetaldehyde, the levels of ATP increased initially, which is totally in contrast to the usually observed drop in ATP when a glucose perturbation is provided. This indicates that the ATP level is not dictated by the glycolytic flux but is much more coupled to the cytosolic NADH/NAD⁺ ratio through the equilibrium pool from F-1,6-BP to 2/3PG.

In chapter 7, the effect of the gaseous stimulus compound CO₂ is tested by using high dissolved CO₂ concentration to pseudo steady state in *S. cerevisiae* is probed in a short time scale (120 minutes) in the fermentor. It is shown that high CO₂ has a pronounced effect during short term perturbation on the physiology of the culture. This effect is clearly not well understood and may be relevant for industrial process where *S. cerevisiae* is used. Furthermore, increase in CO₂ concentration in aerobic glucose/ethanol limited chemostat cultures leads to a transiently (\approx 2 hours) increase (factor 2) of the O₂ uptake and CO₂ production as well as the glycolytic flux apparently due to the mobilization of storage carbohydrates, i.e. trehalose and glycogen.

Samenvatting

Dit proefschrift bevat de resultaten van een onderzoek naar de ontwikkeling van experimentele technieken voor kwantitatief onderzoek aan het metabooloom (concentraties van relevante metabolieten in de cel) van de gist *Saccharomyces cerevisiae* (bakkersgist). Voor dit onderzoek is het essentieel om een momentopname te verkrijgen van intracellulaire en extracellulaire metabolietconcentraties onder bepaalde condities en als functie van de tijd. Hiervoor is het noodzakelijk om binnen een fractie van een seconde een representatief monster uit de populatie van cellen te nemen en op hetzelfde moment het cellulaire metabolisme te fixeren.

In hoofdstuk 2 wordt een methode beschreven voor snelle monsternames uit een fermentor en stillegging van het metabolisme door onmiddellijke afkoeling van het monster in een buisje gevuld met ijskoude stalen kogeltjes gevolgd door een snelle scheiding van cellen en omringend medium door middel van filtratie. Met deze methode kunnen momentopnamen worden gemaakt van de concentraties van door de cel in het medium uitgescheiden metabolieten alsmede extracellulaire substraatconcentraties, zoals ethanol, acetaat en glucose.

In hoofdstuk 3 wordt een methode gepresenteerd waarmee zowel een aantal problemen die inherent zijn aan het kwantificeren van stoffen met vloeistofchromatografie (HPLC) gekoppeld via electrospray ionisatie aan een massaspectrometer (LC-ESI-MS/MS) alsmede degradatie van metabolieten gedurende de extractie kunnen worden gecorrigeerd. Hiertoe werd voor elke te analyseren component een chemisch identieke, stabiele en uniform gelabelde ^{13}C isotoop toegevoegd als interne standaard. Deze ^{13}C metabolieten worden verkregen door gistcellen te kweken op uniform ^{13}C gelabeld medium. Een vaste hoeveelheid van deze gistcellen werd vervolgens toegevoegd aan elk (ongelabeld) monster waarna het gecombineerde monster werd geëxtraheerd. Vervolgens werd iedere component het relatieve piek oppervlak ten opzichte van de ^{13}C gelabelde standaard gekwantificeerd. Op deze wijze kon voor verzadiging van de electrospray ionisatie, drift van de analyseapparatuur alsmede voor degradatie van componenten tijdens de extractie worden gecompenseerd. In hoofdstuk 4 wordt in vivo-evolutie van een gistcultuur in een glucose gelimiteerde chemostaat beschreven. Gevonden werd dat cultivatie gedurende 90 generaties leidde tot grote veranderingen in de extracellulaire substraat concentratie alsmede intracellulaire metaboliet concentraties en enzym activiteiten terwijl er geen verandering optrad in specifieke substraat en zuurstofopnamesnelheden, kooldioxideproductie en biomassa yield. Blijkbaar leidt de specifieke selectiedruk die in een glucose gelimiteerde chemostaat op de cellen wordt uitgeoefend tot aanpassing van de cellen aan de specifieke omstandigheden. Uit deze resultaten blijkt dat er in een chemostaat eigenlijk alleen sprake is van een pseudo steady state en dat, om redenen van vergelijkbaarheid, stimulus reponse experimenten moeten worden

uitgevoerd binnen een gedefinieerd tijdsbestek van bijvoorbeeld niet meer dan 20 generaties. Hoofdstuk 5 beschrijft vervolgens een verbeterd ontwerp van de BioScope, een mini propstroom reactor voor het uitvoeren van stimulus respons experimenten. Voordelen van het nieuwe ontwerp zijn een grotere robuustheid, eenvoudiger fabricage en de mogelijkheid om tijdens stimulus respons experimenten tevens de samenstelling van de gasfase te manipuleren. Aan de hand van de resultaten van vergelijkbare glucose pulse experimenten uitgevoerd in de BioScope en direct in de chemostaat werd de bruikbaarheid van dit instrument gedemonstreerd. De resultaten van een aantal verschillende puls response experimenten uitgevoerd in de BioScope worden behandeld in hoofdstuk 6. Hier wordt aangetoond dat het toedienen van verschillende stimuli leidt tot een verschillende dynamische respons van het metabolisme en dus een verrijking van de dataset voor de uiteindelijke bepaling van de in-vivo kinetische parameters. In hoofdstuk 7 wordt tenslotte het effect van een gasvormige stimulus, in dit geval CO₂, beschreven binnen een kort tijdsbestek van 180 seconden alsmede gedurende een langere periode van 120 minuten. Gevonden werd dat een verhoging van de volumetrische CO₂ concentratie in de gasfase van de fermentor van 1 naar 2 % leidde tot mobilisatie van reservekoolhydraten (trehalose en glycogeen) en daarmee resulteerde in een tijdelijke verhoging met maximaal een factor 2 van de ademhaling (O₂ consumptie en CO₂ productie) een verhoging van de glycolytische flux en daarmee samenhangende veranderingen in de intracellulaire metaboliet concentraties.

Acknowledgements

First and foremost, a word of caution: The chronological order in which various people or organizations are listed under this part of the thesis do not in anyway suggest nor reflect their level of contribution to the success and timely completion of this thesis. I would like to extend my gratitude to Dr. W. M. van Gulik for his immense and significant contribution to the work presented in this thesis. He is also acknowledged for the Dutch translation of the summary of this thesis as well as the statements accompanying this thesis. Walter has been instrumental in my settlement to the lab; hence I thank you for being more than a supervisor. I hope you continue the excellent way in which you supervise your PhD students, and wish that your methodology could be extended or be assimilated by others especially upcoming young PhD supervisors. Ko Vinke is acknowledged for his technical assistance, especially running chemostats “the BPT way”. Professor Sef Heijnen is acknowledged for taking a chance in hiring me for the PhD ship. I could write a chapter on my first encounter with Sef, but due to the production costs of the thesis, I will summarize it as follows: I met Sef in the advanced course in Microbial Physiology and Fermentation Technology, in December of 1996, during which I enquired about the possibility of doing a PhD in Delft. His answer was a string of questions about my former university as well as my Professors. However, the names of the institutions and professors were not familiar to him, so he showed no enthusiasm at the time. Professor Sef Heijnen has been instrumental to the successful realization of the thesis, thank you.

The Fermentatie en Technische Dienst personnel, Rob Kerste, Dirk Geerts and Susan are acknowledged for always willing to technically assist whenever needed. Gertan van Zuijlen is acknowledged for introducing me to the rapid sampling equipment and the boiling ethanol procedure for extracting intracellular metabolites. LC-MS/MS team, Jan van Dam, Cor Ras, Angie ten Pierick and Johan Knoll are acknowledged for the outstanding contribution in the analytical part of the thesis. Also Max Zomerdijk is acknowledged for the GC work. Of course, the rapid sampling team, Wouter, Liang, Uly, Penia, Roelco, Andre, Roeland, Frederick, Emrah, Michiel without which rapid sampling would not have been possible. Industrial Microbiology group is acknowledged, especially Prof. dr J. T. Pronk and Mickel Jansen for their contribution in the in vivo evolution work (chapter 4). Viktor Boer and Zeyneb Vuralhan, Arthur Oudshoorn, Rob Hoogendijk, Han de Winde, Roel Bovenberg, Dick Schipper, Bas Romein in their capacity as members of the Amino acid project and SRT project. Graduate students, Jordi Corcoi and Dennis Krook are acknowledged for their contributions. The workshop team, Arno van den Berg, Joop Langeveld, Rob Suijkerbuijk and Ronald Bode for their outstanding contribution in the construction and maintenance of the 2nd generation BioScope. Astrid van Uijen and Apilena Sapioper are acknowledged for their assistance with sterilizations of fermentors. Sjaak Lispet, Herman Frumau and Wim Morien for always prepared to assist with ordering of special gases and consumables. Hans Kemper and Marcel van de Broek are acknowledged for their

contribution to solving IT related problems. Bart Kurpershoek is acknowledged for his assistance with library matters.

Industrial partners, DSM Limited and Applikon BV are acknowledged for their involvement and financial support in the SRT project and the Japan tech programme. Nederlandse Organisatie for Scientific Research (NWO) as well as Advanced Chemical Technologies for Sustainability (ACTS) are acknowledged for financial support.

My family and friends are acknowledged for supporting me directly or indirectly while far away from home.

Curriculum Vitae

Mlawule Reginald Mashego was born on 12 May 1972 in Bushbuckridge (South Africa). He obtained a BSc. Honours Degree (Microbiology) from the University of the North (South Africa) in 1995. In 1996, he obtained a MSc. Degree (Biotechnology) from the University of Zimbabwe. From 1997-2000, he worked as a research Scientist (fermentation) at the Council for Scientific and Industrial Research (CSIR) and later that year moved to AECI Limited (South Africa) in the same capacity. He then moved back to academia at the University of the North (South Africa) as a Lecturer (Industrial Microbiology). In June 2001, he joined the Bioprocess Technology group of Prof. dr. ir J. J. Heijnen as a PhD student. He worked on the development of robust experimental methods to study in vivo perturbation kinetics of primary metabolism in *Saccharomyces cerevisiae*, which has led to this thesis. From June 2005, he is a Post Doctoral Scientist working for the MEMORE project, a joint initiative between 1. Ghent University; 2. Free University Brussels; 3. Technical University of Delft.

List of publications

Mashego M. R, van Gulik W.M, Vinke J. L, and Heijnen J. J, 2003. Critical Evaluation of Sampling Techniques for Residual Glucose Determination in Carbon-Limited Chemostat Culture of *Saccharomyces cerevisiae*. Biotechnol. Bioeng. 83 (4), 395-399

M. R. Mashego, L. Wu, J. C. Van Dam, C. Ras, J. L. Vinke, W. A. Van Winden, W. M. Van Gulik, J. J. Heijnen, 2004. MIRACLE: mass isotopomer ratio analysis of U-13C-labeled extracts. A new method for accurate quantification of changes in concentrations of intracellular metabolites. Biotechnol Bioeng. 85, 620-628

Mashego M. R, Jansen M. L. A, Vinke J. L, van Gulik W. M and Heijnen J. J, 2005. Changes in the Metabolome of *Saccharomyces cerevisiae* Associated with Evolution in Aerobic Glucose-Limited Chemostats. FEMS Yeast Research. 5, 419-430

Liang Wu, Mlawule R. Mashego, Jan C. van Dam, Angela M. Proell, Jacobus L. Vinke, Cor Ras, Wouter A. van Winden, Walter M. van Gulik, Joseph J. Heijnen, 2005. Quantitative analysis of the microbial metabolome by isotope dilution mass spectrometry using uniformly ¹³C-labeled cell extracts as internal standards. Anal Biochem. 336, 164-171

Mickel L. A. Jansen, Adham Hassane, Mlawule Mashego, Pascale Daran-Lapujade, Jasper A Diderich, Johannes H. de Winde, Johannes P. van Dijken and Jack T. Pronk, 2005. Adaptive evolution of *Saccharomyces cerevisiae* during prolonged chemostat cultivation under glucose limitation leads to a reduced fermentative capacity. Microbiology. 151, 1657-1669

Liang Wu; Mlawule R Mashego; Angela M Proell; Jacobus L Vinke; Cor Ras; Jan van Dam; Wouter A van Winden, Walter M van Gulik; Joseph J Heijnen, 2005. In vivo kinetics of primary metabolism in *S. cerevisiae* studied through prolonged chemostat cultivation, Metab Eng, Accepted